CRANFIELD UNIVERSITY

H V DE CASTRO

FLYING AND HANDLING QUALITIES OF A FLY-BY-WIRE BLENDED-WING-BODY CIVIL TRANSPORT AIRCRAFT

SCHOOL OF ENGINEERING

PhD THESIS

CRANFIELD UNIVERSITY

SCHOOL OF ENGINEERING

PhD THESIS

Academic Year 2002-2003

Helena V de Castro

Flying and Handling Qualities of a Fly-by-Wire Blended-Wing-Body Civil Transport Aircraft

Supervisor: M V Cook

December 2003

This thesis is submitted in partial fulfillment of the requirements for the Degree of Doctor of Philosophy

ABSTRACT

The *blended-wing-body* (BWB) configuration appears as a promising contender for the next generation of large transport aircraft. The idea of blending the wing with the fuselage and eliminating the tail is not new, it has long been known that tailless aircraft can suffer from stability and control problems that must be addressed early in the design. This thesis is concerned with identifying and then evaluating the flight dynamics, stability, flight controls and handling qualities of a generic BWB large transport aircraft concept.

Longitudinal and lateral-directional static and dynamic stability analysis using aerodynamic data representative of different BWB configurations enabled a better understanding of the BWB aircraft characteristics and identification of the mechanisms that influence its behaviour. The static stability studies revealed that there is limited control power both for the longitudinal and lateral-directional motion. The solution for the longitudinal problem is to limit the static margins to small values around the neutral point, and even to use negative static margins. However, for the directional control problem the solution is to investigate alternative ways of generating directional control power. Additional investigation uncovered dynamic instability due to the low and negative longitudinal and directional static stability. Furthermore, adverse roll and yaw responses were found to aileron inputs.

The implementation of a pitch rate command/attitude hold *flight control system* (FCS) improved the longitudinal basic BWB characteristics to satisfactory levels, or Level 1, *flying and handling qualities* (FHQ). Although the lateral-directional command and stability FCS also improved the BWB flying and handling qualities it was demonstrated that Level 1 was not achieved for all flight conditions due to limited directional control power.

The possibility to use the conventional FHQs criteria and requirements for FCS design and FHQs assessment on BWB configurations was also investigated. Hence, a limited set of simulation trials were undertaken using an augmented BWB configuration. The longitudinal Bandwidth/Phase delay/Gibson dropback criteria, as suggested by the military standards, together with the *Generic Control Anticipation Parameter* (GCAP) proved possible to use to assess flying and handling qualities of BWB aircraft. For the lateral-directional motion the MIL-F-8785C criteria were used. Although it is possible to assess the FHQ of BWB configurations using these criteria, more research is recommended specifically on the lateral-directional FHQs criteria and requirements of highly augmented large transport aircraft.

To my parents

Acknowledgements

A work of this size always involves large amounts of time and effort where other people are involved or just make their influence. This research thesis is no different and I would like to pay contribute to a few individuals and institutions.

I would like to thank first of all the Fundacao para a Ciencia e a Tecnologia without whom support this research would have not been possible.

To Prof. Mulder and all Staff of the Control and Simulation Department of Delft University of Technology, the Netherlands, my many thanks for receiving me so well and highly boosted this research.

I would like to thank also to Prof. Alan Morris for the opportunity he gave me to participate in the MOB project, and to all MOB people for the inputs and highlights on the blended-wing-body subject.

To the research test pilots, Erik Cornelisse, Roger Bailey, Jeremy Purry, Rick Pope and Ian Burrett, for all helpful comments and willingness of flying, my greatest thanks and that the sky be always yours.

Further, I would like to thank the Cranfield and Abbey National Volleyball Clubs for helping me to keep "sane in body as in mind", and in special to the players George Goudinakis, Roger Groves, Lionel Mason, Yoshihiro Takahashi, Alberto Sarchiapone, Geraint Roberts, Layne Walker and Sabine.

The Portuguese community in Cranfield was also an invaluable support when homesickness was stronger. All dinners with "bacalhau" will never be forgotten. Special thanks go to Vitor Pereira, Olinda Canhoto, the couple Rui and Cristina Pires, and their lovely children, Catarina and Miguel.

To Mike Cook who has been my mentor through this research with his invaluable knowledge, sense of humour, patience and wisdom, my deepest thanks.

At last but not least, I would like to thank Mischa de Brouwer, the reason to change Portugal for Cranfield, my rock and safe port in many storms since them, my source of motivation and concentration. If I began and finished this thesis that is due to him.

CONTENTS

LIST OF FIGURES

CHAPTER 1

CHAPTER 2

CHAPTER 3

CHAPTER 4

CHAPTER 5

CHAPTER 6

CHAPTER 7

CHAPTER 8

CHAPTER 9

LIST OF TABLES

CHAPTER 1

CHAPTER 2

CHAPTER 3

CHAPTER 4

CHAPTER 5

CHAPTER 6

CHAPTER 7

CHAPTER 8

CHAPTER 9

NOMENCLATURE

A	State matrix
b	Wing span
B	Input matrix: Spring damping parameter
$\bar{\bar{c}}$	Mean aerodynamic chord (*mac*)
cg	Centre of gravity
C_D	Drag coefficient
C_{D_o}	Zero angle of attack drag coefficient
C_l	Rolling moment coefficient
C_L	Lift coefficient
C_{L_o}	Zero angle of attack lift coefficient
C_{L_α}	Lift curve slope
C_m	Pitching moment coefficient
C_{m_o}	Pitching moment coefficient about aerodynamic centre of wing
C_{m_α}	Slope of $C_m - \alpha$ plot
C_n	Yawing moment coefficient
C_W	Weight coefficient
C_X	Axial force coefficient
C_Y	Side force coefficient
C_Z	Normal force coefficient
d_a	Pilot's aileron input
d_{CG}	Longitudinal distance between the main landing gear and the centre of gravity
d_M	Distance between the main landing gear and the centre of gravity
$d_{M_{CG}}$	Longitudinal distance between the main landing gear and the centre of gravity
d_N	Distance between the nose landing gear and the centre of gravity
d_{NG}	Longitudinal distance between the nose and main landing gear
$d_{N_{CG}}$	Longitudinal distance between the nose landing gear and the centre of gravity
d_r	Pilot's rudder input
d_T	Lateral distance from the thrust line to the aircraft centreline
F_{as}	Aileron stick force
F_M	Main landing gear normal friction force
F_N	Nose landing gear normal friction force
g	Acceleration due to gravity
h	Height: Centre of gravity position on reference chord
h_o	Aerodynamic centre position on reference chord
h_{CG}	Centre of gravity height
h_m	Controls fixed manoeuvre point position on reference chord

h_n Controls fixed neutral point position on reference chord

h_M Main landing gear height to the centre of gravity

h_N Nose landing gear height to the centre of gravity

h_T Thrust action line height to the main and nose landing gear level

H_m Controls fixed manoeuvre margin

I_{xx} Moment of inertia in roll

I_{yy} Moment of inertia in pitch

I_{zz} Moment of inertia in yaw

k Spring stiffness coefficient: Lateral-directional flying and handling qualities parameter

k_1 Drag polar parameter

k_2 Drag polar parameter

K Feedback gain

K_{ARI} Aileron to rudder interconnection gain

K_i Integral feedback gain

K_m Feedforward gain

K_n Controls fixed static stability margin

K_p Proportional feedback gain: Roll rate feedback gain

K_q Pitch rate feedback gain

K_r Yaw rate feedback gain

K_u Axial velocity feedback gain

K_α Angle of attack feedback gain

K_β Sideslip angle feedback gain

K_θ Pitch attitude feedback gain

l Rolling moment

L Lift

m mass: Pitching moment

n Load factor: Yawing moment

n_y Lateral load factor

n_z Normal load factor

p Roll rate perturbation

q Pitch rate perturbation

q_m Pitch rate overshot value to a step elevator input

q_s Pitch rate steady state response to a step elevator input

r Yaw rate perturbation

R_M Main landing gear axial friction force

R_N Nose landing gear axial friction force

s Laplace operator

S	Wing reference area
t	Time
$t_{\phi=30\,\mathrm{deg}}$	Time to change 30 degrees of bank angle
T	Time constant: Thrust
T_r	Roll mode time constant
T_s	Spiral mode time constant
T_{θ_2}	Second numerator zero in pitch rate and attitude transfer functions
u	Axial velocity perturbation
U_e	Axial component of steady equilibrium velocity
v	Lateral velocity perturbation
V_o	Steady equilibrium velocity
w	Normal velocity perturbation
W	Weight
W_e	Normal component of steady equilibrium velocity
x	Longitudinal coordinate in axis system
$x_{M_{ext}}$	Main landing gear extended deflection
$x_{N_{ext}}$	Nose landing gear extended deflection
x_{o_M}	Main landing gear static deflection
x_{o_N}	Nose landing gear static deflection
X	Axial force component: Axial position
X_{CG}	Centre of gravity longitudinal position
X_n	Neutral point longitudinal position
y	Lateral coordinate in axis system
Y	Lateral force component
z	Normal coordinate in axis system
Z	Normal force component

α	Angle of attack
β	Sideslip angle
δ	Control angle
Δ	Characteristic polynomial: Transfer function denominator: Increment
ε	Throttle level angle: Closed loop system error
ϕ	Bank angle
γ	Flight path angle perturbation
Γ	Wing dihedral angle
Λ	Wing sweep angle
η	Elevator angle
μ	Mass ratio: Lateral-directional flying and handling qualities parameter
μ_f	Friction coefficient

θ	Pitch angle perturbation
ρ	Air density
ς	Rudder angle
τ_e	Time equivalent delay
τ_{ph}	Phase delay
ω	Undamped natural frequency
ω_{BW}	Bandwidth frequency
ω_d	Dutch roll undamped natural frequency
ω_n	Damped natural frequency
ω_p	Phugoid undamped natural frequency
ω_s	Short period undamped natural frequency
ξ	Aileron angle
ψ	Yaw angle perturbation
ζ	Damping ratio
ζ_d	Dutch roll damping ratio
ζ_p	Phugoid damping ratio
ζ_s	Short period damping ratio

Subscripts

b	Aircraft body axes
com	Command
d	Dutch roll
D	Drag
e	Equilibrium, steady or initial condition
l	Rolling moment
L	Lift
m	Pitching moment: Manoeuvre
max	Maximum
M	Main landing gear
n	Neutral point: Yawing moment
N	Nose landing gear
p	Roll rate: phugoid
ph	Phase
pk	Peak
q	Pitch rate
r	Yaw rate: Roll mode: Root
s	Short period: Spiral mode

t	Time: Thrust: Tip
$trim$	Trim or equilibrium
u	Axial velocity
v	Lateral velocity
w	Aircraft wind or stability axes: Normal velocity
x	Axial force
y	Side Force
z	Normal force

α	Angle of attack
β	Sideslip angle
δ	General control surface
ϕ	Roll angle
η	Elevator
θ	Pitch attitude
ς	Rudder
ξ	Aileron
ψ	Yaw angle

Other symbols and notations

x_u	A shorthand notation to denote a concise derivative, a dimensional derivative divided by the appropriate mass or inertia parameters
C_{X_u}	A shorthand notation to denote a coefficient derivative $\frac{\partial C_X}{\partial u}$
$N_u^y(s)$	A shorthand notation to denote a transfer function numerator polynomial relating the output response y to the input u

ABBREVIATIONS

ACAH	Attitude Command/Attitude Hold
ACT	Activity Control Technology
AR	Aspect Ratio
ARI	Aileron to Rudder Interconnection
BWB	Blended-Wing-Body
BWR	Bedford Workload Rate
CAP	Control Anticipation Parameter
CAS	Command Augmentation Systems
CFD	Computational Fluid Dynamics
CCV	Control Configured Vehicle
CHR	Cooper-Harper Rate
CSAS	Command and Stability Augmentation System
FAA	Federal Aircraft Administration
FAR	Federation Aviation Requirements
FBW	Fly-By-Wire
FCS	Flight Control System
GCAP	General Control Anticipation Parameter
ICAD	Intelligent Computer Aid Design
ILS	Instrument Landing System
JAA	Joint Aviation Authority
JAR	Joint Aviation Requirements
LE	Leading Edge
LG	Landing Gear
LOES	Low Order Equivalent Systems
MIL-F	Military Specifications
MIL-STD	Military Standard
MLW	Maximum Landing Weight
MTE	Mission Task Element
MTOW	Maximum Take Off Weight
OEW	Operational Empty Weight
PF	Pre-Filter
PIO	Pilot Induced Oscillations
RCAH	Rate Command/Attitude Hold
SAS	Stability Augmentation System
UCE	Usable Cue Environment
WO	Washout

CHAPTER 1
Introduction

"It is important to know where we are today, but it is equally important to know a little about the route that we took, and how we came to be here"

A. G. Barnes

1.1 Overview

The dream of flying is as old as civilization itself. Since Icarus, human beings jealousy watch the birds in their flight, wishing they could also see the earth from the sky, they could also climb to high heights, feeling the wind passing by.

From Leonard Da Vinci and his novel machines, to Jules Verne and his fantastic stories, for years and years men dreamed of extensions and devices that could fulfil this dream, but all without success. It was only in more recent times that the dream came true. Firstly, Montgolfier and his hot air balloons, Sir George Cayley and his treatise "On Aerial Navigation" and flying models, then Otto Lilienthal and his gliders. But, it was the Wright brothers with their first powered flight and many pioneers like them with the invention of the flying machine or aircraft, who initiated the true flying adventure.

During this development many configurations and designs were constructed, and tested with more or less success. Some of them just had a wing, others had many protuberances and appendices that although unnecessary, were thought to be important, or were kept just because it looked nice. In the end the particular configuration of a wing, fuselage and tail that separate several functions to make flight possible, earned more and more recognition and over time has been successively developed into the conventional aircraft.

The conventional aircraft concept treated always the several parts of the aircraft according to its role in the final aircraft. The wing has been optimised over the years for the production of lift, tails for the production of stability and fuselage to carry passengers and cargo and so to pay off the aircraft use. Although easy in treatment of each individual part, these sometimes will conflict with each other. For example, in stability matters the tail produce a down force, which counteracts with the up force, lift, produced by the wing. Another example is the wing, being optimised to produce the best efficiency possible, and thus less drag, to be connected to a fuselage afterwards, increasing the drag due to interference.

From this background one might think, why not integrate all parts and optimise for a common purpose? The problem is that this task is not an easy one, since there are many interactions and conflicting issues when treating all functions together: lift generation, stability generation and cargo containment. Hopefully, helped by the today's increasingly available computer technology, this task becomes easier and might become very affordable: actually tools are being developed to integrate and to optimise all aircraft design parameters. Such examples are the multi-disciplinary programs ongoing worldwide, as described by Morris[1] or Chudoba[2].

The idea of combining the several aircraft functions in just the wing is not new and revisits the beginning of aviation. Already at that time aerodynamicists would have liked to omit all parts that increase the drag, such as fuselage and tails. However the problems arising when considering the integration of all functions seemed to be impossible to solve. The natural evolution led to the evolution of the conventional aircraft, as it is known today. Nevertheless, there have been several attempts throughout all this time to integrate the functions in just one surface, the wing, giving rise to flying-wing or all-wing concepts, or just to omit some of the aircraft parts, such as the tail, giving rise to tailless configurations.

1.2 Aircraft Classification

Before dealing with the main subject of the thesis, it was considered important to define what is meant by flying wings, blended-wing-bodies and tailless aircraft. The first to suggest or define an aircraft classification in relation to its configuration was Lippisch[3]. As presented in Figure 1.1, he suggested classifying the aircraft by its planform shape, where a normal standard aircraft represents the conventional aircraft with wing, fuselage and a rearward tail. Variations could then be on the position of

the wing relatively to the stability surface: canard, or tail-first aircraft, when the main wing is behind the tail and tandem when both surfaces are of the same dimensions.

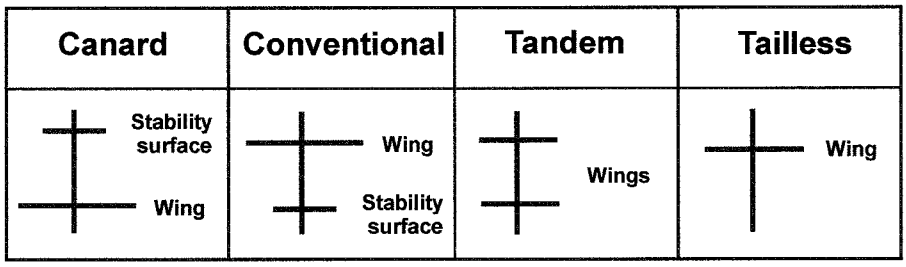

Figure 1.1 Lippisch's aircraft classification (Ref. 3)

A tailless aircraft, then, following Lippisch classification would be an aircraft without tail, although no particular reference exists to define the addition, or not, of a vertical tail or fin. The definitions of canard or tail first, tailed or "conventional", tandem and tailless aircraft given by Lippisch[3] were adopted in this thesis. The assumption in this research is that the tailless definition still allows for one, or more, vertical tail surfaces, somewhere attached to the fuselage or wing.

Based on this primary Lippisch classification, further definition of the tailless configuration was made, as shown in Figure 1.2. Thus, a particular kind of tailless aircraft is one where the fuselage is blended with the wing itself, known as *blended-wing-body* (BWB). In this configuration the thick central body is still partly discernible from the wing although, since it is streamlined, it also contributes to the generation of total lift and reduction of fuselage drag. When there is completely no division between central body and wing, but all of it is just a wing, or a lifting body, and carrying in its interior all the load, this is classified then as a flying wing or lifting-body.

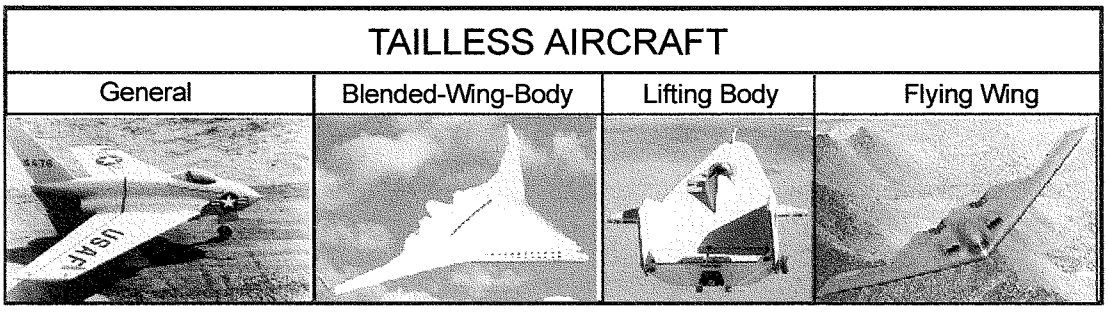

Figure 1.2 Tailless aircraft classification (Ref. W1 to W4)

The blended-wing-body is a further step in the development of the tailless aircraft concept towards the all-wing concept. However, this concept can still be tailless or tailed, since its definition depends only whether the wing and fuselage are blended or

not. Some authors, as Wood and Bauer[4], consider this configuration as a *lift fuselage*. However, such classification is not considered here since a fuselage has mainly a payload carrying function. For this research, lifting-bodies are those particular tailless configurations where the wing is so small, that the "fuselage", or better the central-body, is the main generator of lift, although also including a vertical surface. Although some authors regard these as being blended-wing-bodies, the wing is of such reduced dimensions that in this thesis it is considered as part of the "unusual" body section, rather than being a wing itself.

The presence of a vertical tail is not always well defined. In general for this thesis, it is considered that being tailless just accounts for the horizontal tail, still being possible for a tailless aircraft to possess a vertical tail somewhere attached to the fuselage or wing. However, for many authors a flying-wing or all-wing configuration is one which possesses neither fuselage nor horizontal tail, and also no vertical tail. The Northrop-Grumman B-2 is an example of such an aircraft. The Northrop XB-35 and the Northrop YB-49 were an approximation to pure wings, but they still had protuberances and appendices that exclude them from this category.

Another possibility for classifying aircraft takes into account the wing planform shape. This is based also in the Lippisch[3] classification. The ones of interest for this study are; the normal trapezoidal (rectangular and tapered) wing, the delta wing, and the cranked wing. Since it is a different classification it is possible to have a delta tailless or tailed configuration, as well as a cranked blended-wing-body aircraft.

1.3 Tailless aircraft history

Almost since the beginning of flight, both designers and pilots have been fascinated with the concept of the flying wing. There are a number of reasons for this, many grounded in engineering concepts of stability, drag reduction and so on, but there are also emotional and aesthetic reasons that are equally compelling. In the past, fuselages have carried the payload and empennage, but aerodynamically have produced little lift, contributing mostly to drag. Therefore, in the aerodynamicist's viewpoint an ideal cruising aircraft is a simple elegant flying wing.

Furthermore, the flying wing somehow captures the imagination as being an aircraft of the purest sort, unencumbered by fuselage, tail or other structures, one in which man could truly soar as free as the birds. As Castro[5] shows with the history of tailless aircraft, flying wings have been the object of what amounts to an obsessive

fascination by a number of engineers; their configuration seemed to exercise an almost mystical control over the minds and careers of the men who developed them.

However, the omission of a fuselage and empennage brings problems, as Northrop[6] pointed out in his lecture to the Royal Aeronautical Society in 1947. Basic requirements, such as the aeroplane being large enough to include all within the wing and that enough stability and controllability for practical operations should exist before any gain in aerodynamic and structural efficiency could be achieved. Therefore, more than understanding the tailless aircraft that existed or exist, it is their basic characteristics and problems faced by designers and constructors that are of concern in this thesis. Thus, a review of static and dynamic stability characteristics of tailless aircraft as well as other flying and handling characteristics follows.

1.3.1 The problems of tailless aircraft

1.3.1.1 Longitudinal stability problems

Jones[7] says that an ordinary wing with a slight reflex camber and dihedral has all the aerodynamic characteristics necessary for both lateral and longitudinal stability. Moreover, longitudinal static stability in gliding flight is practically assured if the centre of gravity is located slightly ahead of the aerodynamic centre of the wing. Moreover, Mair[8] also agrees, suggesting the use of an "auto-stable" airfoil: with a forward convex part, being mainly unstable and generating almost all lift, and a rear concave part, which stabilizes the forward part just like a tail. Thus, the aerodynamicists work would be to calculate an airfoil that generates a maximum lift for minimum drag, with the auto-stabilising characteristics. However, an auto-stabilising wing has the drawback of having a short centre of gravity (*cg*) range.

Further, Jones[7] emphasizes another important stability characteristic of a tailless aeroplane: its pitching motion, or more exactly the reduced kinematic damping of the pitching motion. Moreover, the elevator deflection necessary to change a trim condition is also affected by the reduced damping in pitch. This together with the short *cg* margin makes the pitch control too sensitive: a very small amount of stick resulting in a large change in trim.

Moreover, without a horizontal tail, the fuselage becomes small or even disappears, moving the fins to the tip of the wings and using narrow chord flaps to secure longitudinal control. This shortage of fuselage, among other reasons, contributes to a reduction of the moment of inertia in pitch. Thus, the flap angle used for longitudinal

control has to be increased in order to reduce the camber and thus the moment. However, the upward deflection of flaps decreases the total lift, and higher angles of attack are then necessary in order to restore the lost lift, as presented also by Sears[9]. Shepperd[10] found that by increasing the flap chord (and thus the control surface area) a trimmed increment in lift coefficient could be achieved (less control surfaces is necessary). On the other hand, this loss of maximum trimmed lift can be increased, as Northrop[6] suggests, by using boundary-layer control together with turbo-jets or gas turbines, in combination with low pitching moment flaps and trimming devices and, or, by placing the *cg* behind the aerodynamic centre thereby eliminating inherent longitudinal stability.

To overcome the short *cg* range and short pitching moment arm, the majority of tailless designers decide to sweep back the wing. Thus, the aerodynamic centre is moved backwards, the moment of inertia in pitch increases and there is the possibility to use centre spanwise surfaces as high lift generators, which have a reduced up-nose moment since they are near the *cg*, and outer spanwise surfaces for pitch control. Although Mair[8] suggests the swept forward wing as a solution, Donlan[10] and Northrop[6] actually concluded that sweep back presents the best approach.

As Thorpe[11] found the introduction of sweptback wings solved some tailless configuration problems such as the increasing of elevator power. However, it introduced another worse problem, that of premature wing tip stalling which may induce wing drop, loss of lateral control due to lack of flow over the ailerons and even of longitudinal control if elevons are used instead, as well as loss of longitudinal stability with the associated nose-up change of trim.

Donlan[12] investigated the problems and possible solutions of the inclusion of sweepback as an extension of the work realised by Jones[7]. He comments that part of the stalling problem of sweptback wings can be attributed to high taper and so tapered sweepback wings should be avoided. Furthermore, he suggests wing twist (geometric washout), changes in airfoil section (aerodynamic washout), flat-plate separators, changes in tip planform and leading-edge slats as solutions for wing tip stall. Moreover, he adds that the geometric and aerodynamic washout can be very effective, but they would increase the drag at low angles of attack. Also, the use of leading-edge slats would be the most effective, but also this method would result in an increase of the drag at low angles of attack and so retractable slats would be best.

Lee[13] also comments on wing-tip stall, as well as on the compressibility effects and aeroelastic problems of sweptback wings. Furthermore, Trouncer and Wright[14] add

that the maximum lift coefficient was increased when using slats and flaps up, but was decreased with slats and flaps down. Seacord and Ankenbruck[15] also agree that partial-span wing slats are the most effective way to prevent tip stall and eliminate longitudinal instability. Hills and Kucherman[16] investigated the research of crancked sweepback wings which occurred in Germany. Therefore, they suggested that crancked wings, wings with decreasing sweepback towards the tip, would reduce the tendency for tip stall, as well as having a higher critical Mach number.

About the longitudinal instability due to separation on the trailing edge of a sweptback aerofoil with desirable root-thickness, taper ratio and symmetrical sections together with washout at the tips, Northrop[6] and Bolsunovski *et al*[17] suggest to extend the trailing edge chord backwards. Furthermore, Donlan[18] in another report stated that aspect ratio and sweep angle are the most important influence to the type of pitching moment variation to be expected at the stall. Whilst, airfoil section, wing taper, Reynolds number and surface roughness influence most the lift coefficient at which the first instability occurs. Then, Donlan[18] suggested that the addition of leading-edge flaps covering about 60% of the span most improved the pitching moment curve at the stall. Fences properly located also minimised local unstable pitching moment variations.

About tailless aircraft longitudinal dynamics, Wilkinson *et al*[19] found that the short period mode has in general shorter periods and slightly less damping than comparable conventional types. However, Donlan[12] and Northrop[6] found that although the pitch damping, C_{m_q}, is relatively low, the short period oscillation is highly damped for tailless configurations. This is due to a coupled motion such that the vertical damping, C_{Z_w}, comes into play absorbing the energy from the oscillation. Moreover, the low moment of inertia in pitch makes the small existing C_{m_q} more effective than a similar value would be in conventional types. Northrop[6] comments further that the combination of low static stability in pitch, as previously described, and low moment of inertia in pitch results in periods of oscillation for all-wing aircrafts that are comparable to those of conventional types. About the phugoid, Northrop[6] commented that because flying wings have relatively low drag, the phugoid seems even less damped than for conventional aircraft, however, being a slow motion it is easily controlled.

Northrop[6] presents the response to an abrupt vertical gust as being an especially interesting difference between tailless and conventional types. Two factors contribute to that: 1) the larger wing chord increases the time for transient flight to build up and it is more important in reducing accelerations and, 2) the shorter effective tail length

decreases the time interval between the disturbing impulse at the lift surface and the correcting impulse at the effective tail, so that the aeroplane tends to pitch into the gust. Wilkinson *et al*[19] also found that the growth of acceleration response to an elevator impulse, for forward *cg*, is quicker for tailless aircrafts than for conventional, whilst for linear application both have a similar response. However, with the *cg* at the neutral point, greater differences are shown either for the impulse input as for the linear input, with the tailless aircraft being much more sensitive than the conventional. Wilkinson *et al*[19] suggest that the fundamental reason for the difference with *cg* at neutral point for conventional and tailless aircraft is the difference in the relative importance of the damping moment, depending on C_{m_q}, compared with the elevator applied pitching moment and the moment due to C_{m_w}. It follows that the distance between the neutral and manoeuvre points is less on a tailless than on a conventional aircraft.

Kronfeld[20] comments that when disturbed a tailless aircraft will get out of the trim attitude more quickly with the controls held fixed, but will also seem to return in a much shorter time than conventional aircraft. Most pilots react instinctively by anticipating the amount of correct control movement required when hitting a gust, in accordance with the amount of acceleration felt. Because the acceleration is greater with tailless types, the control movements become too large and over-controlling results. This gives the impression of over-sensitiveness, which, strictly speaking, it is not. Proof of this seems to lie in the fact that, after a few flights pilots seem to forget about their original complaint and find a tailless aircraft usually quite pleasant. The best way to be quickly used to the "flicker" is to let the elevator go on, and, to gain confidence by the perfect flying characteristics that tailless aircraft have, if not disturbed by pilots.

Donlan[12] affirms that a form of dynamic instability of tailless airplanes may be manifested as tumbling. Tumbling consists of a continuous pitching rotation about the lateral axis of the aircraft. The manoeuvre is extremely violent and imposes severe accelerations on parts of the aircraft. So far as is known, there are no authenticated instances of the occurrence of tumbling in flight. The only occurrence has been tumbling of models in a free-spinning tunnel, by forcing the models to simulate a whip-stall. Tests have shown that the position of the centre of gravity has a pronounced effect on the motion. Thus, the provision of a large static margin prevents tumbling, but a stable tumbling condition may exist if the static margin is relaxed. Tests have shown that once the tumbling motion has started, the normal flying controls are relatively ineffective for recovery from this stable tumbling condition.

Northrop[6] also shares this opinion that if a tailless aircraft is under circumstances of induced rotation about the pitch axis, tumbling motion, the recovery is marginal. However he defends that it would never tumble from any normal flight condition, such as a stall, spin, or any other-to-be-expected manoeuvre. Donlan[12] concludes by saying that the permissible centre of gravity range position is a critical factor, because if the static margin becomes negative, there is danger of encountering longitudinal instability, either as a divergence from straight flight or as tumbling. However, Fremaux *et al*[21] in a more recent investigation concluded that *cg* location, mass distribution, and geometric aspect ratio strongly affected the tumbling characteristics and that positive static stability did not necessarily preclude tumbling.

Nevertheless, Donlan[12] presents other reasons to use small static margins. Such as, if the static margin is too great, the elevator control may not be powerful enough to raise the nose wheel off the ground at take-off. Furthermore, if the static margin is large, the elevator deflection required to trim the aircraft in level flight may seriously impair the efficiency of the wing with a consequent loss in performance. Consequently, a range of ultimate static margin from 0.02 to 0.08 appears to be reasonable for tailless airplanes, as suggested also by Thorpe[11]. Although these values for the *cg* range look rather small or limited, one should not forget these are a percentage of the mean aerodynamic chord, and usually tailless or all-wing aircraft have larger chords than conventional aircraft.

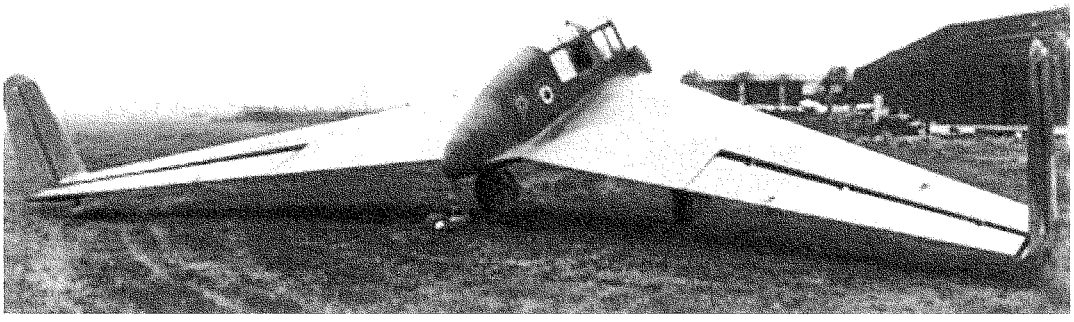

Figure 1.3 General Aircraft Ltd type 56, GAL56 (Ref. W5)

In the test of the GAL 56 glider Kronfeld[20] reports that the very frightening stall characteristics were not found, being impossible to make one or both wings drop in a stall, although it was hardly tried. In fact, there was every indication that a stall should be very good-natured and with plenty of warning. During a stall all that happened was a nosing-up, followed by a dropping of the nose whilst the aircraft gained speed. A warning stall characteristic that may be typical for tailless types was a stick reversal: at most forward *cg* positions, when reducing the speed, the stick started to push back

towards the pilot with a force which increased with decreasing speed. This could be so powerful that full forward trim was required to balance the effect. Even with this reversal of stick force no adverse effect control was noticed and it was possible to fly the glider inside the speed range from stick reversal to the stall.

Another problem sometimes encountered during takeoff, besides the lack of pitching moment to raise the nose wheel off the ground, was how easily some configurations would rise off during the takeoff, followed by a loss of lift, which might bring the aircraft down again. Kronfeld[12] in reporting on the flying and handling qualities of the GAL 56 glider states that when the elevons were deflected upwards in order to give a climbing attitude two effects were felt: 1) there was a loss of lift due to the upward deflection and 2) the pitching moment made the aircraft assume the desired new attitude therefore increasing lift.

How much and how long the loss of lift due to the upward deflection is felt, before the increase of lift due to the pitching moment counteracts, makes this phenomenon more or less important. Although in theory these two effects are expected to be small, in the case of the GAL 56 aircraft it nearly resulted in a serious accident. The solution was for the pilot to hold the glider on the ground until the speed increased to a certain value, instead of letting the glider fly itself off the ground. After a certain speed was reached, the pilot would pull the stick back rather decidedly, until the right attitude was reached. This might increase the takeoff run but improved the takeoff handling qualities.

1.3.1.2 Power effects

In his investigation, Donlan[12] also refers to the effects of power on tailless configurations: in the same way as for conventional aircraft, the further above the centre of gravity the thrust line passes, the greater is the stabilizing effect produced by a given thrust; and the further below the centre of gravity the thrust line passes, the greater are the changes in trim due to the thrust that accompany changes in power.

Another contributing item to the longitudinal stability characteristics is the propeller slipstream, particularly for tractor arrangements, since the location of the aerodynamic centre of the portion of the wing immersed in the slipstream is the controlling factor. If the aerodynamic centre of this portion of the wing is behind the centre of gravity of the aircraft, the slipstream produces a stabilizing effect. If the aerodynamic centre of this portion of the wing is ahead of the centre of gravity, the slipstream produces a destabilizing effect.

1.3.1.3 Lateral-directional stability problems

A main lateral-directional problem of tailless aircraft is the difficulty of achieving reasonable values of directional static stability, C_{n_β}, especially if the vertical surfaces are reduced in size or do not exist at all. At this respect, Donlan[12] suggested that a tailless aircraft of very low directional stability with fixed controls could be flown satisfactorily if an automatic pilot were geared to the directional control.

Northrop[6] comments further that the sweptback wing has inherent directional stability which increases with increasing lift coefficient. Furthermore, if wing tip fins are chosen these will be unsatisfactory at the stall. In the Northrop XB-35 the effective fin area for directional stability was given by the side force derivative of the pusher propellers. The later jet-version, Northrop YB-49, was equipped with four vertical stabilizers and associated fences to compensate for the non-existence of propeller effect. Further, for special occasions when particular steadiness was required, damping in yaw was supplied in the Northrop XB-35 by simultaneously opening both rudders, temporarily increasing the drag at the wing tips.

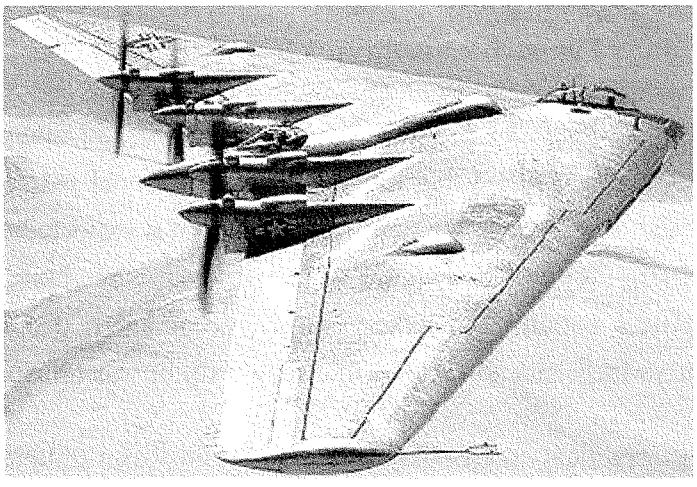

Figure 1.4 Northrop XB-35 (Ref. W6)

A related problem is that of limited rudder control. As for conventional aircraft, rudder control is necessary to counteract the adverse yaw occurring during rolling manoeuvres and to provide sufficient directional control to trim the aircraft directionally at operation under asymmetric power conditions. A first solution suggested by Donlan[12] to this problem is a good design, i.e., reduce rudder control requirements by locating the thrust lines as close as possible to the centre line and provide ailerons that create favourable yawing moments when deflected.

In common with longitudinal controls, conventional directional controls based on lift generation suffer from the small moment arm and may not be high enough. Moreover, the appreciable side-force generated needs to be compensated with higher sideslip and bank angle. Instead, rudders based on drag principles utilizing a double split flap, brake flap, are suggested. However, it is also commented that such rudders may generate undesirable rolling moments, and the drag increments may be large enough to affect the performance of the aircraft.

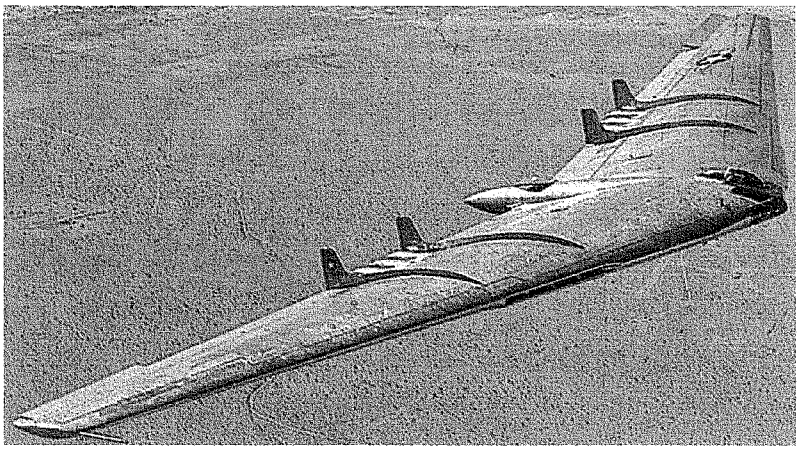

Figure 1.5 Northrop YB-49 (Ref. W7)

Northrop[6] investigated several rudder configurations that had many adverse effects and were not effective. He stated that the normal conventional yaw controls were not considered, only the drag-producing type, since it was not expected to affect pitch or roll, and that the drag they produce would be unimportant when being used, mainly in an asymmetric power condition. Further, Sears[9] commented that the drag penalty resulting from rather large sideslip angles in cruising flight was unusually small.

The best and most practical rudder that Northrop found was a double-split flap at the wing tip which was found to have the most satisfactory all-round characteristics, allowing to combine trim flap and rudder in the same portion of the wing trailing-edge, but it had low effectiveness at low angles of rudder deflection. Northrop[6] also commented that the Northrop XB-35 had no problems of landing with asymmetrical power. Begin[22] describes alternative rudder controls for other Northrop creations such as the XP-56 Black Bullet, which included rudders or split surfaces at the wing tips operated by airflow through special wing tip bellows.

The requirements of lateral static stability are not an issue as long as adequate dihedral is designed for lateral control and steadiness in gusty air, taking into account that the effect of sweepback is to increase the effective dihedral with angle of attack.

In this respect, Northrop[6] stated that C_{l_β} increases quite rapidly with lift coefficient, which gives problems only when its value becomes too large.

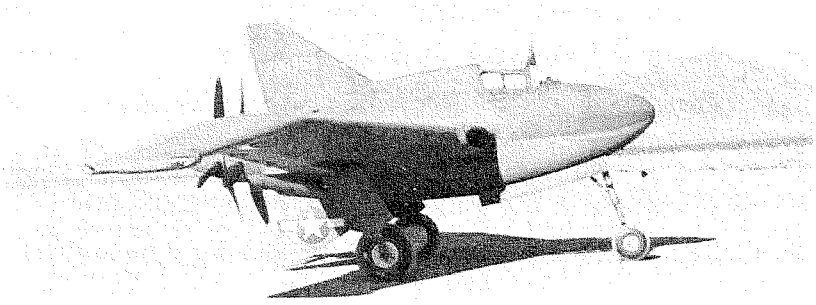

Figure 1.6 Northrop XP-56, Black Bullet (Ref. W7)

The aileron control problems for tailless configurations are the same as for conventional aircraft. However, particular attention to adverse aileron yaw effects should be paid, especially if the directional stability is low. Donlan[12] suggests that adverse aileron yaw moments can be minimized by "up rigging" both ailerons or by utilizing "rotable" wing tips. It can also be advantageous to employ a spring connection between the aileron and rudder to overcome the effects of adverse yaw as suggested by Jones[7]. Furthermore, Northrop[6] comments that if aileron and elevator are put together as elevons, the upward elevator deflection for trim makes the adverse yaw due to aileron deflection disappear. However, further problems may arise if aileron and elevator are combined. Actually, the total effective deflection range for an elevon must be the sum of the ranges required for the aileron and elevator. Large full deflections of elevon for aileron and pitch control may produce high pitching moments and rather small rolling moments, or vice-versa, due to the elevon stall.

Thorpe and Curtis[23] present the probable effect on lateral stability behaviour when changing from conventional to tailless aircraft types. The essential tailless features are represented by large reductions in the absolute values of the derivatives C_{y_β}, C_{n_β} and C_{n_r}. The conclusions of this work are presented in Table 1.1.

Derivative value	**Induces:**
Small $-C_{l_\beta}$	Spiral instability at high speeds
Large $-C_{l_\beta}$	Dutch roll instability at high speeds. Asks for a small C_{l_β} or high C_{n_β} and C_{y_β} values
Large C_{n_r} and C_{y_β}	Spiral instability at low than higher speeds
Small C_{n_r} and C_{y_β}	Dutch roll instability at higher than low speeds. Asks for a small C_{l_β}

Table 1.1 Thorpe and Curtis[23] study results

Shepperd[24] studied the effect of decreasing in 36% the fin and rudder sizes on the GAL 56 glider. He found that the dutch roll and spiral modes were the ones more affected by this reduction. While the spiral mode time constant increases or become slightly unstable, the dutch roll mode frequency and damping decrease. Moreover, Paul and Garrard[25] investigated the reduction of the F-16 vertical tail size in 20%. In the same way they concluded that as the tail size decrease the rudders become ineffective, the dutch roll mode becomes unstable and the spiral mode combines with the roll mode at low speeds (and high angles of attack), and becomes unstable at higher speeds (and low angles of attack).

Northrop[6] states that the dutch-roll oscillation is more critical for tailless types particularly at low speed, high weight and high altitude. This is because of the combination of relatively large effective dihedral, C_{l_β}, and low weathercock stability, C_{n_β} and, under certain conditions specified, is likely to approach neutral damping in the dutch roll mode. In the design of a tailless model, Esteban[26] found that without vertical surfaces the lateral-directional motion would be unstable. Once the winglets were incorporated in the design, the dutch roll mode was stabilised, although the spiral mode would become unstable. Northrop[6] suggests that because of relatively low weathercock stability, the dutch roll is of a rather long period. It is usually assumed that for periods of such length, it is not important to have a high rate of damping since control would seem easily "inside" the motion. However, this may not be true when the rudder is particularly weak, as the time of response to rudder control may be of the same order as the period of the dutch roll motion. This makes directional control extremely difficult in a condition such as landing, where the roll controls are not usable for changing heading.

Northrop[6] points out the low value of the damping coefficient in yaw, C_{n_r}, as another factor contributing to the relative lack of damping in dutch roll motion. Donlan[12] comments that in the same way as for the pitch damping effect on the longitudinal motion, although the rotation damping, C_{n_r} is invariably low due to the reduction of the tail length, the damping of the lateral oscillations is generally greater than would be indicated from only the damping value due to the yawing velocity, this within the usual limits of dihedral and directional stability. Northrop[6] however, comments that for the very low weathercock stability commonly encountered in all-wing aircraft, the conventional solution of increasing weathercock stability to offset increased dihedral does not hold. Increasing C_{n_r} leaves the damping essentially untouched but reduces the period and increases the number of cycles required to damp.

Tailless types seem slightly rougher in turbulent air than conventional types of similar weight due chiefly to the reduced wing loading. However high effective dihedral and low weathercock stability may also have an added effect. Then, Northrop[6] comments that although increasing the weathercock stability has a slight effect on the damping rates, it affects the amplitudes of response to gusts materially. On the other hand, increasing the side force derivative, C_{y_β}, improves the dutch roll damping very much, although it has virtually no effect on amplitude of the response to gusts.

Donlan[12] comments that the damping of the lateral oscillations is likely to be critical at the high-speed conditions because both C_{n_r} and the coupling between yawing and rolling motion tend to diminish at the low angles of attack. Also, associated with the low values of C_{n_r} is some apprehension that large angles of sideslip may develop when the aircraft is subjected to a disturbance of the type produced by asymmetric loss of thrust. Donlan comments that from some wind tunnel tests the effect of C_{n_r} may probably be secondary to other parameters. He adds furthermore that the maximum amplitude of the sideslip oscillation is influenced markedly by the rolling moment due to the sideslip, C_{l_β}, and particularly by the yawing moment due to the sideslip, C_{n_β}. Increasing either the directional stability or the dihedral reduces the magnitude of the sideslip generated by a yawing moment, but the greatest reduction of sideslip appears to result from increasing the directional stability.

Northrop[6] commented also that all-wing aeroplanes, particularly those without fins, have "a very low crosswind derivative". Thus a low side force results from side slipping motion. Some crosswind force is important for precision flight, because with low side force it becomes difficult to judge when sideslip is taking place, as the angle of bank necessary to sustain a steady side slipping motion is small. A sideslip meter may be provided for precision flight. For a very long-range aircraft there is a valuable compensating advantage in being able to fly under conditions of asymmetrical power without appreciable increase in drag.

About spinning characteristics, both Donlan[12] and Northrop[6] agree that steady-spin characteristics are equal to those of conventional aircraft. Donlan[12] says further that the controls required to recover, however, have been found to depend on the type and location of the control surface employed. He goes on to say that rudder controls on vertical tails located at the rear of a fuselage would have the same behaviour as conventional, but on the rear of a wing it would probably be ineffective. If the vertical tails could be located at the wing tips, then it would be effective for spin recovery, particularly if the rudder surface extends below the wing. For tailless aircraft without a fuselage, spin-recovery is more successful by application of rolling moments against

the spin. Drag-rudders were not found very successful, as being able to produce pro-spin rolling moments. The general conclusion was that an investigation should be made for different rudder controls and tailless aircraft designs. On the other hand, Northrop referring to a Northrop N-9M accident probably caused by a spin, says that investigations made have revealed that recovery requires aileron rather then elevator action, and that the spin parachutes were ineffective, both wrongly sized and located. The Northrop XP-79B was another all-wing aircraft that crashed in a spin and it is thought that the pilot was probably overloaded with the stick forces to maintain straight flight, or then some control failed.

The fact that the lateral resistance associated with tailless aircraft is low may preclude the possibility of making flat turns with the rudder alone. It is believed that if the tailless aircraft possesses the same directional stability and dihedral characteristics as are demanded for conventional airplanes, the controlled motions during the normal accelerated manoeuvres should not differ appreciably from those of the conventional aircraft. Kronfeld[20] reported that with the GAL 56, turns with rudder only were satisfactory and that in straight flight a wing could be brought up when dropped with the use of the rudder only.

In view of the likelihood that successful tailless aircraft designs may yet have lower directional stability than conventional aircrafts, the effect of adverse aileron yaw on the handling qualities may be more pronounced. In such cases a spring connection between the aileron and a trimming tab on the rudder may be necessary to satisfy the criterion given by inequality (1.1). Such an arrangement should improve the steadiness of flight.

$$\frac{C_{n_\beta}}{C_{l_\beta}} > \frac{C_{n_\xi}}{C_{l_\xi}} < \frac{C_{n_r}}{C_{l_r}} \tag{1.1}$$

1.3.2 Modern tailless aircraft

From all tailless configurations presented in Castro[5], the Space Shuttle and the Concorde are the ones that approach more closely to large transport aircraft, although both were made for higher speeds. Thus, a close look to these two configurations is desirable. Lastly, the Northrop-Grumman B-2 is also presented, since it is the military equivalent of the blended-wing-body configuration.

1.3.2.1 Concorde

The British Aircraft Corporation/Aerospatiale Concorde is a supersonic and the first fly-by-wire (FBW) civil passenger carrying transport aircraft. Four Rolls Royce/Snecma Olympus 593 turbojet engines power it, each rated at 38,050 lb static thrust with 17% afterburning, under slung at the rear of its delta wing. It has a range of approximately 3500 nm and cruises at Mach 2.02, has a crew of 3 and carries around 100 passengers with a maximum takeoff weight of 408,000 lbs. The Concorde prototype first flew in March 1969 entering service in January 1976 simultaneously in Great Britain and France.

The particular feature of Concorde, besides that of being a tailless supersonic commercial aircraft, is that of having fly-by-wire primary controls. Pitch and roll control are via three elevons on each of the trailing edges of the delta wing. Directional control is by the two-section rudder. The middle and outer elevons are always synchronised, however deflection of the inner elevons for roll control is less than that of the middle and outer elevons. Full deflection of the inner elevons is only achieved in response to pitch commands, while full deflection of the middle and outer elevons is only achieved in response to roll commands. The cockpit controls actuate three signal channels, two electrical (analogue) and one mechanical that send signals to the Powered Flying Control Unit servos on each control surface. The electrical channels are the primary mode with the mechanical back-up channel unclutched at the servos when either electrical channel is operating.

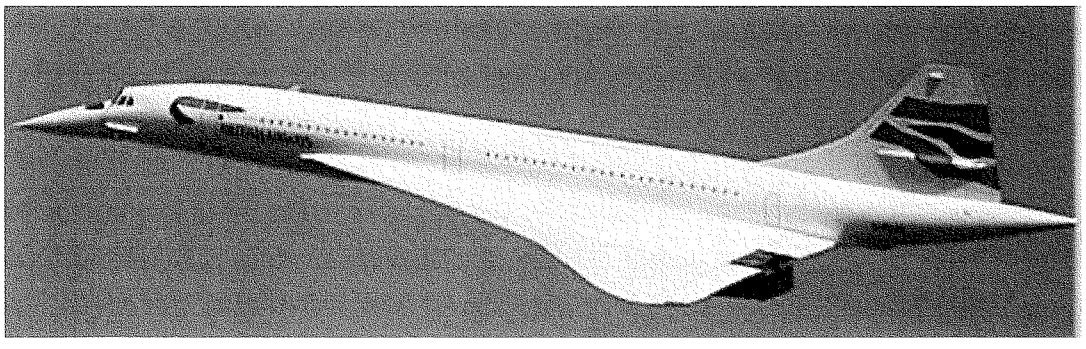

Figure 1.7 BAC/Aerospatiale Concorde (Ref. W8)

Various flight conditions dependent on trim functions, including Mach, incidence and speed trims, feed the hydraulic artificial feel units. These protect the aircraft against excessive aerodynamic loads induced by the pilot through over control. Pitch trim is available via thumb switches on the control yoke. The trim inputs cancel the load of the artificial feel system by changing the feel datum and neutral position of flight controls. The aircraft has no high lift devices or airbrakes/lift spoilers. The fuel

system consists of twelve tanks in the wing and one located in the very rear tail cone to manage the *cg* shift. From takeoff to cruise the *cg* must be shifted aft about seven feet to minimize trim drag, being adjusted during cruise to trim the elevons to zero deflection. For return to subsonic flight transfer from the rear tank is used to accomplish the return to the landing forward *cg*.

The high speed outer windshield retracts into the nose for subsonic low altitude flight. The nose tilts down to 5 degrees for takeoff and 15 degrees when landing for pilot visibility. The nose and high speed windshield is operated hydraulically, but will free fall to the landing position if power is lost.

Although a FBW system was present, no especial use of it was made to improve the flying and handling qualities of the aircraft. This was so mainly because of the mechanical backup and thus the necessity to give the same characteristics to the aircraft as if the FBW were not present.

1.3.2.2 Space Shuttle

The Space Shuttle Orbiter is an early example of a digital fly-by-wire aircraft. However, in this spacecraft there is no mechanical connection between the control stick and the control surfaces. The Shuttle control system was designed in the early 1970's, and although not representing the latest thinking in control system design, it was still a very forward-looking design. A digital control system was made necessary by the wide variety of tasks and flight conditions to be handled by the Shuttle, including launch, on-orbit phases, re-entry, and landing. Some unusual features of the system follow next.

Firstly, during the entry phase of the flight, the control system must rely completely on data from the inertial navigation system, because no air data is available in the hypersonic speed range. The angle of attack during entry is so high that the vertical tail and rudder have no effectiveness. As a result, yaw jets are used in conjunction with the elevons to provide lateral control. Also, during this phase of the flight, the elevons provide more adverse yaw than rolling moments. Therefore, the elevons are used in a reverse direction to yaw the vehicle, in order that the dihedral effect will supply the desirable rolling moments. Later in the entry, the elevon motion for lateral control is reversed so that the elevons assume their normal function of rolling the aeroplane. In normal operations, the only phase of the flight in which flying qualities are important is the approach and landing beginning at 40,000 ft, since before that all is done automatically.

Although it is generally assumed that stability augmentation can solve practically any stability and control problem caused by aerodynamic characteristics of the vehicle, the main conclusion from the Shuttle experience is that not all aerodynamic problems can be solved in this way. The main problem with the Orbiter is that when the elevons are deflected to produce a change in the flight path angle they produce a lift force, which initially causes the flight path to move in the incorrect direction.

1.3.2.3 Northrop-Grumman B-2 Spirit

The Northrop-Grumman B-2 idea was born in 1981 in a program to modernise the American air forces. The reasons for the choice of the B-2 shape were on the aircraft requirements, actually those to evade the enemy defences without being detected (stealth), maximise range while minimizing fuel consumption, and the delivery of large payloads. The supporters of this shape defended that in aerodynamic terms efficiency could be increased dramatically, in structural terms the flying wing concept provided a more uniform distribution of the load, and flying wings possess a low radar signature and low visibility profile, presenting thus the best qualities for the role.

Although there was the knowledge that flying wing designs lack directional stability and have less than desirable directional control, it was believed that with a feedback control system and modern fly-by-wire technology, good flying qualities could be achievable. Couch and Hinds[32] emphasize that flight control is really the key to eliminate the control difficulties which other flying wing designs have had. The B-2 flight control system is a quadruple-redundant fly-by-wire system that has angle of attack limiting. As a safety feature for generic software faults, it has simplified control laws that backup the primary control laws. The B-2 basic aerodynamic directional stability is nearly neutral, but with the yaw feedback system and its mechanization within the flight control system, it exhibits very positive weathercock stability.

A planform view of the aircraft shows that very large portions of the entire trailing edge are control surfaces: three large elevons for pitch and roll control, large drag rudders for directional control, and a centreline surface for gustload alleviation. Elevon utilization varies over the flight envelope and the rudders provide both directional and speed control. The rudders affect yaw by operating asymmetrically and when speedbrakes deploy, both rudders open symmetrically. The quadruple-redundant fly-by-wire FCS provides stability and control augmentation, trim control, *cg* and weight data computation, flight control master modes, multipurpose display unit interface, nose wheel steering, and FCS warnings, cautions, and advisories.

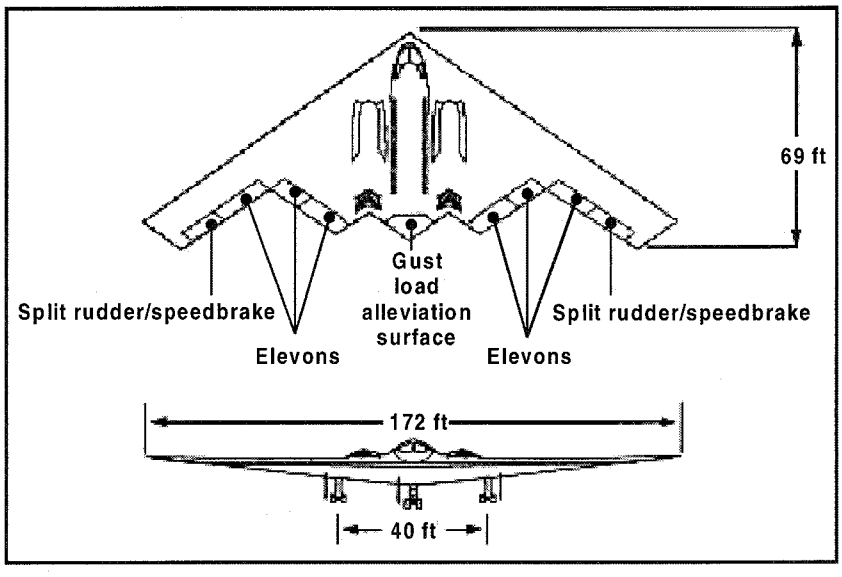

Figure 1.8 Northrop-Grumman B-2 Spirit (Ref. 34)

The B-2A FCS control laws are complex and variable, depending on aircraft mode and flight condition. In all modes, except power approach/takeoff mode and some failure modes, the control system has a proportional plus integral (PPI) architecture that uses normal acceleration and pitch rate as the primary feedback variables. In power approach/takeoff mode the system uses proportional feedback only, using AOA and pitch rate as primary feedback variables. Laterally, feedback includes sideslip angle, bank angle and roll rate. Directional feedback includes sideslip angle, bank angle, and yaw rate. Gains are scheduled with FCS mode, air data system health, autopilot mode, dynamic pressure, pressure altitude, airspeed or Mach number, *cg*, weapon bay door position, and gear position.

In general, the B-2 has Level 1 flying qualities throughout the envelope. The airplane is very stable, yet very responsive in pitch. Roll performance is as designed, and roll control is crisp and predictable. The airplane is very tight directionally and the flight control system keeps the airplane pointed where it is going. Since the B-2 is totally a fly-by-wire aircraft, the software dictates primarily its flight characteristics. At times, it was underestimated how differently the aircraft would behave with new flight control software even well after the aerodynamic performance of the basic airframe was understood.

1.4 Recent large civil transport aircraft

A new transport aircraft would necessarily present an evolution and technology step forward from the aircraft flying today. Thus, it is important to know what are the main

advantages and pitfalls of the most recent advanced large civil transport aircraft, so to apply or avoid in the new configuration.

1.4.1 Airbus A320 and A340

The Airbus A320 was the first civil transport aircraft to fully use the fly-by-wire technology. Previously fly-by-wire fighters had been constructed and flown successfully, opening the way to the transport aircraft. Although many advantages can arrive by using fly-by-wire technology, this use also brings new questions and problems to solve. The possibility of having tailored flying and handling qualities is one example of an advantage. However, with so many response-types to choose from, the question "what is the best for the civil role?" arises.

Another change that arose with fly-by-wire technology is the fact that analogue flight deck instruments could be substituted for simple flat screens to present information. However, the management of the information presented, the cockpit disposition and the cue channels used, representative of the "secondary" flying and handling qualities, may become a problem. But as shown later although still important, these are not crucial for the acceptability of the aircraft.

Some of the Aerospatiale experience in electrical flight control systems gained with the Concorde project: the use of simulation, both ground-based and in flight, has largely contributed to the success of the development process. Thus, the first production Concorde was fitted with a side-stick by the left-hand seat and with a C* type control. This confirmed the very good acceptability of "flying through a side-stick" in all flight phases as well as the advantages of the C* type control law for precise flight path control, autotrim and behaviour in turbulence. Taking advantage of the possibility of tailored flying qualities, the engineers of Airbus implemented a C* control law which exhibits rate command characteristics, but it is modified in the flare by a pitch attitude command law which memorises the pitch attitude at 50ft above the ground and subsequently decreases the attitude by a fixed amount over a period of 8 sec starting at 30ft to provide a more "natural" flare characteristic.

For the lateral motion a roll rate command with bank angle stability up to 33 deg of bank was implemented. Thus, zero stick deflection demands zero roll rate and no change in bank angle, while an increasing stick deflection causes an increasing amount of roll rate to be selected. The bank angle stability allows the bank angle to be maintained without control inputs being required for bank angles up to 33 deg.

Beyond that angle, and up to a limiting value of 67 deg of bank, increasing amounts of control deflection are required to be held by the pilot.

Concluding, the response of the aircraft is no more than that of a classical aeroplane, having instead unconventional characteristics. At first it seemed that these new differences were good news and a change for better. However, once the A320 entered service and a variety of pilots flew them, problems became more apparent. In the flare, although the change of control law to pitch attitude command reduces the floating tendency of the rate command law, there are still no-monotonic forces present, which pilots did not like. Moreover, the A320 C* law exhibits neutral static stability and therefore there is no need for the pilot to trim. The drawback is that there is no tactile airspeed feedback to the pilot, therefore requiring considerable low speed envelope protection. The poor airspeed/thrust control and monitoring when in manual control may be overcome with the very useful Speed Trend Vector, a dominant instrument in all phases of flight for the A320, or by the use of automatic throttle.

However, the use of auto-throttle with static throttle levers, i.e., with no throttle motion when in the automatic motion, thus no feedback of what the aircraft is doing, together with the side-sticks not being linked to each other, and so the pilot which is not flying can only recognize what the other is doing by the aircraft response, gave rise to another problem. Actually, the minimization of tactile and peripheral visual cues, and an overloading of the visual channels resulted in lower situational awareness when taking command from the automatic system or from the flying pilot. Thus, the pilot has to adopt a more open-loop control, reflecting the changing role of the pilot in the fly-by-wire Airbus more to that of a "flight manager" than a conventional pilot. While here it is not aimed to judge whether this is desirable or undesirable, it certainly requires some degree of pilot teaching for him to behave in this role.

The Airbus A340 general design objective was to reproduce the architecture and principles chosen for the Airbus A320 as much as possible for the sake of commonality and efficiency, but taking into account the Airbus A340 differences (long-range four-engine aircraft), as well as the A320 in-service experience. Thus, the Aerospatiale innovation efforts concentrated on system integration and methodology improvements in the FCS, control law and software design. Thus, the next Airbus, the A330/340, used feedback of ground speed to restore speed stability and monotonic stick forces during the flare.

The general philosophy of the flight control laws design of the A320 was maintained, adapted to the aircraft characteristics and used to optimise the aircraft performance such as; the angle of attack protection which was reinforced, the dutch roll damping system, which was designed to survive rudder command blocking, the takeoff performance was optimised by designing a specific law that controls the aircraft pitch attitude during rotation and the flexibility of fly-by-wire was used to optimise the V_{MCG} speeds. Rudder efficiency was increased on the ground by fully and asymmetrically deploying the inner and outer ailerons on the side of the pedal action as a function of the rudder travel - the inner aileron is commanded downwards and the outer aileron, complemented by one spoiler, is commanded upwards.

1.4.2 Boeing B777

The Boeing B777 is another advanced fly-by-wire civil transport aircraft that used the lessons learnt with the Airbus A320 aircraft to implement an improved but "conventional" fly-by-wire aircraft. For that, the first approach taken was to retain the cockpit layout similar to that of a conventional aircraft by maintaining the conventional wheel/column. Besides, the approach was taken to tailor flying and handling qualities to appear almost identical to those of conventional aircraft by exhibiting a positive static stability. This without doubt reduces crew training and helps to improve aircraft ratings by manufacturers since all aircraft types are kept similar.

Boeing also opted for moving throttles, giving visual indication when the system adjusts power, and for linked control wheels that gives information of what the autopilot, or the flying pilot is doing thereby increasing the situational awareness of the pilots. Moreover, the computers warn pilots when they are flying too fast or slow, or when they are overbanking, giving additional audible cues instead of limiting the pilot's ability to override the fly-by-wire computer as protection.

During the B-7J7 development, the forerunner of the B777, a flight path rate/flight path angle hold command control system was adopted as the control law. The pilot commands a selected flight path angle on his display and the aircraft pitchs and adjusts power accordingly with a resultant low workload, but still enabling "pilot-in-the-loop" control. This control law revealed that uncommanded motions were quite natural and that ride qualities in turbulence were excellent without the need for pilot inputs. There was also no need for trim inputs to compensate for flap or gear deployment. However, PIO tendencies were revealed during in-flight tests, as

reported by Sankrithi and Bryant[39]. Instead, Boeing adopted for its Boeing B777 a C*U flight control law which utilises C* flight path control law with an airspeed feedback to give column forces to the pilot and speed stability. Configuration and power changes do not alter flight path and so require no trim change. A linear pitch down command schedule based on radio height was studied for a flare law, although flare with only the C*U control law was also easily managed.

Technically, the fly-by-wire system is in the direct column to elevator mode during takeoff. It then transitions to the C* manoeuvre demand control law where the computer delivers the pitch rate or "g" commanded by the pilot when he moves the control column. This is the case regardless of what else is happening as long as speed remains constant. Thus the computer may command elevator movement to compensate for wind, turbulence or a change in thrust without moving the control column. The B777 roll control surfaces are directed by wheel movement, rather than on a manoeuvre demand-basis. Nevertheless, the B777 is quite agile for a heavy transport providing rapid roll rates of up to 20 deg/sec for evasive manoeuvring.

The B777 first flew in June 1994, undergoing flight testing until March of 1996, when it was ready to enter service. A pilot new to the aircraft encountered a PIO during the de-rotation after landing early in the program. Other lesser PIO tendencies were seen on mode transitions from autopilot overrides and mis-trim takeoffs with large and rapid elevator input, all of which the flying pilot stopped on his own.

Thus, all problems were fixed quickly with software changes and flight tests specially directed to PIO's were made, which included mode transitions with failures and autopilot overrides in high gain tasks, formation flying tasks including simulated air refuelling, in air and on ground attitude tracking tasks following high rate commands and other high gain tasks, such as landing offsets, abused landings, windup turns or approach path tracking in turbulence. The B777 is in-service for some time now, and similar to the Airbus experience, this in-service time will bring the comments of a wide variety of pilots on the acceptance of the aircraft.

1.5 Lessons learned

The tailless aircraft has been introduced. Its classification inside the aircraft category, its history throughout time and its main problems. Although there are still numerous tailless aircraft examples, one can ask why they have never really succeeded the more common conventional tailed ones. The answer may be because the problems inherent

to this kind of configuration have never been truly understood or suitable technology was never available.

Nevertheless, some tailless aircraft have proved very successful in the role for which they were designed, as some fighters, the Concorde, the Space Shuttle and the B-2. Moreover, these aircraft possessed particular characteristics that made them the best configuration for their role, in spite of the tailless aircraft drawbacks. Examples are the delta shape for supersonic flight in the Concorde and some fighters, and for hypersonic flight in the Space Shuttle case, or the low radar signature and wing load in the B-2 case. Today, the characteristic that points to the blended-wing-body as the best configuration for the transport role is the requirement for a large span configuration, taking into account the advantage of the low wing load, span loader, characteristic of the configuration. However, for this concept to become a success the problems inherent to this configuration have to be addressed and solved.

Problems common to tailless aircraft types were reviewed and presented here. Some, if not all, of these are expected in the BWB configuration. However, technology has advanced enough to overcome most of the problems presented, which in the Northrop XB-35 time seemed impossible to solve. In longitudinal motion, instability is no longer a problem, being used as a requirement for many current fighter aircraft. Although a fully unstable aircraft so far has never been flown in the civil transport category, relaxed stability has been used for some time, as well as the reliance on fully flight-computed systems, in the recent fly-by-wire aircraft.

Thus, a natural next step for civil transport aircraft is to evolve into neutral or even unstable configurations, as the confidence in fly-by-wire systems increases. This will enable the solution of many tailless aircraft drawbacks, such as the loss of maximum trimmed lift, low phugoid and short period damping and inherent instability. Through the use of widely known *Computational Fluid Dynamic* (CFD) tools and careful aerodynamic design, stall and pitching moment characteristics can be designed to an optimum, and so solve these tailless problems as well. A last requirement is the careful control power design, since without sufficient control power no control system is able to perform its tasks.

From the aforementioned it seems that success will be easy. However, there is still the lateral-directional motion to be analysed, which has often been overlooked. This, together with inherent lateral-directional problems of tailless aircraft types, may make this motion a lot more critical than the longitudinal. Nevertheless, it is believed that

with the advances in stability augmentation reached so far, as long as enough control power is available, it will be possible to overcome these problems too.

Lastly, the problems raised by the present fly-by-wire transport aircraft need to be mentioned. Actually, the fact that fly-by-wire allows for tailored flying and handling qualities, although, so far, it is still not well understood how this tailoring can be achieved.

1.6 Thesis objectives

Thus, this research project aims to:

- Understand the basic longitudinal and lateral-directional static stability characteristics of the BWB aircraft configuration.
- Assemble a representative mathematical model of the BWB aircraft.
- Develop and validate computer simulation models of the BWB aircraft for flight dynamics analysis.
- Develop a basic understanding of the tailless blended-wing-body flight dynamics by implementation of the equations of motion and the assessment of its handling and flying qualities.
- Develop a flight control system in order to ensure satisfactory stability and flying and handling qualities.
- Verify whether the present criteria and requirements, as defined for conventional aircraft for use in handling and flying qualities assessments, as well as in flight control systems design, are adequate for the blended-wing-body configuration.
- Undertake limited piloted simulation trials to assess flying qualities of a BWB configuration.

CHAPTER 2
Flying and handling qualities review

"...Flying and handling qualities of an aeroplane are those properties which describe the ease and effectiveness with which it responds and the pilot is able to perform the tasks required in support of an aircraft role."

G.E. Cooper and R.P. Harper, 1969

2.1 Overview

Flying and handling qualities are difficult to define: they represent an overall measure of the vehicle's acceptability and suitability for safe and efficient control by the pilot, and ultimately they are assessed by the pilot in a wholly subjective manner. Bisgood[41] goes further when considering "primary" and "secondary" flying and handling qualities. The former is related to the basic stability and response characteristics of the aircraft and control systems, primary characteristics in defining the aircraft acceptability for a mission or role. The latter is related to the fields of view, instrument position, cockpit layout, etc, which although not determining in the acceptance of an aircraft, still play an important role in the pilots comfort.

The subjective advantages of good flying qualities cannot be overstressed. Field[30] reveals that between 1960 and 1990 around 50% of jet transport accidents were attributed to primary flight crew errors and occurred in the presence of adverse weather conditions. Around half were during the touchdown and landing roll-out. Thus, a very high priority should be given to design aircraft with good flying qualities, especially in the presence of adverse weather, which is when poor flying and handling qualities may be fatally revealed. Since good flying and handling qualities are so important, it is not acceptable that these qualities are evaluated only at

the end of the project to discover at once that the flying and handling qualities are inappropriate, all work done so far is wrong and changes required will be of immeasurable cost. Thus, since the beginning of aviation flying and handling qualities are estimated during design through known quantities such as stability and control characteristics, i.e. basic aircraft flight dynamics, an approach that has worked well for the classical aircraft.

However, the increasing speed, performance improvements and expansion of the flight envelope saw the introduction of new technology such as power boosted systems, stability augmentation systems, irreversible control systems, feel systems, etc. In this scenario, the flying and handling qualities are also affected by the dynamics of these technologies and their relationships are no longer simple. Lastly, in a fly-by-wire aircraft and in the era of superaugmentation, the trend is for flying and handling qualities to be defined almost entirely by the flight control system with little interference from the basic aircraft flight dynamics.

The introduction of fly-by-wire technology allows for aircraft with excellent flying qualities in all flight phases. However, the tailoring of flying and handling qualities requires clear and adequate criteria. This seems to be not completely present in the military standard, MIL-STD-1797[48], although quoted mainly in flying and handling qualities terms. However, the civil requirements, JAR[50] and FAR[51], do not even refer to the flying and handling qualities field explicitly at all.

Therefore, the trend in the civil transport aircraft industry has been for manufacturers to produce aircraft with a wide range of different flying qualities due mainly to the fairly loose constraints that the civil requirements impose. The operators then have to learn how to fly each type, incorporating many operational procedures to overcome deficiencies in their inherent flying qualities. With the introduction of fly-by-wire technology this situation will not be much different if the requirements do not change accordingly. The Airbus A320 and Boeing B777 mentioned in chapter 1 are typical examples of inappropriate flying qualities requirements.

2.2 Flying and handling qualities requirements

Phillips[44] states that in the first years of aviation no formal handling qualities requirements existed yet. There was a lack of understanding of the relation between stability theory and flying qualities, since it was difficult to apply the mathematical theory to practice. Thus, dynamic stability was all important criterion, and so great emphasis was placed on the long period modes since these tended to instability.

Philipps[44] says that in 1935 Edward P. Warner made the first effort to write a set of requirements for satisfactory flying qualities. Ashkenas[45] comments that most of the early requirements were largely based on direct flight experience with experimental, prototype, and production airplanes. Then, this experience was distilled into acceptable or unacceptable characteristics and criteria. Such distillation and correlation of good to unsatisfactory characteristics of existing aircraft is still very used practice nowadays. In 1943 Gilruth[44] published the report "Requirements for satisfactory flying qualities of aeroplanes" based on 16 different aircraft ranging from the light to the largest aircraft at that time. Later in 1948 the number of aircraft tested for flying qualities had elevated to 60, and new information was obtained from almost every additional aircraft studied. Furthermore, Ashkenas[45] adds that the first flying quality requirements reflected the realities of purely manual control systems. Design guidance in these early requirements was mostly on the aircraft geometry. Accordingly, handling quality requirements were used for sizing control surfaces, settling hinge moment parameters, and in establishing *cg* locations.

Philipps[44] goes further saying that after the *World War II* (WWII), the appearance of compressibility effects and the consequent use of sweep, thinner airfoils and devices such as Mach trim compensators, and the introduction of powered flying controls, as well as simple augmentation systems revealed the need for changing requirements. Ashkenas[45] comments that it was when designers started using higher gains and feedbacks other than "natural" ones, they encountered servo response, stability, and coupling problems that were not elementary in terms of old classical design tools. Moreover, additional handling qualities problems were introduced as the short period modes became less stable due to the abilities to fly higher and the interaction of the airframe modes (aeroelasticity) with automatic control systems. On the other hand, the development of systems such as power boosted controls and dampers led to a reduced attention to flying qualities requirements in the design stage in the belief that those systems would solve any deficiency. This idea still persists today.

Therefore, the subject of dynamic stability of aeroplanes and the associated analysis assumed new importance. It was at this time that Laplace-Transform methods were introduced and the use of frequency response methods proved useful for analysis. Variable stability aircraft provided a tool by which a large variety of control characteristics could be studied in a systematic manner, rather than relying on tests of a wide variety of different aircraft to cover a range of characteristics. About 1950, versatile ground based flight simulators became available, which where used to study particular problems involving flying qualities. Also by this time, a better knowledge of the characteristics of the human pilot allowed more accurate predictions of

desirable stability and control characteristics, or at least in explaining flying qualities problems.

Accompanying this evolution military flying qualities specifications were produced. First, in September 1954, the "Flying qualities of piloted airplanes", best known as MIL-F-8785 (ASG), then second the "Military Specification, Flying qualities of piloted airplanes" or MIL-F-8785B (ASG), in August 1969. Later, in November 1980 a new issue of the military specifications was released, the MIL-F-8785C[46]. The latter document followed a military directive to place all military specifications under a same particular format. In this format, quantitative specifications are left blank in the statements of requirements. However, with the help of a backup document totalling more than 700 pages, which present the analysis procedures to be used, the contractor and the procuring agency would negotiate the determination of values and verification procedures for each aircraft.

More recently, investigations and developments in Control Configured Vehicle (CCV), Activity Control Technology (ACT), Command Augmentation Systems (CAS) and currently Superaugmentation enabled exploitation of capabilities such as relaxed static stability, manoeuvre load alleviation, structural mode suppression and gust load alleviation. Digital control systems, and the complete fly-by-wire aircraft are now widely accepted for high-performance aeroplanes. These techniques introduced the capability of providing new flying qualities characteristics, possibly unlike those encountered with conventional control systems. These developments opened up new problems and whole new fields for research.

To take into account the use of high gain, high authority augmentation, and to more directly reflect the requirements of the intended missions into the specifications a new Military Standard was issued. This is best known as MIL-STD-1797[48], issued in March 1987. However, it seemed that MIL-STD-1797A did not completely address the flying and handling qualities problems of the new generation of aircraft and so an update of the last issue to the MIL-STD-1787B was expected to have been published by about 1997, including also Mission Oriented Requirements[49].

Since the publication of Gilruth's original flying-qualities requirements, the civil and military agencies all over the world have followed different procedures for ensuring satisfactory flying qualities of new aeroplanes. In the certification of new airplanes, Federal Aircraft Administration (FAA) in the USA and Joint Aircraft Authority (JAA) in Europe, have stated their requirements in qualitative terms, retaining the flexibility to rule out undesirable characteristics determined by actual flight tests after the

aircraft is flown. Mooij[55] agreed that the civil requirements are essentially qualitative, since their purpose is to ensure safety of operation rather than effectiveness of the "mission". However, a failure to provide good flying qualities may lead to unsafe operations, especially in bad weather and emergency procedures. Fortunately, most of the companies producing civil aircraft are sufficiently familiar with the military handling quality requirements to be able to produce satisfactory aeroplanes for civil purposes.

2.2.1 Civil requirements: FAR's and JAR's - Part 25

As commented above, there is a general feeling among flight dynamicists and flight control designers that the current civil requirements, JARs and FARs, are very sparse compared to their military counterparts, relevant only to conventional aircraft and when employing only limited augmentation. The large aeroplanes category JAR-25[50] and FAR-25[51] are the civil requirements of interest for this thesis. Both documents are very similar, with a numbering corresponding to the same requirements. A summary of the relevant requirements for the design of satisfactory flying and handling qualities is presented in Appendix A.

With the design, construction and operation of aircraft embodying advanced concepts, such as the fly-by-wire technology of the supersonic Concorde, the Airbus A320 and the Boeing B777, the normal requirements had to be modified to take into account these concepts. In the case of Concorde, special requirements were imposed uniquely upon the Concorde[31]. A similar approach was taken for the A320[37]. However, with the Boeing B777 and later airplanes of the Airbus family, it is clear that the fly-by-wire technology became an integral part of the design. Thus, a need for the civil requirements update is urgent.

2.2.2 Military requirements: mission-oriented requirements approach

As Mitchell *et al*[49] defend, the idea of mission-oriented requirements intends to define requirements based on realistic *mission elements* and not in general *flight phases*. Moreover, it should be the aircraft's mission and not its weight that should matter. Therefore, reference or subdivision into aircraft size intends also to be eliminated. About the latter, Mitchell *et al*[49] comment further that in a thoroughly mission-oriented flying qualities specification, aircraft class would not appear at all, but would be inferred by the specific *Mission Task Elements* (MTEs) to be applied.

As an example, if precision tracking is required for a particular new aeroplane, it should be irrelevant whether the aeroplane is to be a light trainer or a heavy transport, the requirement for precision tracking will be the same whatever the size, although it may be more difficult and challenging to achieve good precision tracking qualities with a larger aeroplane.

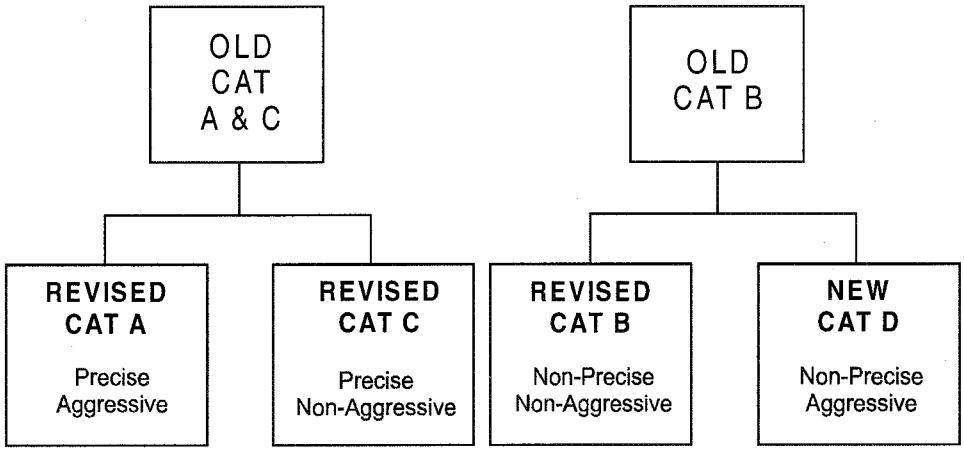

Figure 2.1 New flight phases categories (Ref. 49)

Categorization of Mission-Task-Elements			
Non-Precision Tasks		**Precision Tasks**	
Non-Aggressive (Cat B)	**Aggressive (Cat D)**	**Non-Aggressive (Cat C)**	**Aggressive (Cat A)**
Reconnaissance (RC)	Gross acquisition using loaded roll	Aerial recovery (AR)	Tracking manoeuvring tank (CO)
In-Flight Refuelling – Tanker (RT)	Missile defence using loaded roll	In-flight refuelling – receiver (RR)	Ground attack (GA)
VMC and IMC loiter/cruise/climb/descent, including emergency descent (LO, CR, CL, D, ED, DE)	Anti-submarine search and manoeuvring (AS)	Low altitude parachute extraction (LAPES)	Weapon delivery and launch (WD)
Normal Takeoff	High speed max g turn	Catapult takeoff (CT)	Terrain following
Waveoff/Go-around (WO)	'Herbst' turn	Approach (PA)	"Herbst" turn
Non-precision landing (L)	Split S, chandelle, hammerhead turn, loop, barrel roll, snap roll, etc	Precision Landing	Precision aerobatics, e.g., S point roll, etc.
	Scissors high and low speed "yo-yo"	Close formation (FF)	
		Tactical final approach	

Table 2.1 Grouping of the new mission-task-elements under the new aircraft categories (Ref. 49)

MTEs are specific handling qualities tasks that a mission is subdivided into, so permitting requirements to be written in terms of the task to be accomplished. MTEs are used to make a distinction between criterion boundaries for aircraft with different missions. Further they are also used as *Demonstration Manoeuvres*, and in

combination with the *Usable Cue Environment* (UCE) to determine the proper response type. The new and better defined MTEs are now grouped into four categories, so that requirements for a given category are sufficiently similar so that a single criterion boundary will apply. Figure 2.1 presents the relation between the old A, B and C flight phase categories and the new A, B, C and D categories. Table 2.1 presents the MTEs under each new category. Although the division of aircraft into different weight classes I, II, III and IV is maintained, the requirements dependence on them is eliminated.

2.2.3 Longitudinal response types

Response type is another new concept proposed by Mitchell *et al*[49] to incorporate into the new standard. Response-type refers to the shape of the response to inputs, characterized in either the time domain or frequency domain. It is important to properly match the response type to the mission-task-elements.

RESPONSE TYPEs	ADVANTAGES	DISADVANTAGES
Conventional Aircraft	Well accepted flare characteristics	- Lightly damped phugoid mode - Requires trimming to change airspeed during the approach - Angle-of-attack sensing required – gust sensitivity problems
Rate Command/ Attitude Hold (RCAH)	No trimming required to accomplish airspeed changes during the approach	- Not as desirable for flare - Not Level 1 if $1/T_q < 1/T_{\theta_2}$ - Tendency to float in flare - Tendency for airspeed control problems during the approach (associated with division of attention)
Attitude Command/ Attitude Hold (ACAH)	Highly desirable flare characteristics	- Requires trimming during approach
Flight Path Command/Flight Path Hold	Highly desirable flare characteristics	- Requires trimming during approach - May result in excessive speed bleedoff for unpowered approach windshear - Sensing requirements more complex than for ACAH

Table 2.2 Advantages and disadvantages of response-types for the approach and landing task (Ref. 49)

Table 2.2 presents the advantages and disadvantages of the main response-types for the approach and landing task. An understanding of the strengths, weaknesses and idiosyncrasies of each response-type is essential for a successful design of the flight control system. This is done based on Figure 2.2, which represents the pitch attitude and flight path to stick bode plots, as well the time response plot.

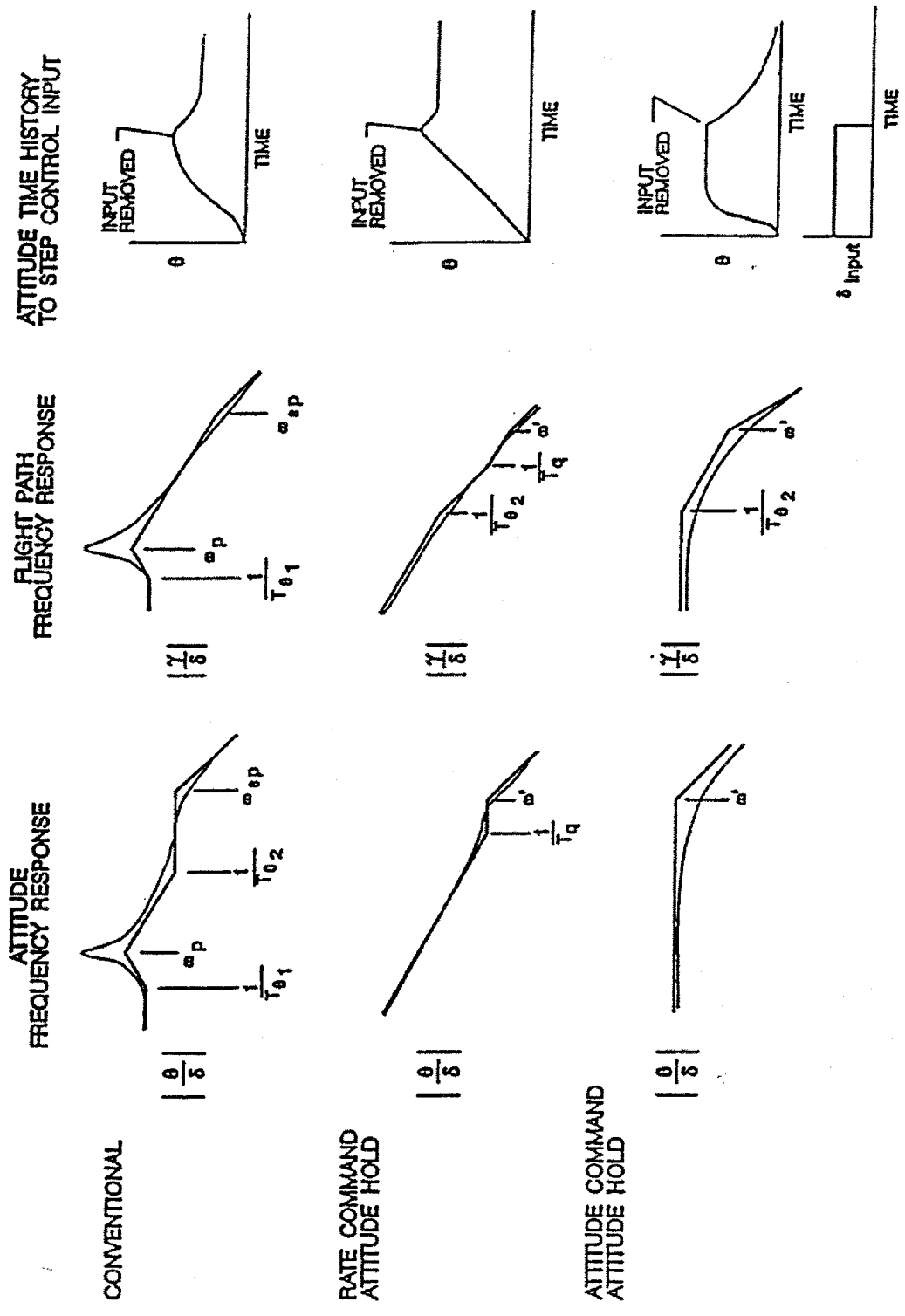

Figure 2.2 Response types characteristics (Ref. 49)

2.2.3.1 Conventional response type

These characteristics are associated with conventional unaugmented airplanes, although it is possible to achieve a conventional response type in an augmented aircraft by feeding back pitch-rate and angle-of-attack, assuming adequate elevator control power. Some important observations that can be made regarding the generic characteristics in terms of the flare and landing task are as follows.

- Short period and phugoid modes are well separated and easily identified. The phugoid mode is typically lightly damped, with an oscillation that occurs at constant angle-of-attack.

- The bode plot of flight path response to longitudinal control inputs is K/s between the phugoid and short period modes.

- The flat region of the θ/δ bode plot between $1/T_{\theta_2}$ and ω_{sp} leads to pitch rate overshoot in the time domain. The longer this region, e.g. when augmenting the short period frequency or decreasing $1/T_{\theta_2}$, the higher the pitch rate overshoot.

- The flight path response lags the attitude response by 90 degrees at frequencies much above $1/T_{\theta_2}$ and is in phase with the attitude response at frequencies much below $1/T_{\theta_2}$. Thus, a low value of $1/T_{\theta_2}$ will lead to a large lag between pitch attitude and flight path.

- Flight path lag (response to stick input) does not exist, i.e., $1/T_{\theta_2}$ does not appear in the γ/δ response.

- The time response of pitch attitude to a step controller input increases monotonically in the short term, and returns to trim when the controller is released.

One problem of conventional response-types in augmented aircraft is that with adequate values of equivalent short-period frequency, it suffers from a lightly damped phugoid mode and excessive response to turbulence and windshear.

2.2.3.2 Rate command/attitude hold (RCAH) response type

This response type usually results from feeding back pitch rate and including an integral term in the pitch-rate loop. The generic characteristics of this response-type are as follows.

- Phugoid dynamics are eliminated
- Attitude numerator is defined by $1/T_q$ instead of $1/T_{\theta_2}$. Thus, the flat region of the attitude-to-stick bode plot is defined by the augmentation zero, $1/T_q$.
- Flight path frequency response is K/s^2 between $1/T_{\theta_2}$ and $1/T_q$, when $1/T_q > 1/T_{\theta_2}$. Since the flare manoeuvre involves control of flight path, it is expected poor flying qualities if $1/T_q$ is much greater than $1/T_{\theta_2}$, since there is introduction of flight path lag. It is important that the pure rate response in pitch is not achieved at the expense of the flight path response.

Time response of pitch attitude increases monotonically to a step controller input, and holds attitude at point of release.

A further comment on this response type is that if $1/T_{\theta_2}$ is low, it may not be possible to obtain a sufficiently high bandwidth with pitch-rate feedback alone, while keeping $1/T_{\theta_2} = 1/T_q$. In such a case, angle-of-attack feedback may be employed to further increase ω', see Figure 2.2, while retaining the conventional response-type. An alternative is to use attitude command/attitude hold (ACAH) response type, as follow.

2.2.3.3 Attitude command/attitude hold (ACAH) response type

Attitude Command/Attitude Hold response type results usually from the feedback of pitch attitude input to elevator. The generic characteristics of this response-type are dramatically different from conventional or RCAH response-types. These are as follows.

- The flight path to stick bode plot has the desired K/s above $1/T_{\theta_2}$ and K below $1/T_{\theta_2}$, or steady flight path change is proportional to controller input with lag defined by $1/T_{\theta_2}$
- Attitude response is proportional to controller input with some lag (defined by ω')

- Time response of pitch attitude to a step controller input is a constant attitude, which returns to trim when input is removed.

Note that this response-type has more phase margin in flight path response to stick at frequencies below $1/T_{\theta_2}$ than RCAH or the Conventional response-types, and hence might be expected to be the best response-type for the approach and landing. However, this ACAH response type is highly dependent upon trim, and therefore the trim system must be carefully optimised. Besides, the very same stability that produces excellent touchdown performance causes problems for an aggressive manoeuvre and excessive phase lag will result in pitch bobbling. This response-type may also require more control power, with consequent rate limiting (if control power is not available) causing pitch bobbling at best and possibly PIO.

2.2.3.4 Flight path angle rate response type

A Flight path angle rate is the last response-type presented here. This response type results from the combination of a flight control system that holds angle of attack constant with pitch, and airspeed constant with an auto-throttle. Although the pitch attitude and flight path response to stick bode plots and time response to step input are not presented, this response type experiences the same touchdown problems as an RCAH response type. It is important either to turn off the auto-throttle prior to flare, or to allow the pilot to override the auto-throttle in the flare.

The response types presented do not limit the possibility of flight control system structure. They are included to allow a distinction to be made between the response shape and the dynamics, and as guidance as to which quantitative criteria to use. Hoh and Mitchell[42] also share this idea that such an input/output definition does not dictate a specific control system architecture, but does provide very specific guidelines for the control law designer.

Mitchell *et al*[49] commented that experience has shown that the "best" response type depend on the task or MTE, and it is desirable that a future standard should contain guidance to the flight control designer on the preferred response type. For the approach and landing task it was shown that ACAH response-types might provide excellent handling qualities for landing. RCAH response types have a tendency to float in the flare and Conventional response types tend to be excessively responsive to turbulence. From here it follows that an ACAH response type would be chosen for the approach and landing mission tasks. However, this response-type may not be the best for other tasks to be performed in the same flight. Thus, the preference would be to

have different response-types for different mission-task-elements. Mitchell *et al*[49] emphasize that since modern digital fly-by-wire aircraft are capable of mode switching, the pilot would have the best flight characteristics through all mission tasks. However, that is still not the common control solution.

Generally a unique response-type is chosen to perform all tasks. Although not optimum for all tasks, a trade of study can be done to achieve satisfactory Levels of flying and handling qualities. Thus, a trade study to determine the proper response-type for landing should include significant low-frequency turbulence and windshear on short final approach to expose potential weaknesses of the conventional response type, an aggressive go-around for the ACAH response-type, and precision touchdown requirements for the rate command response-type. However, Mitchell *et al*[49] state further that certain MTEs in combination with a degraded visual environment may require a specific response type, or in other words, certain response types should not be used in certain levels of degraded visual environment. A new element, that of *Usable Cue Environment* (UCE) scale is therefore introduced. The UCE is a rating scale that allows the effect of degraded visual cues, consisting of visual displays, visual aids, etc, on handling qualities to be quantified, based on the ability of the pilot to manoeuvre with precision and aggressiveness, and not on the pilot's perception of the available cueing. UCE is an important factor in determining the response type together with MTEs, although relations applicable to fixed wing were still not established[49].

A last new feature of the proposed military standard modifications is the inclusion of demonstration manoeuvres. This aim to have not only predicted Levels of flying and handling qualities based on flying qualities parameters, but also assigned levels based on flight test manoeuvres when performing a set of well defined flight test manoeuvres using a team of at least 3 pilots. Therefore, the flying qualities Levels will have a direct reference to the *Cooper-Harper rating* (CHR) and a more clear meaning: Level 1 correspond to a CHR 1 to 3, Level 2 to a CHR 4 to 6, and, Level 3 to a CHR 7 to 8.

The introduction of the demonstration manoeuvres is based on the fact that the quantitative criteria are based on CHR data from engineering in-flight and ground-based simulation. This knowledge is not complete: data is not available to fully define the required limits for all flying qualities parameters which taken together will ensure good handling qualities for all mission tasks. Thus, the predicted handling qualities could be in error. Similarly, the flight test manoeuvres are not sufficiently comprehensive to represent all mission manoeuvres in all environments that a

particular aircraft may be called upon to perform. Comparisons with both the quantitative criteria and the flight test manoeuvres are necessary to maximize the likelihood of an accurate assessment of the Level of handling qualities.

2.2.4 Longitudinal short-term small amplitude criteria

So, after this introduction for mission-oriented requirements, the choice of relevant criteria and requirements for good handling and flying qualities is the next step. Under this subject new features were also proposed by Mitchell *et al*[49]. Actually, the introduction of several manoeuvre amplitudes and definition of criteria for all manoeuvre amplitudes. The manoeuvre amplitudes were proposed as; small amplitude or continuous closed-loop control, moderate amplitude or quasi-open-loop pursuit agility and large amplitude or open-loop control.

For civil transport aircraft the relevant manoeuvre amplitudes used are the small amplitude manoeuvres, or continuous closed-loop control, e.g. for pitch attitude tracking during approach, or large amplitude manoeuvres, or open-loop control, e.g. turning onto a specific heading. The short-term small amplitude pitch response criteria are of primary importance because they are a measure of the pilot's ability to control the aircraft with precision. Therefore, only the criteria related to the short term small amplitude pitch response are presented next.

The MIL-STD-1797A[48] possesses six different short-term small amplitude criteria. Low Order Equivalent System/Control Anticipation Parameter (LOES/CAP), Bandwidth, Time response, Dropback, Nichols charts and Neal-Smith. Although this variety of criteria gives a large choice how to use each criterion is not so well understood. Thus, the flight control designer, without a proper flying and handling qualities background or without experience, might use all criteria with consequent contradictory results. Another scenario might be to use criteria when they are not valid. An example is the common, but inappropriate, use of the LOES/CAP criterion with non-conventional response types. Thus, Mitchell *et al*[49], proposed in the new mission-oriented requirements a main short term small amplitude criterion, the Bandwidth/Phase delay/Dropback criterion . Alternative criteria are also presented together with the situations where their application is valid. The LOES/CAP criterion is the most used alternative criterion, and is the most preferred for conventional aircraft. Therefore, this criterion is here presented. The Bandwidth/Phase delay/Dropback criterion as the name suggests is actually not only one, but three different criteria as follow.

2.2.4.1 Bandwidth criterion

Historically, the bandwidth criterion is an evolutionary development of the Neil and Smith criterion, and it is due to Hoh, Mitchell and Hodgkinson[59] that this criterion exists. They state that a measure of the handling qualities of an aircraft is its stability margin when operated in a closed pilot-in-the-loop compensatory pitch attitude tracking task. The maximum frequency at which such closed loop tracking can take place without threatening stability is referred to as bandwidth.

The control bandwidth of the aeroplane is critically important to good handling and the FCS easily modifies it. The control of bandwidth is further complicated by the fact that it varies according to the input-output variables involved. Control and handling difficulties may arise when the bandwidth of an input-output relationship is lower than it should be. Thus, all input-output bandwidth properties should be consistent with good handling and adequate stability margins. However, it is the pitch attitude bandwidth criterion that is referred to here.

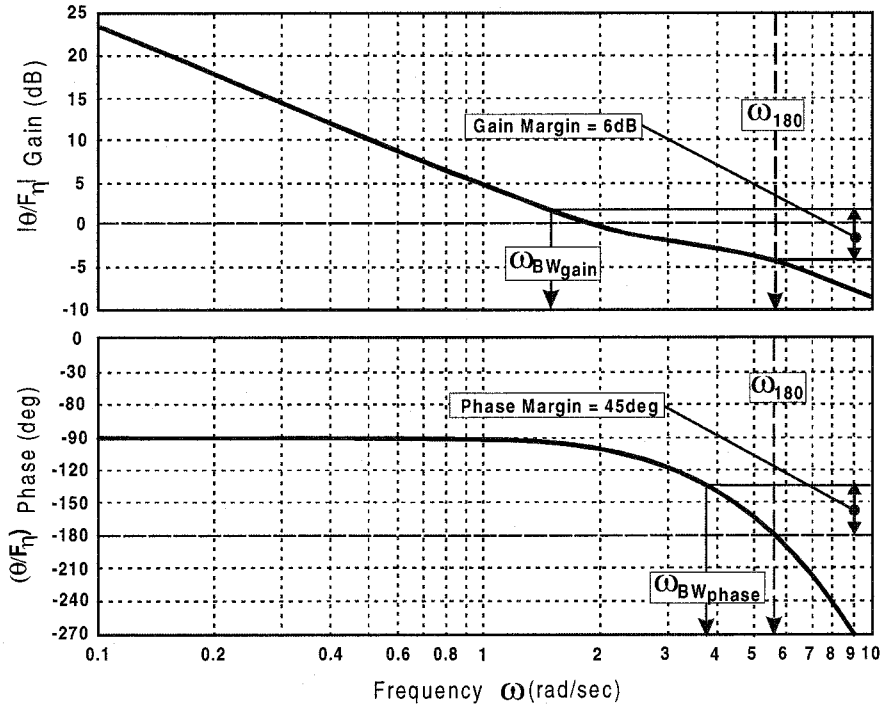

Figure 2.3 Bandwidth frequency definition (Ref. 59)

The pitch attitude bandwidth is defined as the lower of the pitch attitude gain bandwidth, $\omega_{BW_{gain}}$, and the pitch attitude phase bandwidth, $\omega_{BW_{phase}}$. With reference to Figure 2.3, the gain bandwidth, $\omega_{BW_{gain}}$, is defined by the frequency at which the gain margin is 6 dB, in other words, is the frequency correspondent to the gain 6 dB higher than the gain when the phase is −180 deg. The phase gain bandwidth, $\omega_{BW_{phase}}$, is

defined by the frequency at which the phase margin is 45 deg, or in other words, it is the frequency at which the phase first passes –135 deg (is 45 deg higher than –180 deg).

2.2.4.2 Phase delay criterion

Cook[59] states that the roll off in phase due to a time delay τ is a linear function of frequency and is given by $\Phi_\tau = -\tau\omega$. It is observed that, at frequencies around and higher than the bandwidth frequency, the shape of the Bode phase response for a high order is reasonably well matched by the equivalent phase delay. Consequently, an approximate expression for equivalent phase delay may be defined by equation (2.1).

$$\tau_{ph} = \frac{-\left(\Phi_{2\omega_{180}} + 180\right)}{\left(57.3 \times 2\omega_{180}\right)} \tag{2.1}$$

Where $2\omega_{180}$ is twice the neutral stability frequency, i.e., the frequency at –180 degrees phase, and, $\Phi_{2\omega_{180}}$ is the phase at twice the neutral stability frequency, i.e., is the phase for the frequency with a value twice the frequency for phase equal to –180 degrees. The criterion Bandwidth/Phase delay is then expressed graphically as boundaries of equivalent phase delay as a function of pitch attitude bandwidth. For the mission-task-elements to be accomplished for this aircraft, these boundaries are as given in Figure 2.4.

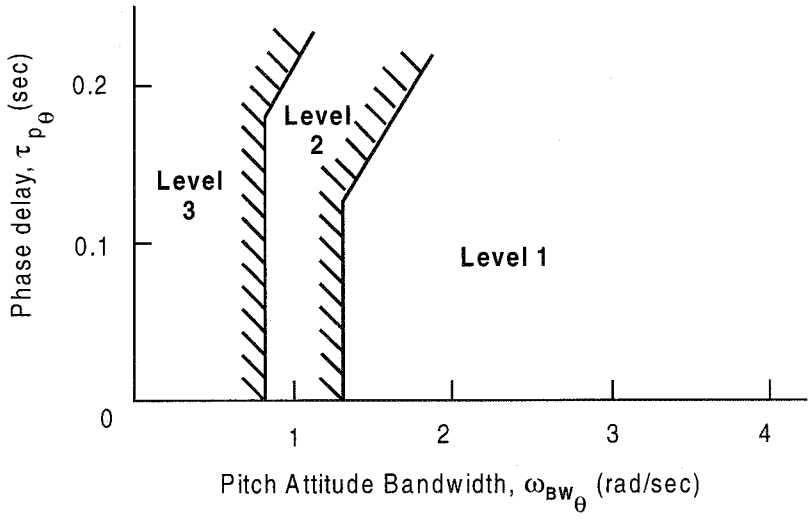

Figure 2.4 Pitch attitude bandwidth/phase delay criterion boundaries, for new categories B and C (Ref. 49)

2.2.4.3 Gibson's dropback criterion

The Gibson Criteria[59], *Dropback* and *Phase Rate*, grew out of the need to know how to design command and stability augmentation system that would endow an aircraft with acceptable flying and handling qualities. The foundations were laid by carrying out a very extensive analytical study of the longitudinal response characteristics of many aircraft, whose flying and handling qualities were known. Eventually, patterns began to emerge such that it was possible to identify those parameters, which are important in determining the handling characteristics to which pilots are most sensitive. The Dropback criterion is concerned with the pitch attitude response to pilot command, and is based on the fact that it is the relationship between pitch attitude and flight path angle that can give rise to handling qualities problems.

In Figure 2.5 the parameters of the pitch rate overshoot ratio, q_m/q_s, actually the first peak and the steady state of the pitch rate response, are given. The pitch attitude dropback, $\Delta\theta_{peak}$ i.e., the difference between the pitch attitude value when the input is removed and the steady state pitch attitude value, is also defined. Then, the pitch attitude Dropback criterion is defined in terms of limiting values on pitch rate overshoot ratio, q_m/q_s, and on the ratio of the attitude dropback to steady state pitch rate, $\Delta\theta_{peak}/q_s$, as shown also in Figure 2.5.

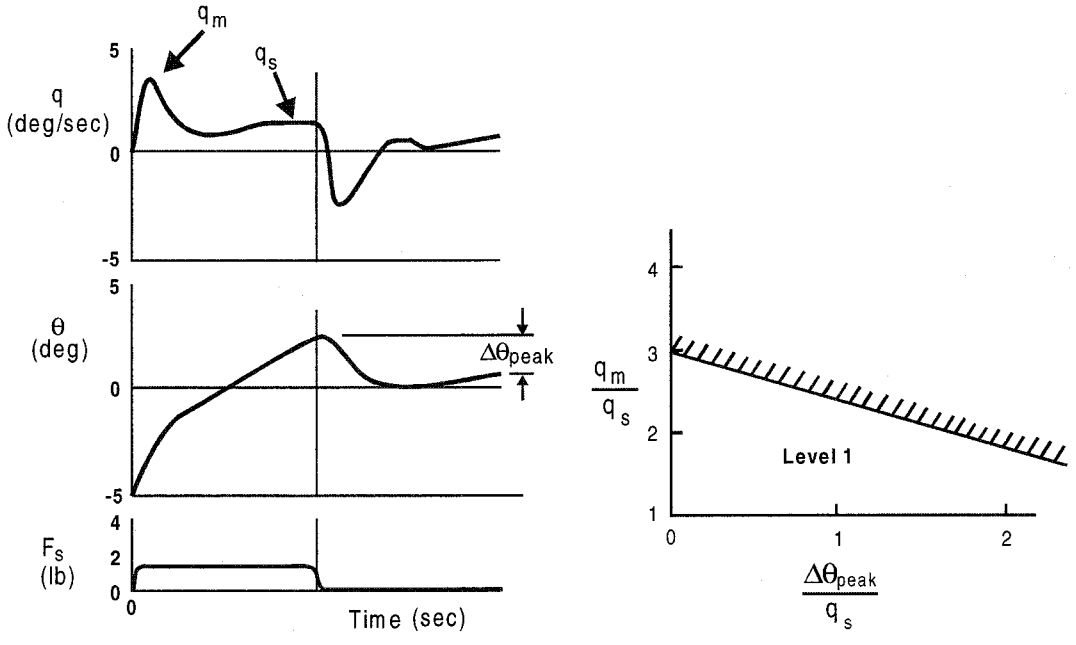

Figure 2.5 Gibson's dropback criterion parameters definition (left) and boundaries (right) (Ref. 59 and 49)

Dropback is a valuable auxiliary flying qualities criterion for rate response types. However, Mitchell *et al*[49] state that dropback is not applicable to the flight path or attitude systems since this criterion is a measure of pitch rate overshoot, and these systems have essentially zero steady-state pitch rate in response to a step control input.

2.2.4.4 Control Anticipation Parameter (CAP) and low order equivalent systems (LOES)

According to Bihrle[61], in order to make precise adjustments to the flight path, the pilot must be able to anticipate the ultimate response of the airplane and angular pitching acceleration is used for this purpose. In order to assess the handling of aircraft, Bihrle[61] defined a quantifiable measure of the anticipatory nature of the response called *Control Anticipation Parameter* (CAP). The formal definition of CAP is, the amount of instantaneous angular pitching acceleration per unit of steady state normal acceleration. In equation (2.2) the value of CAP is given in terms of second-order like parameters and which is currently in use.

$$CAP = \frac{\dot{q}(0)}{n_z(\infty)} = \frac{g\omega_s{}^2 T_{\theta_2}}{U_e} \tag{2.2}$$

Equation (2.2) is easily applicable to unaugmented aircraft since the later usually presents second order like behaviour. However, in augmented aircraft the flight control system dynamics modify the basic aircraft response. Furthermore, they introduce many modes making it difficult to interpret and apply the analytical tools. As Cook[59] says, an analytical technique has been developed which approximate the high order system to a *low order equivalent system* (LOES), as that presented in equation (2.3).

$$\frac{q(s)}{\eta(s)} = \frac{K_q\left(s + 1/T_{\theta_2}\right)e^{-\varpi}}{\left(s^2 + 2\zeta_s\omega_s s + \omega^2\right)} \tag{2.3}$$

The parameter $e^{-\varpi}$ is the system phase delay, and is intended to approximate the accumulated phase lag arising from all of the additional dynamics in the high order system transfer equation. This approximation is done through equivalent system matching, usually applied only to the short term dynamics, as shown in equation (2.3). A computational curve fitting process is used to match the frequency response of usually high order and low order equivalent reduced order models. The matching is done for the Bode gain and phase over a limited range of frequency whilst varying

transfer function variables such as K_q, T_{θ_2}, τ, ζ_s and ω_s. During the process, gain and phase errors are calculated at each frequency point between the high and low order systems. A cost function of the weighted sum of the square errors is then evaluated and minimised iteratively by adjusting the LOES transfer function variables until the best match is achieved.

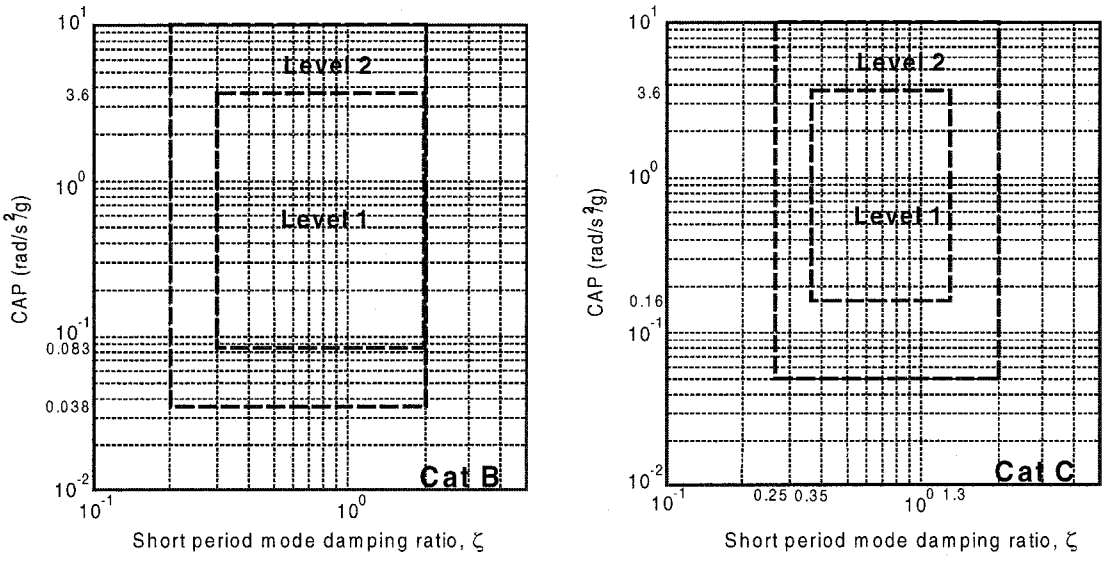

Figure 2.6 CAP criterion limits for new B and C categories (Ref. 49)

From Mitchell *et al*[49] it was taken the CAP limits for the new B and C categories, as presented in Figure 2.6. The limits for the equivalent time delay allowed were taken from the MIL-STD-1797A[48], and are presented in Table 2.3.

Level	τ_e (sec)
1	0.10
2	0.20
3	0.25

Table 2.3 Limits of equivalent time delay, τ_e (Ref. 48)

2.2.5 Lateral-directional requirements

The present mission-oriented requirements as given by Mitchell *et al*[49], have modifications for the lateral-directional motion. However, these are few and concerning agility, characteristic not important in large civil transport aircraft. The requirements in the MIL-F-8785C[46] are then, the most appropriate at the moment, and the ones used in this research. These are divided in lateral and directional axis.

2.3 Research into flying and handling qualities of transport aircraft

2.3.1 Earlier research

2.3.1.1 Booz's work

Booz[64] in 1988 studied the longitudinal flying qualities for the approach and landing flare task of a transport aircraft. For that Booz[64] applied the six MIL-STD-1797A longitudinal short-term small amplitude criteria, presented above in paragraph 2.3.3, to the same configurations as used by Weingarten[64].

Booz[64] concluded that the best correlation for both the approach and landing flare task was the gain attenuation and phase lag rate of Gibson's criteria. This is not surprising since the standard requirement states that this criterion was intended for fly-by-wire control law design optimisation. Its only drawback being that Level 1 boundary only is established.

Furthermore, Booz[64] concluded that none of the remaining criteria adequately corresponded with the pilot evaluations for either the approach or flared landing tasks. All but the bandwidth criterion yielded 53% correlation with the average approach pilot ratings. The bandwidth criterion seemed more applicable for the more demanding flared landing task, where there was 60% correlation with the average pilot ratings if the boundaries for Category A requirements were used instead. His explanation for these results was that most of the criteria were derived from MIL-F-8785C requirements, and so suitable only for unaugmented aircraft.

2.3.1.2 Rossitto *et al* work

Rossitto *et al*[65] presents some initial results of an in-flight evaluation of longitudinal flying qualities for augmented large transport aircraft in approach and landing phases. The objective of this experiment was to examine the preferred modal characteristics of angle-of-attack and pitch attitude command response-types, the Level 2 CAP boundary, and desired and adequate boundaries of equivalent time delay. For that, the acceleration sensitivity, n/α, was varied, as well as short period frequency, by means of a selected CAP value, and overall equivalent time delay, τ_e.

Two response types, angle-of-attack, or conventional, and pitch attitude command, were used in a generic advanced technology large transport aircraft for two different

weights of 750,000 lb and 500,000 lb. Four experimental test pilots evaluated between 8 to19 configurations by performing a lateral and longitudinal offset approach and flared landing.

For the conventional angle of attack command configurations, Rossitto *et al*[65] concluded that there was a consistency of the ratings for constant CAP values, which supports the CAP theory. Moreover, pilot comments supported the good angle of attack command characteristics with a CAP value of 0.5 rad/sec. Pilots suggested, furthermore, that for airplanes of this size the trend is to fly more in a precognitive open-loop fashion than in a compensatory closed-loop fashion.

The results for unconventional aircraft dynamics were inconclusive, with turbulence effects and lack of conventional cues presented as the reasons for this uncertainty. Nevertheless, some pilots initially objected to the large trim changes required for large thrust changes. The floating tendencies in the flare were also disliked. On the other hand, the aircraft was very stable once trimmed out on glide slope being difficult to be upset by turbulence.

2.3.2 Research at Cranfield University

2.3.2.1 Field's work

Field[66] divided his study into three different experiments. The impact of cockpit information available to the pilot, an evaluation of flying qualities for about 10 different current aircraft and piloted flight simulations of one aircraft configuration with several control laws.

For the first and second experiment Field used the training simulators of the following aircraft: BAC 111-500, Lockheed L-1011-1 Tri-star, BAC/Vickers Armstrong VC 10 K Mk 3 Tanker, Lockheed C-130 K Hercules, Boeing 737-300, BAe E-3D Sentry AEW Mk 1, BAC/Aerospatiale Concorde, Boeing 747-400 and Airbus A320-100. Only one pilot during one standard four-hour session evaluated these aircraft, performing 3 different tasks to accomplish different objectives. These tasks were evaluation of changes in configuration, evaluation of visual and ILS approach, correcting for lateral and longitudinal offsets, with engine inoperative, and evaluation for degraded modes of aircraft controls. In this experiment the pilot did not only attributed a *Cooper-Harper rating*, but also gave a "pilot interpreted" rating which concentrated more on the pilot's perception of the performance attained, rather than

on the measured performance. This was intended to identify pertinent characteristics of the aircraft flying qualities.

Field[66] concluded that all the aircraft evaluated clearly presented deficiencies in their flying qualities, limiting the frequency at which the pilot is able to close the control loop. None of the aircraft could be flown accurately in a compensatory manner with low workload. However, Field[66] concluded that the flying qualities of the A320 are a clear improvement over all other aircraft evaluated when flown in an open loop manner, with a resultant reduction in workload. However, when the pilot attempted to enter the control loop at any appreciable gain level, it exhibited probably the worst flying qualities of all aircraft.

The third experiment was designed to investigate the characteristics of various response types and was divided in two parts:

1) All response types were designed to have two common short term frequencies of 1.5 and 0.7 rad/sec, and

2) The preferable response types were improved further, so as to investigate whether it is the modal properties or response shape that best defines the short term response.

The command sensitivity of the pitch attitude and flight path command systems were also investigated, as well as the effect of restoring speed stability to a pitch rate command system. The pitch sensitivity of all the baseline configurations was defined to give an initial acceleration overshoot of 0.5 deg/sec^2/lb. However, although this was adequate for the angle of attack and rate command systems, it often produced heavy forces for the pitch attitude and flight path command systems, especially when away from the trim. Six different pilots performed the piloted flight simulation comprising two approaches, one instrument and one visual, simultaneously correcting for lateral and longitudinal offsets.

Field[66] concluded that the conventional angle of attack response type appeared to be the one to allow the full range of control techniques from precognitive to compensatory. Furthermore, angle of attack command has the characteristics of speed stability, allowing minimum attention to manual speed control, and the associated monotonic stick forces in the flare. Lastly, Field concluded that new flying qualities requirements are needed for commercial transport aircraft that take into account higher order systems effects, all elements in the pilot/aircraft closed loop system and the introduction of alternative response types.

2.3.2.2 Gautrey's work

A very important result from Gautrey's work was the derivation of a new criterion for flying and handling qualities evaluation as presented by Gautrey and Cook[67], called the *Generic Control Anticipation Parameter* (GCAP). This criterion is a modified interpretation of the control anticipation parameter and is applicable to both unaugmented and augmented aircraft.

Many of the handling criteria were developed for classical aircraft responses. Thus, they are not strictly valid for application to aircraft with command augmentation, which have non-classical response characteristics. However, many of the experimental databases are founded on and correlated with pilot opinion, so they are potentially adaptable for application to aircraft with non-classical response characteristics. Such an example is the CAP criterion presented in paragraph 2.3.3.4, where equation 2.2 translates the CAP definition applied to systems that approach a second order system behaviour.

For aircraft that do not exhibit conventional second order like dynamic response, a generic CAP is proposed in which the normal acceleration measure used is the peak value and an equivalent steady value is derived from knowledge of the damping ratio of the short period mode. Gautrey and Cook[67] found that the initial instantaneous pitch acceleration is nearly the same as the maximum pitch acceleration achieved at the first peak in a typical lagged response. Thus, in the evaluation of CAP or GCAP the value of $\dot{q}(0)$was replaced with the value of $\dot{q}(t_{pk})$ measured at the first peak with little loss of accuracy. As a result the definition of GCAP was amended to that in equation (2.4).

$$GCAP = \frac{\dot{q}(t_{pk})}{n_z(t_{pk})}\left(1+\exp\left(\frac{-\zeta_s \pi}{\sqrt{1-\zeta_s{}^2}}\right)\right) \qquad (2.4)$$

Where ζ_s is the damping ratio of the short-term second order mode and varying between $0<\zeta_s<1$. The value of GCAP as given in equation (2.4) may be applied to any aircraft in any flight phase. However, Gautrey and Cook[67] have only applied this concept to a large transport aircraft operating in terminal phases. Thus, more investigation is needed to confirm this results for other flight phases and aircraft types. Nevertheless, since the interpretation of CAP and GCAP is the same, the same boundary limits should apply. In spite of that, Gautrey and Cook[67] suggest to redefine the upper and lower Level 1 boundaries as shown in Figure 2.7.

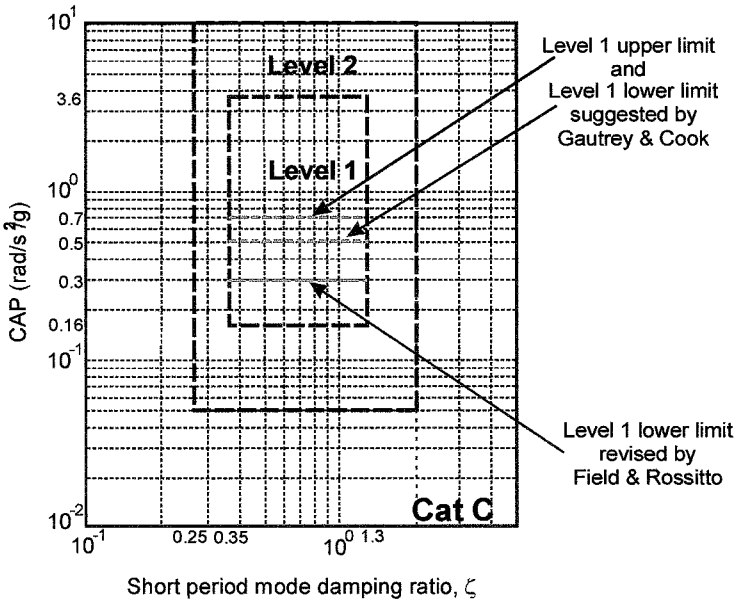

Figure 2.7 Revised CAP criterion limits

Further, in his research Gautrey[68] realized two experiments. In the first experiment five pilots flew several reconfigurations and ILS approach tasks in a ground-based fixed simulator to evaluate a generic regional transport aircraft augmented with several unconventional response-types. The control laws used were:

(i) Conventional angle of attack command,
(ii) Pitch rate/attitude hold command,
(iii) C* command,
(iv) Normal acceleration/flight path hold command, and
(v) "g"/flight path hold command.

From this experiment, Gautrey[68] concluded that the normal acceleration law had the lowest workload and received the best CHR due to its low workload and ability to hold flight path, though it does require a non-conventional piloting technique. The pitch rate law with trim to airspeed gave the most conventional feel, with good attitude stability and good airspeed awareness. Furthermore, the normal acceleration law with airspeed feedback did not give quite such a conventional feel. In the second experiment Gautrey[68] performed more piloted flight simulations, this time for a formation task and windshear approach task, using the same generic regional transport aircraft. The basic configuration was augmented with the following flight control systems:

(i) Angle of attack command,
(ii) Pitch rate command with trim to airspeed,
(iii) Normal acceleration command,

(iv) Normal acceleration command with trim to airspeed, and

(v) Normal acceleration with trim to angle of attack.

With this experiment Gautrey[68] concluded that good pitch dynamics give the pilot more time for airspeed control, and that for the windshear penetration task, the "pure" normal acceleration command law gives the best performance. Moreover, for the formation task, no benefit was found from having to trim to airspeed or angle of attack, and the benefit of trimming for the approach and landing task to improve airspeed awareness is questionable, especially with the benefits found with non-airspeed stable laws during windshear. Lastly, Gautrey[68] found that the pilot is sensitive, in classical terms, to manoeuvre margin, and not to static margin, although he is aware of the presence of a positive static margin.

2.3.3 Recent research

2.3.3.1 Rossitto and Field's work

Rossitto and Field[69] continued the work of Rossitto *et al*[65] described in paragraph 2.4.1.2. The goal of the research was to investigate flying qualities criteria for very large transport aircraft and the approach taken was pretty much the same: using in-flight simulations of configurations with various levels of short period frequency, acceleration sensitivities and equivalent time delays. The results from the experiments were used to appraise three common flying qualities criteria: LOES/CAP, pitch and flight path bandwidth criteria.

In this experiment Rossitto and Field[69] considered the feel system separately. It was assessed using different criteria, to ensure it was tuned to the aircraft's dynamics introducing no deficiencies. Three different response types were implemented: conventional or angle of attack command, pitch attitude command and flight path command. However, only the results for the conventional response type were reported. The piloted simulation task was that of a lateral and longitudinal offset during approach and landing flare.

The results of this experiment support to raise the lower Level 1 CAP criterion boundary for transport aircraft in the terminal flight phase, possibly to 0.3, as shown in Figure 2.7. Moreover, the Level 2 boundaries of the Bandwidth criterion are over restrictive for transport aircraft in terminal phases and a new boundary have been proposed, as shown in Figure 2.8. Furthermore, a multi-parameter correlation between CAP and time delay was identified, and this correlation is reflected in proposed new

boundaries, as shown in Figure 2.9. Lastly, the influence of pitch sensitivity on flying qualities was demonstrated.

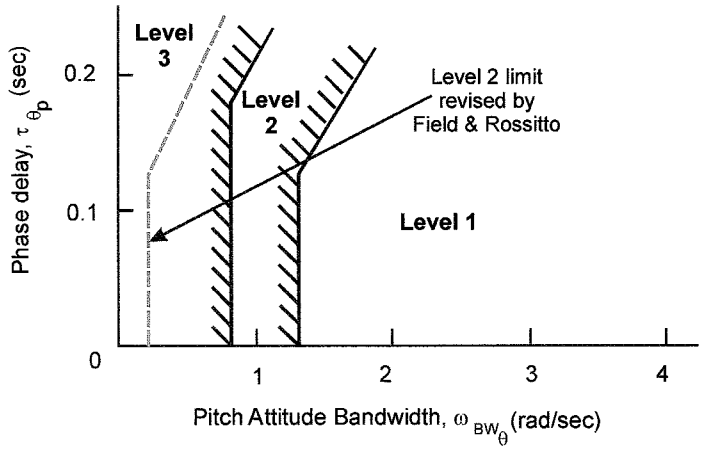

Figure 2.8 Pitch attitude bandwidth versus phase delay limits

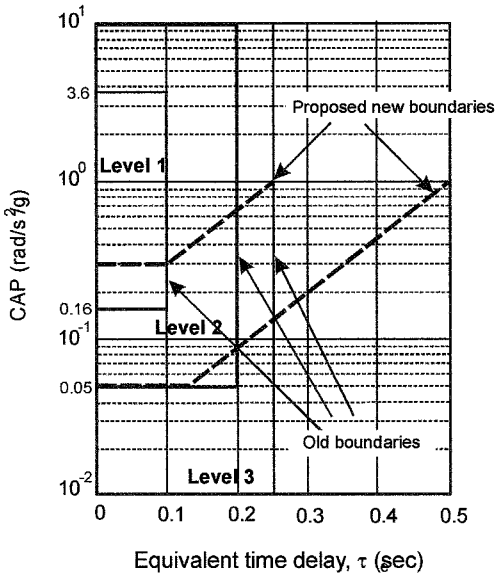

Figure 2.9 Equivalent time delay limits

2.3.3.2 Shweyk *et al* work

Shweyk *et al*[70] investigated the applicability of the pitch attitude and flight path bandwidth criteria in large transport aircraft with non-conventional response-types. The NASA Ames Vertical Motion Simulator was used to simulate a modern large supersonic transport with a flight path rate command/speed hold system. A group of seven evaluation pilots with extensive experience in transport aircraft assessed various test configurations by performing approach and land tasks. The experiment aimed to vary the model's pitch attitude and flight path bandwidth characteristics. The influence of head up displays use was also investigated.

The flight path bandwidth criterion is defined in a similar way as the pitch attitude bandwidth criterion presented before, but using the flight path bode plot instead. The flight path bandwidth requirement is added intending to ensure that the consonance between flight path and pitch attitude is consistent with the pilot's expectations. It was developed to address the ability to use pitch attitude to affect flight path changes, and, as such, specifies the rapidity with which sink rate follows attitude changes for, say, flared manual landing. Shweyk *et al*[70] concluded that the flying qualities Level 1 boundaries of the flight path bandwidth criterion could be relaxed somewhat, however, an inspection of the plots seems not to be conclusive.

2.3.3.3 Shweyk and Rossitto's work

Shweyk and Rossitto[71] performed two simulation experiments in order to develop/validate lateral flying qualities requirements for large transport aircraft. The objectives were to specify the optimum levels of roll control effectiveness and roll control sensitivity, the combination of which determines the shaping functions for lateral control inceptors. The fundamental concept behind roll stick shaping is to have a low stick shaping gradient for small stick inputs in order to provide acceptable levels of roll sensitivity and high stick shaping gradient for large stick inputs to provide adequate levels of roll performance. A stick shaping function defines the relationship between the pilot's stick-input and the stick-output into the lateral control system.

The subject aircraft model represented a large, modern, supersonic, civil transport, with centre control stick. The key experiment variables were the model's real time capability to reach 30 degrees of bank angle change, $t_{\phi=30^o}$, for the roll control effectiveness study, and the initial roll acceleration per pound force of roll stick input, $\dot{p}/F_{as}$, as well as the roll mode time constant, t_r, for the roll control sensitivity study. The roll control effectiveness study employed four evaluation manoeuvres designed to promote large lateral stick inputs. Two of the manoeuvres described closed-loop tasks one for terminal and the other for non-terminal areas. The other two described open-loop tasks also for terminal and non-terminal areas. The roll control sensitivity study adopted two closed-loop tasks, one for terminal and non-terminal areas, designed to promote small, continuous, roll stick inputs.

Shweyk and Rossitto[71] concluded that the roll control effectiveness, described in terms of the time required to bank 30 degrees, as given in the MIL-STD-1797A[48] are too conservative for non-terminal areas and new limits are proposed as shown in Table 2.4. They also developed flying qualities Level boundaries for roll control

sensitivity and roll control mode time constant. The results suggest that the optimum Level 1 roll acceleration per pound force of lateral stick input is in the range 2 to 5 and 3 to 7 deg/sec^2/lbf, for the terminal and non-terminal flight-phases respectively. The corresponding roll mode time constant was found to be in the range of 0.5 to 0.8 seconds, contrasting with the Level 1 limit specified in the requirements[48].

FQ Levels	Minimum time to achieve 30deg angle change, $t_{\phi=30^o}$ (sec)		
	Terminal Flight Phases	Non-Terminal Flight Phases	
	$V < 200KEAS$	$0.32 \leq M < 0.85$	$0.85 \leq M < M_{MO}$
1	2.5	3.0	3.5
2	4.0	6.0	
3	6.0	8.0	

Table 2.4 Proposed roll control effectiveness criterion (Ref. 71)

2.4 Special criterion for tailless aircraft

Monnich and Dalldorff[72] when studying the tailless sailplane Akaflieg Braunschweig SB-13 found it exhibits very poor flying and handling qualities in a turbulent atmosphere, although having good qualities in calm air. Then, they compared the SB-13 to the Schleicher ASW 19, a conventional sailplane with known good flying qualities in calm air as well as in turbulent. Monnich and Dalldorff[72] found dramatic differences between the ASW 19 and the SB-13 responses to vertical gust inputs. Both aircraft would initially pitch up as a response to an "up" gust, and so both pilots would push the stick forward on recognizing this. However, after about half a second, the SB-13 would start to pitch down, coming out of the gust sooner, whereas the ASW 19 would still pitch up. Unfortunately, this change on pitching direction together with the pilot reaction would amplify the pitching down of the SB-13, giving an indication to the pilot of a too responsive aircraft.

The explanation for this behaviour is that a conventional aircraft enters the gust first with its wing. Assuming an upward gust, this results in an increased lift and a pitch-up moment, since the centre of gravity lies usually behind the neutral point of the wing. A little later, as the horizontal tail enters the gust, the lift at the tail increases and the aircraft pitches down. However, when a flying wing enters a gust, since the *cg* now lies in front of the neutral point of the wing, the increase in lift produces automatically a pitch-down moment. In the first seconds the pitching gust velocity is dominant making the SB-13 still pitch up. But as the angle of attack due to the gust increases, the increase of lift becomes dominant.

Monnich and Dalldorff [72] concluded in this investigation that in designing a tailless aircraft the inequality (2.5) must be met in order for a tailless aircraft to have good flying qualities in turbulent air. For the SB-13, C_{m_α} was the only parameter in inequality (2.5), which could be easily changed. Using computer simulation they proved that by moving the *cg* backwards it was possible to make the SB-13 have a response to gust similar to that of the ASW 19.

$$M_\alpha + \frac{M_q Z_\alpha}{V_e} > 0 \qquad (2.5)$$

2.5 Lessons Learned

It is not possible to overstress how important good flying and handling qualities are for safe flight. This need is subtle since a competent pilot can develop the skills required to overcome a handling quality deficiency and he may then even consider it an enhancement. However, even the most skilled pilots make fundamental errors when confronted with highly stressful real-life scenarios, e.g. tired crew, short runway, turbulence, windshear, night, etc. While such an unfortunate combination is rare, that is precisely when safety dictates good handling qualities. Furthermore, the primary way to introduce good flying and handling qualities in a design is through clear and adequate criteria.

Flying and handling qualities criteria are laid down in the JAR and FAR for civil aircraft and in the military standards for military aircraft. However, the present civil requirements are qualitative in nature and therefore rather relaxed. Furthermore, with the introduction of fly-by-wire aircraft there are more possibilities for the design of aircraft response. Without competent regulatory criteria civil aircraft will be designed with a width characteristic between them. Then the operator will need extra training for its pilots.

The military counterpart requirements are more complete and deal with flying and handling qualities directly. However, the MIL-STD-1797A still gives a misleading orientation to the design of highly augmented aircraft. A new approach into mission-oriented requirements was then proposed in the hope to fill this gap with a better orientation on how to use the longitudinal criteria. For the lateral-directional motion no relevant changes really exists to the main requirements.

As shown in Chapter 1, the use of fly-by-wire in the Airbus A320 and Boeing B777, open the possibility of new response types in the civil transport aircraft category. On

the other hand, the military requirements although being more complete in this field, are still military and differences exist between the role of these aircraft and civil transport aircraft. Therefore, research in the large civil transport aircraft field is on going to find the best response types, criteria and boundaries specifically for this category. While for conventional response types this research has been successful, for unconventional response types it has not been so. The new blended-wing-body configuration type is in study to possibly fill the market of large civil transport aircraft. Being a new aircraft it must present a better evolution to its predecessors. There are mainly two problems in the flying and handling qualities field, first which response type to use, and second, which criteria to apply then. It seems there is no clear ideas whether a conventional or which unconventional response type is the best for the civil transport role.

Thus, in this research the mission task to accomplish will be the determinant factor in deciding the response-type to use when designing the blended-wing-body flight control systems. About the flying and handling criteria to use, the new mission-oriented requirements approach seems clearer. Thus, the proposed Bandwidth/Phase Delay/Dropback criteria, together with the GCAP criterion, will be used to assess the longitudinal flying and handling qualities requirements. For the lateral-directional flying and handling qualities assessment the requirements from the MIL-F-8785C will be used. The new limits proposed from research directed towards large transport aircraft as presented in the last part of this chapter will also be used in this evaluation.

CHAPTER 3
BWB Aircraft Model

"... (CFD) nicely and synergistically complements the other two approaches of pure theory and pure experiment, but it will never replace either of these approaches."

Anderson, 1995

3.1 Overview

Before any kind of flight dynamic, stability, control or flying qualities study can be made some aerodynamic, geometric and other general data is necessary. The quantity and accuracy of this data will depend on the kind of study to be done. For example, a simple flying simulation will require an appreciable amount of aerodynamic data, such as aerodynamic coefficients as functions of angle of attack, speed and controls deflection, if accuracy is to be maintained. Whilst, static stability analysis only needs few stability derivatives for one condition of speed, angle of attack and controls deflection, commonly known as a flight condition.

The BWB concept was at an early stage of its development when this thesis began and has evolved since. The aircraft data used in this research has evolved in the same way. Moreover, since many projects are commercial and thus confidential, it was not always an easy task to obtain this precious data. Although some approximate analytical methods for calculating data for flight dynamic applications[76 to 83] are available, some are not accurate enough since they are based on conventional aircraft configurations, and being analytical methods their application to the BWB aircraft is difficult.

This is the same problem designers are facing at the moment in the design of the BWB aircraft, as well as other new aircraft concepts. Due to non-existence of tail, or fuselage, and the fact that the control surfaces are part of the wing, the optimisation

for maximum aerodynamic efficiency needs to take into account not only trim aspects, but also aspects of stability and control simultaneously, which makes the problem more complex. Then, the design rules are no longer conventional and approximations are not always possible to make so easily.

To ease the problem new technologies are now available to the designer; actually digital computers that can handle drawings easily and enable configuration change in a "blink of eye". Digital computers also enable faster and more complex calculations to be done, making possible the optimisation of several variables simultaneously. However, many of these tools are still under development[1], needing first to be implemented and validated before becoming widely available.

To obtain quickly more complete and reasonable aerodynamic data for a new aircraft concept, the best approach may be to use classical wind tunnel tests complemented with *Computational Fluid Dynamics* (CFD) tools. While low fidelity panel methods from the latter CFD tools already offer lots of information with a reasonable accuracy and within certain approximations (inviscid and linear flow), it takes more effort, money and time to build a good model and run enough wind tunnel experiments to obtain accurate data. Other CFD codes based on the solution of the full Navier-Stokes and Euler equations, although giving more accurate and hence valuable data using fewer approximations, are still under development and require powerful digital computers and huge amounts of processing time to reach few results. Thus, this option may remain expensive, even when compared with wind tunnel experiments.

A further problem is whether to consider the aerodynamic body as part of the wing or as an individual item, a fuselage. Thus how should the reference area be defined? This is a very important concept for flight dynamics since it is used to make the coefficient derivatives dimensionless and its definition is important, especially when comparing coefficients of different blended-wing-body configurations. Although the adoption of the same reference area is desirable, so far for the BWB concept it has been the individual performing the calculations who chooses his own definition. Hopefully, only two options need be considered, the total area of wing and body, or the area of a fictitious trapezoidal wing coincident with most of the wing and extending to the aircraft centre line. During this research there was an exchange of information with designers, aerodynamicists and other flight dynamicists. Thus, there was an assumption that all were using the same convention, actually the trapezoidal wing area. However, not all data sets came from the same team, with others using the wing-body area as the reference area. Thus, whenever possible the first convention is used, since this seems the general trend, and this will be referred with a "trapezoidal" index,

or no index at all. When the reference area is relative to the combined wing-body the index "gross" is used.

The BWB models and data presented in this chapter were obtained from different sources and have evolved with time in complexity and the amount of data becoming available, just like the evolution of the concept itself. The final model used for simulation is, in some ways, a blend of data from all of the models and may therefore be regarded as a generic BWB aircraft.

The first set of aircraft data was obtained from designers and was calculated using simple approximate design rules. The second set of aerodynamic data was obtained from wind tunnel tests of a different aircraft geometry. However, the wind tunnel experiments looked more like an academic experiment and some doubts of the validity and accuracy of the data still remains. Moreover, this wind tunnel data was still not sufficiently complete for the research described here.

The third set of aerodynamic data was obtained from CFD panel code methods for a similar geometry to the first set of data. This data set is the most complete and includes rotational aerodynamic coefficients for several *cg* positions. The fourth and last data set used was made for exactly the same configuration as previously, but was made by a different team and using different tools, although CFD panel codes were also used to obtain this last data set.

All four models are presented next with more information, where available, on the methods of calculation and the configurations used, together with other details that seemed important to this thesis. However, a brief description of the reference geometry and aircraft axes systems is given first.

3.2 Reference axes

3.2.1 Body axes system

The body axes system $(ox_b y_b z_b)$, as the name suggests, is a reference axes fixed in the aircraft and moving along with it. In Figure 3.1 the orientation of the body axes is shown, along with the notation for positive linear force (X,Y,Z), velocity (u,v,w), moment (L,M,N) and angular velocity (p,q,r) components. The body axes are very important for both flight dynamics and simulation, since they are the reference axes used to define the equations of motion.

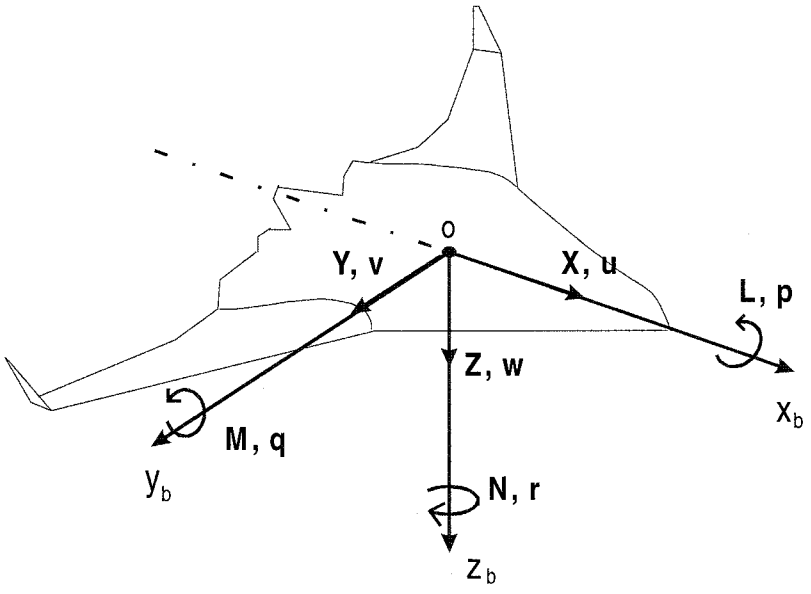

Figure 3.1 Body reference axis orientation

3.2.2 Wind or stability axes system

The wind, or stability, axes system $(OX_W Y_W Z_W)$ in symmetric flight is just a particular version of the body axes system, which is rotated by the angle of incidence α around the oy_b axis as Figure 3.2 shows. It has the convenience that the total velocity vector V_o is parallel to the OX_W axis. This system of reference is often used in wind tunnel tests to give the values of the aerodynamic lift, drag and side force, which are measured with respect to the OZ_W, OX_W and OY_W axes respectively.

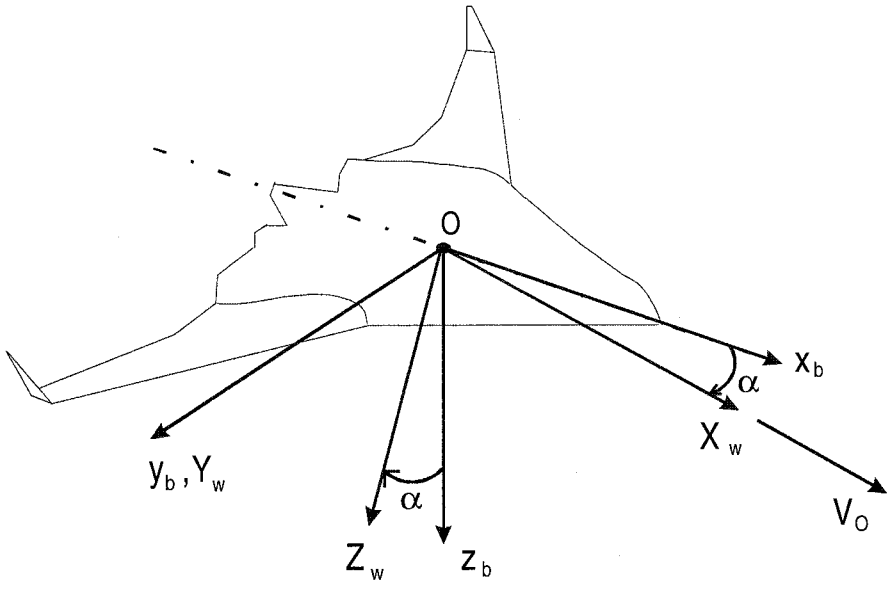

Figure 3.2 Wind reference axis orientation relatively to the body reference axis

3.3 Data sets

3.3.1 BWB1 configuration data

The configuration named BWB1 constitutes the first set of available data used in this research. This was the data specification[84] given for the group project of the Aerospace Vehicle Design MSc course at Cranfield University. This data was the result of the preliminary design, so the data presented is very simple and not completely fitted for a flight dynamic analysis, let alone a flight simulation. Besides, being only preliminary data, it is certain that more design iterations are necessary to achieve a fixed final design which has more accurate values representing the real configuration. Moreover, most of the tools used in preliminary design are based on conventional aircraft databases. Thus, there were many doubts as to whether this data would actually be representative of a BWB configuration or not, since comparative data for a BWB configuration is extremely rare.

Nevertheless, at the time the BWB1 data was the only set of data readily available, and although not complete, accurate or representative, it was enough to begin simple flight dynamic analyses and to gain some insight into the basic blended-wing-body stability and control characteristics. Moreover, the results of a flight dynamics analysis could be used as input to direct the next design iteration. The three view drawings, a more detailed view of the planform shape and other general geometric and aerodynamic information are given in Appendix B, paragraph B.1.

3.3.2 BWB2 configuration data

Although the second data set was also incomplete, it was very welcomed, since it came from a completely different source – wind tunnel tests[85 to 90]. Thus, greater fidelity and accuracy was expected. The BWB2 data would also enable a first comparison to be made between these two different blended-wing-body configurations. However, when more was known about the project behind the data, the feeling was that it had been just an academic exercise, and that the fidelity expected may not be present. Moreover, more information about the basic geometric configuration, and the mass distribution data was necessary which was not completely available. Thus, in the long run, it was not possible to use this data to its greatest potential.

The geometric, aerodynamic and other general data available for the full-scale aircraft are presented in Appendix B, paragraph B.2. It can be seen that some values do not

seem very appropriate and others are missing altogether. The 3-view drawings representative of the BWB2 configuration are also given in appendix B together with a detailed planform drawing showing the location of the control surfaces. Although values for the rotational derivatives were missing and other information was not entirely "right", this second set of aerodynamic data permitted additional insight of the blended-wing-body characteristics. A parametric study was done to investigate the flight dynamic characteristics that might be expected with blended-wing-bodies of this kind. Lastly, the most important contribution of this data set was the information on aerodynamic drag.

3.3.3 BWB3 configuration data

This third set of data came to complete all that was missing from previous data sets. The general aerodynamic data was calculated using the QUADPAN[91] commercial code, an inviscid panel code based on a Source/Doublet method, modified to include calculation of rotational flow and hence, rotational derivatives. The control surface derivatives data was calculated using a Vortex-Lattice method. As these codes run relatively fast, it was also possible to calculate aerodynamic data for several *cg* positions. The *cg* range used was that defined for BWB1.

The basic configuration used was the same as that of configuration BWB1 as presented in Figure B.1 of Appendix B. However, the wing twist distribution was optimised for a desired lift distribution[94]. Furthermore, the grid generation was done in a manual way using a coarse scale, i.e., reading the measurements directly from 3-view drawings[93], thereby trading computational simplicity with accuracy.

Axes transformations were done with the CFD data thus obtained, since the reference axis used on CFD calculations have a different orientation than that used for flight dynamic studies. However, instead of transforming the data into stability axes as aerodynamic data is usually presented, it was preferred to transform it directly to body axes, since it would simplify simulation later. All relevant data about this BWB3 configuration is presented in Appendix B, paragraph B.3.

3.3.4 BWB4 configuration data

This is the fourth and last set of data used in this research. It was decided to use this data since it presented better lateral-directional characteristics than the previous BWB3, although this data set was not as complete as the previous. The configuration

used for this data is the same of that already presented for BWB1 and BWB3, whose layout drawings are presented in paragraph B.1 of Appendix B.

Although the same planform was used, differences still exist between the three configurations. The wing twist distribution used was the same as optimised for the BWB3 configuration, but this time the CFD grid was generated automatically through the use of an *Intelligent Computer Aid Design* (ICAD) program[96]. Two CFD panel codes different from that used for the BWB3 data generation were used. One team used the *NLR (National Aerospace Laboratory, the Netherlands)* code PDAERO based on linear potential flow. Whilst the CFD code WINGBODY existent in Cranfield University was by other team. Furthermore, a more advanced code based on Euler equations, actually the NLR code ENSOLV was used to calculate a few data such as the maximum angle of attack with slats deflected. The geometric and aerodynamic data of this fourth set is presented in paragraph B.4 of Appendix B. Later investigations revealed that basic aerodynamic properties also change with deflections of the control surfaces. However, since this was only revealed at a very late stage of the research it was not possible to include it in this study.

3.4 Moments of inertia

The moments of inertia of an aircraft are important quantities in a flight dynamics analysis. However, for configurations BWB3 and BWB4, that had the most complete data sets, there was only information on the longitudinal moment of inertia. The proportions between moments of inertia of the other two configurations, BWB1 and BWB2, were calculated and used as a guide to estimate the roll and yaw moments of inertia for configurations BWB3 and BWB4.

		$I_{xx}\ (Kg.m^2)$	$I_{xx}:I_{yy}$	$I_{yy}\ (Kg.m^2)$	$I_{yy}:I_{yy}$	$I_{zz}\ (Kg.m^2)$	$I_{zz}:I_{yy}$
BWB1	**MTOW**	1.087×10^{8}	2.3	4.712×10^{7}	1	1.558×10^{8}	3.3
	OEW	2.835×10^{7}	1.2	2.431×10^{7}	1	5.266×10^{7}	2.2
BWB2		4.832×10^{11}	9.2	5.283×10^{10}	1	2.517×10^{11}	4.8
BWB3		4.703×10^{7}	1.9	2.507×10^{7}	1	9.973×10^{7}	3.9
BWB4		4.703×10^{7}	1.9	2.507×10^{7}	1	9.973×10^{7}	3.9

Table 3.1 Moments of inertia for several BWB configurations

In the end, as Table 3.1 shows, it was decided to use a proportion of approximately 2:1:4 (Ixx:Iyy:Izz) for the moments of inertia. Values for roll and yaw moments of inertia for BWB3 and BWB4 were then estimated from the pitch moment of inertia given for the BWB3 and BWB4.

3.5 Summary

In this chapter, four sets of aircraft data were presented; BWB1, BWB3 and BWB3 have the same basic planform in different stages of development, and BWB2 which although possessing a different planform design, still has common features with the first configuration, namely the fact of being a blended-wing-body configuration of similar dimensions. To evaluate the accuracy and validity of the data used the methods and processes to obtain them are considered.

BWB1 was the first data set available from preliminary design data. The methods used to obtain this data were probably analytical methods, based on conventional aircraft configurations. Thus, it is probably not very accurate. Nevertheless, as a first BWB data set it presented enough accuracy to gain a first insight into the stability of BWB configurations and for comparison purposes.

The BWB2 data was obtained from wind tunnel experiments, thus a better accuracy was believed. However, general geometric and mass information did not completely exist and its accuracy was dubious. Furthermore, it has a different BWB planform than that of BWB1, and, the aerodynamic data did not include information on rotational derivatives and it was given only for one *cg* position. Nevertheless, this data set presented valuable drag information that no other data set possessed.

BWB3 and BWB4 data sets are believed to be the most complete and accurate information obtained. However, since inviscid CFD panel methods were used some assumptions exist. Firstly, no influence of drag is present due to the assumption of inviscid flow, and, secondly, the data is only valid within linear flow regime. Finally, the aerodynamic data is only valid at low speeds.

In conclusion, although the present data sets may not present the highest accuracy, they present the best data available for the research. Furthermore, within the assumptions, the data sets are considered representative enough of BWB configurations. Moreover, since no single data set was complete, in the end the approach was to consider a general BWB configuration based on a combination of the actual data sets. Namely, the more complete BWB3 and BWB4 data sets were used in the flight simulation, complemented with the BWB2 drag information.

CHAPTER 4
Static and manoeuvre stability of the basic blended-wing-body aircraft

"... Inability to balance and steer still confronts students of the flying problem ... when this one feature is worked out the age of flying machines will have arrived, for all the other difficulties are of minor importance"

Wilbur Wright

4.1 Overview

As Wilbur Wright commented around 100 years ago the (in)ability to balance and steer remains one of the most important problems in aircraft design. Designers are often primarily interested in optimising the structural weight, the aerodynamic efficiency, the maximum payload, and performance so as to win a place in the market. However, if insufficient care is paid to steer and balance at the early stage of design, at a later stage it may mean deficient aircraft flying and handling qualities and, possibly the complete loss of a promising project.

"Steer and balance" technically are referred to as "control and stability". Control or steering is the ability that the pilot has to change the aircraft condition in speed, direction and altitude. Balance, or stability, is the aircraft inherent characteristic to resist disturbances due to external inputs, either desirable as in pilot commands, or undesirable as in atmospheric turbulence.

An aircraft, like any other mechanical system following a perturbation, can be considered stable if the aircraft returns by itself to the initial equilibrium condition,

neutral if it returns to a different equilibrium condition, or unstable if it diverges from any equilibrium, probably being lost if no corrective control action is taken. Furthermore, stability can be divided into static and dynamic stability. Static stability describes the aircraft tendency to recover equilibrium in the long-term, whilst dynamic stability describes the short term aircraft response. This means that static stability describes whether the aircraft, following a perturbation, is stable, neutral or unstable in the steady state response after the transients die away, whilst dynamic stability determines whether these transients are stable, neutral or unstable. The worst and most undesirable condition that can exist is an unstable aircraft both statically or dynamically. Clearly, the most desirable situation is a stable aircraft, both statically and dynamically. An aircraft that is statically unstable will always be unacceptable unless the period of the associated dynamic mode is very long, or an augmentation system is installed to restore stability artificially.

To summarise, stability describes the tendency to maintain an equilibrium condition in the presence of perturbation, whilst control describes the ability to change from one equilibrium condition to another by means of deliberate inputs. Thus, it can be concluded that these two characteristics work against to one another. The right amount of both stability and control has then to be found – the solution is inevitably a compromise. If high inherent stability is present it will not be possible to change the equilibrium of the aircraft unless very high control power is used. If low, or neutral, inherent stability is present, small control inputs or small outside perturbations will easily change the aircraft equilibrium. If there is no stability any control input or external perturbation will cause the aircraft to diverge if left unchecked.

In Chapter 2 it was shown that "flying and handling qualities" are very related to the aircraft stability and control characteristics. Thus, it is important to understand these inherent aircraft characteristics in order to properly understand its flying and handling qualities. The static stability and control, since they are very much interrelated and conflict with one another, are treated together in this chapter. Dynamic stability embraces much wider and important aspects of flight control, thus it is treated separately in Chapters 5 and 6.

4.2 Longitudinal motion

4.2.1 Static stability

Castro[97] applies the classical stability theory to the particular features of tailless aeroplanes to develop a simple longitudinal static stability and manoeuvrability

theory. This theory is then applied to the blended-wing-body transport aircraft, actually the model BWB1 presented in the previous chapter. Some interesting conclusions were drawn from that study and are presented next, together with results for the other BWB configurations studied.

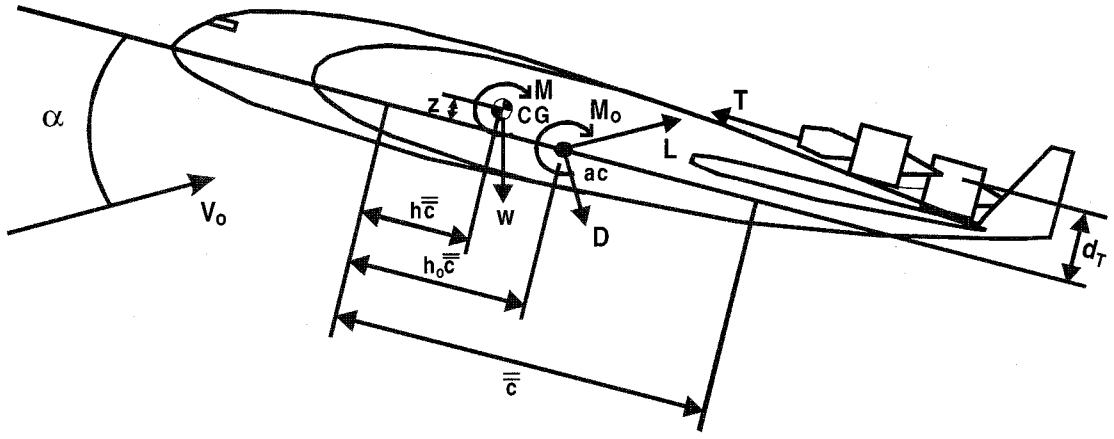

Figure 4.1 Forces and moments acting on an aircraft.

From Figure 4.1 the pitching moment for tailless aircraft for trimmed equilibrium and quasi-steady flight, constant mass, normal atmosphere, without compressibility effects and for small angles of attack can be derived. This is given by equation (4.1). This shows that the pitching moment is a function of the lift coefficient, C_L, the distance from the *cg* to the aerodynamic centre, $h_o - h$, as it would be expected, and if taking these effects also into account, of pitching moments due to the power plant and of the normal displacement of the *cg* relatively to the aerodynamic centre.

$$C_m = C_{m_o} - C_L(h_o - h) - (C_L\alpha - C_D)\frac{z}{\bar{\bar{c}}} + C_{m_p} \tag{4.1}$$

If the pitching moments due to the power plant, C_{m_p}, and the *cg* normal displacement, z, are neglected equation (4.1) becomes a linear relation only as a function of the coefficient of lift for a constant *cg* position as presented in equation (4.2).

$$C_m = C_{m_o} - C_L(h_o - h) \tag{4.2}$$

One interesting and well-known result for tailless aircraft with fixed controls, or irreversible controls, as with fly-by-wire technology, is presented in equation (4.3), which shows that a tailless aircraft will be statically stable if the *cg*, $h\bar{\bar{c}}$, is ahead of the aerodynamic centre, $h_o\bar{\bar{c}}$. Furthermore, from the definition of static margin, $K_n = h_n - h$, equation (4.3) shows that for a tailless aircraft the neutral point is coincident with the aerodynamic centre.

$$K_n = -\frac{dC_m}{dC_L} = (h_o - h) \tag{4.3}$$

However, this simple result is based on extreme simplifications, such as presented for equation (4.2), and may not be always valid. Therefore, if thrust effects or the normal *cg* displacement cannot be neglected, and, or the trimmed angle of attack is higher, this relation does not hold true. A more complete relation is that given by equation (4.4), taken also from Castro[97].

$$K_n = \left(1 + \frac{\partial C_D}{\partial C_L}\alpha_e\right)(h_o - h) + \left(\alpha_e - \frac{\partial C_D}{\partial C_L}\right)\frac{z}{\bar{c}} - \frac{\partial C_{m_p}}{\partial C_L} \tag{4.4}$$

From this relation it can be seen that if the thrust pitching moment due to variations in lift coefficient is negative, and if the *cg* is displaced below the aerodynamic centre, these two terms will contribute to a more stable aircraft. In other words, the *cg* can be placed aft of the aerodynamic centre while retaining a positive static margin.

Nevertheless, in a study of small perturbations about a trim condition, the thrust effects can possibly be neglected without large errors, as well as the term of the normal *cg* displacement since this is usually small and becomes even smaller when divided by the mean aerodynamic chord, which is much larger than the *mac* of conventional aeroplanes. Thus, subject to these conditions the better-known version of equation (4.3) results, which is commonly used in flight tests to calculate the neutral point. Equation (4.3) is also used in appendix B to calculate the neutral point of configuration BWB3, and in configuration BWB2 to find the *cg* position, respectively.

Table 4.1 presents the *cg* range considered for configurations BWB1 and BWB3, as well as the static margin corresponding to the most forward and the most aft *cg* positions. For configurations BWB2 and BWB4 only one *cg* position is shown with the static margin as presented in Table 4.1. The values for BWB1 and BWB3 of the "study case" column present the static margin used in the following studies of this chapter.

	CG range $(h_{aft} - h_{fwd})$	**Static margin,** $K_n = (h_o - h)$		
		Fwd	**Aft**	**Study case**
BWB1	29.0%	20.9%	-8.3%	3.3%
BWB2	-	-	-	3.22%
BWB3	40.6%	18.1%	-22.4%	-14.4%
BWB4	-	-	-	-13.2%

Table 4.1 *cg* range and static margins for four BWB configurations

From Table 4.1 it is seen that the *cg* range considered is quite large for the BWB1 configuration and even more for the BWB3 configuration. The forward *cg* position for both configurations is lower than the usual for conventional aircraft. The aft *cg* position for both configurations gives an unusually unstable configuration for a large civil transport aircraft, although having been used in the fighter category for some time now. Nevertheless, a positive static margin is considered for BWB1, although it is small. Whilst for BWB3 a large negative static margin is considered. For the BWB2 configuration, the *cg* position, although stable, has a small static margin. While the BWB4 configuration has an unusually large negative static margin. Therefore, the case studies of configurations BWB1 and BWB2 are for a stable configuration, although almost neutral, while BWB3 and BWB4 are completely unstable. Thus, some kind of stability augmentation may be necessary for the first two configurations and absolutely necessary for the last two configurations. Therefore, this research is concerned only with fixed controls stability.

4.2.2 Trimmability

The interest in controls fixed static stability and manoeuvrability analysis is not so much about the positive and negative static and manoeuvre margins, but is more about the control surface deflections necessary to trim the aircraft in a flight condition, or to manoeuvre the aircraft. Nevertheless, static stability and manoeuvrability margins are closely related to control angles to trim and to manoeuvre respectively.

The control surface deflections to trim or manoeuvre are especially important for tailless aircraft, because a tail does not exist and controls are located in the trailing edge of the wing with much smaller moment arms. Thus, the designer, the flight dynamicist and the flight control system designer has to be sure that there is enough control power to trim or to manoeuvre in all situations. This is an important aspect in tailless aircraft and history has shown this may be the reason why tailless aircraft, and in particular flying wings, never achieved complete success. To calculate the controls deflection and the angle of attack to trim, Castro[97] gives the relations presented in equations (4.5) and (4.6).

$$\alpha_{trim} = \frac{\hat{C}_m C_{L_\eta} - \hat{C}_L C_{m_\eta}}{\det} \tag{4.5}$$

$$\eta_{trim} = \frac{\hat{C}_L C_{m_\alpha} - C_{L_\alpha} \hat{C}_m}{\det} \tag{4.6}$$

Where $\hat{C}_m = -\overline{C}_{m_o} - C_{m_\beta}\beta$, $\hat{C}_L = C_{L_{trim}} - C_{L_o} - C_{L_\beta}\beta$ and $\det = C_{L_\eta} C_{m_\alpha} - C_{L_\alpha} C_{m_\eta}$.

Substituting values for the four BWB configurations, with their *cg* positions as given in the case study column of Table 4.1, gives the trim relationships shown in Figure 4.2 and Figure 4.3. It can be seen from Figure 4.2 that for the BWB1 and BWB2 configurations, which have smaller static margin magnitudes, the elevator angle to trim is smaller than that for configurations BWB3 and BWB4, which have higher static margin magnitudes. On the other hand, BWB3 and BWB4 configurations trim at lower angles of attack than configurations BWB1 and BWB2, as shown in Figure 4.3. This is the case, since to trim an unstable aircraft the elevator is deflected down instead of deflected up as shown in the elevator angle to trim plot. Since these controls are located on the trailing edge of the wing they directly affect the generation of lift, as they change the wing camber. Thus, when the elevators are deflected down the camber increases, increasing the wing lift slope. If the elevators are deflected up the opposite happens: the wing camber decreases and the lift slope decreases. Thus, less angle of attack is necessary to generate the same amount of lift when the elevators are deflected down.

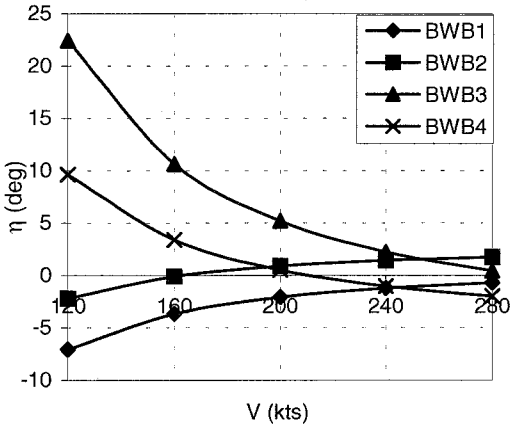

Figure 4.2 Elevator angle to trim as function of speed for several BWB configurations.

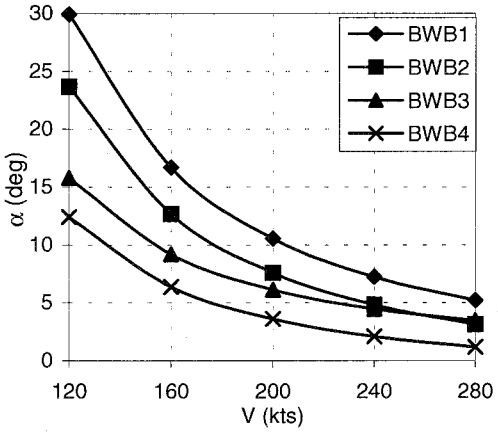

Figure 4.3 Angle of attack to trim variation with speed for several BWB configurations.

From here a conclusion, which is presented in Castro[97] and previously cited by John Northrop in his Wilbur Wright lecture[6], is drawn that an inherently unstable tailless configuration may be the best design. This can be better understood through equation (4.7) taken from Castro[97]. This equation gives the trimmed lift slope and it can be seen that for a stable aircraft, positive static margin, the lift slope is decreased and for an unstable aircraft, negative static margin, it is increased (note that the quotient C_{L_η}/C_{m_η} is negative).

$$\left(\frac{dC_L}{d\alpha}\right)_{trim} = C_{L_\alpha}\left(1-\frac{C_{L_\eta}}{C_{m_\eta}}(h-h_n)\right) = C_{L_\alpha}\left(1+K_n\frac{C_{L_\eta}}{C_{m_\eta}}\right) \quad (4.7)$$

Thus, since fly-by-wire has been around for a while and its technology has become reasonably mature, the choice of a neutral, or slightly unstable, aircraft should not be a problem, even if it is for the transport of passengers, especially when it brings good compensations.

Similar conclusions were obtained by Cook and Castro[98] when analysing the static stability of configuration BWB3 for the full *cg* range given. They found that for the same static margin magnitude, unstable configurations would need smaller angle of attack values to trim. However, Cook and Castro[98] concluded that higher elevator deflections were needed for larger static margins, irrespective of the configuration being stable or unstable. They concluded that, due to the limited control power available, the BWB3 static margin magnitude should not exceed $K_n = 0.10$ *mac* for safe operation at low speeds.

In Figure 4.2 it can be seen that although configuration BWB4 has a negative static margin similar to configuration BWB3, the elevator deflection needed to trim for the same speed is much lower for the BWB4. This is due to the control surface derivatives, which are larger for the BWB4 configuration indicating higher control power. The same is true for configurations BWB1 and BWB2 that have similar static margins. The BWB2 configuration, which has larger longitudinal control surface derivatives, or higher longitudinal control power, needs less elevator deflection than BWB1 to trim at the same speed.

4.2.3 Manoeuvrability

An analysis of the classical manoeuvre stability of tailless aircraft is presented by Castro[97]. This theory was then used by Cook and Castro[98], who applied it to the BWB3 configuration varying the *cg* position and speed. From that analysis, Cook and Castro[98] concluded that the practical control effectiveness for manoeuvring is limited and dependent on static margin. Furthermore, the unstable configurations showed more favourable since the required elevator angle per 'g' and corresponding angle of attack per 'g' were lower. The classical manoeuvre stability as derived by Castro[97] is also used here to compare the four study case configurations. Equation (4.8) and equation (4.9) represent respectively the angle of attack per 'g' and the elevator angle per 'g'.

$$\frac{\delta\alpha}{(n-1)} = \frac{1}{C_{L_\alpha}}\left(C_W - C_{L_q}\frac{C_W}{2\mu} - C_{L_\eta}\frac{\delta\eta}{(n-1)}\right) \tag{4.8}$$

$$\frac{\delta\eta}{(n-1)} = -\frac{\left(1-\frac{C_{L_q}}{2\mu}\right)C_W C_{m_\alpha} + C_{m_q}\frac{C_W}{2\mu}C_{L_\alpha}}{C_{L_\alpha}C_{m_\eta} - C_{L_\eta}C_{m_\alpha}} \tag{4.9}$$

In equations (4.8) and (4.9) $\mu = \frac{2m}{\rho S\bar{c}}$ is the mass ratio and $C_W = \frac{mg}{\frac{1}{2}\rho V^2 S}$ is the weight coefficient.

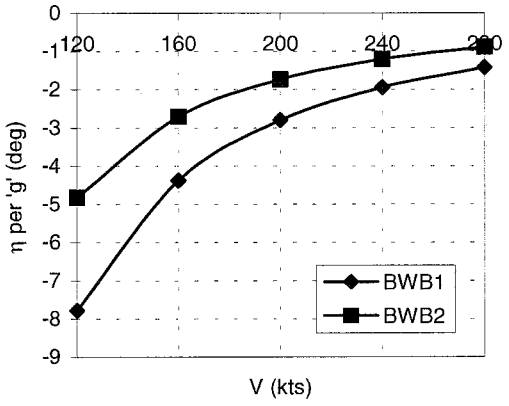

Figure 4.4 Elevator angle per 'g' variation with speed for the BWB1 and BWB2 stable configurations.

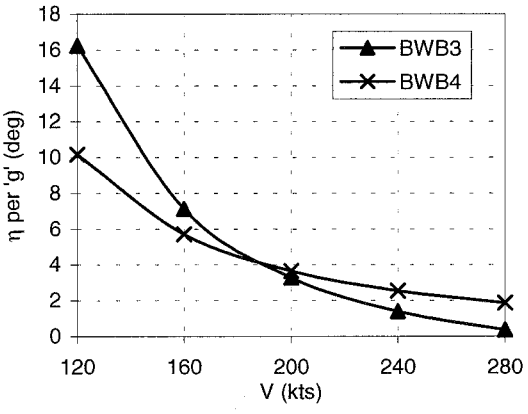

Figure 4.5 Variation of elevator angle per 'g' with speed for the BWB3 and BWB4 unstable configurations.

Figures 4.4, 4.5 and 4.6 present the results of the application of equations (4.8) and (4.9) to the four BWB configurations. From Figures 4.4 and 4.5, the elevator per 'g' plots it can be seen that, in the same way as for the elevator angle to trim, the control surface deflection sense to manoeuvre is different depending on the aircraft stability: - elevator deflected up (negative elevator value) for a stable aircraft, and deflected down (positive elevator value) for an unstable aircraft. As before, this results in a corresponding lower angle of attack per 'g', as shown in Figure 4.6. In Figures 4.4 and 4.5 the influence of the static margin on the elevator angle per 'g' can be seen. Configuration BWB1 has a slightly bigger static margin than BWB2, therefore requiring more elevator angle per 'g' at the same speed. The same happens in Figure 4.5 for BWB3 and BWB4 at low speeds. On the other hand, although the magnitude of the BWB3 and BWB4 static margin is much bigger than that of BWB1 and BWB2, the increase in elevator angle per 'g' seems not so large. This correlates with the result given by Cook and Castro[98] that unstable configurations need less elevator angle per 'g' than the corresponding stable configurations.

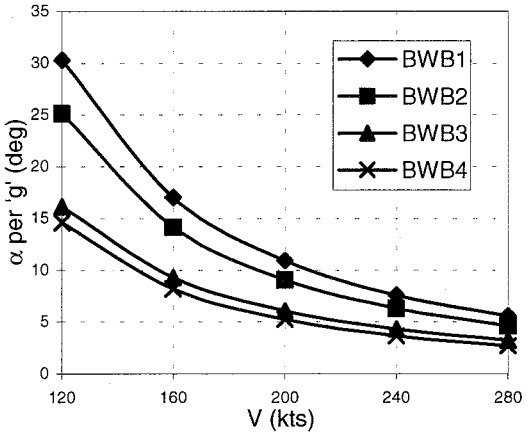

Figure 4.6 Angle of attack per 'g' versus speed for the four BWB configurations

Since the rotational derivatives were not known for configurations BWB1 and BWB2, these were assumed to be zero, $C_{L_q} = 0$ and $C_{m_q} = 0$. This implies that there is no pitch damping, which also dynamically opposes a change of equilibrium and hence manoeuvre. Figure 4.7 shows the variation of the elevator angle per 'g' for several values of pitch damping. It is possible to see then, that an increase in the pitch damping also increases the elevator angle per 'g' required for a pull-up of 1g.

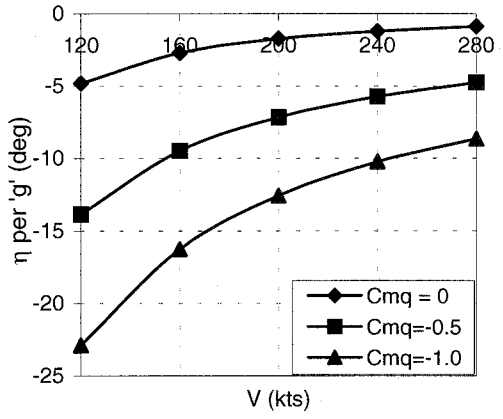

Figure 4.7 BWB2 elevator angle per 'g' versus speed and pitch damping

Actually, when the *cg* position moves backwards, the longitudinal rotational derivatives decrease as shown in the data for the BWB3 configuration, and reproduced here in Figure 4.8. Furthermore, Figure 4.8 shows that the normal force coefficient due to the pitch rate, C_{Z_q}, decreases to almost half of its initial value, decreasing more than the pitching moment coefficient due to pitch rate, C_{m_q}. From this observation follows the justification of the decrease in the angle of attack per 'g' as seen in Figure 4.6.

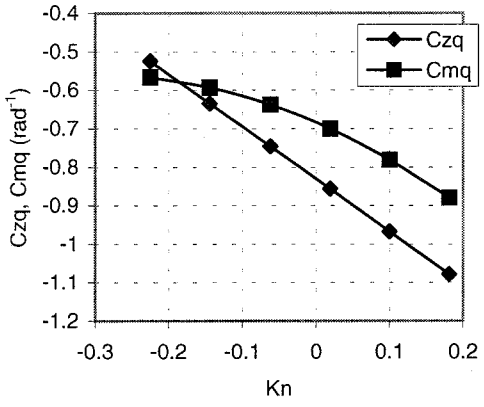

Figure 4.8 BWB3 rotational derivatives function of the static margin

One last point seems worthy to mention here. From Cook and Castro[98] the manoeuvre point of configuration BWB3 is given as being at $h_m = 0.407\,mac$ and was considered normal when compared with conventional aircraft. On the other hand, the neutral point was determined from CFD data as $h_n = 0.297\,mac$. Subtracting these two values, it gives a distance of 0.11 *mac* between the neutral and manoeuvre points. This result seems slightly lower than that for conventional aircraft and may explain some of the BWB characteristics as mentioned in Chapter 1.

4.3 Lateral-directional motion

4.3.1 Lateral static stability

In any stability book[99 to 103] it can be found that the lateral static stability is concerned with the aircraft ability to maintain wings level equilibrium in the roll sense. Wing dihedral is the most visible parameter that confers static stability on an aeroplane, and the easiest parameter to adjust in the design process in order to "tune" the degree of stability to an acceptable level. It can also be found that the condition for an aeroplane to be laterally stable is that the rolling moment resulting from a positive disturbance in roll attitude must be negative, as given by equation (4.10).

$$C_{l_\phi} = \frac{dC_l}{d\phi} < 0 \quad \text{or} \quad C_{l_\beta} = \frac{\partial C_l}{\partial \beta} < 0 \tag{4.10}$$

Although being of a different layout compared with conventional configurations dihedral effect is present to the same degree. Thus, the same amount of lateral static stability as for conventional configurations would be expected. Other factors, for example high angles of sweepback, may change the BWB lateral static stability.

From Figure 4.9 it can be seen that all except the BWB2 configuration possess lateral static stability. Moreover, for the lateral stable configurations, the lateral static stability increases with angle of attack. Although lateral static stability is desirable, too much static stability can also be detrimental as it makes roll control more difficult, so the right balance has to be found.

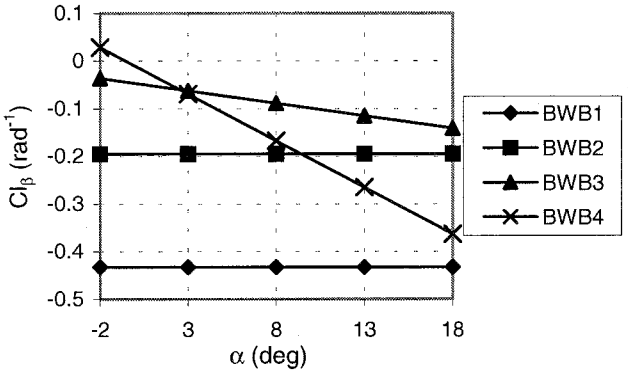

Figure 4.9 Levels of lateral static stability for four BWB aircraft

Configuration BWB1 possesses the highest basic lateral static stability of the four configurations, probably as a result of the conventional approximate methods used in its estimation[76 to 83]. Lateral static stability derivatives for configurations BWB3 and BWB4 were obtained for the same planform, although by different processes as explained in Chapter 3, and they present the most consistent results. As a conclusion, the values of Figure 4.9 indicate that lateral static stability should not present a problem for blended-wing-body configurations.

4.3.2 Directional static stability

Directional static stability is concerned with the aircraft's ability to yaw or weathercock into wind in order to maintain directional equilibrium. The fin is the most visible contributor to directional static stability, although there are many other contributions some of which are destabilizing. A yawing moment is stable and so restoring, if it causes the aeroplane to yaw in the sense to reduce the disturbing sideslip angle. The mathematical condition for directional static stability is given by equation (4.11).

$$C_{n_\beta} = \frac{dC_n}{d\beta} > 0 \qquad (4.11)$$

Directional static stability is not only a function of angle of attack, but also of the *cg* position, as can be seen from the BWB3 and BWB4 configuration data, Figure 4.10.

As the *cg* is moved aft the distance to the aerodynamic centre of the fins decrease, and so the yawing moment arm also decreases resulting in a decrease in directional static stability, possibly becoming unstable for the most aft *cg* positions.

From Figure 4.10 it can be seen that the directional static stability degrades with angle of attack. The highest directional static stability value is for configuration BWB2, as expected, since this configuration possesses the largest vertical surfaces, more similar to those of conventional aircraft.

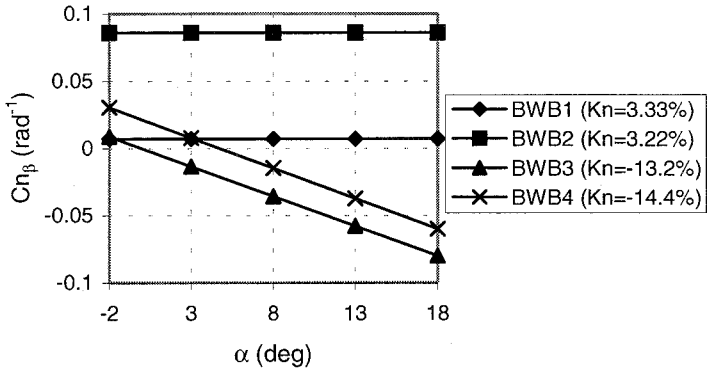

Figure 4.10 Levels of directional static stability for four BWB

From here it is concluded that directional static stability is critical for blended-wing-body configurations, as reviewed in Chapter 1, principally because vertical surfaces are near to the *cg* and decreased to a minimum area or even do not exist at all. Stability augmentation will probably be needed to restore directional static stability in some, if not all, configurations to acceptable levels.

4.3.3 Trimmability

The ability to trim in lateral-directional sense is not so important as in the longitudinal sense, because the aircraft is not to be flown asymmetrically, except for turns, in crosswinds and in case of asymmetric thrust as a result of an engine failure. Actually, the two latter cases constitute very important requirements within the civil requirements, as can be seen in Appendix A, paragraph A1, and are usually critical in fin and rudder design. The case of turns, although not so much, is still important, principally concerning the rate of roll needed to acquire a determined bank angle and the possibility for coordinating turns. These aspects of lateral control represent the critical cases for aileron design, however these are more in the dynamics domain and will be analysed later.

4.3.3.1 Engine failure

An engine failure will result in an unbalanced yawing moment, which will have to be compensated by control surface deflections. In principle only the rudder is used to compensate for the yawing moment, however, when rudders are deflected rolling moment is generated which is then compensated with aileron deflection, resulting in a non-zero bank angle. The engine failure case is represented by equations (4.12) and (4.13).

$$T \times d_T = \frac{1}{2}\rho S V^2 b\left(C_{n_\beta}\beta + C_{n_p}p + C_{n_r}r + C_{n_\xi}\xi + C_{n_\varsigma}\varsigma\right) \tag{4.12}$$

$$C_l = C_{l_\beta}\beta + C_{l_p}p + C_{l_r}r + C_{l_\xi}\xi + C_{l_\varsigma}\varsigma \tag{4.13}$$

Where T is the value of thrust generated by the asymmetric operating engine and d_T is the normal lateral offset of the thrust line to the *cg* of the same operating engine. When the yawing moment generated by the asymmetric thrust is fully compensated with rudder and aileron, the aircraft will be in a trimmed symmetric steady flight. Thus, the roll and yaw rate, sideslip angle and rolling moment are all zero. Substituting these values in equations (4.12) and (4.13), and solving the equations for the rudder and aileron deflection, results in equations (4.14) and (4.15).

$$\varsigma = \frac{2Td_T}{\rho S V^2 b\left(C_{n_\varsigma} - C_{n_\xi}\dfrac{C_{l_\varsigma}}{C_{l_\xi}}\right)} \tag{4.14}$$

$$\xi = -\frac{C_{l_\varsigma}}{C_{l_\xi}}\zeta \tag{4.15}$$

$\left(C_{n_\varsigma} - C_{n_\xi}\dfrac{C_{l_\varsigma}}{C_{l_\xi}}\right)$ of equation (4.14) is the determining factor for the engine failure case. If the rudders were perfect, all rudder deflection would solely be used for yawing moment generation. However, deflecting the rudder always induces some rolling moment which is balanced with the aileron deflection. The ailerons in turn, when deflected, also produce some yawing moment which may be favourable or unfavourable. In the latter case, part of the rudder deflection will then be used to compensate for the ailerons. How much this is necessary depends on the adverse yaw and roll effects of the ailerons and rudders, respectively. Table 4.2 shows some of the components of equation (4.14) for the four BWB configurations and from which inference concerning control effectiveness may be made.

	C_{n_ζ}	C_{n_ξ}	$\frac{C_{l_\zeta}}{C_{l_\xi}}$	$-C_{n_\xi}\frac{C_{l_\zeta}}{C_{l_\xi}}$
BWB1	-0.0087	0.0093	-0.0125	-0.00012
BWB2	-0.0344	0.0017	-0.0518	-0.00001
BWB3	-0.0092	0.0052	-0.1135	-0.0006
BWB4	-0.0158	0.0041	-0.1145	-0.00047

Table 4.2 Lateral-directional control derivatives

An important fact relating to equation (4.14) is that the reference area used is different for each BWB configuration. For BWB1 and BWB2 the gross wing area was used while for BWB3 and BWB4 the trapezoidal wing area was used. With reference to Figure 4.11 this explains why the BWB1 configuration has lower rudder deflections than the BWB3 configuration, although having a weaker rudder. Moreover, BWB4 configuration although having a lower reference area than that used for the BWB1, has a control rudder derivative as high as the BWB1, hence, the similarity between the BWB4 and BWB1 rudder deflections. The BWB2 configuration has the highest control rudder derivative, more than twice of the BWB4 configuration, and thus also has the lowest rudder deflection necessary to counteract the asymmetric thrust effect.

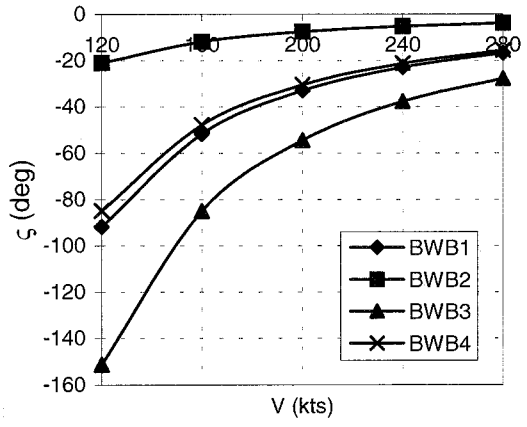

Figure 4.11 Rudder angle to trim an engine failure versus speed

Figure 4.12 shows the corresponding aileron deflection to trim following engine failure. Figure 4.12 correlates well with Table 4.2 and the results shown on Figure 4.11. The BWB3 configuration needs the highest rudder deflection. Since Table 4.2 shows the highest rolling moment coefficient due to rudder and aileron ratio for BWB3, this is the configuration where more ailerons need to be deflected in an engine failure manoeuvre. As the BWB4 configuration is similar, it also shows similar results. Although the BWB1 configuration has slightly higher rudder deflections than BWB4, it has a lower rolling moment coefficient due to rudder and aileron ratio, and so it has very low aileron demands.

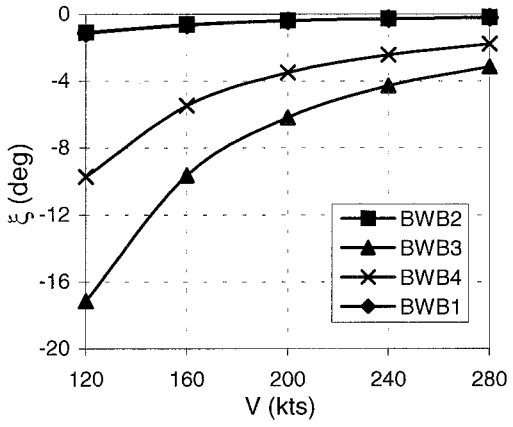

Figure 4.12 Aileron angle to trim an engine failure versus speed

From the four blended-wing-body configurations only the BWB2 configuration shows acceptable values of rudder and aileron deflection to compensate for an engine failure. Furthermore, in this analyse the value of thrust and engine offset from the centreline was, for convenience, taken to be the same for all aircraft. However, BWB2 actually has its engines closer to the centreline with a smaller offset than the value used here. Thus, for the real BWB2 design, even lower values of what was here obtained would be expected.

4.3.3.2 Crosswind

The crosswind case is not of so easy treatment as the engine failure, since both the rudder and aileron are used to compensate for moments generated both in the roll and yaw axes, due to the asymmetric flight. The general equations for the aerodynamic rolling and yawing moment coefficients are given by equations (4.16) and (4.17).

$$C_l = C_{l_\beta}\beta + C_{l_p}p + C_{l_r}r + C_{l_\xi}\xi + C_{l_\varsigma}\varsigma \tag{4.16}$$

$$C_n = C_{n_\beta}\beta + C_{n_p}p + C_{n_r}r + C_{n_\xi}\xi + C_{n_\varsigma}\varsigma \tag{4.17}$$

$$\beta = \tan^{-1}\left(\frac{V_g}{V_o}\right) \cong \frac{V_g}{V_o} \tag{4.18}$$

For small perturbations a crosswind can be converted into a sideslip angle when dividing it by the forward speed, as shown in equation (4.18) where V_g is the speed of the crosswind gust. In trimmed steady sideslip flight the roll and yaw rate are null, as well as the total rolling and yawing moments. Thus, the rudder and aileron positions can be found by solving the above system of two equations, equation (4.16) and

equation (4.17). The resulting solution is given for the aileron angle by equation (4.19), and for the rudder angle by equation (4.20).

$$\xi = \frac{C_{l_\varsigma} C_{n_\beta} \beta - C_{n_\varsigma} C_{l_\beta} \beta}{C_{l_\xi} C_{n_\varsigma} - C_{l_\varsigma} C_{n_\xi}} \tag{4.19}$$

$$\varsigma = \frac{C_{n_\xi} C_{l_\beta} \beta - C_{l_\xi} C_{n_\beta} \beta}{C_{l_\xi} C_{n_\varsigma} - C_{l_\varsigma} C_{n_\xi}} \tag{4.20}$$

The rolling and yawing moments due to sideslip angle are, respectively, $C_{l_\beta}\beta$ and $C_{n_\beta}\beta$, and it is these which must be compensated by control deflection. Thus, the higher the lateral and directional stability, the higher the rudder and aileron deflections have to be in order to compensate for the crosswind. In principle, aileron deflections will compensate mainly for the rolling moment generated while rudder deflections will compensate for the yawing moment generated. Thus, high lateral stability will require higher aileron deflections, and high directional stability will require higher rudder deflections. However, due to the adverse yaw and adverse roll generated by the deflection of ailerons and rudders this generalisation may not always be true.

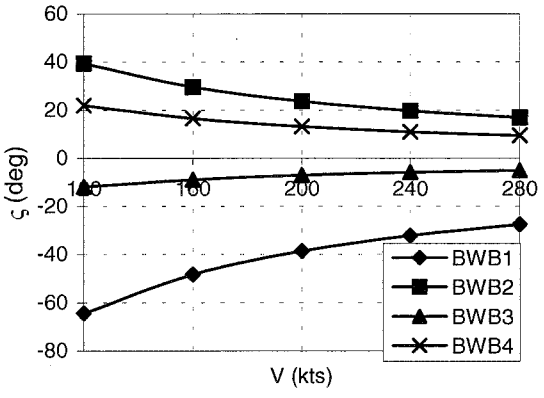

Figure 4.13 Rudder angle to trim a crosswind of 30deg versus speed

From Figure 4.10 it was seen that the BWB2 has the highest directional static stability followed by the BWB4 and then the BWB1 configuration. The BWB3 configuration has the lowest directional static stability, since it is actually directionally unstable. For the BWB2, BWB3 and BWB4 configurations, Figure 4.13 correlates well with this observation, since greater rudder deflection for the BWB2 configuration is necessary, and less for the BWB3 configuration, the least stable. However, BWB1 does not correlate with this because although it has the lowest directional static stability, it needs the highest rudder deflection to compensate for the crosswind. An inspection to Figure 4.14 reveals why this is so.

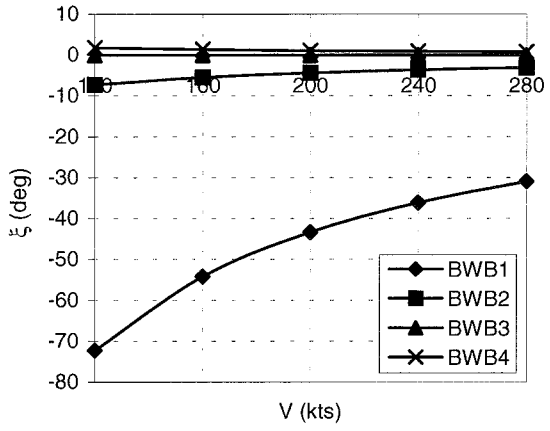

Figure 4.14 Aileron angle to trim a crosswind of 30deg versus speed

From Figure 4.9 it was seen that configuration BWB1 had the highest lateral stability, followed by the BWB2, BWB3, and BWB4 configurations, being the configuration with the lowest lateral static stability (at zero angle of attack). From here it is not surprising to find in Figure 4.14 that the BWB1 configuration has not only the largest aileron deflections of the four configurations, but also that these deflections exceed the maximum limits for ailerons to compensate for the crosswind. This aileron deflection also induces a yawing moment, which has to be compensated with rudder, which explains the large amount of rudder deflection required as shown in Figure 4.11 for the BWB1 configuration.

On the other hand, Figure 4.14 shows that the BWB3 configuration needs less aileron deflection than the BWB4 configuration, although the BWB3 configuration has the higher lateral static stability. This is explained in the same way as for the BWB1 configuration. From Figure 4.13, the BWB4 configuration needs more rudder deflection, and from Table 4.2 it may be seen that the BWB4 configuration has the highest rudder adverse roll, which means that it needs more aileron deflection to compensate for the same amount of adverse roll. Since the BWB3 configuration does not deflect its rudder so much, the amount of aileron to compensate for the rudder adverse roll is smaller, and thus the total aileron deflection is less than that for the BWB4 configuration.

4.4 Control allocation

Through the entire chapter it was shown that the control power available, at the moment, is not enough. However, so far only the conventional control surfaces were considered. i.e., ailerons to control roll, rudder to control yaw and elevators to control pitch. This is the classical view of a single moment generating controller designed to

control a single rotational degree-of-freedom (DOF). However, nowadays, high performance as well as large aircraft possess other control surfaces such as leading edge flaps, trailing edge flaps, spoilers each left and right and operating independently, vertical lift, side-force generators, and even thrust vectoring is in common use nowadays. A future BWB aircraft will also possess some or all of these "extra" controls.

Then, these several controls need to be allocated, or blended, in order to achieve specific objectives, actually, that of controlling the aircraft. This allocation of the control surfaces is known as the control allocation problem. In control allocation the several possible controls are viewed as pure moment generators constrained to certain physical limits as geometry of the actuators, or aerodynamic considerations. Taking account the pure moment generated and the physical constraints, admissible control deflections are determined using allocation methods so that will generate the desired moments.

4.5 Summary

At the beginning of this chapter it was stated that nowadays controls fixed static stability and manoeuvrability analysis is not so much about positive or negative static and manoeuvre margins, but more about having enough control power available to trim and manoeuvre the aircraft in all flight conditions. Taking this into consideration limited trimmability and manoeuvrability studies were completed.

It was then found that some of the present BWB configurations almost reach or even exceed their control power available either to trim and, or to manoeuvre at low speeds. On one hand, large elevator angles to trim and to manoeuvre were found necessary principally for the BWB3 and BWB4 configurations, almost reaching saturation. While, on the other hand, high angles of attack to trim and to manoeuvre, already in the non-linear regime, were found necessary for BWB1 and BWB2 configurations. In the lateral-directional motion the picture was even worse. To trim an engine failure, BWB1, BWB3 and BWB4 needed more rudder control power than available, while, BWB1 and BWB2 reached rudder saturation on trimming a crosswind asymmetric flight.

However, it must not be forgotten that in the previous chapter some of the data was calculated on the assumption that linear flow existed. However, linear flow cannot be assured near control saturation and at high angles of attack. Thus, care must be taken with these results since they are valid only for well-behaved flow. In reality, near

saturation and at high angles of attack other effects may be present and the picture may be worse than that presented here.

CHAPTER 5
Longitudinal dynamic stability of the unaugmented blended-wing-body aircraft

"A theory which is properly founded does not require to be quantitatively complete in order to constitute an adequate guide to scientific laboratory investigation."
F. W. Lanchester, "*The flying machine*"

5.1 Overview

Dynamic stability is a very important field for the understanding of aircraft flying and handling qualities. As seen in the historical introduction of Chapter 2, the understanding and limitation of dynamic stability parameters was the first attempt to get aircraft flying and handling qualities right. Although flying qualities requirements have changed since then, dynamic stability parameters remain the basis of such requirements. Therefore, a good understanding of what dynamic stability means and knowing the dynamic stability characteristics of blended-wing-body configurations is very important as a way to understand the flying and handling qualities of these configurations.

While static stability determines the steady state, or trim, of an aircraft, the dynamic stability is related to the dynamic, or transient, part of the aircraft response to pilot or disturbance inputs. Therefore, although the steady state is the ultimate objective of a pilot, the way an aircraft behaves to reach that end, i.e. the transient response, may be more determinative for pilots when assessing a certain configuration for accomplishing a specified task. Moreover, in certain tasks such as tracking, or combat flight, the pilot is continuously inputting commands, thereby rendering the steady

state response less importance and increasing that of the dynamic response. This explains why dynamic stability is so important in the assessment of flying and handling qualities and why the formal civil requirements are limited, since they make no explicit reference to dynamic stability parameters.

Now, since dynamic stability defines the transient response of a system, its characteristics are not dependent on just a few basic aerodynamic parameters, but on the more complex relationships and interaction of all characteristics. The equations of motion represent the complete analytical source of an aircraft response, both transient and steady state, to pilot inputs. However, the analysis of the complete non-linear equations of motion is very complex. Thus, the usual approach is to assume small perturbations and to linearize the equations of motion around a flight condition, to obtain the well-known state space model. A further simplification is to separate the longitudinal motion from the lateral-directional motion due to the symmetry of the airframe.

Since many books on aircraft stability[99 to 103] present all necessary theory, this will not be repeated here and possible questions on these matters are forwarded to these references. Once the longitudinal and lateral-directional state space matrices are established, the transfer functions representing the aircraft response to inputs can be obtained through Laplace transforms, a procedure also well established and presented in the same books.

A first important observation of aircraft response transfer functions is that the denominator is common to all of the longitudinal or lateral-directional transfer functions, although its coefficients may vary in value with flight condition. These common longitudinal and lateral-directional denominators are also the characteristic polynomials and they describe the stability of the aeroplane. The second important observation is that the numerators of each response transfer function are different and describe the differences in the response shapes. It may be concluded that stability is about the provision of safe, controllable aeroplanes: it determines the "general shapes" of the response variables and is governed by the common denominator of the response transfer functions. On the other hand, handling is about the provision of the correct relationships between input and output, the "shapes" of the response variables, and is governed by the unique numerators in combination with the common denominator of the response transfer functions.

Although linearization of the equation of motion and the state space and transfer functions approach simplifies analysis a great deal, before the advent of digital

computers such an approach was analytically complex for dynamic stability analysis and reduced order models were used instead to give initial valuable insight into the physical phenomena governing the dynamical behaviour of aircraft. Reduced order models are used in this research to find out in which way stability parameters are influenced by the aerodynamic parameters. With this approach it is possible to understand the differences between the blended-wing-body aircraft and conventional configurations. With this knowledge, and using the criteria presented in Chapter 2, it will be possible to assess flying and handling qualities and to identify the deficiencies to overcome.

The possibility of separating the longitudinal and lateral-directional aircraft motion makes it easier to analyse and understand the aircraft behaviour. The longitudinal dynamics are dealt in this chapter, whilst the lateral-directional dynamics are dealt with in the next chapter. The longitudinal dynamics are important since the pilot flies in the aircraft plane of symmetry most of the time. Moreover, it is by the longitudinal motion that forward speed and altitude are controlled.

5.2 Longitudinal equations of motion

With the advent of digital technology, the calculation and manipulation of matrices and more complex equations became much quicker and easier. The longitudinal linearized equations of motion in state space form as taken from Cook[99], are presented in equation (5.1). The coefficients of the matrices are the aerodynamic and control stability derivatives, referred to aeroplane body axes, in concise form.

$$\begin{bmatrix} \dot{u} \\ \dot{\alpha} \\ \dot{q} \\ \dot{\theta} \end{bmatrix} = \begin{bmatrix} x_u & x_w V_o & x_q & x_\theta \\ z_u/V_o & z_w & z_q/V_o & 0 \\ m_u & m_w V_o & m_q & 0 \\ 0 & 0 & 1 & 0 \end{bmatrix} \begin{bmatrix} u \\ \alpha \\ q \\ \theta \end{bmatrix} + \begin{bmatrix} x_\eta \\ z_\eta/V_o \\ m_\eta \\ 0 \end{bmatrix} \eta \qquad (5.1)$$

The longitudinal dynamics of the four blended-wing-body configurations were calculated using the landing approach flight condition as presented in Table 5.1. General characteristics of each configuration for this flight condition are presented in Table 5.2.

FLIGHT CONDITION DATA	
Altitude h (ft)	0
Velocity V_e (m/s)	100.0
Mach number M_e	0.294

Table 5.1 Flight condition data for a landing approach

Referring to Table 5.2, two points are highlighted; firstly, since there was no information on the pitching moment and lift coefficient due to pitch rate, C_{m_q} and C_{L_q}, these were assumed zero in the first instance. Later, a parametric flight dynamic study was done using a range of values, as given in brackets for BWB1 and BWB2 configuration. Secondly, the pitch moment of inertia for the BWB2 configuration as presented in Appendix B was reduced by a factor of 10^3 because no consistent confirmation could be obtained for the value in Appendix B.

	BWB1	**BWB2**	**BWB3**	**BWB4**
Mass m (Kg)	322,599	460,869.0	371,280.0	371,280.0
I_y **(Kg.m2)**	32.63 x 10^6	52.83 x 10^6	25.40 x 10^6	25.40 x 10^6
Static margin K_n	0.033	0.0322	0.019	-0.142
α_e **(deg)**	7.69	7.49	8.49	3.58
η_e **(deg)**	-2.75	0.91	-4.44	0.51
C_{L_q}	(0.0/0.5)	(0.0/0.5)	1.0964	2.9862*
C_{m_q}	(0.0/-0.3/-0.6)	(0.0/-0.3/-0.6)	-0.7001	-2.5395*
* Refers to $C_{L_{\hat{q}}}$ and $C_{m_{\hat{q}}}$, respectively, where $\hat{q} = qV/2\bar{c}$				

Table 5.2 Landing approach data for several BWB configurations

Substituting for the data of the several blended-wing-body configurations and landing approach flight condition, typical values for the A and B matrices of the linear state equation resulted, as presented in Table 5.3.

	A	**B**
BWB1	$\begin{bmatrix} -0.0188 & -6.0736 & -13.3897 & -9.7183 \\ -0.0020 & -0.8705 & 0.9910 & -0.0131 \\ 0 & -1.3289 & 0 & 0 \\ 0 & 0 & 1 & 0 \end{bmatrix}$	$\begin{bmatrix} 0 \\ -0.4321 \\ -3.0499 \\ 0 \end{bmatrix}$
BWB2	$\begin{bmatrix} -0.0201 & -6.4497 & -13.3897 & -9.7230 \\ -0.0020 & -0.6600 & 0.9910 & -0.0128 \\ 0 & -0.4869 & 0 & 0 \\ 0 & 0 & 1 & 0 \end{bmatrix}$	$\begin{bmatrix} 0 \\ -0.2354 \\ -2.5640 \\ 0 \end{bmatrix}$
BWB3	$\begin{bmatrix} -0.0238 & -11.3900 & -14.7658 & -9.6992 \\ -0.0020 & -0.7535 & 0.9744 & -0.0145 \\ 0 & -0.2560 & -0.2153 & 0 \\ 0 & 0 & 1 & 0 \end{bmatrix}$	$\begin{bmatrix} 0 \\ -0.1667 \\ -1.8009 \\ 0 \end{bmatrix}$
BWB4	$\begin{bmatrix} -0.0238 & -12.1122 & -6.2459 & -9.7875 \\ -0.0020 & -0.8086 & 0.9470 & -0.0061 \\ 0 & 1.8480 & -0.7810 & 0 \\ 0 & 0 & 1 & 0 \end{bmatrix}$	$\begin{bmatrix} 0 \\ -0.3135 \\ -1.7892 \\ 0 \end{bmatrix}$

Table 5.3 State equation matrices A and B for a landing approach flight condition

5.3 Transfer functions

The Laplace transform method was developed to make it easy to calculate the equations of motion solution. This method transforms the differential equations into algebraic equations expressed in terms of the Laplace operator s. To calculate then the equations of motion solution it is necessary only to solve a system of simultaneous linear algebraic equations. From this solution input-output response relationships, or transfer functions, in terms of the Laplace operator s result. To calculate the time response solution inverse Laplace transform must be applied to the transfer function of interest.

Nowadays, digital computers can calculate the equations of motion time solution directly from the equations of motion. Thus, it would be concluded that transfer functions and Laplace transform are no more in use. However, transfer functions are the principal tool of the control system engineer. Besides, transfer functions can rapidly give a picture of the system dynamic behaviour, principally stability, and are the basis of frequency response information. Thereafter, transfer functions are still an important tool, and are presented next. Equations from (5.2) to (5.5), taken from Cook[99], represent the longitudinal transfer functions, i.e. dynamic relationships between the input variable, the elevator deflection, and the output variable, any of the longitudinal variables. The numerators and denominators factorisation presented in equations (5.2) to (5.5) are typical of a conventional aircraft. These may not be representative of the blended-wing-body transfer functions.

$$\frac{u(s)}{\eta(s)} = \frac{N_\eta^u(s)}{\Delta(s)} = \frac{k_u\left(s+1/T_u\right)\left(s^2+2\zeta_u\omega_u s+{\omega_u}^2\right)}{\left(s^2+2\zeta_p\omega_p s+{\omega_p}^2\right)\left(s^2+2\zeta_s\omega_s s+{\omega_s}^2\right)} \tag{5.2}$$

$$\frac{\alpha(s)}{\eta(s)} = \frac{N_\eta^\alpha(s)}{\Delta(s)} = \frac{k_\alpha\left(s+1/T_\alpha\right)\left(s^2+2\zeta_\alpha\omega_\alpha s+{\omega_\alpha}^2\right)}{\left(s^2+2\zeta_p\omega_p s+{\omega_p}^2\right)\left(s^2+2\zeta_s\omega_s s+{\omega_s}^2\right)} \tag{5.3}$$

$$\frac{q(s)}{\eta(s)} = \frac{N_\eta^q(s)}{\Delta(s)} = \frac{k_q s\left(s+1/T_{\theta_1}\right)\left(s+1/T_{\theta_2}\right)}{\left(s^2+2\zeta_p\omega_p s+{\omega_p}^2\right)\left(s^2+2\zeta_s\omega_s s+{\omega_s}^2\right)} \tag{5.4}$$

$$\frac{\theta(s)}{\eta(s)} = \frac{N_\eta^\theta(s)}{\Delta(s)} = \frac{k_\theta\left(s+1/T_{\theta_1}\right)\left(s+1/T_{\theta_2}\right)}{\left(s^2+2\zeta_p\omega_p s+{\omega_p}^2\right)\left(s^2+2\zeta_s\omega_s s+{\omega_s}^2\right)} \tag{5.5}$$

As shown from equation (5.2) to equation (5.5), each transfer function is written as a ratio of two polynomials; a unique numerator, such as $N_\eta^u(s)$ or $N_\eta^q(s)$, and a denominator common to all transfer functions, $\Delta(s)$, also called the characteristic polynomial. In Tables 5.4 and 5.5 the numerators and denominators for the four BWB aircraft in the landing approach flight condition are presented.

	BWB1	BWB2
$N_\eta^u(s)$	$43.5s(s+0.3232)(s+1.4222)\ (m/s)$	$34.9s(s+0.2929)(s+1.4787)\ (m/s)$
$N_\eta^\alpha(s)$	$-0.43([0.1067,0.1379])(s+6.9837)\ (rad)$	$-0.24([0.1134,0.1378])(s+10.7902)\ (rad)$
$N_\eta^q(s)$	$-3.05s(s+0.0013)(s+0.6997)\ (rad/s)$	$-2.56s(s-0.0004)(s+0.6358)\ (rad/s)$
$N_\eta^\theta(s)$	$-3.05(s+0.0013)(s+0.6997)\ (rad)$	$-2.56(s-0.0004)(s+0.6358)\ (rad)$
$\Delta(s)$	$([0.0707,0.1395])([0.3836,1.1335])\ (rad)$	$([0.0191,0.1411])([0.4975,0.6781])\ (rad)$

Table 5.4 Longitudinal transfer function numerators and denominator for BWB1 and BWB2

Comparing the conventional numerators of equations (5.2) to (5.5) with those presented for the BWB configurations in Tables (5.4) and (5.5) it can be concluded that except for $N_\eta^u(s)$, all the other BWB numerators present the same factorisation. $N_\eta^u(s)$, although not having a pair of complex roots, still has the same number of roots as for conventional aircraft. This reveals that the individual characteristic of each response as given by the transfer function numerator may be equal to that of conventional aircrafts.

	BWB3	BWB4
$N_\eta^u(s)$	$28.5s(s+0.2480)(s+1.7621)\ (m/s)$	$15.0s(s+0.4152)(s+3.1684)\ (m/s)$
$N_\eta^\alpha(s)$	$-0.17([0.1336,0.1371])(s+10.7286)\ (rad)$	$-0.31([0.1004,0.1326])(s+6.1834)\ (rad)$
$N_\eta^q(s)$	$-1.8s(s-0.0065)(s+0.7602)\ (rad/s)$	$-1.79s(s+0.0028)(s+1.1534)\ (rad/s)$
$N_\eta^\theta(s)$	$-1.8(s-0.0065)(s+0.7602)\ (rad)$	$-1.79(s+0.0028)(s+1.1534)\ (rad)$
$\Delta(s)$	$([-0.0342,0.1082])([0.7827,0.6388])\ (rad)$	$(s-0.5904)([0.2368,0.1675])(s+2.1244)\ (rad)$

Table 5.5 Longitudinal transfer function numerators and denominator for BWB3 and BWB4

5.4 Longitudinal characteristic modes

5.4.1 Characteristic modes analysis

The characteristic polynomial when equated to zero defines the characteristic equation, $\Delta(s)=0$. The longitudinal characteristic equation completely describes the longitudinal characteristic modes; the short period and the long period phugoid modes. Table 5.6 present the short period and phugoid modes of the four BWB configurations in the landing approach flight condition defined above.

In Table 5.6 it is seen that the BWB1 and BWB2 configurations, which have the largest positive static margins, are the ones that have both the short period and the phugoid mode stable. The BWB3 configuration with a *cg* position very close to the

neutral point, $K_n = 0.019$, although having a stable short period mode, its phugoid is unstable (positive pair of complex roots). Lastly, the BWB4 configuration which has the largest negative static margin, $K_n = -0.142$, has an unstable short period mode, although its phugoid mode is stable. The incidence lag, T_{θ_2}, is also presented in Table 5.6. The incidence lag is, actually, the second zero of the pitch rate to elevator control transfer function, $1/T_{\theta_2}$, as shown in equations (5.4) and (5.5) and another important flight dynamic characteristic for flying and handling qualities.

	K_n	**Short period mode**		**Phugoid mode**		T_{θ_2} (sec)
		ζ_s	ω_s (rad/s)	ζ_p	ω_p (rad/s)	
BWB1	0.033	0.384	1.13	0.0707	0.139	1.43
BWB2	0.032	0.497	0.678	0.0191	0.141	1.57
BWB3	0.019	0.783	0.639	-0.0342**	0.108**	1.32
BWB4	-0.142	(-0.472)*	(+1.7)*	0.237	0.168	0.867
* Time constants, in seconds, of two real roots: one positive (unstable) and other negative (stable) ** Pair of positive complex roots with negative damping (unstable mode)						

Table 5.6 Longitudinal characteristic modes and incidence lag for four BWB

In general, it can be said that the blended-wing-body longitudinal dynamic stability characteristics are similar to those of conventional aircraft. Cook and Castro[98] obtained similar results for a BWB3 configuration with about a static margin of $K_n = 0.1$ in a landing approach flight condition. Further, Cook and Castro[98] analysed the variation of the characteristic longitudinal modes of the BWB3 configuration with *cg* position and speed. They concluded that the levels of stability deteriorate rapidly as the *cg* moves aft, and the static margin becomes negative.

It was also found that the short period undamped natural frequency had it highest value for the most forward *cg* position and decreases to about half that value at a mid *cg* position around the neutral point. The short period damping ratio increases until it becomes critically damped at the mid *cg* position. For further aft *cg* positions two real roots replace the short period mode, one of which is positive, and so the mode is unstable. With respect to variation in speed, the short period frequency increases significantly with increasing speed, whilst the short period damping ratio decreases, but rather slightly.

For the phugoid mode it was found that the undamped natural frequency and damping ratio decrease with aft *cg* to become unstable at a mid *cg* position, around the neutral point, becoming stable again for further aft *cg* movements. This variation in damping with *cg* movement becomes almost unnoticed at higher speeds. However, the phugoid frequency also increases with increasing speed.

5.4.2 Reduced order models

As stated in the introduction, with the advent of digital computers and programs such as Matlab[104] it became easy to handle the linearized small perturbations equations of motion, and even the complete non-linear equations of motion. Although this progress made calculations quicker and faster, insight into the parameters that most influence the characteristic modes was lost.

The longitudinal small perturbation equations of motion were established to help to understand the aircraft behaviour. Although simpler than the complete non-linear equations of motion, they were still difficult to handle, before the advent of digital computers. Reduced order models were then used to more easily estimate the characteristic modes. The reduced order models still constitute today a better means to identify the longitudinal modes, to understand their mechanisms and to identify the derivatives that most influence them. However, since the reduced order models were developed for conventional aircraft, before applying them to blended-wing-body configurations it is necessary to revise the simplifying assumptions used in the reduced models to confirm they still apply to blended-wing-body configurations.

5.4.2.1 Short period reduced order model

The longitudinal response usually comprises two oscillatory modes: the short period motion and the long period phugoid motion. As its name says, the long period phugoid motion usually comprises a rather long period, and thus is usually of no concern to the pilot. Therefore, as the short period motion is the most important for flying and handling qualities, only the short period mode approximation will be considered here. This reduced order model is based on the short period nature of this mode, sometimes also called the "rapid incidence adjustment". Thus, it is not surprising to find that the terms in the reduced order equations are those dominant in the short term dynamics, actually pitch rate and angle of incidence. The reduced order model state equation has given by Cook[99] in non-dimensional parameters is presented here in equation (5.6).

$$\begin{bmatrix} \dot{w} \\ \dot{q} \end{bmatrix} = \begin{bmatrix} z_w & z_q \\ m_w & m_q \end{bmatrix} \begin{bmatrix} w \\ q \end{bmatrix} + \begin{bmatrix} z_\eta \\ m_\eta \end{bmatrix} \eta \tag{5.6}$$

$$\frac{w(s)}{\eta(s)} = \frac{z_\eta \left(s - \left(m_q - z_q \frac{m_\eta}{z_\eta} \right) \right)}{s^2 - (m_q + z_w)s + (m_q z_w - m_w z_q)} \tag{5.7}$$

$$\frac{q(s)}{\eta(s)} = \frac{m_\eta\left(s + \left(m_w \frac{z_\eta}{m_\eta} - z_w\right)\right)}{s^2 - (m_q + z_w)s + (m_q z_w - m_w z_q)} \tag{5.8}$$

$$\Delta(s) = s^2 + 2\zeta\omega s + \omega^2 = s^2 - (m_q + z_w)s + (m_q z_w - m_w z_q) = 0 \tag{5.9}$$

Applying Laplace transform to the reduced state equation, equation (5.6), and solving for the two state variables, the two transfer functions as presented in equations (5.7) and (5.8) result. As presented in equation (5.9), the common denominator of the transfer functions gives the characteristic equation when equated to zero. The short period frequency and damping result then from solving equation (5.9). These are presented in equations (5.10) and (5.11).

$$\omega_s{}^2 = (m_q z_w - m_w z_q) \tag{5.10}$$

$$2\zeta_s\omega_s = -(m_q + z_w) \tag{5.11}$$

A simplification is presented in equation (5.12) based on the usual magnitude of conventional aerodynamic properties, as shown on equation (5.13). $\overset{o}{Z}_q$ and $\overset{o}{Z}_{\dot{w}}$ are derivatives largely dependent on tail surface. Therefore, these derivatives have lower values for tailless aircraft than for conventional configurations. For the particular case of this research, because insufficient data is available, $\overset{o}{Z}_{\dot{w}}$ is considered null for all configurations. Thus, it is completely right to assume that $m >> \overset{o}{Z}_{\dot{w}}$

$$z_q = \frac{\overset{o}{Z}_q + mU_e}{m - \overset{o}{Z}_{\dot{w}}} \cong U_e \tag{5.12}$$

$$\text{Since } \overset{o}{Z}_q << mU_e \text{ and } m >> \overset{o}{Z}_{\dot{w}} \tag{5.13}$$

On the other hand, since the mission tasks are still the same, the speed values, U_e, are also of the same order as for conventional aircraft. Moreover, the tailless aircraft mass is larger than that of conventional aircraft, as shown in Table 5.2, since larger dimensions are considered in the design of this configuration. Therefore, it is still valid to consider $\overset{o}{Z}_q << mU_e$ for BWB as well. Thus, introducing simplification of equation (5.12) into equation (5.10), follows that the short period frequency, ω_s, and damping, ζ_s, are, in terms of dimensional derivatives, as given in equations (5.14) and (5.15).

$$\omega_s{}^2 = \frac{\overset{o}{M}_q}{I_y}\frac{\overset{o}{Z}_w}{m} - \frac{\overset{o}{M}_w U_e}{I_y} \tag{5.14}$$

$$2\zeta_s\omega_s = -\left(\frac{\overset{o}{M}_q}{I_y} + \frac{\overset{o}{Z}_w}{m} + \frac{\overset{o}{M}_{\dot{w}} U_e}{I_y}\right) \tag{5.15}$$

As before, since the tail is the main contribution to $\overset{o}{M}_{\dot{w}}$, for blended-wing-body types which have no tail, this derivative is previewed to be of lower value than for conventional configurations. Nevertheless, similar to $\overset{o}{Z}_{\dot{w}}$, in this research $\overset{o}{M}_{\dot{w}}$ is also considered null since there is no data available on aerodynamic derivatives dependent on $\dot{w}$. The remaining aerodynamic derivatives are dependent on several well-known aerodynamic parameters as given in equations (5.16) to (5.18).

$$\overset{o}{Z}_w = -\frac{1}{2}\rho V S\left(\frac{\partial C_L}{\partial \alpha} + C_D\right) \tag{5.16}$$

$$\overset{o}{M}_w = \frac{1}{2}\rho V S\bar{\bar{c}}\frac{\partial C_m}{\partial \alpha} = -\frac{1}{2}\rho V S\bar{\bar{c}}\frac{\partial C_L}{\partial \alpha}K_n \tag{5.17}$$

$$\overset{o}{M}_q = \frac{1}{2}\rho V S\bar{\bar{c}}\frac{\partial C_m}{\partial q} \tag{5.18}$$

As shown in equation (5.16) $\overset{o}{Z}_w$ is dependent on the lift curve slope and on drag, while $\overset{o}{M}_w$, given in equation (5.17), is proportional to the product of lift slope and static margin, or the pitch moment slope. Thus, the aerodynamic parameters that most influence the short period frequency and damping are the lift curve slope, the static margin and the pitch damping or pitching moment derivative due to pitch rate, as given in equation (5.18). Cook[99] states that for a typical conventional aircraft the relative magnitudes of the aerodynamic derivatives are such that, to a crude approximation equations (5.14) and (5.15) can be simplified further to that given in equations (5.19) and (5.20).

$$\omega_s^{\,2} = -\frac{\overset{o}{M}_w U_e}{I_y} \tag{5.19}$$

$$2\zeta_s\omega_s = -\frac{\overset{o}{M}_q}{I_y} \tag{5.20}$$

Relatively to the short period frequency, comparing equations (5.14) and (5.19) this means that for a typical conventional aircraft, which has usually large positive static margins, $\overset{o}{M}_w$ influences the short period frequency more. However, for BWB configurations large static margins are not expected, and, as it can be seen in Figures 5.1 and 5.2, for small static margin values the influence of the $\overset{o}{Z}_w$ and $\overset{o}{M}_q$ product plays also an important part.

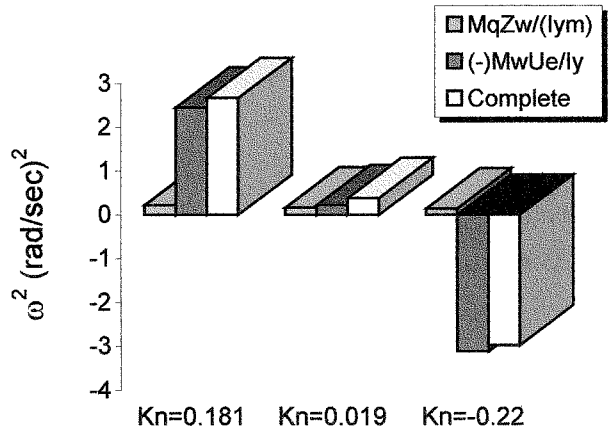

Figure 5.1 Short period frequency squared compounds variation with *cg*

From figure 5.1 it can be seen that equation (5.19) is adequate for configurations with a large static margin magnitude, either positive or negative. However, around the neutral point equation (5.19) does not hold true and it is advised to use equation (5.14) instead. This result is not surprising, since it was seen in equation (5.17) that $\overset{o}{M}_w$ is directly proportional to the static margin, being null for a null static margin, neutral stability, and higher for large static margin magnitudes. For figure 5.2, the same conclusion holds true.

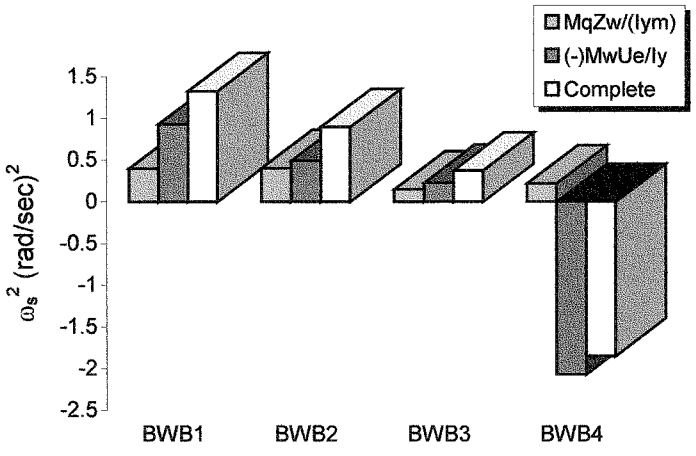

Figure 5.2 Short period frequency squared compounds for four BWB

Relatively to the damping, comparing equations (5.15) and (5.20) it is concluded that for a typical conventional aircraft the pitching moment due to the pitch rate is the most influencing parameter, and thus the name of pitch damping. However, for BWB configurations, which have no tail and the lift curve slope is optimised to a maximum, the importance of the pitch damping parameter decreases. This can also be seen in Figures 5.3 and 5.4. Figure 5.3 shows that equation (5.20) is not valid for BWB3 configurations since the contribution from the $\overset{o}{M}_q/I_y$ term is smaller than that from the $\overset{o}{Z}_w/m$ term. Moreover, when the *cg* moves aft the contribution from $\overset{o}{M}_q/I_y$

becomes even smaller, due to the decrease of the rotational derivatives, with the $\overset{\circ}{Z}_w/m$ term becoming dominant. Figure 5.4 also supports the use of equation (5.15). The differences between the parameters $\overset{\circ}{M}_q/I_y$ and $\overset{\circ}{Z}_w/m$ of the several configurations are due to the different pitch damping and lift curve slope values for each configuration, but the general conclusion is that the pitch damping parameter, $\overset{\circ}{M}_q/I_y$, is not the dominant factor in the damping value.

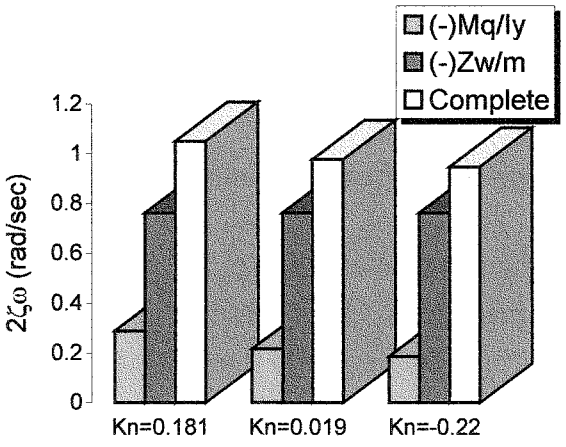

Figure 5.3 Short period $2\zeta\omega$ compounds variation with *cg* for BWB3

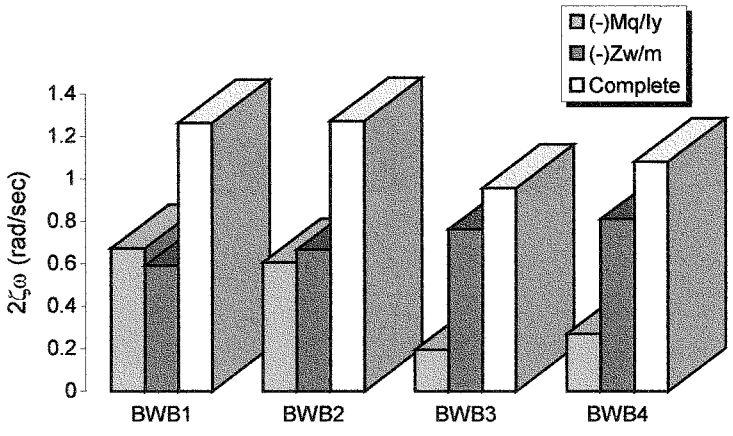

Figure 5.4 $2\xi\omega$ short period compounds for four BWB configurations

A comparison between the short period frequency and damping for the reduced order model and for the complete longitudinal model is given in Table 5.7. Based on this table, it can be concluded that the reduced order model given by equations (5.14) and (5.15) is a good approximation to the complete model. Moreover, the relative simplicity of equations (5.14) and (5.15) already allowed to see which aerodynamic parameters influence the short period frequency and damping.

	Full order model		Reduced order model	
	ζ_s	ω_s (rad/s)	ζ_s	ω_s (rad/s)
BWB1	0.384	1.13	0.379	1.15
BWB2	0.497	0.678	0.475	0.695
BWB3	0.783	0.639	0.755	0.642
BWB4	(+1.7)*	(-0.47)*	(+1.9)*	(-0.47)*
* Time constants, in seconds, of two real roots: one positive (unstable) and other negative (stable) ** Pair of positive complex roots with negative damping (unstable mode)				

Table 5.7 Short period characteristic mode for four BWB

5.4.3 Simple parametric study

Since there was no data for the pitch rate derivatives, C_{L_q} and C_{m_q}, a parametric study was done to investigate the influence of these derivatives on the longitudinal characteristic modes. From the reduced order model for the short period it is not expected that C_{L_q} will influence the short period significantly. However, since the full order model solution was considered, this was considered useful for comparison with the preview results. Although being tailless configurations, and therefore having smaller rotational derivatives, their contributions are still important. This is better seen in Tables 5.8 and 5.9, where the BWB1 and BWB2 C_{L_q} and C_{m_q} rotational derivatives were given the notional values presented in brackets in Table 5.2.

BWB1		Short period		Phugoid	
C_{L_q}	C_{m_q}	ζ_s	ω_s (rad/s)	ζ_p	ω_p (rad/s)
0.0	**0.0**	0.384	1.13	0.0707	0.139
0.0	**-0.3**	0.543	1.34	0.0581	0.118
0.0	**-0.6**	0.670	1.52	0.0529	0.104
0.5	**-0.3**	0.550	1.33	0.0554	0.119
0.5	**-0.6**	0.677	1.51	0.0506	0.105

Table 5.8 Longitudinal modes variation with C_{L_q} and C_{m_q} for BWB1

Table 5.8 shows that when the pitching moment derivative due to pitch rate, C_{m_q}, is considered in the BWB1 configuration, both the short period frequency and damping ratio increase with an increase in the pitching stiffness. Although the effect of C_{m_q} on the phugoid mode is to decrease both the frequency and damping, the mode remains stable. When considering the effect of lift coefficient derivative due to pitch rate, C_{L_q}, on configuration BWB1, Table 5.8 shows an increase in the short period damping, and a slightly decrease of the short period frequency. The effect on the phugoid is opposite, still with a trend of decreasing both the phugoid frequency and damping, but decreasing the damping slightly more and the phugoid frequency slightly less. Similar results can be found in Table 5.9 for the BWB2 configuration.

BWB2		Short period		Phugoid	
C_{L_q}	C_{m_q}	ζ_s	ω_s (rad/s)	ζ_p	ω_p (rad/s)
0.0	**0.0**	0.497	0.678	0.0191	0.141
0.0	**-0.3**	0.615	0.845	0.0173	0.113
0.0	**-0.6**	0.715	0.982	0.0161	0.0975
0.5	**-0.3**	0.621	0.837	0.0143	0.114
0.5	**-0.6**	0.720	0.975	0.0139	0.0981

Table 5.9 Longitudinal modes variation with C_{L_q} and C_{m_q} for BWB2

5.5 Longitudinal time responses

The time history responses for the BWB1, BWB2 and BWB3 configurations are presented in Figures 5.5 and 5.6. BWB4 is not included whereas BWB3 is, because the instability of the BWB3 configuration is of the phugoid mode, which has a large period. The BWB4 configuration is unstable in the short period mode where the time to double amplitude is much smaller, in the order of 1.18 seconds as calculated from the values of Table 5.6. The short period mode is usually faster then the phugoid, thus occurring in the first seconds of the variables response. The phugoid is a much rather slow mode, which takes long to develop. This is better seen in Figure 5.6. Figure 5.5 shows what happens in the first seconds, thus the influence of the short period, with more detail.

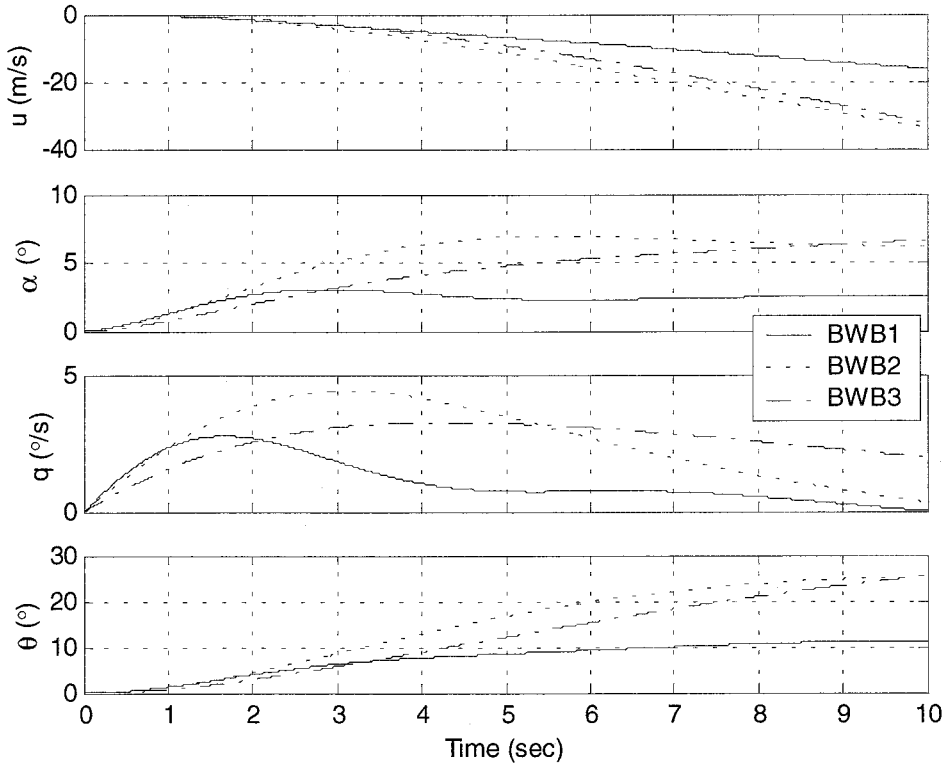

Figure 5.5 Longitudinal short-term response to an elevator step input of –1deg

Figures 5.5 and 5.6 show both dynamic stability modes in all responses. However, the magnitude of each stability mode is different for each response variable. For instances, in Figure 5.6 it seems that both short period and phugoid mode are present in the same proportion in the pitch rate and angle responses, q and θ. However, the axial velocity, u, seems to be dominated by the phugoid since there is no oscillations in the short-term response of Figure 5.5. On the other hand, the BWB1 angle of attack response, α, seems to be dominated by the short-period mode, as it seems constant in the long-term response, as shown in Figure 5.6. However, for the BWB2 and BWB3 angle of attack responses, oscillations due to the phugoid exist also in the long term.

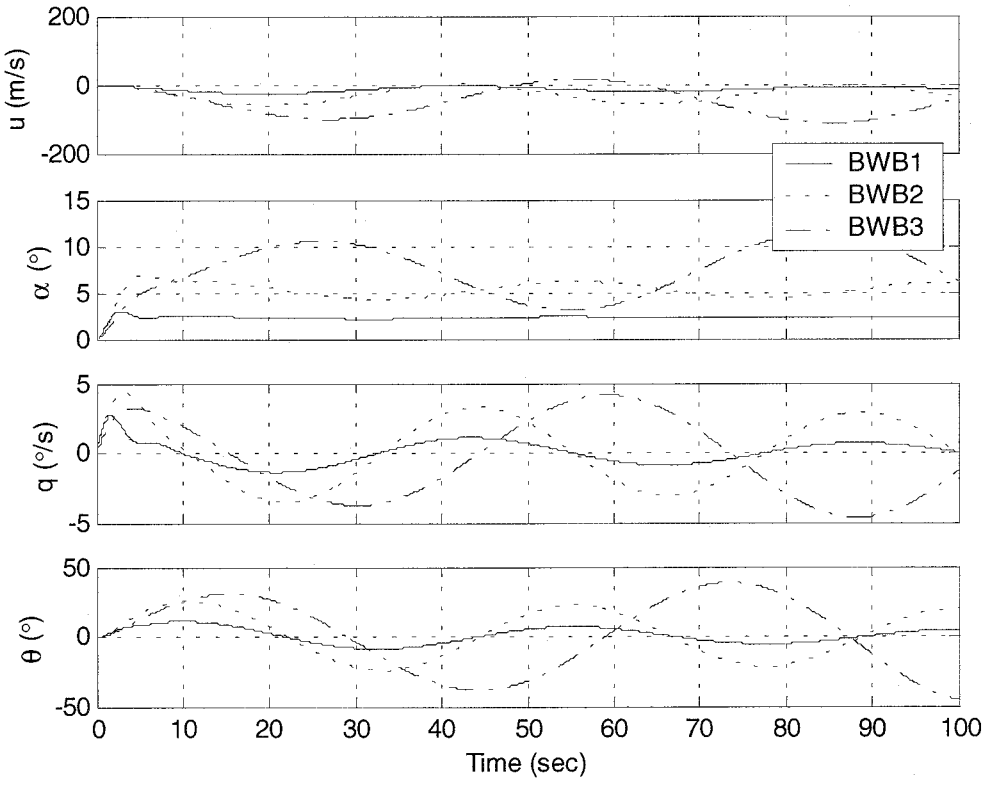

Figure 5.6 Longitudinal long-term response to an elevator step input of –1deg

Clearly from Figure 5.6, the stability of all responses is the same as determined by the common denominator. In Table 5.6 it was seen that all three BWB configurations here considered have stable short period modes, with BWB1 having the highest short period frequency. The short period stability is well noticed in all responses of Figure 5.5, together with the faster response from BWB1. Besides, BWB1 and BWB2 have a stable low damped phugoid, while BWB3 have an unstable phugoid. Therefore, from all responses of Figure 5.6 the BWB3 phugoid instability can be seen, as the amplitude responses increase.

5.6 Comparison with flying and handling qualities requirements

As seen in Chapter 4, due to the limited control power available in blended-wing-body configurations, the static margin must be limited to small values around the neutral point. Furthermore, since there are noticeable advantages, a negative static margin may be preferable. In this chapter it is shown that for *cg* positions near, or aft of the neutral point dynamic instability exists, being more critical as the *cg* moves backwards. For forward *cg* positions, but within a small positive static margin, it is shown that both the short period and phugoid mode are relatively low damped. The existence of unstable configurations determines the requirement for some kind of automatic stability augmentation system. On the other hand, the need to have a small positive static margin, say $K_n = 0.1$, imposed by the low control power, makes stability augmentation necessary for the stable configuration as well.

CHAPTER 6
Lateral-directional dynamic stability of the unaugmented blended-wing-body aircraft

"...model aircraft builders have found that they must have good spiral stability, and so they use large dihedral angles and small vertical tails to favour spiral mode. As a result their dutch roll damping may be light, and in fact, the constant swaying or rocking motion of their models indicates that this is so. But, they have no pilots to complain about handling qualities and no passengers to make ill."

Seckel

6.1 Overview

In Chapter 5 it was stated that the longitudinal motion is very important since the pilot flies most of the time in the aircraft's plan of symmetry. However, it is also important to know the lateral-directional dynamic behaviour, since the aircraft still has to perform asymmetric operations such as turning or even fly asymmetrically.

As it was said in Chapter 5, dynamic stability establishes the form of the variables transient responses. In Chapter 4 it was found about the possibility of trim in asymmetric conditions such as crosswind or in the event of an engine failure. However, it is also important to know the transient modes as soon as an engine is failed, when lateral or directional gust are sensed, or when controls are input.

The procedures to investigate the lateral-directional dynamics of an aircraft are much the same as those used to investigate the longitudinal dynamics, already presented in Chapter 5. However, some major differences exist; Firstly, there are two aerodynamic

inputs, the ailerons and rudder, possible to be used to control the lateral-directional motion. Nonetheless, since the aerodynamic inputs are considered one at a time, i.e. one equal to zero and the other not, the problem resumes to a single input as before, only it has to be done twice, one time for each input. Secondly, the lateral-directional motion includes rolling and yawing that may couple between each other giving rise to complex motions.

A particularity in the present research and one of the blended-wing-body configurations problems is that since it has no horizontal tail and the fuselage is blended with the wing, a place where to place the vertical surface is difficult to find. One solution is to not have vertical tail at all, yet a solution must be find then about the place and way of working of the rudders. On the other hand, when opting for having vertical surfaces, the moment arm is in principle smaller than that when an extension for tail is considered. This definitely leads to differences between blended-wing-body and conventional types. However, the extent of these differences has still to be found.

6.2 Lateral-directional equations of motion

To proceed with a dynamic stability analysis, it is first necessary to establish the lateral-directional equations of motion. However, as it was stated in Chapter 5, due to the complexity of the non-linear equations of motion, a linearization around a trimmed flight condition is usually considered. Similar to what was done for the longitudinal case, the linear lateral-directional state equation is presented in equation (6.1), as taken from Cook[99].

$$\begin{bmatrix} \dot{\beta} \\ \dot{p} \\ \dot{r} \\ \dot{\phi} \\ \dot{\psi} \end{bmatrix} = \begin{bmatrix} y_\beta & y_p/V_o & y_r/V_o & y_\phi/V_o & 0 \\ l_v V_o & l_p & l_r & 0 & 0 \\ n_v V_o & n_p & n_r & 0 & 0 \\ 0 & 1 & 0 & 0 & 0 \\ 0 & 0 & 1 & 0 & 0 \end{bmatrix} \begin{bmatrix} \beta \\ p \\ r \\ \phi \\ \psi \end{bmatrix} + \begin{bmatrix} y_\xi/V_o & y_\varsigma/V_o \\ l_\xi & l_\varsigma \\ n_\xi & n_\varsigma \\ 0 & 0 \\ 0 & 0 \end{bmatrix} \begin{bmatrix} \xi \\ \varsigma \end{bmatrix} \tag{6.1}$$

Equation (6.1) was solved for all configurations for the same landing approach flight condition as given in Tables 5.1 and 5.2 of Chapter 5. Other lateral-directional general characteristics are given in Table 6.1. Since there is no information on the lateral-directional rotational derivatives for configuration BWB2, the values in parenthesis in Table 6.1 were used. The coupling derivatives, C_{l_r} and C_{n_p}, were assumed zero. Introducing these values in equation (6.1) the state equation A and B matrices result, as given in Table 6.2.

	BWB1	BWB2	BWB3	BWB4
I_x (Kg.m2)	67.5 x 10^6	48.3 x 10^7	47.0 x 10^6	47.0 x 10^6
I_z (Kg.m2)	74.3 x 10^6	25.2 x 10^7	99.7 x 10^6	99.7 x 10^6
C_{l_p}	-0.1854	(-0.3)	-0.3453	-0.4563
C_{n_r}	-0.0157	(-0.03)	-0.0240	-0.0347

Table 6.1 BWB general lateral-directional data

	A	B
BWB1	$\begin{bmatrix} -0.0735 & 0.2153 & -0.9863 & 0.0981 & 0 \\ -4.3660 & -1.4972 & 1.4084 & 0 & 0 \\ 0.0642 & -0.6647 & -0.1152 & 0 & 0 \\ 0 & 1 & 0 & 0 & 0 \\ 0 & 0 & 1 & 0 & 0 \end{bmatrix}$	$\begin{bmatrix} 0 & 0.0099 \\ -0.9721 & 0.0121 \\ 0.0853 & -0.0798 \\ 0 & 0 \\ 0 & 0 \end{bmatrix}$
BWB2	$\begin{bmatrix} -0.0404 & 0.1303 & -0.9915 & 0.0981 & 0 \\ -0.2992 & -0.3687 & 0 & 0 & 0 \\ 0.2536 & 0 & -0.0708 & 0 & 0 \\ 0 & 1 & 0 & 0 & 0 \\ 0 & 0 & 1 & 0 & 0 \end{bmatrix}$	$\begin{bmatrix} 0.0058 & 0.0161 \\ -0.5105 & 0.0264 \\ 0.0050 & -0.0855 \\ 0 & 0 \\ 0 & 0 \end{bmatrix}$
BWB3	$\begin{bmatrix} -0.0328 & 0.1726 & -1.0076 & 0.0981 & 0 \\ -0.7986 & -2.4225 & 0.7708 & 0 & 0 \\ -0.1323 & -0.3652 & -0.0795 & 0 & 0 \\ 0 & 1 & 0 & 0 & 0 \\ 0 & 0 & 1 & 0 & 0 \end{bmatrix}$	$\begin{bmatrix} -0.0021 & 0.0064 \\ -0.5647 & 0.1035 \\ 0.0099 & -0.0422 \\ 0 & 0 \\ 0 & 0 \end{bmatrix}$
BWB4	$\begin{bmatrix} -0.0194 & 0.0530 & -1.0095 & 0.0981 & 0 \\ -0.7069 & -1.2803 & -0.0873 & 0 & 0 \\ 0.0213 & 0.0145 & -0.0459 & 0 & 0 \\ 0 & 1 & 0 & 0 & 0 \\ 0 & 0 & 1 & 0 & 0 \end{bmatrix}$	$\begin{bmatrix} -0.0050 & 0.0122 \\ -1.3154 & 0.2316 \\ 0.0039 & -0.0562 \\ 0 & 0 \\ 0 & 0 \end{bmatrix}$

Table 6.2 Lateral-directional A and B state equation matrices

6.3 Lateral-directional transfer functions

Applying Laplace transform to equation (6.1) and solving for each input independently, the transfer functions due to ailerons and rudder result. These are better seen from equation (6.2) until equation (6.11), as taken from Cook[99]. The factorisation presented for each input-output relationship is typical of stable conventional aircraft.

$$\frac{\beta(s)}{\xi(s)} = \frac{N_\xi^\beta(s)}{\Delta(s)} = \frac{k_\beta s(s+1/T_{\beta_1})(s+1/T_{\beta_2})}{(s+1/T_s)(s+1/T_r)(s^2+2\zeta_d\omega_d s+\omega_d{}^2)} \tag{6.2}$$

$$\frac{\phi(s)}{\xi(s)} = \frac{N_\xi^p(s)}{\Delta(s)} = \frac{k_p s(s^2+2\zeta_\phi\omega_\phi s+\omega_\phi{}^2)}{(s+1/T_s)(s+1/T_r)(s^2+2\zeta_d\omega_d s+\omega_d{}^2)} \tag{6.3}$$

$$\frac{r(s)}{\xi(s)} = \frac{N_\xi^r(s)}{\Delta(s)} = \frac{k_r s(s+1/T_\psi)(s^2+2\zeta_\psi\omega_\psi s+\omega_\psi{}^2)}{(s+1/T_s)(s+1/T_r)(s^2+2\zeta_d\omega_d s+\omega_d{}^2)} \tag{6.4}$$

$$\frac{\phi(s)}{\xi(s)} = \frac{N_\xi^\phi(s)}{\Delta(s)} = \frac{k_\phi s(s^2+2\zeta_\phi\omega_\phi s+\omega_\phi{}^2)}{(s+1/T_s)(s+1/T_r)(s^2+2\zeta_d\omega_d s+\omega_d{}^2)} \tag{6.5}$$

$$\frac{\psi(s)}{\xi(s)} = \frac{N_\xi^\psi(s)}{\Delta(s)} = \frac{k_\psi(s+1/T_\psi)(s^2+2\zeta_\psi\omega_\psi s+\omega_\psi{}^2)}{(s+1/T_s)(s+1/T_r)(s^2+2\zeta_d\omega_d s+\omega_d{}^2)} \tag{6.6}$$

$$\frac{\beta(s)}{\varsigma(s)} = \frac{N_\varsigma^\beta(s)}{\Delta(s)} = \frac{k_\beta s(s+1/T_{\beta_1})(s+1/T_{\beta_2})(s+1/T_{\beta_3})}{(s+1/T_s)(s+1/T_r)(s^2+2\zeta_d\omega_d s+\omega_d{}^2)} \tag{6.7}$$

$$\frac{p(s)}{\varsigma(s)} = \frac{N_\varsigma^p(s)}{\Delta(s)} = \frac{k_p s^2(s+1/T_{\phi_1})(s+1/T_{\phi_2})}{(s+1/T_s)(s+1/T_r)(s^2+2\zeta_d\omega_d s+\omega_d{}^2)} \tag{6.8}$$

$$\frac{r(s)}{\varsigma(s)} = \frac{N_\varsigma^r(s)}{\Delta(s)} = \frac{k_r s(s+1/T_\psi)(s^2+2\zeta_\psi\omega_\psi s+\omega_\psi{}^2)}{(s+1/T_s)(s+1/T_r)(s^2+2\zeta_d\omega_d s+\omega_d{}^2)} \tag{6.9}$$

$$\frac{\phi(s)}{\varsigma(s)} = \frac{N_\varsigma^\phi(s)}{\Delta(s)} = \frac{k_\phi s(s+1/T_{\phi_1})(s+1/T_{\phi_2})}{(s+1/T_s)(s+1/T_r)(s^2+2\zeta_d\omega_d s+\omega_d{}^2)} \tag{6.10}$$

$$\frac{\psi(s)}{\varsigma(s)} = \frac{N_\varsigma^\psi(s)}{\Delta(s)} = \frac{k_\psi(s+1/T_\psi)(s^2+2\zeta_\psi\omega_\psi s+\omega_\psi{}^2)}{(s+1/T_s)(s+1/T_r)(s^2+2\zeta_d\omega_d s+\omega_d{}^2)} \tag{6.11}$$

Again, each transfer function is composed by a unique numerator, $N_\xi^\chi(s)$, and a common denominator, $\Delta(s)$. This denominator is common to either the transfer functions due to ailerons and the transfer functions due to the rudder. The numerators and denominators for the present landing and approach flight condition are given in Table 6.3 to Table 6.6 for all the four BWB configurations.

To aileron control	
$N_\xi^\beta(s)$	$-0.3s(s-0.0009)(s+2.9209)\ (rad)$
$N_\xi^p(s)$	$-0.97s^2(s-0.5297)(s+0.5948)\ (rad/s)$
$N_\xi^r(s)$	$0.09s([0.3937,0.1991])(s+8.992)\ (rad/s)$
$N_\xi^\phi(s)$	$-0.97s(s-0.5297)(s+0.5948)\ (rad)$
$N_\xi^\psi(s)$	$0.09([0.3937,0.1991])(s+8.992)\ (rad)$
To rudder control	
$N_\varsigma^\beta(s)$	$0.01s(s-0.0886)(s+1.4683)(s+8.4223)\ (rad)$
$N_\varsigma^p(s)$	$0.012s^2(s-14.6645)(s+1.9987)\ (rad/s)$
$N_\varsigma^r(s)$	$-0.08s([0.2436,0.5536])(s+1.3940)\ (rad/s)$
$N_\varsigma^\phi(s)$	$0.012s(s-14.6645)(s+1.9987)\ (rad)$
$N_\varsigma^\psi(s)$	$-0.08([0.2436,0.5536])(s+1.3940)\ (rad)$
Denominator	
$\Delta(s)$	$s(s+0.0115)(s+1.6392)([0.0120,1.4675])\ (rad)$

Table 6.3 BWB1 lateral-directional transfer functions

To aileron control	
$N_{\xi}^{\beta}(s)$	$-0.07s(s+0.0685)(s+0.7500)\ (rad)$
$N_{\xi}^{p}(s)$	$-0.5s^{2}([0.1142,0.5017])\ (rad/s)$
$N_{\xi}^{r}(s)$	$0.005s(s-1.8185)(s+0.8014)(s+1.7174)\ (rad/s)$
$N_{\xi}^{\phi}(s)$	$-0.5s([0.1142,0.5017])\ (rad)$
$N_{\xi}^{\psi}(s)$	$0.005(s-1.8185)(s+0.8014)(s+1.7174)\ (rad)$
To rudder control	
$N_{\varsigma}^{\beta}(s)$	$0.016s(s+0.0054)(s+0.3817)(s+5.5172)\ (rad)$
$N_{\varsigma}^{p}(s)$	$0.026s^{2}(s-0.8846)(s+0.8129)\ (rad/s)$
$N_{\varsigma}^{r}(s)$	$-0.09s([0.1329,0.2267])(s+0.4214)\ (rad/s)$
$N_{\varsigma}^{\phi}(s)$	$0.026s(s-0.8846)(s+0.8129)\ (rad)$
$N_{\varsigma}^{\psi}(s)$	$-0.09([0.1329,0.2267])(s+0.4214)\ (rad)$
Denominator	
$\Delta(s)$	$s(s+0.0173)(s+0.3993)([0.0576,0.5487])\ (rad)$

Table 6.4 BWB2 lateral-directional transfer functions

To aileron control	
$N_{\xi}^{\beta}(s)$	$-0.11s(s+0.0125)(s+2.6004)\ (rad)$
$N_{\xi}^{p}(s)$	$-0.56s^{2}(s-0.3371)(s+0.4329)\ (rad/s)$
$N_{\xi}^{r}(s)$	$0.01s([0.2494,0.1877])(s+23.1679)\ (rad/s)$
$N_{\xi}^{\phi}(s)$	$-0.56s(s-0.3371)(s+0.4329)\ (rad)$
$N_{\xi}^{\psi}(s)$	$0.01([0.2494,0.1877])(s+23.1679)\ (rad)$
To rudder control	
$N_{\varsigma}^{\beta}(s)$	$-0.006s(s-9.3542)(s-0.0165)(s+2.4217)\ (rad)$
$N_{\varsigma}^{p}(s)$	$0.1s^{2}(s-0.7579)(s+0.6054)\ (rad/s)$
$N_{\varsigma}^{r}(s)$	$-0.04s([0.2211,0.1841])(s+3.2496)\ (rad/s)$
$N_{\varsigma}^{\phi}(s)$	$0.1s(s-0.7579)(s+0.6054)\ (rad)$
$N_{\varsigma}^{\psi}(s)$	$-0.04([0.2211,0.1841])(s+3.2496)\ (rad)$
Denominator	
$\Delta(s)$	$s(s+0.2090)(s+2.3080)([0.0486,0.1834])\ (rad)$

Table 6.5 BWB3 lateral-directional transfer functions

To aileron control	
$N_{\xi}^{\beta}(s)$	$-0.08s(s+0.0522)(s+1.4215)\ (rad)$
$N_{\xi}^{p}(s)$	$-1.32s^2([0.2215,0.1419])\ (rad/s)$
$N_{\xi}^{r}(s)$	$0.004s(s-3.7578)[0.1947,0.4094]\ (rad/s)$
$N_{\xi}^{\phi}(s)$	$-1.32s([0.2215,0.1419])\ (rad)$
$N_{\xi}^{\psi}(s)$	$0.004(s-3.7578)[0.1947,0.4094]\ (rad)$
To rudder control	
$N_{\varsigma}^{\beta}(s)$	$0.012s(s+0.0165)(s+1.3424)(s+5.6436)\ (rad)$
$N_{\varsigma}^{p}(s)$	$0.23s^2(s-0.3663)(s+0.4157)\ (rad/s)$
$N_{\varsigma}^{r}(s)$	$-0.056s([0.0065,0.2220])(s+1.2323)\ (rad/s)$
$N_{\varsigma}^{\phi}(s)$	$0.23s(s-0.3663)(s+0.4157)\ (rad)$
$N_{\varsigma}^{\psi}(s)$	$-0.056([0.0065,0.2220])(s+1.2323)\ (rad)$
Denominator	
$\Delta(s)$	$s(s+0.0392)(s+1.2856)([0.0403,0.2583])\ (rad)$

Table 6.6 BWB4 lateral-directional transfer functions

In the same way as for the longitudinal motion, comparing the results of Tables 6.3 to 6.6 with the numerators and denominator factorisation presented in equations (6.2) to (6.11), it can be seen that except for the $N_{\xi}^{p}(s)$ numerator of BWB1 and BWB3, the blended-wing-body aircraft presents the same factorisation. Similar characteristics for each variable response are thus expected.

6.4 Lateral-directional characteristic modes

6.4.1 Characteristic modes analysis

The lateral-directional roll, spiral and dutch roll mode characteristics are found by solving the characteristic equation, $\Delta(s)=0$. The solution of the characteristic equation is presented in Table 6.7 for the four BWB configurations.

	Roll mode	**Spiral mode**	**Dutch-roll mode**	
	T_r (sec)	T_s (sec)	ζ_d	ω_d (rad/sec)
BWB1	0.610	86.96	0.0120	1.47
BWB2	2.5	57.80	0.0576	0.549
BWB3	0.433	4.78	0.0486	0.183
BWB4	0.775	25.51	0.0403	0.258

Table 6.7 Lateral-directional characteristic modes for four BWB aircraft

From Table 6.7 it can be seen that, except for the BWB2 configuration, all others have a fast stable roll mode time constant. The higher roll mode time constant for the BWB2 configuration is due to the higher roll moment of inertia used, as shown in Table 6.1. The spiral mode time constant is positive (stable) for all configurations, having a low value in the BWB3 case, which may become a problem in changing heading. The dutch roll mode for all configurations is stable, although it has very low damping. Configuration BWB1 has the highest dutch roll frequency, more similar to conventional aircraft, followed by the BWB2 configuration which has a frequency one third of that value. BWB3 and BWB4 have the lowest dutch roll frequencies.

Similar to what was done for the longitudinal motion, a lateral-directional dynamic stability study variation with *cg* movement was done for the BWB3 configuration. In Figure 6.1 it is presented the angle of attack necessary to trim the BWB3 configuration as function of the *cg* movement and speed. As shown in Chapter 4, configurations with positive static margin need a higher angle of attack to trim than configurations with negative static margin. Moreover, the need for angle of attack increases as the speed decreases.

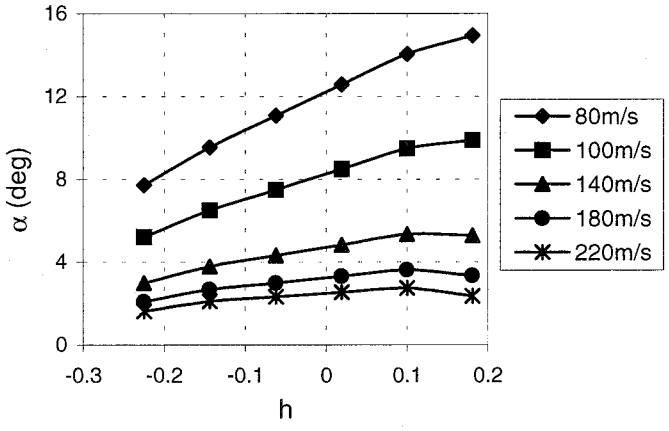

Figure 6.1 Angle of attack to trim variation with *cg* position and speed

Figures 6.2 to 6.4 give the variation of the lateral-directional characteristic modes, roll, spiral and dutch roll, with *cg* position and speed. In Figure 6.2 the roll mode time constant, T_r, variation with *cg* position and speed is shown. As it can be seen in Figure 6.2, the roll mode time constant decreases with increasing speed. This means, the roll mode is faster for higher speeds. Moreover, T_r is independent of the *cg* position for large values of speed. Actually, comparing Figure 6.2 with Figure 6.1 it can be seen that they are similar. This is so because the rolling moment derivative due to roll rate, C_{l_p}, which is the dominant factor in the roll mode time constant as it will be shown later, varies only with angle of attack.

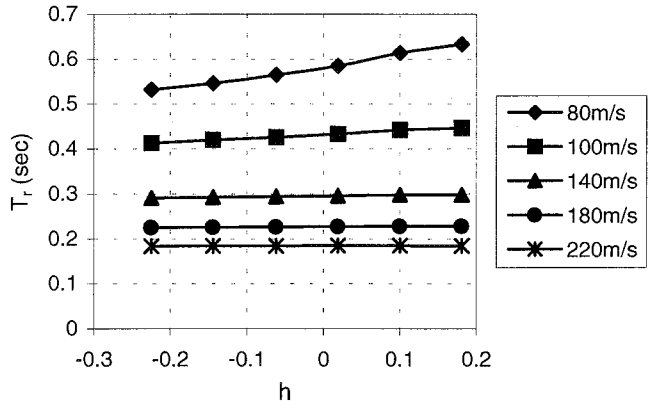

Figure 6.2 Roll mode time constant variation with *cg* movement and speed

Figure 6.3 shows the spiral mode time constant variation with *cg* position and speed. The spiral mode is faster, smaller time constant, for larger negative static margin configurations and high speeds. However, as the *cg* moves forward, the spiral mode becomes slower, time constant increases, slowing even further as the speed increases. The spiral mode is usually a rather slow mode, or very high time constant, being in this case acceptable an unstable spiral mode.

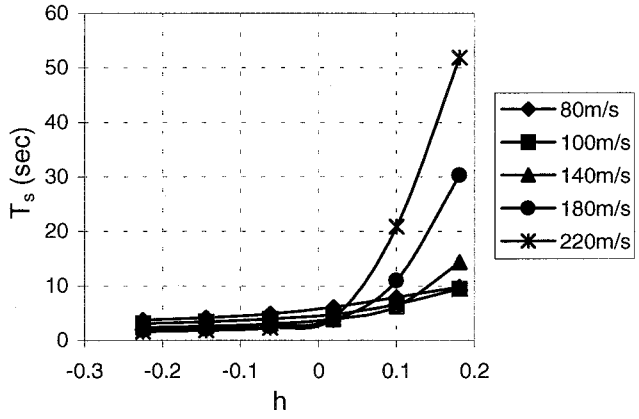

Figure 6.3 Spiral mode time constant variation with *cg* position and speed

The dutch roll mode frequency versus damping for several *cg* positions and speeds is given in Figure 6.4. The variation of frequency and damping with *cg* position and speed is now rather complex. There is instability for aft *cg* positions, which become worse with increasing speed. In general, the dutch roll mode frequency, ω_d, decreases with aft *cg* movement and increasing speed. The dutch roll mode damping, ζ_d, for low speeds also decreases as the *cg* goes backwards, becoming negative and so rendering the dutch roll mode unstable. However, for increasing speeds, the damping initially increases as the *cg* goes backwards, decreasing again as the *cg* approaches the neutral point. For unstable *cg* positions, as the *cg* goes backwards, the damping becomes more negative until becoming critically damped, originating then two positive real roots.

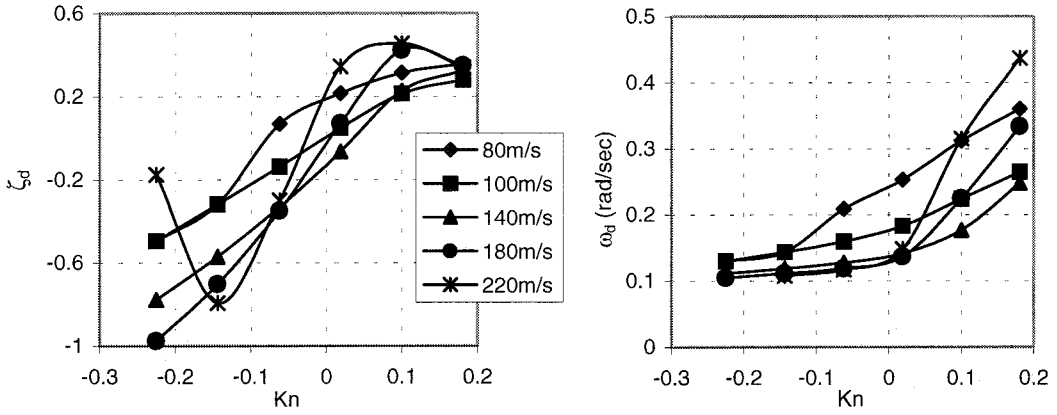

Figure 6.4 Dutch roll mode frequency and damping versus *cg* position and speed

6.4.2 Reduced order models

In paragraph 6.2.3 it was shown through the use of digital computers and fast programs the lateral-directional characteristic modes of four BWB configurations. Furthermore, the variation of the characteristic modes with *cg* position and speed for one BWB configuration was also shown. However, no insight was given to which parameters influence the lateral-directional characteristic modes, or the reasons for the variations seen. In the same way as it was done for the longitudinal motion, reduced order models were used to give some more understanding about the characteristic modes. However, since the theory is developed only for conventional aircraft, a review of the simplifying assumptions is made before applying it to BWB configurations.

6.4.2.1 Roll subsidence mode

The roll mode is a non-oscillatory lateral characteristic, which is usually substantially decoupled from the spiral and dutch roll modes. Its approximation is based on the fact that if a perturbation is small, the roll mode involves almost only pure rolling motion. From the complete state equation (6.1) a reduced state equation for this mode is taken, as defined in Cook[99] and presented in equation (6.12).

$$\begin{bmatrix} \dot{p} \\ \dot{\phi} \end{bmatrix} = \begin{bmatrix} l_p & l_\phi \\ 1 & 0 \end{bmatrix} \begin{bmatrix} p \\ \phi \end{bmatrix} + \begin{bmatrix} l_\xi \\ 0 \end{bmatrix} \xi \qquad (6.12)$$

As it can be seen from equation (6.12), only the aileron input is considered. Furthermore, as Cook[99] suggests, wind axes are assumed, so $l_\phi = 0$ and equation (6.12) is reduced to equation (6.13), a single degree of freedom rolling moment

equation. Applying Laplace transform to equation (6.13) the transfer function for this reduced order model results as shown in equation (6.14).

$$\dot{p} = l_p p + l_\xi \xi \tag{6.13}$$

$$\frac{p(s)}{\xi(s)} = \frac{l_\xi}{(s - l_p)} \equiv \frac{k_p}{(s + 1/T_r)} \tag{6.14}$$

Since the roll subsidence mode is non-oscillatory, a single real root of the characteristic polynomial describes it, as shown in equation (6.14). Thus, the pilot sees the roll mode manifestation as an exponential lag characteristic in rolling motion following a command input. Equation (6.15) gives the approximate value of the roll mode time constant, as taken from Cook[99].

$$T_r \equiv \frac{1}{l_p} = -\frac{\left(I_x I_z - I_{xz}^{\,2}\right)}{\left(I_z \overset{\circ}{L}_p + I_{xz} \overset{\circ}{N}_p\right)} \tag{6.15}$$

For the particular case where I_{xz} is null, as assumed for the configurations of this thesis, equation (6.15) is simplified further into equation (6.16). It is seen then from equation (6.16) that the roll mode time constant is largely dependent on the moment of inertia in roll, and on the rolling moment due to the roll rate, C_{l_p}, as shown in equation (6.17).

$$T_r = -\frac{I_x}{\overset{\circ}{L}_p} \tag{6.16}$$

$$\overset{o}{L}_p = \frac{1}{2}\rho S V^2 C_{l_p} \tag{6.17}$$

For BWB configurations the moment of inertia in roll is about the same order as for conventional aircraft. However, as the dihedral effect is also increased due to the high wing sweepback, the rolling moment derivative due to roll rate may be higher than that for conventional aircraft. Table 6.8 presents the roll time constant as calculated with the full order model and with equation (6.7). From here it can be concluded that the approximate model compares well with the results for the full order roll mode solution.

T_r (sec)	Full order model	Reduced order model
BWB1	0.885	1.076
BWB2	2.525	2.712
BWB3	0.431	0.412
BWB4	0.8	0.798

Table 6.8 Roll time constant for the full and reduced order models

6.4.2.2 Spiral mode

The spiral mode approximation is based on the fact that since the spiral mode is a slow mode, v, p and r are quasi-steady and $\dot{v}$, $\dot{p}$ and $\dot{r}$ are approximately null. Therefore, in the full state equation (6.1), $\dot{v}$, $\dot{p}$ and $\dot{r}$ are made equal to zero and it is assumed controls fixed, so that $\xi = \varsigma = 0$. Then, re-arranging by eliminating variables v and r, giving a reduced order model in p and ϕ only, the reduced state equation (6.18), as taken from Cook[99], results.

$$\begin{bmatrix} 0 \\ \dot{\phi} \end{bmatrix} = \begin{bmatrix} \tilde{a} & y_\phi \\ 1 & 0 \end{bmatrix} \begin{bmatrix} p \\ \phi \end{bmatrix} \tag{6.18}$$

$$\text{where } \tilde{a} = \frac{n_r l_p - n_p l_r}{n_v l_r - l_v n_r} y_v + y_p + \frac{l_v n_p - n_v l_p}{n_v l_r - l_v n_r} y_r \tag{6.19}$$

In the same way as for the roll mode reduced order model, equation (6.18) reduces to a single degree of freedom equation, as shown in equation (6.20). Applying then Laplace transform the transfer function for the spiral reduced order model results as presented in equation (6.21). The spiral mode time constant of this approximate model is then given by equation (6.22).

$$\dot{\phi} + \frac{y_\phi}{\tilde{a}} \phi = 0 \tag{6.20}$$

$$\phi(s)\left(s + \frac{y_\phi}{\tilde{a}}\right) = \phi(s)\left(s + \frac{1}{T_s}\right) = 0 \tag{6.21}$$

$$T_s = \frac{\tilde{a}}{y_\phi} \tag{6.22}$$

For usual stable conventional aircraft, equation (6.19) can be simplified to that given in equation (6.23), since the y_v and y_p terms are usually smaller than the y_r term. This simplified model is based on the fact that the spiral mode characteristics are very dependent on the lateral and directional static stability of the aeroplane. Therefore, the situation is one in which the fin effect, directional static stability, and the dihedral effect, lateral static stability, act in opposition. When the dihedral effect is greater the spiral mode is stable, and hence convergent, and when the fin effect is greater the spiral mode is unstable, and hence divergent.

$$\tilde{a} = \frac{l_v n_p - n_v l_p}{n_v l_r - l_v n_r} y_r = -\frac{U_e\left(\overset{o}{L}_v \overset{o}{N}_p - \overset{o}{L}_p \overset{o}{N}_v\right)}{\overset{o}{L}_r \overset{o}{N}_v - \overset{o}{L}_v \overset{o}{N}_r} \tag{6.23}$$

For all present BWB configurations, except the BWB2, the only vertical surfaces are the winglets working as fins. However, by being small the fin effect is not strong and the dihedral effect dominate. This leads to stable spiral modes, and in some cases to very stable modes, which may not be so desirable. The contributing terms of equation (6.19) are presented in Figure 6.5, for the four BWB configurations, and in Figure 6.6, for several *cg* positions of the BWB3 configuration.

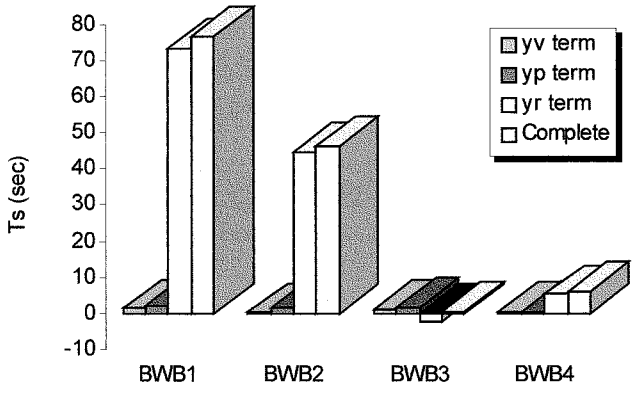

Figure 6.5 Spiral mode approximation for four BWB aircraft

In Figure 6.5 it is seen that for configurations BWB1 and BWB2 the y_r term really dominates comparatively to y_p and y_v terms. For these two configurations, equation (6.23) could be used. For the BWB4 configuration the y_r term is higher than y_v and y_p, although of smaller magnitude than that of BWB1 and BWB2. However, for the BWB3 configuration y_r, y_p and y_v are all of similar magnitudes, and y_r is even of opposite sign, therefore, making the use of equation (6.23) completely invalid.

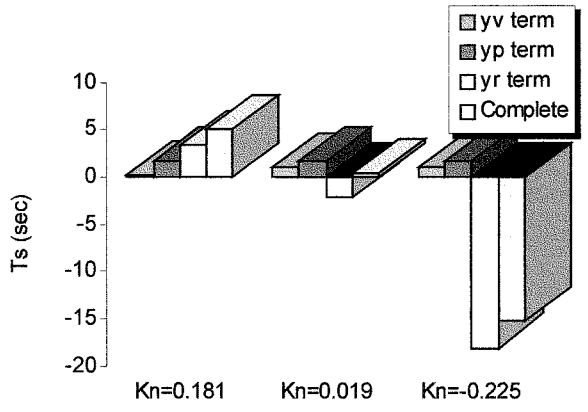

Figure 6.6 BWB3 Spiral mode approximation variation with *cg*

In Figure 6.6, it is seen that for larger static margin magnitudes the y_r term increases becoming dominant, although of opposite sign for the most forward and the most aft *cg* positions. Furthermore, the y_p term is constant for all *cg* positions, as shown also

in the approximation of equation (6.24). Lastly, the y_v term, from the Figure 6.6 and from equation (6.25), although increasing with aft *cg* positions, its variation is smaller than that of the y_r term. Thus, it can be concluded that the differences in the spiral mode time constant are related with to levels of lateral and directional stability due to the y_r term in equation (6.12).

$$y_{p_{term}} = \frac{\overset{\circ}{Y}_p}{m} + W_e \approx W_e \tag{6.24}$$

$$y_{v_{term}} = \left(\frac{\overset{\circ}{N}_r \overset{\circ}{L}_p - \overset{\circ}{N}_p \overset{\circ}{L}_r}{\overset{\circ}{N}_v \overset{\circ}{L}_r - \overset{\circ}{N}_r \overset{\circ}{L}_v} \right) \frac{\overset{\circ}{Y}_v}{m} \tag{6.25}$$

Tables 6.9 and 6.10 show the variation in lateral and directional stability derivatives for the several BWB configurations and with static margin for the BWB3 configuration. For BWB1 and BWB2, it is not so much the fact that the lateral stability C_{l_β} is high, but it is more a positive directional stability, C_{n_β}, coupled with a high C_{l_p}. In the BWB3 and BWB4 cases, the even higher C_{l_p}, coupled with negative directional stability C_{n_β}, in most cases is higher than the lateral directional stability giving rise to an unstable spiral mode. The same applies to the BWB3 *cg* variation, where an aft shift results in deterioration in directional stability, increasing magnitude of unstable C_{n_β}, together with a decrease in C_{n_p}, making the spiral mode unstable.

	C_{l_β}	C_{n_β}	C_{l_p}	C_{n_p}
BWB1	-0.4325	0.007	-0.1854	-0.0906
BWB2	-0.1948	0.086	-0.1	0
BWB3	-0.0887	-0.036	-0.3459	-0.1173
BWB4	-0.1679	-0.015	-0.4465	-0.0538

Table 6.9 Lateral directional derivatives for four BWB aircraft

Static margin K_n	C_{l_β}	C_{n_β}	C_{l_p}	C_{n_p}
0.181	-0.0887	-0.0239	-0.3459	-0.1090
0.019	-0.0887	-0.0299	-0.3459	-0.1038
-0.225	-0.0887	-0.0389	-0.3459	-0.0960

Table 6.10 Lateral directional derivatives variation with static margin

However, from Table 6.11 it is seen that the reduced order model does not always compare well with the solution of the full order linear state equation. Although it gives a good indication for configurations with positive static margins, it may not be so for configurations with negative static margins.

Spiral time constant Ts (sec)	Static margin K_n	Full order model	Reduced order model
BWB1	0.033	98.04	76.70
BWB2	0.032	57.80	46.49
BWB31	0.181	9.90	5.048
BWB33	0.019	4.808	0.479
BWB36	-0.225	2.915	-15.34
BWB4	-0.132	24.94	5.514

Table 6.11 Spiral mode time constant for the full and reduced order models

6.4.2.3 Dutch roll mode

The lateral-directional dutch roll mode is comparable to the short period mode in longitudinal motion. The dutch roll mode is a classical damped oscillation in yaw which couples into roll and into sideslip, to a lesser extent. The usual reduced order model assumes that the dutch roll motion involves no rolling motion. Although not completely correct, this assumption is reasonable if the roll to yaw ratio in dutch rolling motion is small. Therefore, the lateral-directional state equation (6.1) is simplified by assuming that $\dot{p} = p = \dot{\phi} = \phi = 0$, aircraft wind axes are in use or $l_\phi = n_\phi = 0$, and controls fixed or $\xi = \varsigma = 0$. The dutch roll mode reduced order model results then as presented in equation (6.25), as taken from Cook[99].

$$\begin{bmatrix} \dot{v} \\ \dot{r} \end{bmatrix} = \begin{bmatrix} y_v & y_r \\ n_v & n_r \end{bmatrix} \begin{bmatrix} v \\ r \end{bmatrix} \tag{6.25}$$

From the reduced state equation (6.25) the characteristic equation is found, as presented in equation (6.26). Comparing this equation with the standard second order equation of an oscillatory system, $\Delta(s) = s^2 + 2\zeta\omega s + \omega^2$, the dutch roll mode frequency and damping approximations follow easily. These are better seen in equations (6.27) and (6.28)

$$\Delta(s) = s^2 - (n_r + y_v)s + (n_r y_v - n_v y_r) = 0 \tag{6.26}$$

$$\omega_d{}^2 \cong (n_r y_v - n_v y_r) \cong \left(\frac{\overset{\circ}{N}_r}{\overset{\circ}{I}_z} \frac{\overset{\circ}{Y}_v}{m} + V_o \frac{\overset{\circ}{N}_v}{\overset{\circ}{I}_z} \right) \approx V_o \frac{\overset{\circ}{N}_v}{\overset{\circ}{I}_z} \tag{6.27}$$

$$2\zeta_d \omega_d \cong -(n_r + y_v) \cong -\left(\frac{\overset{\circ}{N}_r}{\overset{\circ}{I}_z} + \frac{\overset{\circ}{Y}_v}{m} \right) \tag{6.28}$$

Equations (6.27) and (6.28) define the stability characteristics in the solution of the state equation (6.25), together with the simplifications used for conventional aircraft,

as given also by Cook[99]. Plotting the several terms, which compose equation (6.27), it is found that the approximation given holds true for blended-wing-body configurations as well, as shown in Figures 6.7 and 6.8.

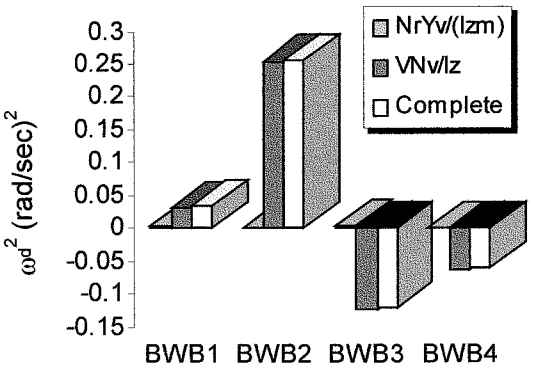

Figure 6.7 Squared dutch roll frequency components for four BWB

With this reduced order model, it can be seen in Figures 6.7 and 6.8, that because BWB3 and BWB4 configurations have negative directional stability, the dutch roll mode is unstable giving rise to a negative value of $\omega_d{}^2$. Nevertheless, when compared to the solution of the full order state equation, as given in Tables 6.12 and 6.13, it is seen that the reduce model does not compare well.

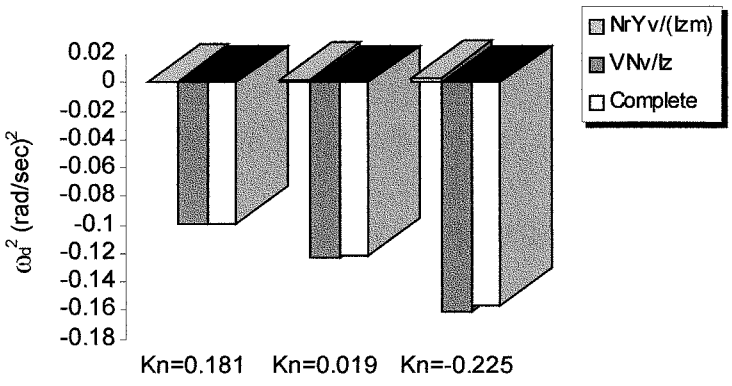

Figure 6.8 BWB3 Squared dutch roll frequency components variation with *cg*

For conventional aircraft the dutch roll mode frequency and damping are largely determined by the fin. However, the complexity of the dutch roll dynamics suggests that there may be other additional contributions. Since for blended-wing-body configurations the fin is usually small, the additional effects may therefore be even more important. However, configuration BWB2 possesses large vertical surfaces, in addition to the small winglets. Thus, for the BWB2 case the reduced order model gives a reasonable value for the dutch roll frequency, as shown in Table 6.12.

Dutch roll mode	Full order model		Reduced order model	
	ζ_d	ω_d (rad/sec)	ζ_d	ω_d (rad/sec)
BWB1	-0.0507	1.02	0.0032	0.427
BWB2	0.0594	0.550	0.1097	0.506
BWB3	0.0244	0.177	-0.165	0.348
BWB4	0.0411	0.376	-0.132	0.247

Table 6.12 Dutch roll mode frequency and damping for the full and reduced order models

Static margin K_n	Full order model		Reduced order model	
	ζ_d	ω_d (rad/sec)	ζ_d	ω_d (rad/sec)
0.181	0.231	0.230	-0.111	0.314
0.019	0.0244	0.177	-0.165	0.348
-0.225	-0.341	0.156	-0.183	0.396

Table 6.13 BWB3 dutch roll mode frequency and damping given by full and reduced order models

As an indication, usually when the peak roll to peak yaw ratio is less than one, the dutch roll mode is stable. As given, the reduced order model and the full order model solutions show that the dutch roll mode may be marginally stable, or even unstable, for most of the configurations. It may therefore be concluded that the peak roll to peak yaw ratio is greater than one. In this application, the assumption that the dutch roll mode involves no rolling motion is not correct and the reduced order model should not be used to estimate the dutch roll mode.

6.4.3 Simple parametric study

A parametric study can also be a way to find out the influence of stability derivatives in the characteristic modes. Since there was no information on the rotational stability derivatives of configuration BWB2, a parametric study was realized, in the same way as done for the longitudinal motion and presented as follow. In Table 6.14, the values of C_{l_p} and C_{n_r} were varied for the BWB2 configuration and its influence in the characteristics modes found. Increasing C_{l_p} decreases the roll mode time constant, but increases the spiral mode time constant. It also increases the dutch roll damping and frequency, stabilizing this mode, although high levels of C_{l_p} would be necessary to increase the damping to a desirable level.

BWB2		Roll mode	Spiral mode	Dutch-roll mode	
C_{l_p}	C_{n_r}	T_r(sec)	T_s(sec)	ζ_d	$\omega_d(rad/\text{sec})$
0	**0**	0	10.1	-0.0539	0.544
-0.1	**-0.01**	5.21	83.3	-0.0157	0.548
-0.3	**-0.01**	2.48	175.4	0.0228	0.550
-0.1	**-0.03**	5.78	24.7	0.0186	0.544
-0.3	**-0.03**	2.5	57.80	0.0576	0.549
-0.4	**-0.04**	1.96	54.95	0.0907	0.547
-0.4	**-0.02**	1.96	110.3	0.0550	0.547

Table 6.14 Lateral-directional characteristic modes variation with C_{l_p} and C_{n_r}

The effect of increasing C_{n_r} is to slow the roll mode, and to fasten the spiral mode. For the dutch roll mode, increasing this derivative decreases the dutch roll frequency, but increases damping. From here it is seen that C_{l_p} has a strong influence on all modes, while C_{n_r} has a stronger influence on the spiral mode, followed by the dutch roll mode and, to a lesser extent, on the roll mode. This confirms that both the dutch roll and spiral modes depend on mechanisms other than just those presented by the reduced order model.

6.5 Lateral-directional time responses

Time history responses can be obtained from solving the equations of motion relatively to each input. Since the lateral-directional motion has two possible controls, the state variable time history responses are divided in two; due to ailerons and to rudder, as follow.

6.5.1 Time responses due to aileron inputs

Figures 6.9 and 6.10 show the lateral-directional state variables time response to an aileron pulse of –1deg applied during 10 seconds. From these figures it appears that the dutch roll mode is dominant in almost all response variables. While that is usual for variables such as sideslip angle, yaw rate and bank angle, in the remaining variables this dominance is due mainly to the low dutch roll damping. Nevertheless, the roll mode is dominant in the roll rate response, and it can be better seen in Figure 6.9 by the roll rate rise and recovery when the ailerons are applied and when they are removed after 10 seconds respectively. The spiral mode influence is better seen in the convergence of the BWB2 bank angle response of Figure 6.10.

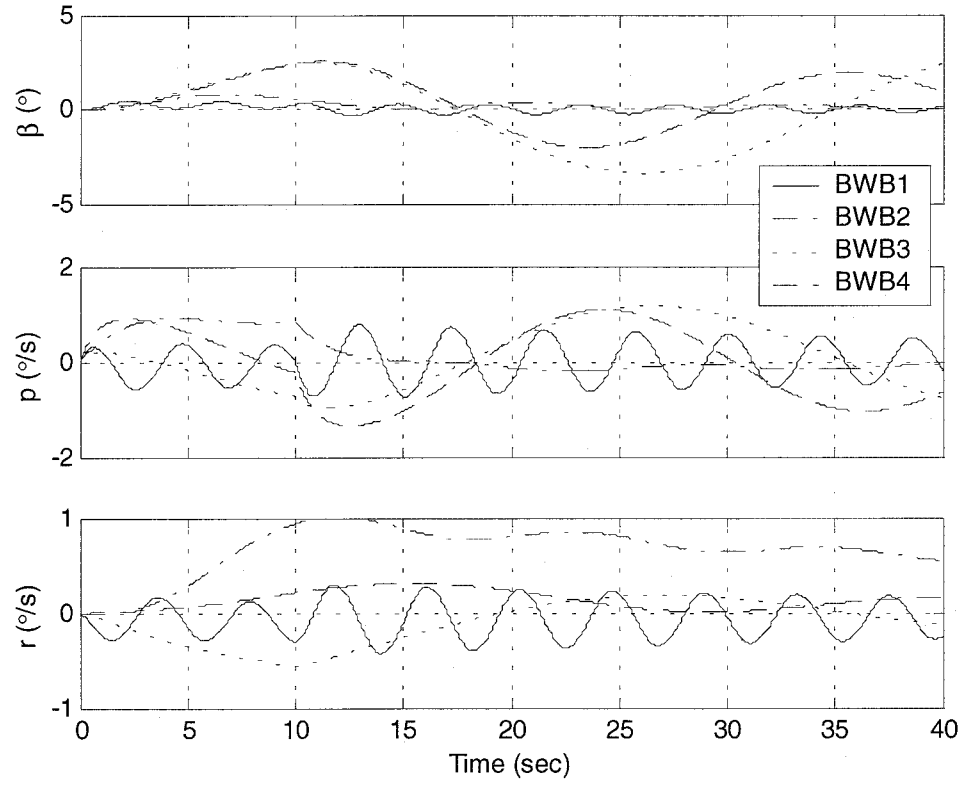

Figure 6.9 BWB responses to an aileron pulse of –1deg for 10 seconds

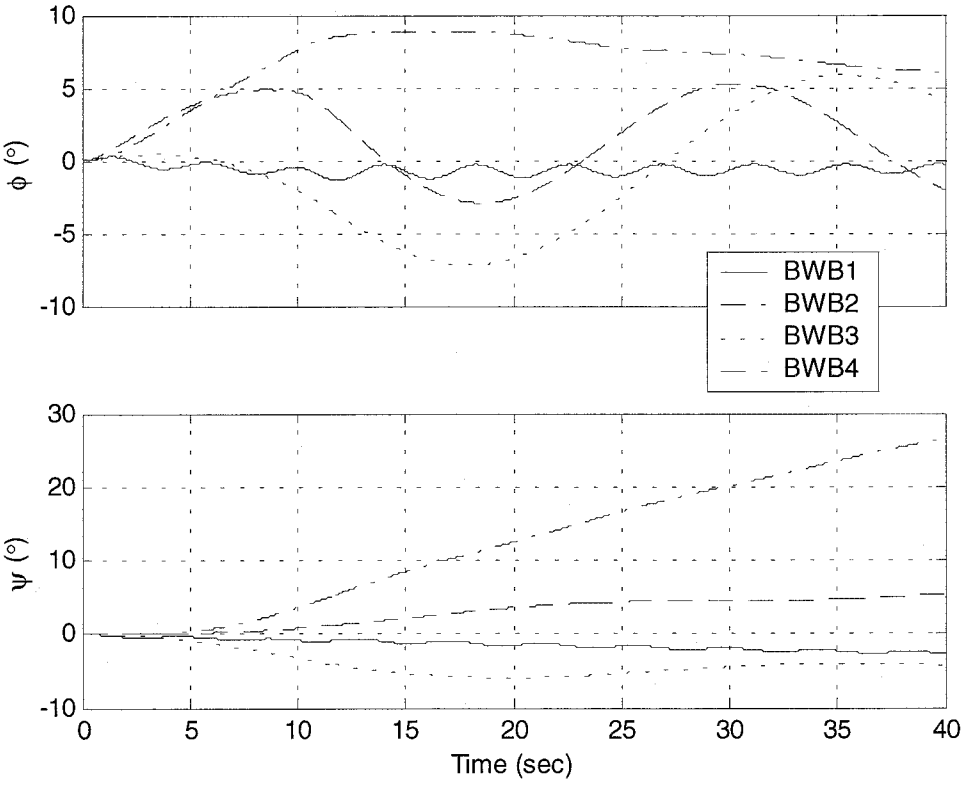

Figure 6.10 BWB responses to an aileron pulse of –1deg for 10 seconds

The goal when applying an aileron input is a certain roll rate to give an effective bank angle followed by a change in heading. Examining more closely Figures 6.9 and 6.10 it is seen that only in the case of the BWB2 configuration this is achieved. For the BWB2 configuration it is seen that 1 degree of negative ailerons deflection rotates the aircraft at a roll rate of almost 1 deg/sec, increasing the bank angle, until almost 10 degrees in 10 seconds. Once the input is removed, the roll rate returns almost to zero and the bank angle is steady for almost another 10 seconds, and then begins to converge to zero, probably as a result of the spiral mode influence. As a result of the aircraft banking, the BWB2 yaw rate increases until reaching 1 deg/sec at 10 seconds, thus increasing the aircraft heading. Lastly, the BWB2 sideslip angle generated is higher than 0.7 degrees in the positive side, in the first seconds, which can be considered significant and a probable source of problems.

The BWB4 configuration behaves approximately in the same way as the BWB2 for the first three seconds: the roll rate increases positively reaching 1 deg/sec and, with the bank angle increasing positively at that rate. However, after that the roll rate begins to decrease, until it changes direction a little before the input is removed. As a result, the bank angle increases until the roll rate becomes null and decreases when the roll rate changes sign. To increase the bank angle more the ailerons would probably have to be deflected further for this configuration. On the other hand, the BWB4 yaw rate increases with the aileron deflection, and it is still increasing when the input is removed. This is so that when the input is removed the BWB4 roll rate is negative when the yaw rate is positive and vice-versa. In this way the heading still increases but with a smaller rate. A last effect of the ailerons deflection is the positive sideslip angle generated with negative aileron deflection, of more than 2deg maximum at the moment the input is removed.

Moreover, Figures 6.9 and 6.10 show that the BWB1 time responses to a negative aileron deflection are completely inadequate. This is due not only to the high dutch roll frequency and very low damping ratio, as shown before in Table 6.7, but also due to the direction of the roll and yaw angle. I.e., the BWB1 response to a negative aileron input is a negative bank angle and a decrease in the aircraft heading, when the opposite is desirable and expected by the pilot. On the other hand, the BWB1 sideslip angle oscillation has the smallest amplitude of less than 0.5deg.

Lastly, Figures 6.9 and 6.10 show for the BWB3 configuration the worse response to a negative aileron pulse of 1 deg applied during the first 10 seconds. It is considered the worse response, because when the ailerons are deflected negatively, the roll rate has an initial positive value, but reverse to negative values after few seconds,

probably influenced by the negative yaw rate developed. Thus, the BWB3 configuration initially banks positively, reversing its bank into the wrong sense after few seconds. The high increase of negative yaw rate then induces a decrease in the aircraft heading instead of an increase, as was desired when deflecting the ailerons negatively. Lastly, the maximum sideslip angle achieved is more than 2 degrees after the input is removed, which is also highly unacceptable.

In Figures 6.11 and 6.12 the time responses to an aileron pulse of –1deg for three different static margins of the BWB3 configuration are presented. These 3 configurations were named BWB31, BWB33 and BWB34. Configuration BWB31 has a static margin of $K_n = 0.181$, BWB33 has a static margin of $K_n = 0.019$ and, BWB34 has a negative static margin of $K_n = -0.062$.

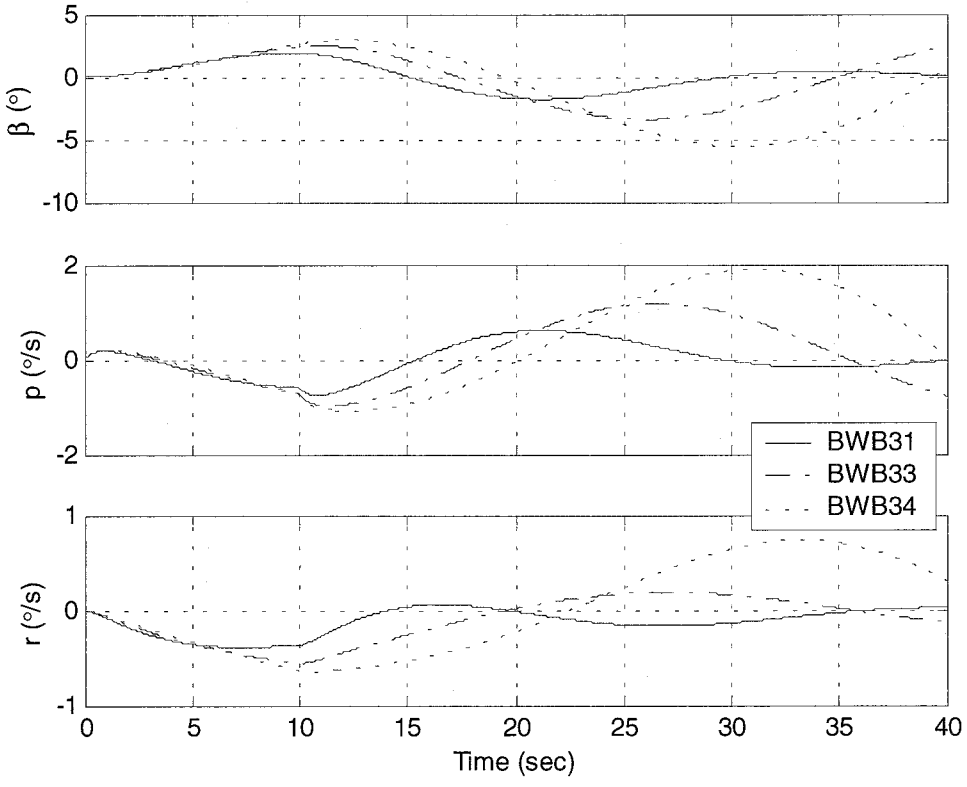

Figure 6.11 BWB3 responses to an aileron pulse of –1deg for 10 seconds

Shown in Figures 6.11 and 6.12 is that whilst the control is applied all the different BWB3 configurations have essentially the same response. This is because the ailerons stability derivatives are independent of the static margin (or *cg* position). When the control is removed an oscillatory motion exists in all responses due to the dominance of the dutch roll mode. The differences seen in each variable response, once the control is removed, are due to the characteristic modes change with static margin, as shown before in Figures 6.2 to 6.4.

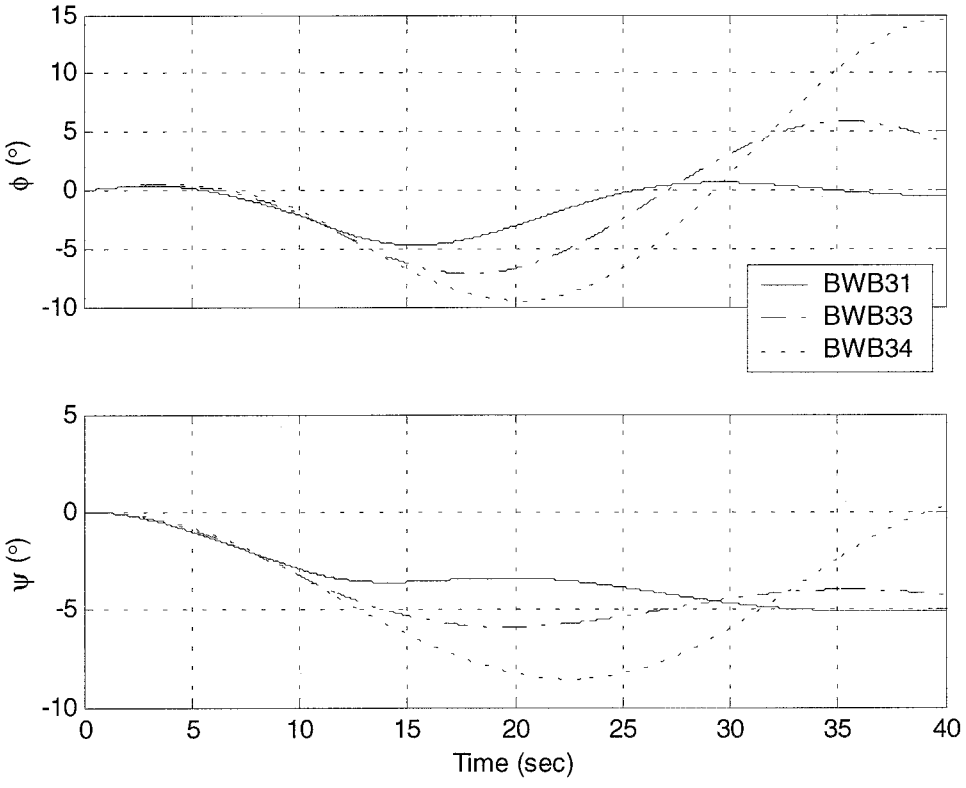

Figure 6.12 BWB3 time responses to an aileron pulse of -1deg for 10 seconds

From the differences in the BWB3 responses it is well seen that the dutch roll mode damping and frequency decrease with decreasing static margin, i.e., from configuration BWB31 to BWB34 where the *cg* is pushed aft. The mode becomes possibly unstable for the BWB34 configuration, as shown by the increasing of amplitude for all variables. In the same way as seen in Figure 6.9, the sideslip angle generated is high and increases as the *cg* moves aft. Moreover, even when the BWB3 configuration is very stable, as for the BWB31, the response to an aileron deflection presents adverse roll and yaw rate, and consequently the bank and yaw angles are opposite to what would be expected when the controls were first deflected.

6.5.2 Discussion of responses to aileron inputs

From the previews analysis it was seen that differences between the pairs (BWB2, BWB4) and (BWB1, BWB3) exist. From here it is possible to classify the use of ailerons in the pair (BWB2, BWB4) as conventional and normal behaved, while in the pair (BWB1, BWB3) the use of ailerons is completely inadequate and a re-design of ailerons seems to be needed. In this paragraph the reason for this inadequacy of the lateral controls of the pair (BWB1, BWB3) is sought.

	BWB1	BWB2	BWB31	BWB33	BWB34	BWB4
C_{n_ξ}	0.0093	0.0017	0.0028	0.0024	0.0022	0.0010

Table 6.15 Control derivative C_{n_ξ} for several BWB aircraft

In Table 6.15 the adverse yaw due to aileron deflection control derivative, C_{n_ξ}, is presented for several BWB configurations. Table 6.15 shows that BWB1 and BWB3 have the highest C_{n_ξ} control derivative followed then by BWB2 and BWB4. However, calculating the time response for the BWB33 configuration for several values of C_{n_ξ}, as presented in Figure 6.13, it is found that even when C_{n_ξ} is made equal to zero, no adverse yaw effect, the BWB33 response still has a negative rolling and yawing following a negative aileron deflection.

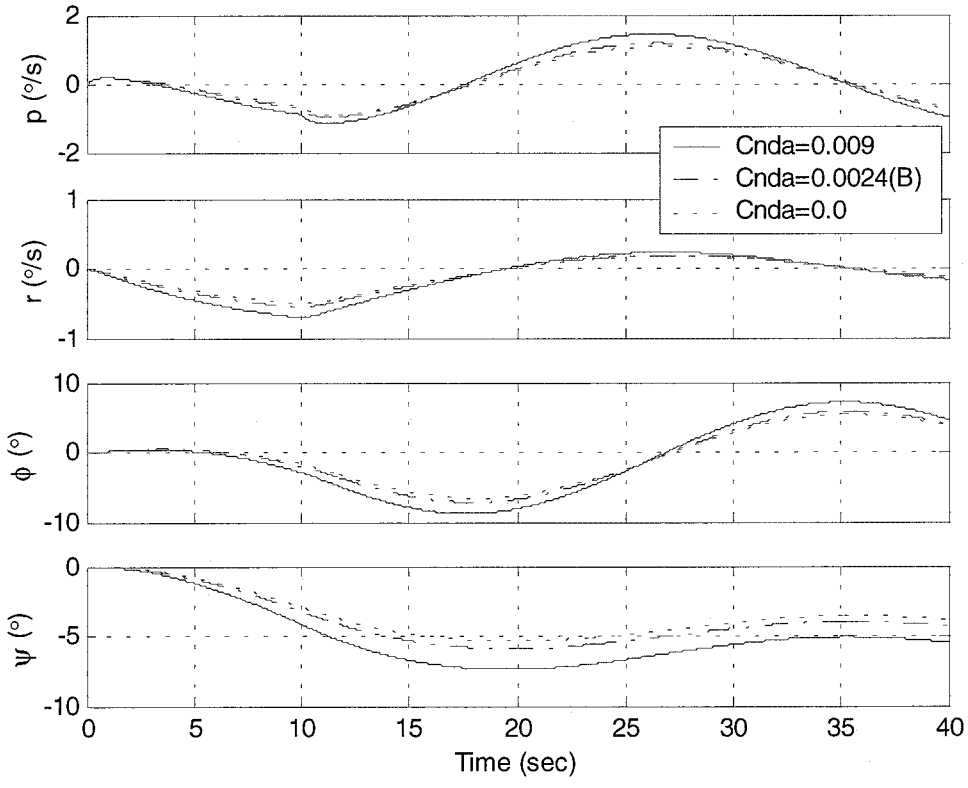

Figure 6.13 BWB3 responses to an aileron pulse of –1deg for 10 seconds for several C_{n_ξ} values

Therefore, based on Figure 6.13 and Table 6.15 it can be concluded that the control derivative C_{n_ξ} is not the main reason for the BWB1 and BWB3 adverse yaw response to aileron inputs. Therefore, it was continued the research into the main factors for this response. In Table 6.16 the aerodynamic derivatives for BWB configurations here in study are presented.

	C_{l_β}	C_{n_β}	C_{l_p}	C_{n_r}	C_{l_r}	C_{n_p}
BWB1	-0.433	0.007	-0.185	-0.016	0.174	-0.091
BWB2	-0.195	0.086	-0.1	-0.01	0	0
BWB31	-0.098	-0.033	-0.344	-0.017	0.128	-0.137
BWB33	-0.091	-0.032	-0.345	-0.024	0.110	-0.110
BWB34	-0.086	-0.030	-0.347	-0.028	0.098	-0.094
BWB4	-0.081	0.005	-0.456	-0.035	-0.03	0.011

Table 6.16 BWB lateral and directional aerodynamic stability derivatives

Analysing Table 6.16 it is found that only for the coupling derivatives C_{n_p} and C_{l_r}, last two columns, a difference exists for the values of pairs (BWB1, BWB3) and (BWB2, BWB4). While the pair (BWB1, BWB3) has negative C_{n_p} values and positive C_{l_r} values, the pair (BWB2, BWB4) has exactly the opposite; positive C_{n_p} values and negative C_{l_r} values. Actually, BWB2, which was considered to have the best response to aileron inputs, has zero C_{n_p} and C_{l_r} values, due to lack of information on these derivatives.

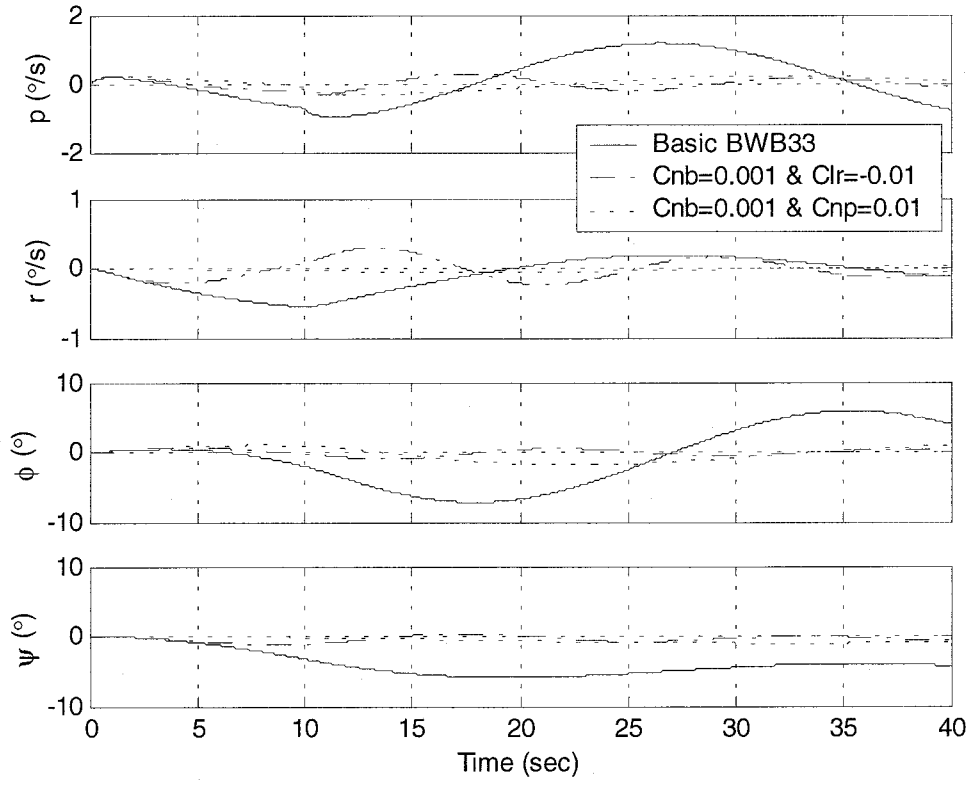

Figure 6.14 BWB33 responses to an aileron input for several C_{n_β}, C_{l_r} and C_{n_p} values

In Figure 6.14 the roll and yaw rates and angles responses to an aileron input are presented, where the values and signs of derivatives C_{l_r} and C_{n_p} are changed. The value of the directional static stability, C_{n_β}, was also changed to give stable

configurations, thus emphasizing once more the need for some static stability. From Figure 6.14 it is seen that the derivatives C_{l_r} and C_{n_p} have a great influence over the roll and yaw rates responses, and consequently over the roll and yaw angles.

Physically what happens is, when the ailerons are deflected negatively the first and desirable reaction is a positive rolling moment, through the C_{l_ξ}, which induces a positive roll rate. Since C_{n_p} is negative, a positive roll rate induces a negative yawing moment, and thus a negative yaw rate appears. Moreover, due to the positive C_{l_r}, the just created negative yaw rate induces a negative roll rate which will oppose to the initial roll rate, reason why the ailerons where deflected. Thus, C_{n_p} and C_{l_r} actually oppose the initial desirable roll rate.

Furthermore, the C_{l_p} derivative opposes also to the initial positive roll rate, since it is negative, therefore, a positive roll rate induces a negative rolling moment. Only the C_{n_r} derivative will be helping the C_{l_ξ} effect, while the yaw rate is negative, by decreasing the yawing moment value and thus the C_{l_r} effect. On the other hand, for the BWB2 and BWB4 configurations, although C_{n_p} is contributing to a desirable positive yawing moment when the roll rate is positive, the C_{l_r} derivative will oppose the increase of rolling moment, since it is negative. However, the opposite effect of the derivatives C_{l_p} and C_{l_r} are not enough to overcome the C_{l_ξ} effect.

The C_{n_p} cross derivative is almost entirely determined by the wing contribution, due to the increase of drag in the wing that goes down, and decrease of drag in the wing that goes up, during a rolling manoeuvre. This contribution is usually positive, i.e., a positive roll rate induces a positive yawing moment. Other contributions to this derivative comes from, usually large, fins. Since BWB configurations do not have large fins, it would be expected a positive C_{n_p} as it happens for the BWB2 and BWB4 data, which is very desirable.

In the same way as for C_{n_p}, the C_{l_r} derivative is due mainly to the wing contribution. When yawing the difference in the lift increase of the wing that goes forward and the lift decrease of the wing that goes backwards, induces a rolling moment. Usually, a positive yaw rate produces a positive rolling moment, and thus, a positive C_{l_r} due to the wing. Another contribution arrives from the fin, which when yawed a sideslip angle develops, viewed as an angle of attack increase by the fin. Thus, a side force appears in the fin, which usually works above the centre of gravity, creating a rolling moment. Hence, the fin also contributes for a positive C_{l_r} derivative.

6.5.3 Time responses due to rudder inputs

The lateral-directional time history responses are analysed here for when a rudder control is inputted. Figures 6.15 and 6.16 give the lateral-directional variables response to a rudder step input of –1deg of several BWB configurations. Observing these figures the dutch roll mode is well seen in the sideslip angle and roll rate responses to a greater extent, and in the yaw rate and roll angle to a lesser extent. In general, the goal when applying a rudder input is for a certain yaw rate to give an appropriate yaw angle or sideslip angle. For this role and based on Figures 6.15 and 6.16, the BWB4 configuration appears to be the most adequate.

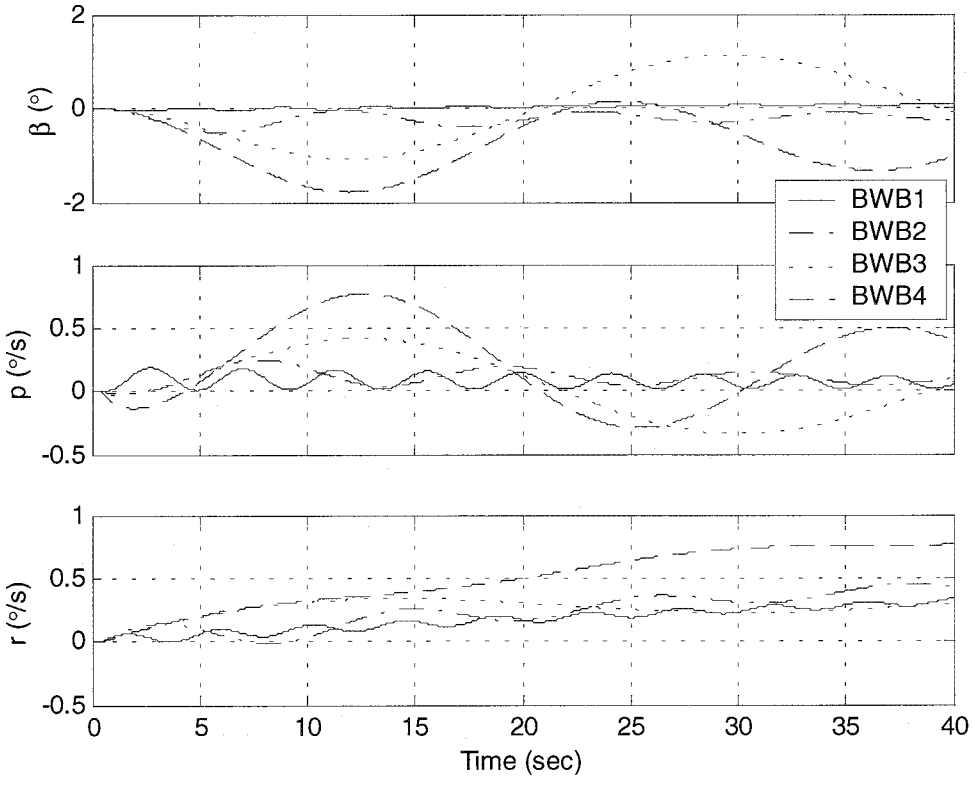

Figure 6.15 BWB responses to a rudder step input of –1deg

Figure 6.15 shows that for a negative rudder deflection the BWB4 yaw rate increases in the positive sense and increasing rate, and without dutch roll influence. Consequently, the yaw angle increases steadily at an increasing rate, as shown on Figure 6.16. During this time the BWB4 sideslip angle response is negative and highly influenced by the dutch roll mode. Although not show on Figure 6.15, the BWB4 steady state sideslip angle value appears to be the highest of all configurations. However, the BWB4 roll rate response to rudder input appears to be from Figure 6.15 the worse response with the highest initial adverse roll rate and highly oscillatory.

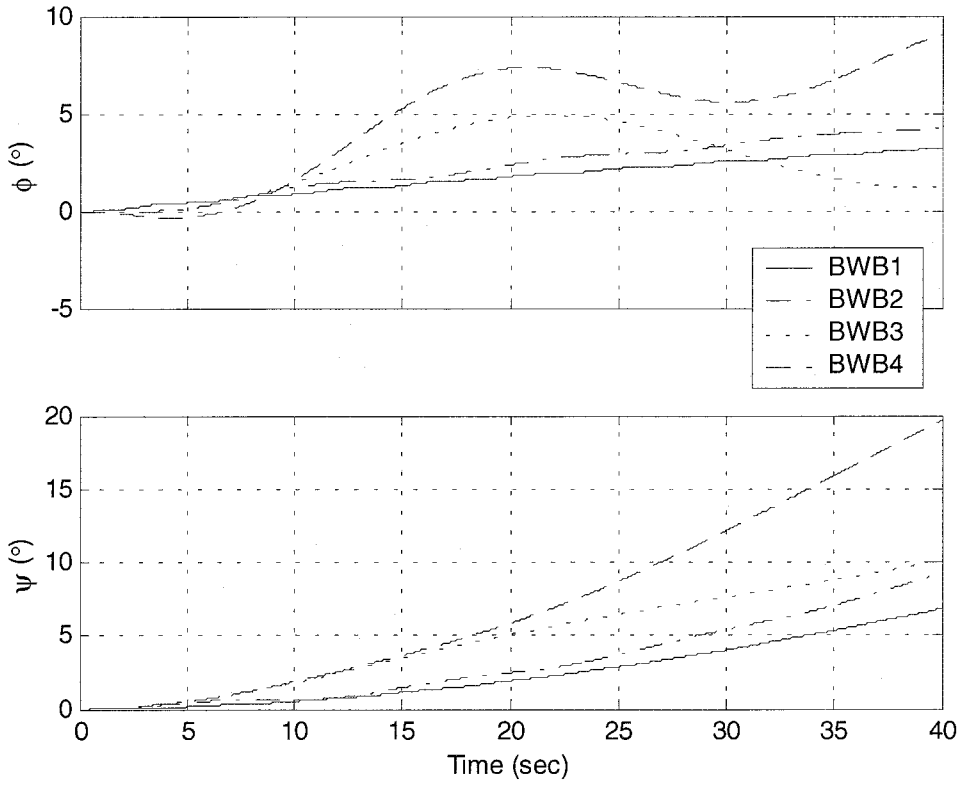

Figure 6.16 BWB responses to a rudder step input of –1deg

The BWB2 configuration has a similar response as for the BWB4 configuration, but with a lower magnitude and with lower oscillations in the roll rate response. Figures 6.15 and 6.16 show that when the rudder is deflected negatively, a positive yaw rate is developed, although oscillating due to the low dutch roll mode. This results in a slow increase of heading, being necessary almost 30 seconds to reach only 5 degrees of yaw angle. The BWB2 roll rate generated by the rudder input is also positive, although there is an incursion on the negative side in the very first seconds, referred to as adverse roll in the rudder response. Since this incursion is very small, there appears to have no effect on the bank angle, which increases steadily in the positive sense without oscillations. Lastly, the sideslip angle response to rudder input is oscillatory due to the dutch roll influence, being the maximum amplitude generated around half degree in the negative side, which is less than that generated by ailerons deflection.

For the BWB3 responses Figures 6.15 and 6.16 presents similar characteristics as the BWB4 responses, although with a lower magnitude. Besides, for the variables highly influenced by the dutch roll, such as sideslip angle, roll rate and roll angle, when this mode is full developed the BWB3 responses are different from the BWB4 responses due to a noticeable neutral or slightly unstable dutch roll mode. Nevertheless, the

BWB3 configuration presents the second highest yaw angle generation per rudder deflection.

Lastly, configuration BWB1 has the lowest yaw rate and yaw angle response of the four configurations to a rudder input. Furthermore, although the high oscillation of the sideslip angle response due to the dutch roll high frequency, also noticeable in all other BWB1 variables response, the BWB1 steady state sideslip angle appears to be zero. The only positive note of the BWB1 configuration is the inexistence of adverse roll in the roll rate response to rudder inputs.

Figures 6.17 and 6.18 present the lateral-directional responses to a rudder step input of –1deg for the BWB31, BWB33 and BWB34 configurations defined in the previous paragraph. As for the responses to aileron inputs, the initial responses of all three configurations are equal, but differentiate as soon as the characteristic modes are developed. Furthermore, it can be seen from Figures 6.17 and 6.18 that the BWB31 configuration, which has the highest positive static margin, $K_n = 0.181$, presents the most conventional response.

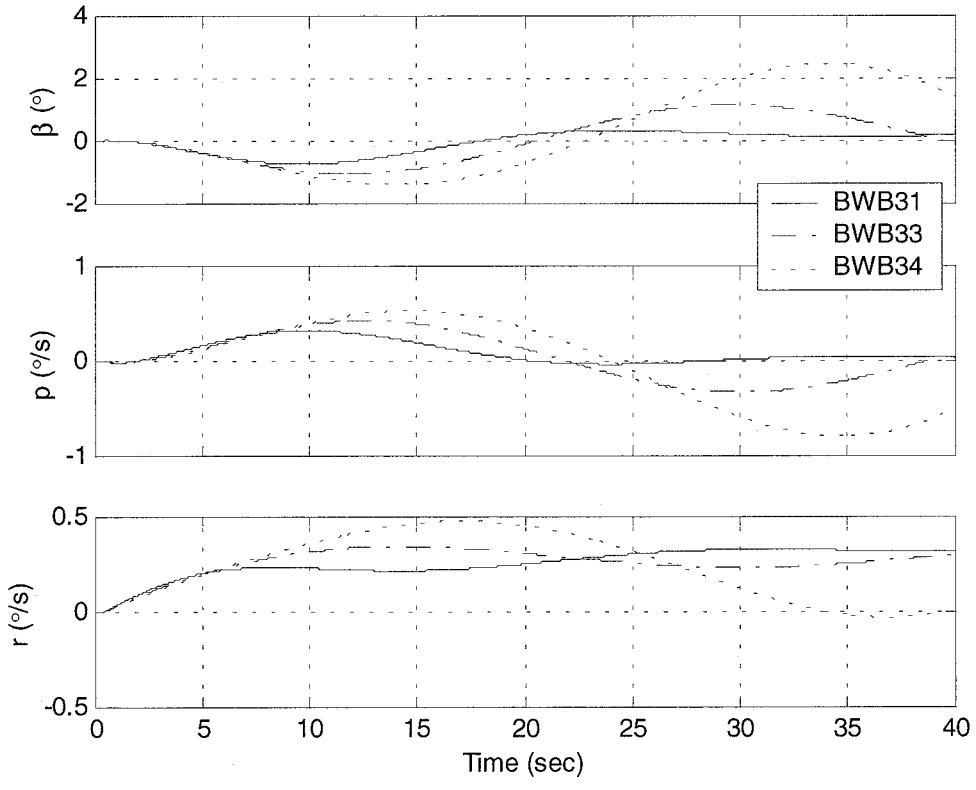

Figure 6.17 BWB3 responses to a rudder step input of –1deg

This means that when the rudder is deflected negatively the yaw rate increases positively for the first seconds maintaining more or less constant for the remaining time. Consequently, the yaw angle is very slow to begin to change, but then increases

in the positive sense at a constant rate. Furthermore, the roll rate increases positively in the first 10 seconds becoming null again after that. As a consequence the aircraft banks positively for 10seconds keeping then the bank constant. Lastly, the sideslip angle increases negatively for 10 seconds and then decreases again to near zero, similar to the roll rate response.

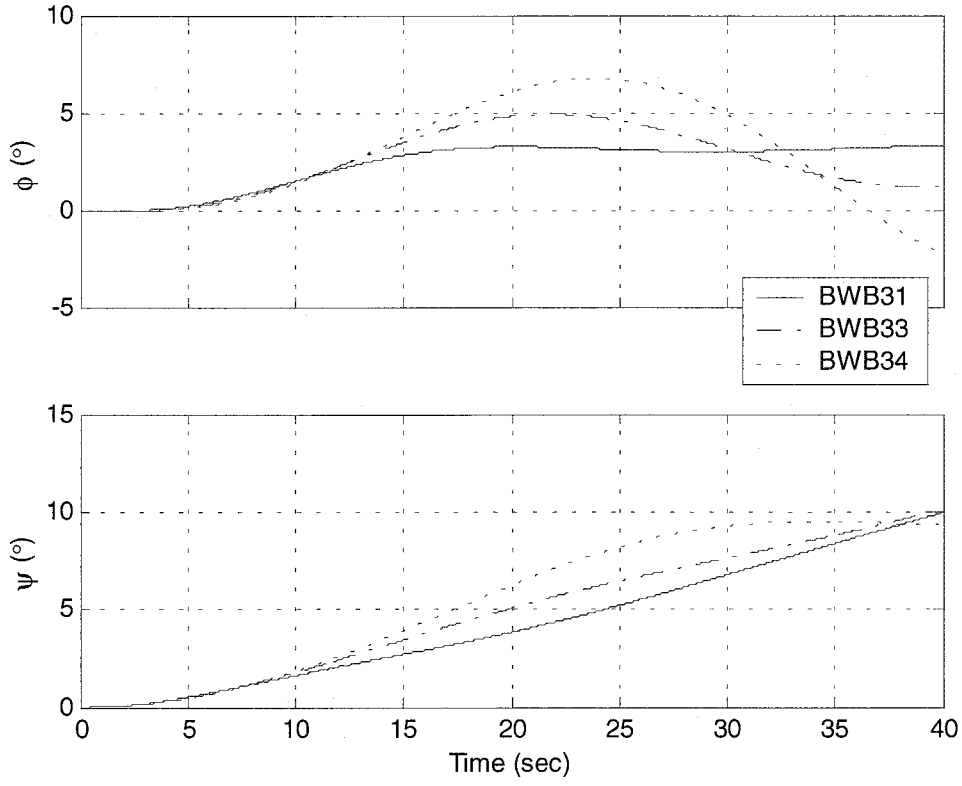

Figure 6.18 BWB3 responses to a rudder step input of –1deg

The differences existent between BWB31 and BWB33 and BWB34 are due to the different characteristic modes, as shown in Figures 6.2 to 6.4. From Figures 6.17 and 6.18 it is well seen the lower damping and lower frequency as the static margin decreases and becomes negative, in the same way as for the responses to aileron inputs.

6.6 Comparison with the flying and handling qualities requirements

From the lateral-directional dynamic analysis done, more was revealed about the lateral-directional stability characteristics and behaviour of blended-wing-body configurations. Comparing these results with the lateral-directional requirements of

MIL-F-8785C[46], an assessment of the lateral-directional flying and handling qualities of blended-wing-body is made.

Firstly, comparing the several configurations basic modes with those given by the requirements, one can see that the dutch roll mode is very low damped for a landing approach flight condition, and still low damped or even unstable for other flight conditions, principally for unstable *cg* positions or for high levels of static lateral stability. For most of the configurations the dutch roll mode frequency is also low, needing improvement.

In general, the roll and spiral mode do not present the usual problems of fulfilling the minimum lower limits of the requirements, on the contrary. The blended-wing-body problems with roll and spiral modes may be the low time constant values achieved in certain configurations and flight conditions. For a stable spiral mode, a decrease in time constant means a faster mode, which may be undesirable during turns. A roll mode faster than usual may bring problems of excessive lateral abruptness and roll ratcheting.

A further problem is the sideslip angle generated by some configurations when ailerons or rudders are applied. In some cases 2 degrees of sideslip is generated per degree of aileron or rudders deflected. This means 20 degrees of sideslip angle when the ailerons or rudders are deflected 10 degrees, which is completely undesirable. The roll and yaw rate responses to aileron inputs for some configurations are also undesirable. Due to the coupling derivatives signs, a desirable roll rate induces an undesirable yaw rate, which will oppose the initial roll rate. This connected with underpowered controls and a low damped dutch roll, makes it impossible to control a blended wing body configuration using conventional techniques.

Finally, the rudders adverse roll effect makes the aircraft to initially roll in the direction contrary to the direction of turn, giving a wrong feeling to the pilot, and thus degrading the handling qualities. Furthermore, although possessing large vertical surfaces and thus more rudder control power, the BWB2 aircraft also possesses high levels of directional stability, making the increased control power not sufficient. In general, all configurations lack control power, since the fastest configuration needs more than 20 seconds to achieve 0.5 deg/sec of yaw rate and none of the remaining achieve that value after 40 seconds of rudder deflection.

CHAPTER 7
Longitudinal Flight Control System

"As the science of air travel has expanded the safety of the vehicle has more or less kept pace ... the importance of continuity in development and safety cannot be overstressed"
Black, 1968

7.1 Overview

Using the flying and handling qualities requirements set out in Chapter 2, which relate the stability and control characteristics to flying and handling qualities, it was shown that the blended-wing-body configuration suffers from flying and handling qualities problems. Thus, some kind of stability augmentation system has to be implemented, for both the longitudinal and lateral-directional motions, in order to augment the blended-wing-body flying and handling qualities to satisfactory levels.

In Chapter 5 it was shown that a negative static margin presents advantages in blended-wing-body applications, hence an unstable configuration is preferred. Thus, a fly-by-wire system is required to be on line at all times. Fly-by-wire technology not only enables augmentation of the basic aircraft stability, but also the complete optimisation of the aircraft response to pilot commands, an aspect already discussed in Chapters 1 and 2.

The question arises again of what the optimised aircraft response should be, or what the pilot desires most. A pilot usually learns how to fly in smaller non-augmented aircraft. Thus, he develops his skills in the expectation that aircraft in general have conventional response-type characteristics. As Philipps[44] suggests, some of the typical characteristics of conventional aircraft considered desirable or expected by

pilots are, for instance, that the control forces appear approximately in phase with the control deflection, thereby providing the pilot with anticipation of the magnitude of the response that will follow. Aerodynamic damping moments on the control surfaces suppress control oscillations. With stable aeroplanes, the variation of stick position and force with airspeed give the pilot a warning of speed changes from the trim condition, and give him appreciation of approach to the stall. The aerodynamic hinge moments increase with the dynamic pressure, thereby maintaining an appropriate stick force per g and helping to prevent the pilot from overloading the airplane in flight at high speed.

In Chapter 2 several response-types were presented: the angle of attack or conventional, the pitch rate command/attitude hold, the pitch attitude command/attitude hold and the flight path angle rate command. Since the pilot expects a conventional response, one could doubt the implementation of unconventional response-types. However, Hoh[57] and Mitchell *et al*[49] showed that, depending on the mission element task, other response-types may be more useful, or should be completely avoided. Moreover, once a decision on the response-type is made, it is still necessary to design the flight control system structure.

In this and the next chapters, flight control system designs are described which improve the basic blended-wing-body flying and handling qualities. In the present chapter a longitudinal flight control system is devised, while a lateral-directional flight control system will be treated in the following chapter.

7.2 Flight control system design rules

The requirements used in the design of longitudinal flight control systems are those as presented in Castro and Cook[98], and resulted from the findings of Gautrey[68]. These are repeated here in equations (7.1) to (7.4) and represent ideal characteristics for a civil transport aircraft.

Short-term mode damping ratio, $\zeta_s = 0.7$ (7.1)

Generic Control Anticipation Parameter, $GCAP = 0.6\, rad/s^2/g$ (7.2)

Gibson dropback criterion $\frac{DB}{q_s} = 0$ or $T_{\theta_2} = \frac{2\zeta_s}{\omega_s}$ (7.3)

Long-term mode damping ratio, $\zeta_p > 0.1$ (7.4)

The requirements of equations (7.1) and (7.2) impose limits to the short period damping and frequency. Namely, equation (7.1) requires a minimum damping of 0.7, whilst equation (7.2) defines GCAP and hence a value for the short-period frequency, ω_s. The definition of GCAP was presented in Chapter 2 and it is here repeated in equation (7.5). However, as it can be seen in equation (7.5), this GCAP definition depends on the values of the closed-loop augmented system. Thus, in order to have an initial value of the short-period frequency, the definition of CAP, as given in equation (7.6), is used instead.

$$GCAP = \frac{\dot{q}(t_{pk})}{n_z(t_{pk})}\left(1+\exp\left(\frac{-\zeta_s \pi}{\sqrt{1-\zeta_s{}^2}}\right)\right) \tag{7.5}$$

$$CAP = \frac{g\omega_s{}^2 T_{\theta_2}}{U_e} \Rightarrow \omega_{sp} = \sqrt{\frac{U_e CAP}{gT_{\theta_2}}} \tag{7.6}$$

Furthermore, calculating the short-period frequency required for a given CAP value for several values of speed and different *cg* positions of configuration BWB3, it was found that high values of frequency were required in some cases as shown in Figure 7.1. Since the control power available is limited, if the requirement for a GCAP of $0.6 rad/s^2/g$ demands unusually large feedback gains this is not used. In this case, constant values for the short period mode frequency as presented in equation (7.7) are used instead, and the resultant GCAP value is calculated afterwards for comparison purposes.

$$\omega_s = 2.0(rad/\sec) \text{ or } \omega_s = 2.5(rad/\sec) \tag{7.7}$$

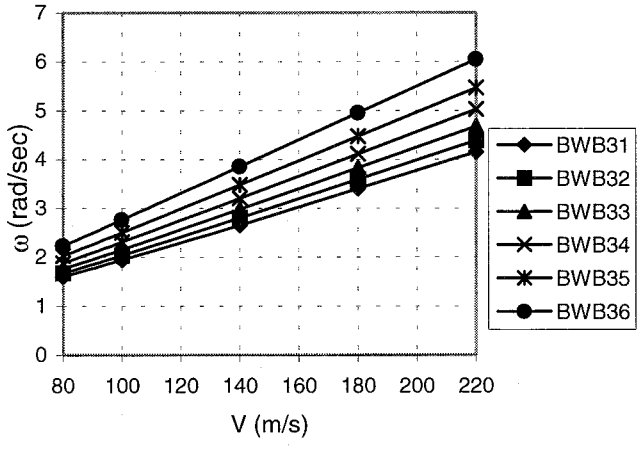

Figure 7.1 Short-period frequency for a CAP of 0.6 rad/s^2/g

Since the flight path angle is controlled through knowledge of the pitch attitude behaviour, the relation between these two variables is important and the relation

should be optimised. The requirement described by equation (7.3) imposes limits on that relationship, so that by using pitch attitude information the flight path angle can be controlled easily. The phugoid mode is generally of rather long period and usually it is not of concern to the pilot. However, depending on the structure of the flight control system to design this can change. Therefore, the requirement of equation (7.4) is used to keep the long-term response within acceptable limits.

7.3 Simple stability augmentation system

Cook[43] states that if there is no reason to complicate the flight control system design, then do not do it. With this idea in mind, the initial goal when beginning the longitudinal flight control system design was solely to increase the aircraft static stability. The pole placement method was used in this case. The pole placement is a powerful method for designing feedback gains based on the manipulation of the equations of motion in state space form. If stability characteristics for the augmented aircraft are specified, this method enables to place the poles of the closed loop on the s-plane exactly as required. The open-loop state and output matrix equations are given by equations (7.8) and (7.9) respectively. The control law is given then by equation (7.10), where v is the vector of input demand variables and K is the matrix of feedback gains.

$$\dot{x} = Ax + Bu \tag{7.8}$$

$$y = Cx + Du \tag{7.9}$$

$$u = v - Kx \tag{7.10}$$

Substituting equation (7.10) into equations (7.8) and (7.9), the closed loop state and output equations follow as given by equations (7.11) and (7.12). The augmented aircraft characteristic equation is then calculated as presented in equation (7.13), and the roots of this equation completely describe the stability of the augmented aircraft.

$$\dot{x} = (A - BK)x + Bv \tag{7.11}$$

$$y = (C - DK)x + Dv \tag{7.12}$$

$$\Delta_{aug}(s) = |sI - A + BK| = 0 \tag{7.13}$$

As it was seen in the design rules of the previous paragraph 7.2, limits are imposed mainly to the short period mode damping and frequency, through equations (7.1), (7.2) and (7.7). Actually, equation (7.7) is used here instead of equation (7.2) so to study the influence of higher frequencies in the feedback gains. The actual phugoid

mode damping and frequency are acceptable. Thus, these are adopted for the augmented aircraft. Thus, the closed loop stability characteristics are defined by $\zeta_s = 0.7$, $\omega_s = 2.0(rad/\sec)$ or $\omega_s = 2.5(rad/\sec)$, $\zeta_p = (\zeta_p)_{actual}$ and $\omega_p = (\omega_p)_{actual}$. In possession of this information the closed loop characteristic equation is given by equation (7.14). The values of the feedback gains matrix can be calculated then by equating equation (7.14) to equation (7.13).

$$(s^2 + 2\zeta_s\omega_s s + \omega_s{}^2)(s^2 + 2\zeta_p\omega_p s + \omega_p{}^2) = 0 \qquad (7.14)$$

The flight control system structure resultant from this design is given in Figure 7.2. It can be seen that all four longitudinal state variables, angle of attack, pitch rate, pitch attitude and axial speed are fed back. Before being summed with the pilot command, each variable is multiplied by a gain. It is also seen in Figure 7.2 that the elevator actuator dynamics are also included. Equation (7.8) actually is equivalent to equation (5.1) presented in Chapter 5, augmented with the elevator actuator dynamics as follow.

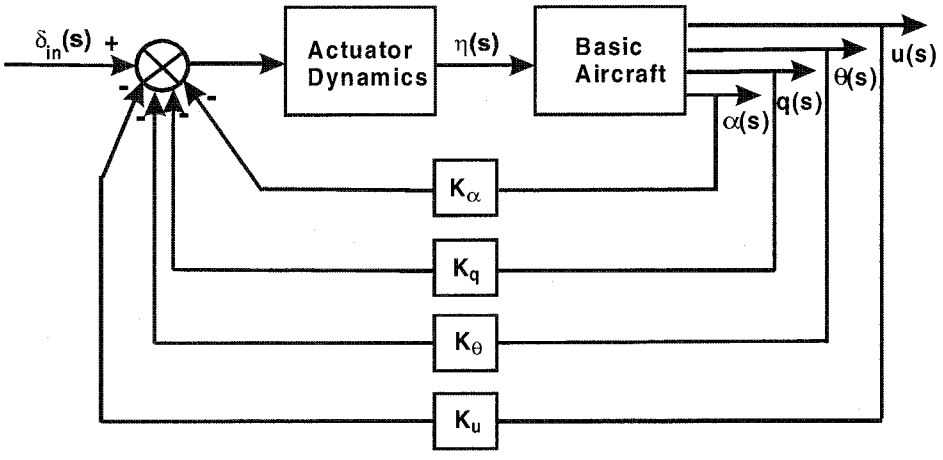

Figure 7.2 Stability augmentation system structure

The actuator system, as that of Figure 7.3, is supposed to be represented by a second order equation as shown in equation (7.15). The transfer function which gives the relation between the actuator output, y_{ac}, and the actuator input, u_{ac}, is presented in equation (7.16).

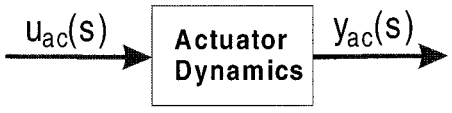

Figure 7.3 Actuator dynamics diagram

$$\ddot{y}_{ac}(t)+2\zeta_{ac}\omega_{ac}\dot{y}(t)+\omega_{ac}{}^{2}y_{ac}(t)=\omega_{ac}{}^{2}u_{ac}(t) \tag{7.15}$$

$$\frac{y_{ac}(s)}{u_{ac}(s)}=\frac{\omega_{ac}{}^{2}}{s^{2}+2\zeta_{ac}\omega_{ac}s+\omega_{ac}{}^{2}} \tag{7.16}$$

Two state variables are then used to describe this second order system as shown in equations (7.17) and (7.18), and the differential equations representing this system are given in equations (7.19) and (7.20). Introducing these last two equations in the state equation (5.1) results the state equation as presented in equation (7.21).

$$\eta = y_{ac} \tag{7.17}$$

$$V_{\eta} = \dot{y}_{ac} \tag{7.18}$$

$$\dot{\eta} = V_{\eta} \tag{7.19}$$

$$\dot{V}_{\eta} = \omega_{ac}{}^{2}u_{ac} - 2\zeta_{ac}\omega_{ac}V_{\eta} - \omega_{ac}{}^{2}\eta \tag{7.20}$$

$$\begin{bmatrix}\dot{u}\\ \dot{\alpha}\\ \dot{q}\\ \dot{\theta}\\ \dot{\eta}\\ \dot{V}_{\eta}\end{bmatrix}=\begin{bmatrix} x_u & x_w V_o & x_q & x_\theta & x_\eta & 0\\ z_u/V_o & z_w & z_q/V_o & 0 & z_\eta/V_o & 0\\ m_u & m_w V_o & m_q & 0 & m_\eta & 0\\ 0 & 0 & 1 & 0 & 0 & 0\\ 0 & 0 & 0 & 0 & 0 & 1\\ 0 & 0 & 0 & 0 & -\omega_{ac}{}^{2} & -2\zeta_{ac}\omega_{ac}\end{bmatrix}\begin{bmatrix}u\\ \alpha\\ q\\ \theta\\ \eta\\ V_{\eta}\end{bmatrix}+\begin{bmatrix}0\\ 0\\ 0\\ 0\\ 0\\ \omega_{ac}{}^{2}\end{bmatrix}u_{ac} \tag{7.21}$$

The feedback gains are presented in Tables 7.1 and 7.2 for a short period frequency of $2.0(rad/\sec)$ and $2.5(rad/\sec)$ respectively. From Tables 7.1 and 7.2 it is seen that, except for K_θ, the magnitude of the gains increases as the *cg* moves aft. Moreover, gains of magnitude equal to those of K_α may be dangerous for safety reasons. Comparing Tables 7.1 and 7.2 it is also seen that the gains increase to achieve a higher short period frequency.

***cg* position** h	K_u	K_α	K_q	K_θ
0.019	0.0015	-1.31	-0.94	0.015
-0.062	0.0017	-2.16	-1.03	0.011
-0.144	0.0019	-3.35	-1.12	0.006
-0.225	0.0020	-5.13	-1.16	-0.003

Table 7.1 BWB3 feedback gains variation with *cg* for $\omega_s = 2.0(rad/\sec)$

From Table 7.1 a gain of $K_\alpha = -1.31$ is necessary to increase the short period frequency to $2.0(rad/\sec)$. To increase it further to $2.5(rad/\sec)$, the K_α gain almost doubles value, as shown in Table 7.2. Thus, to reach the higher values of short period frequency, as shown in Figure 7.1, even higher K_α gains would be required, which is

not advisable for safety issues. From here it can be concluded that the requirement of a constant GCAP value as presented in equation (7.2) is definitively not advisable for these BWB configurations. For the remaining of the longitudinal flight control design the requirement (7.7) is used throughout.

***cg* position** h	K_u	K_α	K_q	K_θ
0.019	0.0018	-2.32	-1.28	0.024
-0.062	0.0021	-3.30	-1.41	0.019
-0.144	0.0024	-4.66	-1.54	0.013
-0.225	0.0026	-6.70	-1.63	0.001

Table 7.2 BWB3 feedback gains variation with *cg* for $\omega_s = 2.5(rad/\sec)$

Gains of these larger magnitudes are required due to the weaker control surface power of BWB3 configuration, as commented before. Table 7.3 shows the gains for the BWB3 configuration, using the single surface with the highest pitching moment, as initially intended, and, which is compared with the gains when all trailing edge surfaces for pitch control are used. Compared with these are the gains for the BWB4 configuration which has larger control surface derivatives, as shown. The BWB3 configuration used a static margin of $K_n = -0.144\,mac$, similar to $K_n = -0.132\,mac$ of the BWB4 configuration. From Table 7.3 the influence of control surface power on the gains magnitude is well seen.

	C_{m_η}	K_u	K_α	K_q	K_θ
BWB3 (Single)	-0.121	0.0087	-14.7	-5.27	0.034
BWB3 (All)	-0.532	0.0019	-3.35	-1.12	0.006
BWB4 (All)	-0.716	0.0013	-2.32	-0.35	-0.005

Table 7.3 Flight control system gains variation with control power

In Figure 7.4 the time response variables to an elevator pulse of –1deg for the BWB3 augmented aircraft are presented. From Figure 7.4 it can be seen that since the short period frequency and damping was designed to be the same, the general shape of the responses is similar for all configurations. The most significant differences are in the magnitude of the angle of attack response and the pitch rate overshoot. In the BWB33 configuration, the more forward *cg* position has the higher angle of attack response and pitch rate overshoot. While the BWB36 configuration, with the most aft *cg* position has the lowest angle of attack response and pitch rate overshoot. This means that, since BWB33 has the lowest feedback gains and BWB36 the highest, BWB33 has more control power left to change the aircraft equilibrium than configuration BWB36. This is another important consideration when designing the flight control

system. Since there is only a limited amount of control power, some must be used for stabilisation purposes only.

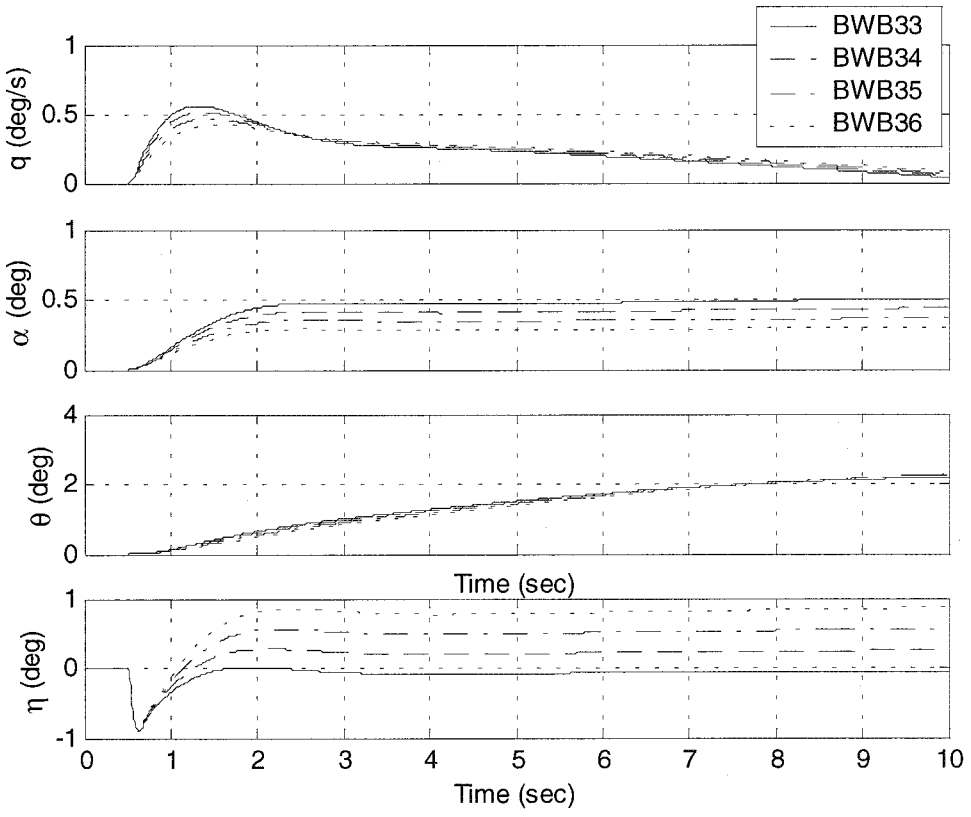

Figure 7.4 Longitudinal response to an elevator step input

This is better seen in the last plot of Figure 7.4 which shows what actually happens to the elevator when the pilot demands an elevator input of –1 deg. Initially the elevator almost deflects to the amount demanded, but once the dynamics are disturbed the flight control system adds feedback inputs, so that the elevator then compensates for the airframe lack of stability. The result is that more compensation is needed for the BWB36 configuration, as shown, with a logical lack of control surface efficiency. This is also seen by the lower angle of attack and pitch rate overshoot attainable.

Since the approach to land is one of the most demanding tasks to be accomplished manually in civil transport missions, this is frequently used in flight simulation trials to assess aircraft flying and handling qualities. The previously designed flight control system gives a conventional, or angle of attack response-type, as shown by the responses. Figure 7.4 also shows that the pitch rate response, after the initial overshoot, decreases although the input is still being applied. However, for a tracking task as in the approach this characteristic is not so desirable, since it requires a continuous input from the pilot implying continuous attention and higher workload. Thus, an alternative different flight control system design was then designed.

7.4 Command and stability augmentation system

During the landing approach the pilot has to follow the glide slope until the aircraft touches the runway at the desired point. The task then, is to track the flight path angle. Since the relation between flight path angle and pitch attitude angle is usually well defined, pilots intuitively use this relation to control flight path by varying pitch attitude. If an integrator is used in the pitch rate feedback path, the pitch rate error is driven to zero. Thus, the pitch rate is held constant for a constant input applied. Therefore, the pitch attitude and flight path will change at a constant rate. Once the input is removed, the pitch rate returns to zero and the pitch attitude remains constant, and so the flight path angle also remains constant.

The structure of the flight control system design is presented in Figure 7.5. The inner loop feedback of angle of attack is necessary to increase the static stability of the unstable configurations. The command variable, as shown in Figure 7.5 is the actual pitch rate, which after being compared with the pitch rate feedback, is integrated to give exactly the amount demanded. This type of command and stability augmentation system (CSAS) is called a pitch rate command/attitude hold control system.

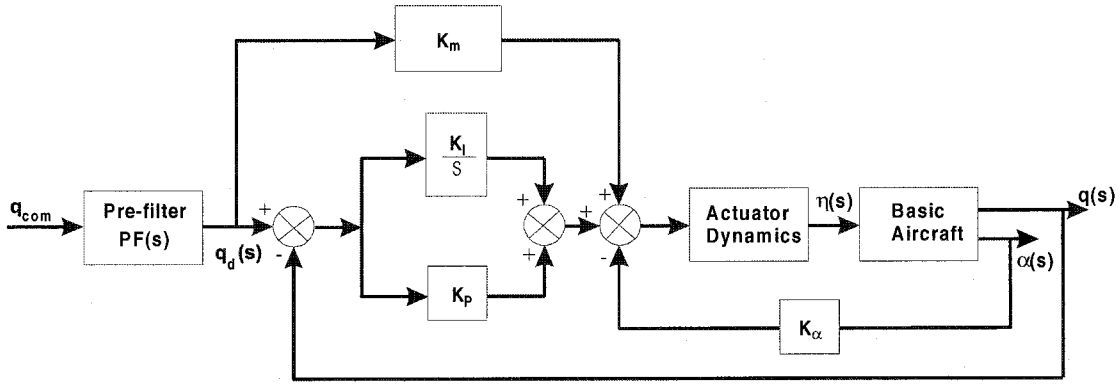

Figure 7.5 Pitch rate command/attitude hold flight control system

Since only angle of attack and pitch rate are used for feedback, a reduced order model is used. Thus, the state equation (5.1) is reduced to that presented in equation (7.22). The elevator actuator dynamics, equations (7.19) and (7.20), are then included in equation (7.22) resulting in the state equation presented in equation (7.23).

$$\begin{bmatrix} \dot{\alpha} \\ \dot{q} \end{bmatrix} = \begin{bmatrix} z_w & z_q/V_o \\ m_w V_o & m_q \end{bmatrix} \begin{bmatrix} \alpha \\ q \end{bmatrix} + \begin{bmatrix} z_\eta/V_o \\ m_\eta \end{bmatrix} \eta \qquad (7.22)$$

$$\begin{bmatrix}\dot{\alpha}\\ \dot{q}\\ \dot{\eta}\\ \dot{V}_\eta\end{bmatrix}=\begin{bmatrix} z_w & z_q/V_o & z_\eta/V_o & 0\\ m_wV_o & m_q & m_\eta & 0\\ 0 & 0 & 0 & 1\\ 0 & 0 & -\omega_{ac}{}^2 & -2\zeta_{ac}\omega_{ac}\end{bmatrix}\begin{bmatrix}\alpha\\ q\\ \eta\\ V_\eta\end{bmatrix}+\begin{bmatrix}0\\ 0\\ 0\\ \omega_{ac}{}^2\end{bmatrix}\eta_d \tag{7.23}$$

To take in account the integration in the state equation, a new state variable is defined. This variable is equal to the integral of the pitch rate error as shown in equation (7.24), where q is the pitch rate and q_d is the demanded pitch rate, as shown in Figure (7.5). Including this differential equation in the state equation (7.23) results the equation (7.25).

$$\varepsilon=\int(q-q_d) \tag{7.24}$$

$$\begin{bmatrix}\dot{\alpha}\\ \dot{q}\\ \dot{\eta}\\ \dot{V}_\eta\\ \dot{\varepsilon}\end{bmatrix}=\begin{bmatrix} z_w & z_q/V_o & z_\eta/V_o & 0 & 0\\ m_wV_o & m_q & m_\eta & 0 & 0\\ 0 & 0 & 0 & 1 & 0\\ 0 & 0 & -\omega_{ac}{}^2 & -2\zeta_{ac}\omega_{ac} & 0\\ 0 & 1 & 0 & 0 & 0\end{bmatrix}\begin{bmatrix}\alpha\\ q\\ \eta\\ V_\eta\\ \varepsilon\end{bmatrix}+\begin{bmatrix}0\\ 0\\ 0\\ \omega_{ac}{}^2\\ 0\end{bmatrix}\eta_d+\begin{bmatrix}0\\ 0\\ 0\\ 0\\ -1\end{bmatrix}q_d \tag{7.25}$$

In matrix form, the state equation (7.25) is represented by equation (7.26). The control law used in this flight control system is as given in equation (7.27). Introducing then equation (7.27) into equation (7.26) and rearranging, results the closed loop state equation (7.28), where $K^T=\lfloor K_\alpha \quad K_q \quad K_\eta \quad K_{V_\eta} \quad K_i \rfloor$ and $M=[K_m]$.

$$\dot{x}=Ax+B\eta_d+Nq_d \tag{7.26}$$

$$\eta_d=-Kx+Mq_d \tag{7.27}$$

$$\dot{x}=(A-BK)x+(BM-N)q_d \tag{7.28}$$

The values of the gains vector, K, establish the stability of the system and are calculated using the pole placement method described in paragraph 7.3. The closed loop characteristic equation has the short period mode damping and frequency as in equations (7.1) and (7.7), the actuator dynamics are kept equal, and the integrator zero is given a convenient value. The feedforward path gain K_m provides the means for tailoring the pitch response transfer function zero to cancel the integral lag. In the pole placement method all state variables are feedback and that is the reason of the appearance of the gains K_η and K_{V_η} referent to the actuator states. However, these gains are usually small, and hence are ignored.

Thus, in a second phase of the design the full order model, as given in equation (7.29), is considered. The control law as given by equation (7.27) is also applied, but now the gains vector is equal to $K^T=\lfloor K_u \quad K_\alpha \quad K_q \quad K_\theta \quad K_\eta \quad K_{V_\eta} \quad K_i \rfloor$ where K_u, K_θ, K_η

and K_{V_η} are made equal to zero and the remaining gains are made equal to those calculated with the reduced order model.

$$\begin{bmatrix} \dot{u} \\ \dot{\alpha} \\ \dot{q} \\ \dot{\theta} \\ \dot{\eta} \\ \dot{V}_\eta \\ \dot{\varepsilon} \end{bmatrix} = \begin{bmatrix} x_u & x_w V_o & x_q & x_\theta & x_\eta & 0 & 0 \\ z_u/V_o & z_w & z_q/V_o & 0 & z_\eta/V_o & 0 & 0 \\ m_u & m_w V_o & m_q & 0 & m_\eta & 0 & 0 \\ 0 & 0 & 1 & 0 & 0 & 0 & 0 \\ 0 & 0 & 0 & 0 & 0 & 1 & 0 \\ 0 & 0 & 0 & 0 & -\omega_{ac}{}^2 & -2\zeta_{ac}\omega_{ac} & 0 \\ 0 & 0 & 1 & 0 & 0 & 0 & 0 \end{bmatrix} \begin{bmatrix} u \\ \alpha \\ q \\ \theta \\ \eta \\ V_\eta \\ \varepsilon \end{bmatrix} + \begin{bmatrix} 0 \\ 0 \\ 0 \\ 0 \\ 0 \\ \omega_{ac}{}^2 \\ 0 \end{bmatrix} \eta_d + \begin{bmatrix} 0 \\ 0 \\ 0 \\ 0 \\ 0 \\ 0 \\ -1 \end{bmatrix} q_d \tag{7.29}$$

The command path pre-filter is the last part to be designed and it remains as the means for fine-tuning the command response characteristics for good handling, essentially by phase adjustment, as shown in equation (7.30). This is done using the design requirement as given in equation (7.3). To design the pre-filter a new state variable is defined as presented in equation (7.31), where the differential equation to be included in the closed loop state equation is that given by equation (7.32).

$$PF(s) = \frac{\left(1 + \dfrac{s}{(T_{\theta_2})_{desired}}\right)}{\left(1 + \dfrac{s}{(T_{\theta_2})_{actual}}\right)} \tag{7.30}$$

$$v = q_d - \frac{(T_{\theta_2})_{desired}}{(T_{\theta_2})_{actual}} q_{com} \tag{7.31}$$

$$\dot{v} = -(T_{\theta_2})_{actual} v + \frac{(T_{\theta_2})_{desired}}{(T_{\theta_2})_{actual}} \left((T_{\theta_2})_{desired} - (T_{\theta_2})_{actual}\right) q_{com} \tag{7.32}$$

In this way, it is possible to place the transfer function zero responsible for the pitch rate response overshoot as desired to give favourable characteristics as seen by the pilot. However, sometimes this cancellation may not be exact, introducing additional lag. Thus, an alternative structure, as presented in Figure 7.6, was tried as well. In this design, the actual pitch rate transfer function zero, $1/T_{\theta_2}$, is eliminated using the integral pole, and the feedforward path is used not only to eliminate the lag introduced by the integral term, but also to place T_{θ_2} in the desirable place. Table 7.4 presents the flight control system gains for the structure with pre-filter, and Table 7.5 for the structure without pre-filter. The values for two different *cg* positions of configuration BWB3 are presented, BWB33 and BWB35, as well as for the BWB4 configuration, which has a static margin similar to BWB35, but more powerful control surfaces.

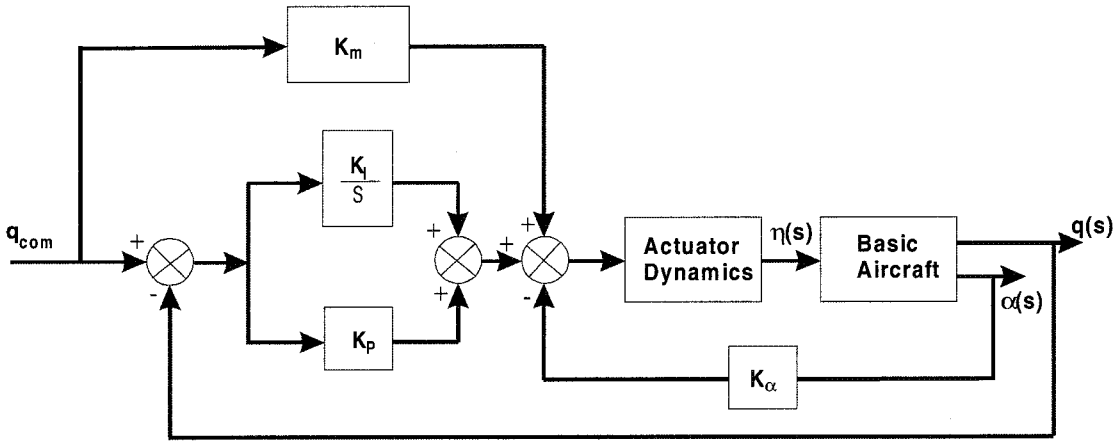

Figure 7.6 Pitch rate command/attitude hold flight control system

Again, control power is important to define the magnitude of the gains. Comparing the values obtained for the BWB35 and BWB4 configurations, which have around the same static margin, it is seen that BWB4 gains are half the value of those for BWB35. Table 7.4 shows further that the integral gain does not change very much with *cg* position, but all gains increase in magnitude with decreasing speed. In table 7.4 the feedforward gain, K_m, is not given because it was made equal to $-K_i/3$ at all times. Table 7.5 contains the values for the flight control system without pre-filter, where K_m is already presented. Comparing the gains of Tables 7.4 and 7.5, it can be seen that the flight control system without pre-filter has, in general, lower gains than with pre-filter.

	BWB33 ($h = 0.019$)		**BWB35** ($h = -0.144$)		**BWB4** ($h = -0.13$)	
	$100m/s$	$180m/s$	$100m/s$	$180m/s$	$100m/s$	$180m/s$
K_P	4.65	0.61	1.83	-1.3	0.9	-0.88
K_i	-9.13	-1.55	-9.0	-1.54	-5.92	-1.01
K_α	-3.3	-0.76	-4.23	-0.99	-2.7	-0.48
$(T_{\theta_2})_{actual}$	1.32	0.75	0.98	0.55	0.87	0.33
$(T_{\theta_2})_{desired}$	0.80	0.76	0.83	0.65	0.78	0.66

Table 7.4 Longitudinal command flight control system gains with pre-filter

This is so because the integral pole is allocated to the same value as $1/T_{\theta_2}$. From Table 7.4 it is seen that $1/T_{\theta_2}$ is always higher than 1/3, the integral time constant for the flight control system with pre-filter. Since with the pre-filter the integral pole is located further away from the origin of the *s*-plane, the integral gain needs to be higher than that of the flight control system without pre-filter, which has the integral

poles more near to the origin. On the other hand, if the cancellation is not exact, the flight control system without pre-filter is more prone to problems.

	BWB33 ($h = 0.019$)		**BWB35** ($h = -0.144$)		**BWB4** ($h = -0.13$)	
	$100 m/s$	$180 m/s$	$100 m/s$	$180 m/s$	$100 m/s$	$180 m/s$
K_P	0.21	0.15	-1.57	-1.57	-1.07	-0.88
K_i	-2.31	-0.69	-3.08	-0.93	-2.28	-1.01
K_α	-1.54	-0.43	-2.18	-0.68	-1.25	-0.48
K_m	0.7	0.7	0.64	0.55	0.64	0.66

Table 7.5 Longitudinal command flight control system gains without pre-filter

It is usual to schedule the gains with speed since, as shown in Tables 7.4 and 7.5, the flight control system gains vary greatly with speed. However, that was not done for this research, since interpolation with two or three values did not give an acceptable response. Instead, constant gains calculated for a mid speed of around 150 m/s were used throughout. Although being more critical at lower speeds, the gains were calculated for a mid speed, because the gains at low speeds would give rise to undesirable oscillations at higher speeds. As shown later in the Chapter 10, the pilots actually only flew one configuration in the flight simulator with one longitudinal and lateral-directional control system. The configuration flown was that for BWB4 and the longitudinal flight control system gains used are presented in Table 7.6. The time history responses for several speeds are given in Figure 7.7.

	K_P	K_i	K_α	$(1/T_{\theta_2})_{actual}$	$(1/T_{\theta_2})_{desired}$
BWB4	-0.58	-2.75	-1.072	0.5883	0.5468

Table 7.6 Longitudinal flight control system gains used in the simulator

From Figure 7.7 it is seen that with this command and stability augmentation system, the pitch rate is held nominally constant as long as the input is applied. There are only a few differences due to the use of a fixed set of gains, for example, in the pitch rate overshoot and rise time, on the initial pitch attitude response and on the "steady state" magnitude of the angle of attack. The latter difference is expected since different speeds need different angles of attack to trim. The pitch rate overshoot and rise time differences, which also make the initial pitch attitude angle different, can degrade the flying and handling qualities if not within the required limits. The last plot of Figure 7.7 shows the elevator angle deflected. Comparing this plot with the elevator angle response of Figure 7.4 it seems that the elevator deflects more for this command and stability augmentation flight control system than in the case of the simple stability

augmentation system. However, while previously the pilot was commanding elevator deflection, achieving a maximum of 2 degrees pitch attitude after 7 seconds with an elevator deflection of around 0.6 degrees, now the pilot commands pitch rate and with the same elevator deflection a larger pitch attitude angle is achieved. Besides, previously it was possible for the pilot to demand more than 10 degrees of elevator deflection, whilst with the present system 5 degrees/sec may represent the maximum pitch rate demanded by the pilot.

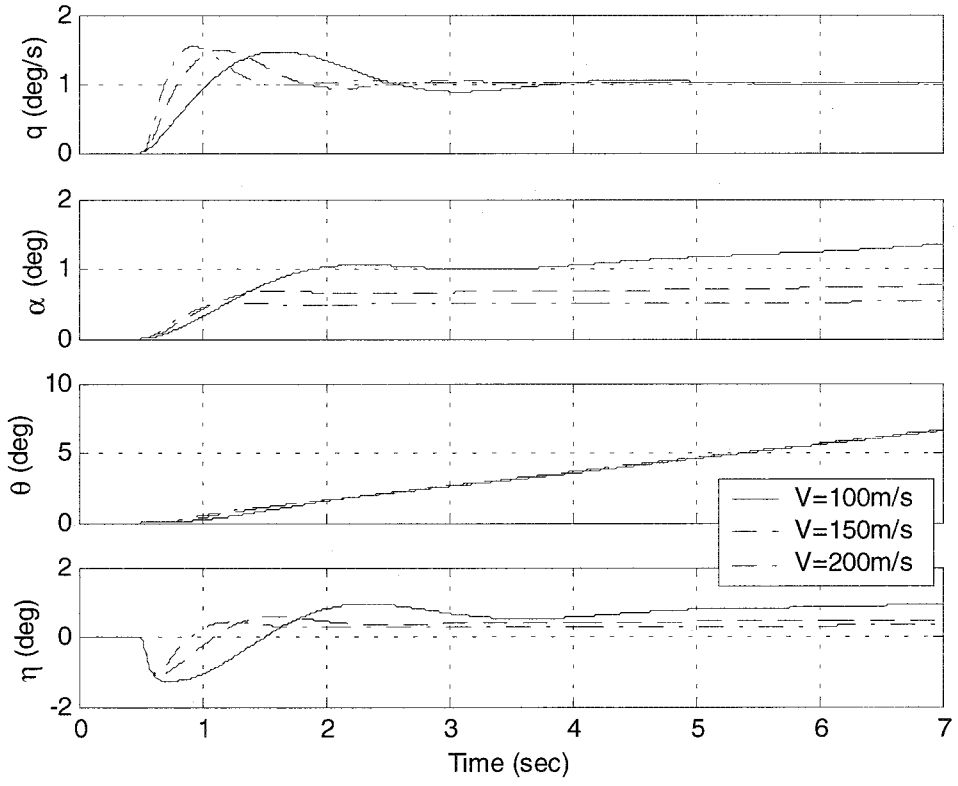

Figure 7.7 Response to 1 deg/sec pitch rate command for the BWB4

A typical characteristic of a pitch rate command/attitude hold system is shown in Figure 7.7, specifically the increase in angle of attack and elevator deflection at low speed, which is necessary to maintain the demanded pitch rate. In other words, what is happening is that when a pitch attitude or pitch rate is demanded, the flight control system attempts to maintain the attitude or pitch rate, irrespective of whether the speed and angle of attack decrease below or increase above their recommended limits. This situation can be dangerous, especially when the pilot has a high workload and is not paying attention, as in the case of an emergency or bad weather. Thus, as seen later in Chapter 9, angle of attack and speed protection must be included.

A last characteristic of a rate command/attitude hold flight control system is the meagre characteristic during flare, as already mentioned in Chapter 2. However, since during the design and test, this flight control system significantly improved the flying and handling characteristics while in normal flight, such characteristic did not seem important and, due to the limited time, it was decided to keep the longitudinal flight control system as designed here. Later, when landings were being carried out and pilots not used to a rate command/attitude hold response-type were flying, this characteristic gained more importance. Thus, when the speed and angle of attack protections were designed an attempt was made to solve the problem for the flare, as shown later in Chapter 8.

7.5 Augmented aircraft flying and handling qualities assessment

The longitudinal criteria presented in Chapter 2, namely the Bandwidth, Phase Delay, Dropback and GCAP criteria, were used to assess the augmented aircraft flying and handling qualities. The special criterion for tailless aircraft presented in paragraph 2.4 is also used here. However, only the configuration used in the flight simulator trials, the BWB4 configuration with the FCS gains as presented in Table 7.7 is assessed here. The augmented configuration was assessed for the flight conditions representative of the mission tasks used in the flight simulation trials. As described later in Chapter 9, the tasks used were representative of the takeoff, climb, descent, approach and precision landing. From Table 2.1 of Chapter 2, it is seen that these tasks are classified as Category C, precision non-aggressive, and Category B, non-precision non-aggressive, mission tasks.

For each mission task, variability in flight conditions were assumed to be due to changes in speed and angle of attack. Thus, the criteria were applied for a range of angle of attack and speed values representative of the flight conditions for each mission task. Actually, using an angle of attack range of $-2^o \le \alpha \le 18^o$, and a speed range of $80 m/s \le V_o \le 200 m/s$.

Due to the empirical form of the several criteria, their application is always difficult, especially when applied several times, as in this case. Thus, the procedure used here was to develop representative Matlab programs, when possible, to easily apply the criteria thereby assuring repeatability and consistency for all combinations of speed and angle of attack.

7.5.1 Bandwidth, Phase delay and Dropback criteria

As presented in Chapter 2, the pitch attitude Bandwidth, Phase delay and Gibson's pitch attitude Dropback criteria were used for assessment of flying and handling qualities of the pitch axis short-term response. A particular interest is when unconventional response-types are used, such as the pitch rate command/attitude hold of the presently used longitudinal flight control system.

Using the definitions presented in Chapter 2, the values of the pitch attitude bandwidth, ω_{BW_θ}, and the phase delay, τ_{ph}, were calculated, as well as the pitch rate overshoot ratio, q_m/q_s, and the ratio of the attitude dropback to steady state pitch rate, $\Delta\theta_{peak}/q_s$, of the Gibson's dropback criteria. The results are presented in Figures 7.8 and 7.9.

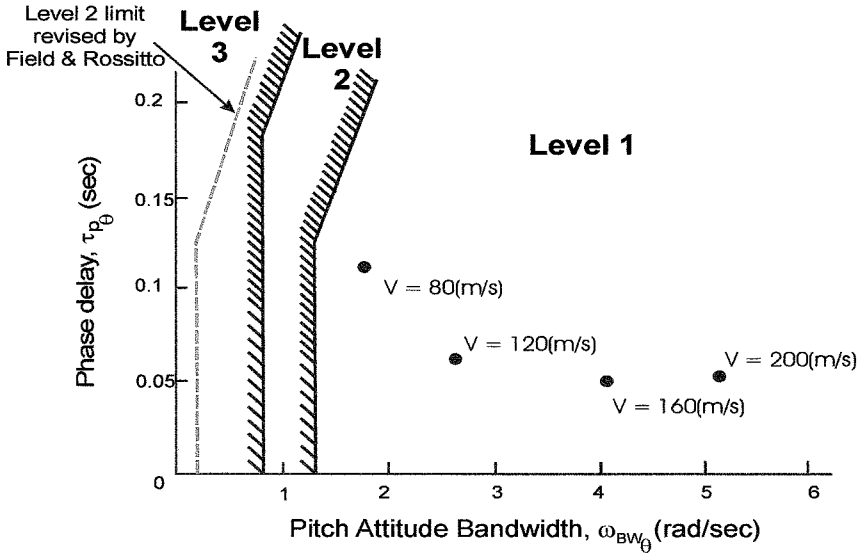

Figure 7.8 Bandwidth/Phase delay assessment of augmented BWB4

As shown in Figure 7.8, for all combinations of speed and angle of attack, the BWB4 augmented configuration is assessed as Level 1 when using the Bandwidth/Phase Delay criteria. Moreover, from figure 7.9 when using the Dropback criterion the BWB4 augmented configuration is also Level 1. This last result was expected, since the requirement for zero pitch attitude dropback was used in the flight control system design. Although not exactly zero, the actual pitch attitude dropback is nevertheless very small.

Actually, from the flying and handling qualities assessment it was found that angle of attack variation has a small effect on the criteria parameters when compared to that of speed. Angle of attack variation was found to have no influence on the Bandwidth and on the ratio of the attitude dropback to steady state pitch rate, $\Delta\theta_{peak}/q_s$. Although

angle of attack affects the phase delay and the pitch rate overshoot ratio, q_m/q_s, this is so small that is not represented in both Figures 7.8 and 7.9. On the other hand, an increase of speed decreases the phase delay and increases the bandwidth significantly, as shown in Figure 7.8, while it decreases the dropback and increases the overshoot ratio in a lesser degree, as shown in Figure 7.9.

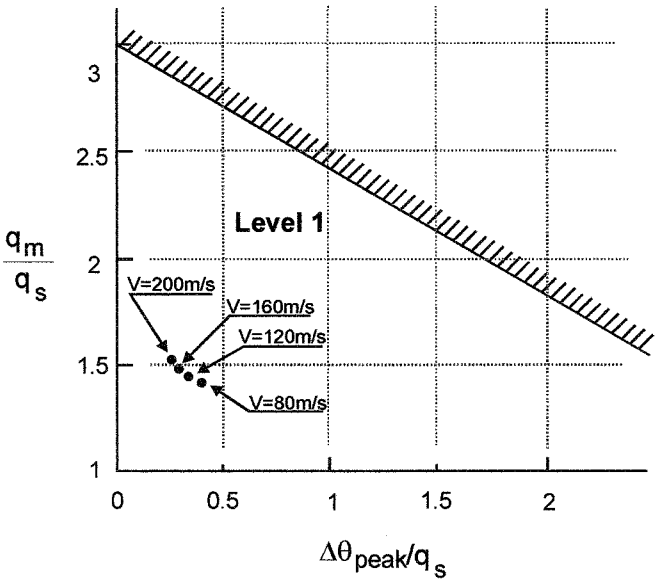

Figure 7.9 Dropback criterion assessment of augmented BWB4

7.5.2 Generic Control Anticipation Parameter criterion

The GCAP criterion was also presented in Chapter 2 as an alternative interpretation of the *Control Anticipation Parameter* (CAP). Its use allows for data gathered for the CAP limits in highly augmented aircraft, mainly those with unconventional response-types, without the need to use *low order equivalent systems* (LOES) analysis. From the longitudinal time response, for all combinations of speed and angles of attack, the values of $\dot{q}(t_{pk})$, $n_z(t_{pk})$ and ζ_s were calculated and substituted in equation (2.7), as repeated here, to calculated the GCAP values. The results are presented in Figure 7.10.

$$GCAP = \frac{\dot{q}(t_{pk})}{n_z(t_{pk})}\left(1+\exp\left(\frac{-\zeta_s \pi}{\sqrt{1-\zeta_s{}^2}}\right)\right) \qquad (2.7)$$

From Figure 7.10 it is seen that for low speeds the BWB4 configuration is out of the revised Level 1 limit given by Gautrey and Cook[67], by Field and Rossitto[69], and even out of the Level 1 limit given for the CAP criterion. Although a requirement for a pitch damping ratio of 0.7 was used during the flight control system design, the

damping ratio varies for the several flight conditions, probably due to the fact that only one set of gains is used. In the same way, initially it was considered appropriate to use the requirement of a GCAP value around 0.6 rad/s^2/g. However, due to the high gains necessary to achieve this it was chosen to use a constant short period frequency of 2.0 rad/sec instead for the FCS design.

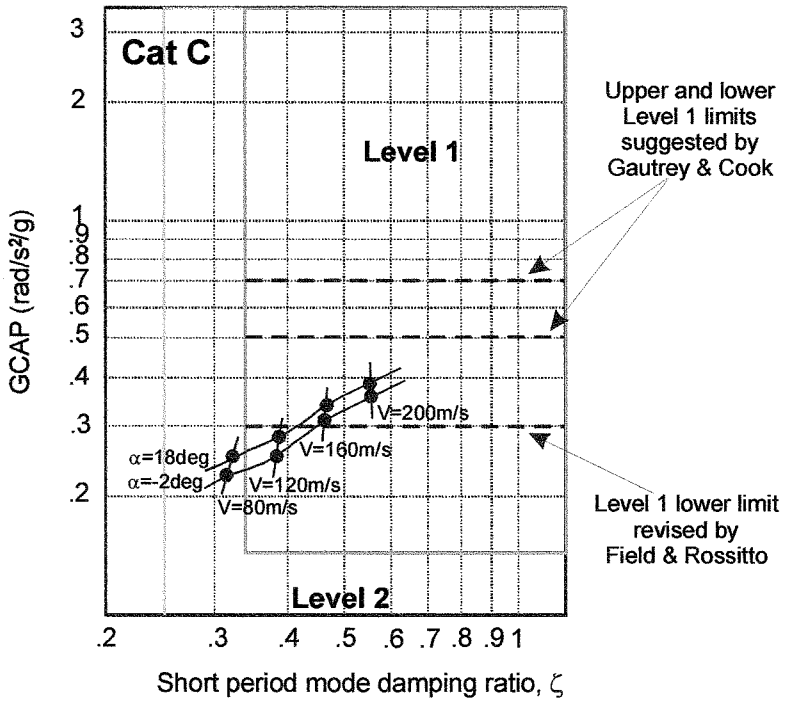

Figure 7.10 GCAP criterion assessment of augmented BWB4

As for the previously evaluated criteria, the influence of angle of attack is small but more significant than for the previous criteria and thus it is presented. However, the variation with angle of attack is still smaller than that due to speed variation. Nevertheless, increasing the angle of attack or increasing the speed increases both the GCAP value and the short period damping ratio.

7.5.3 Special criterion for tailless aircraft

In Chapter 2 it was seen that Monnich and Dalldorff[72] state that for a tailless aircraft to have good flying and handling qualities in turbulent atmosphere inequality (2.5), here repeated, must be fulfilled. Inequality (7.33) is an equivalent expression given by Monnich and Dalldorff[72] when using non-dimensional derivatives.

$$M_\alpha + \frac{M_q Z_\alpha}{V_e} > 0 \qquad (2.5)$$

$$\frac{C_{m_\alpha}}{C_{m_q}} < \left(C_{L_\alpha} + C_{D_e}\right)\frac{\rho S\bar{\bar{c}}}{2m} \tag{7.33}$$

Applying inequality (7.33) to the BWB4 configuration it is seen that the left side of inequality (7.33) is negative, since C_{m_q} is negative while C_{m_α} is positive due to the aft *cg* position of this configuration. On the other hand, the right side of inequality (7.33) is always positive, since all variables present are positive. Therefore it is concluded that inequality (7.33) is fulfilled and it is expected that BWB4 has good flying and handling qualities in turbulent atmosphere.

7.6 Summary

In this chapter a longitudinal flight control system was designed for the BWB4 aircraft with a simple stability augmentation system. However, due to the precise tracking nature of the task to accomplish, approach and landing, a pitch rate command/attitude hold control system was then designed. Both flight control systems were designed based on design rules existing in literature, which were modified to accommodate the particularities of BWB aircraft, in particular the limited control power. Moreover, during all design process the magnitude of the feedback gains were investigated and decreased when possible. Actual elevator deflection time response were plotted to investigate the effect of command and stability augmentation in the control surfaces. Finally, the flying and handling qualities of the BWB4 augmented aircraft system was assessed using analytical flying and handling criteria. This revealed that although the BWB4 has a high negative static stability margin, it is possible using flight control system to achieve Level 1 flying and handling qualities.

Although some attention was paid to the elevator control power available, no real analysis were made on the impact of amplitude and rate saturation in the flight control system. This is an important issue that the reader must consider if using the results of this chapter. A very simple example can be given as follow. From Chapter 4 it was seen that the BWB4 configuration needs about a third of positive elevator control power deflection to trim at low speeds. This may not seem very much, but if a pitch rate command of about 10deg/sec is added, a final positive elevator deflection of about another third is necessary for command and stability purposes. Thus, it remains only a third of control elevator deflection for other purposes such as correcting disturbances, further manoeuvring or even for rolling control since some elevator surfaces are also used as aileron.

The effect of control surface rate saturation is more difficult to show, but in the same way as for amplitude saturation, if reached the result is the pilot feeling he is not able to control the aircraft, generating many times pilot-induced oscillations (PIO). In an extreme situation, control surface amplitude and rate saturation may decrease the flight control system effectiveness. This situation in a negative static stability aircraft may lead to the complete loss of the aircraft.

CHAPTER 8
Lateral-directional flight control system

"We must either find a way or make one"
Hannibal

8.1 Overview

As seen in Chapters 4 and 6, the lateral-directional motion has serious flying and handling qualities deficiencies. Specifically, those deficiencies are the low control power available, the large sideslip angle generated, the poorly damped, or unstable, dutch roll mode, adverse roll and yaw due to cross coupling effects in some configurations and low directional static stability. Thus, if no improvement can be achieved with the introduction of a flight control system, these deficiencies may dictate the premature demise of blended-wing-body configurations, as the history of aircraft has shown several times.

Not so much research has been done on the development of lateral-directional control systems unlike systems development for the longitudinal motion. And, when it has, most of the research is directed to the roll axis. However, in the case of the blended-wing-body configuration, the lateral axis is not the one that presents the critical problems. Rather, the greatest problem is presented by poor directional stability. In the literature[108, 109] some possible solutions were found, however, few were of real use. Thus, new ways have to be devised as presented in this chapter.

Similar to the longitudinal axis, command and stability augmentation systems and several optimal response-types have been developed for the lateral axis. On the other hand, the directional axis has mainly seen development of yaw dampers to increase the dutch roll damping. This is the case since pilots mainly use the lateral axis to control the lateral-directional motion and the directional axis have always had

basically acceptable characteristics. However, due to the lateral-directional coupling, some of the present blended-wing-body configurations need an improvement in the directional axis stability before the lateral axis control system is able to work properly. Stability augmentation is based on feeding back certain aircraft parameters that can be measured in flight by means of motion sensors. When the value of these parameters is compared with what is demanded by the pilot, the resulting error is used to control the aircraft. However, it is not always desirable or possible to feed back all motion variables. Some variables may not be easily measured, or the effect of feeding back some variables back may compete with other feedback loops.

Research into the motion sensing field to know the variables available for feed back is beyond the scope of this research. It will be assumed that all motion variables are available for feedback, or that their values can be estimated with the knowledge of other available variables. Most important in this research is the choice of a variable over another and the effect on the aircraft of feeding back that variable. A root locus analysis is therefore one way to make this choice. Then, with the identified deficiencies given in Chapters 4 and 6, possible solutions found in the literature may be tried, or new solutions may be devised. Throughout the quantitative research the augmented aircraft flying and handling qualities were assessed in order to verify that the flight control systems devised solved the flying qualities deficiencies problems.

8.2 Lateral-directional root locus

The lateral-directional variables most commonly used in feedback control systems are sideslip angle β, roll rate p, yaw rate r and roll attitude ϕ. Sometimes yaw attitude, ψ, is also considered for feedback, although not for stability augmentation purposes. The feedback can be directed either to aileron or rudder input. This means that cross inputs, roll rate or attitude to rudder input, or yaw rate or attitude to aileron input are also possible. However, since these couple the lateral and directional motions even more, their use is not usually advisable. Furthermore, since lateral acceleration is a variable easier to measure than sideslip angle, and since it comprises components of both sideslip angle and yaw rate, it is sometimes also considered for feedback control purposes.

Cook[99] and McLean[108] both present a complete analysis of feeding back lateral-directional variables to both aileron and rudder for a conventional aircraft. However, since a complete analysis would be too extensive and is not the goal of this research, only the following feedbacks are presented, since they were deemed to be more

relevant for the present problem. These are: 1) roll rate feedback to aileron input, 2) sideslip angle feedback to rudder input, 3) yaw rate feedback to rudder input, and 4) lateral acceleration to rudder input. In Appendix C the root locus plots are presented for these four feedback variable-input combinations. The results of this analysis were used as the basis for the flight control system design, and are summarised as follows,

- Low negative gain values for roll rate feedback to aileron input may be useful to improve the stability of the roll and spiral modes. However, extra care should be paid to the dutch roll mode which degrades with this kind of feedback.
- Sideslip angle feedback to rudder input is definitively a feedback to consider, since it improves the dutch roll mode frequency considerably. Furthermore, the roll and spiral modes remain almost unchanged. However, relatively high positive feedback gain K_β may be necessary to obtain the desirable changes.
- Negative gain of yaw rate feedback to rudder may be interesting to increase the dutch roll damping, but this appears to have a low effectiveness. Besides, since the roll and spiral modes tend to combine to create a second oscillatory mode when using this kind of feedback, care is required.
- Lateral acceleration feedback to rudder input does not look useful for the present blended-wing-body configuration application.

8.3 Flight control system design

One of the most obvious deficiencies detected in the BWB configurations is the inherent low directional stability. This would increase the sideslip excursions, degrade the dutch roll mode, and would make the use of ailerons troublesome in some operating conditions. Thus, the flight control system must include, at least, a directional stability augmentation loop. Furthermore, another problem is the adequate augmentation of the dutch roll damping and frequency. This is merely in case the directional stability augmentation loop would not be adequate to put this mode right. The same is also important for the sideslip angle generation, which although decreased with increasing directional stability, does not completely disappear. A significant problem referred in Chapter 6 is the adverse yaw response to aileron inputs for some BWB configurations and flight conditions. This was identified as due to the C_{n_p} and C_{l_r} coupling derivatives.

As stated before, in the present literature[108, 109], the classical lateral-directional flight control systems so far devised, consist of yaw dampers to improve the dutch roll

mode damping as well as lateral flight control systems to improve the rolling characteristics. Since the directional stability is not generally allowed to be as low as in the present configurations, a conventional yaw damper has always been adequate to correct deficiencies of the dutch roll mode. However, that seems to be inadequate in the present application. On the other hand, due to the high dihedral effect and low directional stability of the present configurations, the rolling characteristics of the basic airframe seem not to pose problems. This is seen in the roll mode time constants presented in Chapter 6. However, the basic system response to aileron step inputs seems adverse with results opposite to what would be expected. Thus, the usual flight control systems for the roll axis may not be the best solution for the BWB aircraft.

Therefore, the challenge exists to devise a new flight control system with a loop to augment the directional stability, to improve the dutch roll mode, to diminish the adverse sideslip, and to "correct" the system response to aileron inputs. McLean[108] suggests several loops to increase the basic directional stability, and root locus plots were used to identify the most useful variables for feedback. This, together with a kind of "yaw damper" to improve the dutch roll mode damping are probably the essential minimum inner loops of a new blended-wing-body flight control system.

Another challenge in the design of the lateral-directional flight control system is that of the multi-input control problem, since there are two possible inputs, aileron and rudder controls. The solution to this problem may be firstly, to design a flight control system to correct the problems in one axis and secondly, to correct the remaining axis. In this way, a separation between the control inputs, and thus, the facility to consider a single input problem is retained. Since pilots use the roll axis most, this is considered the most important and usually improved first. Only then is the yaw axis treated. However, since the BWB configurations present more problems in the directional axis the more conventional approach was not followed in this research. Thus, the yaw axis is treated first, and only then the roll axis as presented in the following paragraphs.

8.3.1 Criteria and requirements used in the design

In the same way as for the longitudinal flight control system design, the lateral-directional flight control system should be designed to meet criteria or requirements such that the resultant flight control system will actually improve the flying and handling qualities of the basic airframe. In Chapter 2 it was referred that the criteria and requirements presented in MIL-F-8785C[46] would be used for the lateral-directional motion. These requirements and criteria are suitable for analysis and for

simple assessment of flying and handling qualities. These will be used later in this chapter, to establish that the augmented airframe has the desired qualities. However, due to the "empirical" nature of their presentation, the criteria and requirements presented in MIL-F-8785C[46] are not so suitable for flight control system design. A set of design requirements were therefore devised from those initial requirements as follows,

- Roll mode time constant, $0.33 < T_r < 1.4\,\text{sec}$
- Spiral mode time constant stable, $T_s > 0$
- Dutch roll mode damping ratio and frequency, $\omega_d \geq 0.4\,rad/\text{sec}$ and $\zeta_d \geq 0.19$
- Sideslip angle optimised to a minimum

8.3.2 Lateral-directional matrix state equation

Previously to the flight control system design it is desired to define the matrix state equation used through the design. A linear lateral-directional state equation is presented in equation (6.1) of Chapter 6, and it is here repeated as equation (8.1). In the same way as it was done for the longitudinal motion in Chapter 7 paragraph 7.3, the dynamics of the aileron and rudder actuator were also taken into account. Similar dynamics to those of the elevator actuator were assumed and are given in equation (8.2) and (8.3) for the aileron and rudder, respectively. Including these dynamics in equation (8.1) the state equation (8.4) results.

$$\begin{bmatrix} \dot{\beta} \\ \dot{p} \\ \dot{r} \\ \dot{\phi} \\ \dot{\psi} \end{bmatrix} = \begin{bmatrix} y_\beta & y_p/V_o & y_r/V_o & y_\phi/V_o & 0 \\ l_v V_o & l_p & l_r & 0 & 0 \\ n_v V_o & n_p & n_r & 0 & 0 \\ 0 & 1 & 0 & 0 & 0 \\ 0 & 0 & 1 & 0 & 0 \end{bmatrix} \begin{bmatrix} \beta \\ p \\ r \\ \phi \\ \psi \end{bmatrix} + \begin{bmatrix} y_\xi/V_o & y_\varsigma/V_o \\ l_\xi & l_\varsigma \\ n_\xi & n_\varsigma \\ 0 & 0 \\ 0 & 0 \end{bmatrix} \begin{bmatrix} \xi \\ \varsigma \end{bmatrix} \tag{8.1}$$

$$\ddot{y}_a(t) + 2\zeta_a\omega_a\dot{y}(t) + \omega_a{}^2 y_a(t) = \omega_a{}^2 u_a(t) \tag{8.2}$$

$$\ddot{y}_r(t) + 2\zeta_r\omega_r\dot{y}(t) + \omega_r{}^2 y_r(t) = \omega_r{}^2 u_r(t) \tag{8.3}$$

$$\begin{bmatrix} \dot{\beta} \\ \dot{p} \\ \dot{r} \\ \dot{\phi} \\ \dot{\psi} \\ \dot{a}_1 \\ \dot{a}_2 \\ \dot{r}_1 \\ \dot{r}_2 \end{bmatrix} = \begin{bmatrix} y_\beta & y_p/V_o & y_r/V_o & y_\phi/V_o & 0 & y_\xi/V_o & 0 & y_\varsigma/V_o & 0 \\ l_v V_o & l_p & l_r & 0 & 0 & l_\xi & 0 & l_\varsigma & 0 \\ n_v V_o & n_p & n_r & 0 & 0 & n_\xi & 0 & n_\varsigma & 0 \\ 0 & 1 & 0 & 0 & 0 & 0 & 0 & 0 & 0 \\ 0 & 0 & 1 & 0 & 0 & 0 & 0 & 0 & 0 \\ 0 & 0 & 0 & 0 & 0 & 0 & 1 & 0 & 0 \\ 0 & 0 & 0 & 0 & 0 & -\omega_a{}^2 & -2\zeta_a\omega_a & 0 & 0 \\ 0 & 0 & 0 & 0 & 0 & 0 & 0 & 0 & 1 \\ 0 & 0 & 0 & 0 & 0 & 0 & 0 & -\omega_r{}^2 & -2\zeta_r\omega_r \end{bmatrix} \begin{bmatrix} \beta \\ p \\ r \\ \phi \\ \psi \\ a_1 \\ a_2 \\ r_1 \\ r_2 \end{bmatrix} + \begin{bmatrix} 0 & 0 \\ 0 & 0 \\ 0 & 0 \\ 0 & 0 \\ 0 & 0 \\ 0 & 0 \\ \omega_a{}^2 & 0 \\ 0 & 0 \\ 0 & \omega_r{}^2 \end{bmatrix} \begin{bmatrix} \xi \\ \varsigma \end{bmatrix} \tag{8.4}$$

8.3.3 Directional axis controller design

8.3.3.1 Sideslip angle inner loop

To improve the yaw axis response it was decided to use sideslip angle feedback to rudder first. This was done because in the root locus plots of Appendix C, it was shown that sideslip angle feedback would improve the dutch roll mode without significantly affecting the remaining modes. The initial stability augmentation flight control system structure is shown in Figure 8.1. The equivalent control law is given in equation (8.5). Substituting this equation into the linear open-loop lateral-directional state equation (8.4), the closed loop state equation results as presented in equation (8.6). The sideslip angle gain, K_β, was calculated in an iterative way, i.e., several values were attributed to K_β and the modes characteristic calculated until the design requirements were met.

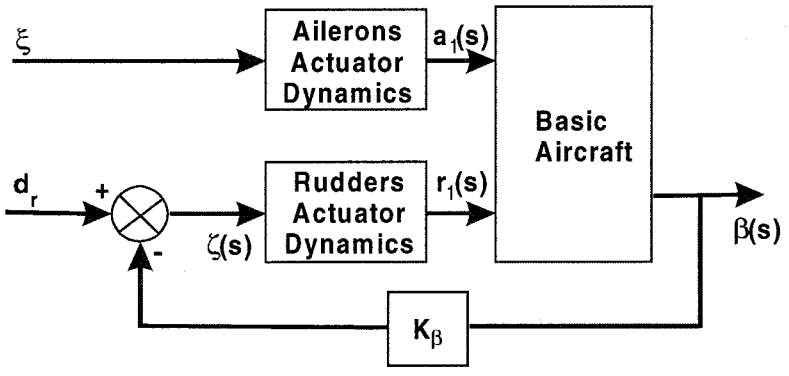

Figure 8.1 Sideslip angle inner loop

$$\varsigma = d_r - K_\beta \beta \tag{8.5}$$

$$\begin{bmatrix} \dot{\beta} \\ \dot{p} \\ \dot{r} \\ \dot{\phi} \\ \dot{\psi} \\ \dot{a}_1 \\ \dot{a}_2 \\ \dot{r}_1 \\ \dot{r}_2 \end{bmatrix} = \begin{bmatrix} y_\beta & y_p/V_o & y_r/V_o & y_\phi/V_o & 0 & y_\xi/V_o & 0 & y_\varsigma/V_o & 0 \\ l_v V_o & l_p & l_r & 0 & 0 & l_\xi & 0 & l_\varsigma & 0 \\ n_v V_o & n_p & n_r & 0 & 0 & n_\xi & 0 & n_\varsigma & 0 \\ 0 & 1 & 0 & 0 & 0 & 0 & 0 & 0 & 0 \\ 0 & 0 & 1 & 0 & 0 & 0 & 0 & 0 & 0 \\ 0 & 0 & 0 & 0 & 0 & 0 & 1 & 0 & 0 \\ 0 & 0 & 0 & 0 & 0 & -\omega_a^2 & -2\zeta_a\omega_a & 0 & 0 \\ 0 & 0 & 0 & 0 & 0 & 0 & 0 & 0 & 1 \\ -K_\beta\omega_r^2 & 0 & 0 & 0 & 0 & 0 & 0 & -\omega_r^2 & -2\zeta_r\omega_r \end{bmatrix} \begin{bmatrix} \beta \\ p \\ r \\ \phi \\ \psi \\ a_1 \\ a_2 \\ r_1 \\ r_2 \end{bmatrix} + \begin{bmatrix} 0 & 0 \\ 0 & 0 \\ 0 & 0 \\ 0 & 0 \\ 0 & 0 \\ 0 & 0 \\ \omega_a^2 & 0 \\ 0 & 0 \\ 0 & \omega_r^2 \end{bmatrix} \begin{bmatrix} \xi \\ d_r \end{bmatrix} \tag{8.6}$$

From Table 8.1, it is seen that the dutch roll mode frequency increases with increasing sideslip angle feedback gain, K_β. For low angles of attack, a K_β gain value higher than 1 is necessary in order to bring the dutch roll mode frequency within the design limits, while for high angles of attack a K_β of 1 is sufficient. As expected, the roll

mode time constant did not change significantly and the dutch roll damping ratio increased only slightly. On the other hand, the spiral mode time constant value increased, but remained stable, even for high feedback gains. At first, high K_β gain seemed appropriate since it increases greatly the dutch roll mode frequency with small adverse effects on the other modes. However, this is not ideal for safety reasons.

	$\alpha = 3.6\,\text{deg}$				$\alpha = 8\,\text{deg}$			
K_β	0	1	5	10	0	1	5	10
T_r (sec)	0.78	0.78	0.78	0.77	0.8	0.8	0.8	0.8
T_s (sec)	25.5	36.4	49.8	54.0	24.9	35.2	62.1	80.6
ζ_d	0.04	0.05	0.06	0.07	0.04	0.05	0.06	0.07
ω_d (rad/sec)	0.26	0.37	0.65	0.88	0.38	0.47	0.73	0.97

Table 8.1 Lateral-directional modes characteristic variation with feedback gains

8.3.3.2 Yaw damper with washout loop

As shown in Table 8.1, sideslip angle gains less than five increase the dutch roll frequency above the minimum required, but the dutch roll damping is still below the minimum required of 0.1. Nevertheless, higher values of K_β are not advisable and as stated in the root locus analysis in paragraph 8.2, feedback of yaw rate to rudder may be more effective to increase the dutch roll damping. Therefore, a yaw rate feedback loop to rudder input was introduced to the previous directional stability augmentation system, as shown in Figure 8.2. The washout filter is included to allow for continuous yaw rate feedback in steady turns.

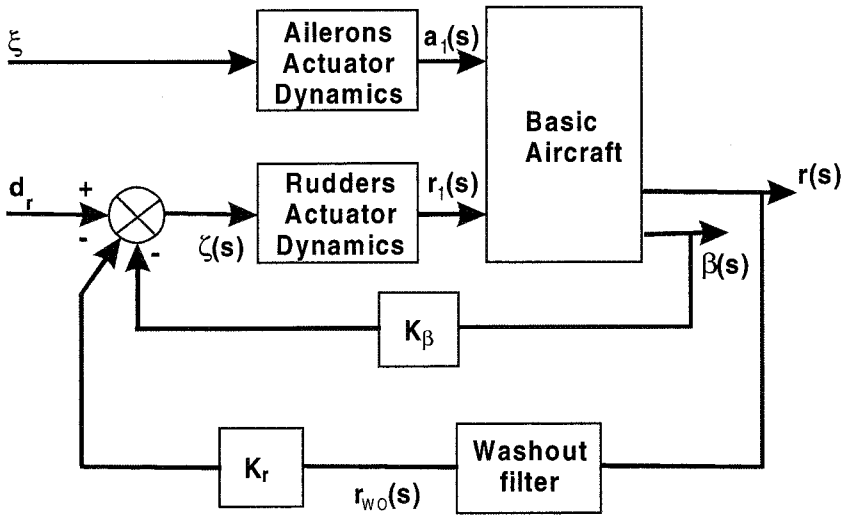

Figure 8.2 Sideslip angle and washed yaw rate inner loops

The washout filter transfer function is given in equation (8.7) as a first order lag of time constant T_{WO}. One state variable is therefore sufficient to represent the washout filter. The lateral-directional state equation with the new washout state variable is presented in equation (8.8). The control law is given now by equation (8.9) which substituting in equation (8.8) results in the closed loop state equation given in equation (8.10).

$$\frac{r_{WO}(s)}{r(s)} = \frac{s}{s + 1/T_{WO}} \tag{8.7}$$

$$\begin{bmatrix} \dot{\beta} \\ \dot{p} \\ \dot{r} \\ \dot{\phi} \\ \dot{\psi} \\ \dot{a}_1 \\ \dot{a}_2 \\ \dot{r}_1 \\ \dot{r}_2 \\ \dot{r}_{WO} \end{bmatrix} = \begin{bmatrix} y_\beta & y_p/V_o & y_r/V_o & y_\phi/V_o & 0 & y_\xi/V_o & 0 & y_\varsigma/V_o & 0 & 0 \\ l_v V_o & l_p & l_r & 0 & 0 & l_\xi & 0 & l_\varsigma & 0 & 0 \\ n_v V_o & n_p & n_r & 0 & 0 & n_\xi & 0 & n_\varsigma & 0 & 0 \\ 0 & 1 & 0 & 0 & 0 & 0 & 0 & 0 & 0 & 0 \\ 0 & 0 & 1 & 0 & 0 & 0 & 0 & 0 & 0 & 0 \\ 0 & 0 & 0 & 0 & 0 & 0 & 1 & 0 & 0 & 0 \\ 0 & 0 & 0 & 0 & 0 & -\omega_a^2 & -2\zeta_a\omega_a & 0 & 0 & 0 \\ 0 & 0 & 0 & 0 & 0 & 0 & 0 & 0 & 1 & 0 \\ 0 & 0 & 0 & 0 & 0 & 0 & 0 & -\omega_r^2 & -2\zeta_r\omega_r & 0 \\ n_v V_o & n_p & n_r & 0 & 0 & n_\xi & 0 & n_\varsigma & 0 & -1/T_{WO} \end{bmatrix} \begin{bmatrix} \beta \\ p \\ r \\ \phi \\ \psi \\ a_1 \\ a_2 \\ r_1 \\ r_2 \\ r_{WO} \end{bmatrix} + \begin{bmatrix} 0 & 0 \\ 0 & 0 \\ 0 & 0 \\ 0 & 0 \\ 0 & 0 \\ 0 & 0 \\ \omega_a^2 & 0 \\ 0 & 0 \\ 0 & \omega_r^2 \\ 0 & 0 \end{bmatrix} \begin{bmatrix} \xi \\ \varsigma \end{bmatrix} \tag{8.8}$$

$$\varsigma = d_r - K_\beta \beta - K_r r_{WO} \tag{8.9}$$

$$\begin{bmatrix} \dot{\beta} \\ \dot{p} \\ \dot{r} \\ \dot{\phi} \\ \dot{\psi} \\ \dot{a}_1 \\ \dot{a}_2 \\ \dot{r}_1 \\ \dot{r}_2 \\ \dot{r}_{WO} \end{bmatrix} = \begin{bmatrix} y_\beta & y_p/V_o & y_r/V_o & y_\phi/V_o & 0 & y_\xi/V_o & 0 & y_\varsigma/V_o & 0 & 0 \\ l_v V_o & l_p & l_r & 0 & 0 & l_\xi & 0 & l_\varsigma & 0 & 0 \\ n_v V_o & n_p & n_r & 0 & 0 & n_\xi & 0 & n_\varsigma & 0 & 0 \\ 0 & 1 & 0 & 0 & 0 & 0 & 0 & 0 & 0 & 0 \\ 0 & 0 & 1 & 0 & 0 & 0 & 0 & 0 & 0 & 0 \\ 0 & 0 & 0 & 0 & 0 & 0 & 1 & 0 & 0 & 0 \\ 0 & 0 & 0 & 0 & 0 & -\omega_a^2 & -2\zeta_a\omega_a & 0 & 0 & 0 \\ 0 & 0 & 0 & 0 & 0 & 0 & 0 & 0 & 1 & 0 \\ -K_\beta\omega_r^2 & 0 & 0 & 0 & 0 & 0 & 0 & -\omega_r^2 & -2\zeta_r\omega_r & -K_r\omega_r^2 \\ n_v V_o & n_p & n_r & 0 & 0 & n_\xi & 0 & n_\varsigma & 0 & -1/T_{WO} \end{bmatrix} \begin{bmatrix} \beta \\ p \\ r \\ \phi \\ \psi \\ a_1 \\ a_2 \\ r_1 \\ r_2 \\ r_{WO} \end{bmatrix} + \begin{bmatrix} 0 & 0 \\ 0 & 0 \\ 0 & 0 \\ 0 & 0 \\ 0 & 0 \\ 0 & 0 \\ \omega_a^2 & 0 \\ 0 & 0 \\ 0 & \omega_r^2 \\ 0 & 0 \end{bmatrix} \begin{bmatrix} \xi \\ d_r \end{bmatrix} \tag{8.10}$$

The feedback gain K_β is the same as calculated in paragraph 8.3.2.1. The feedback gain K_r is calculated in the same way as K_β, i.e., iteratively until the dutch roll damping as the desired value. However, in this calculation the washout filter is not yet taken into account. Table 8.2 shows the lateral-directional modes characteristic variation with increasing K_r gain, for two different values of angle of attack. To increase the dutch roll mode frequency the minimum required, $\zeta_d \geq 0.19$, a $K_r \geq -5$ is necessary.

α (deg)	K_β	K_r	T_r (sec)	T_s (sec)	ζ_d	ω_d (rad/sec)
3.6	3	-1	0.76	31.4	0.102	0.524
		-3	0.75	18.9	0.193	0.510
		-5	0.73	13.0	0.283	0.490
8	3	-1	0.79	26.8	0.102	0.607
		-3	0.77	13.2	0.182	0.583
		-5	0.75	8.2	0.259	0.552

Table 8.2 Lateral-directional modes characteristics variation with K_r

The washout filter is now included and the washout time constant, T_{WO} is therefore calculated in a way that the washout filter dynamics do not interfere significantly with the flight control system. In Figure 8.3 the variation of the dutch roll damping is shown for several values of T_{WO} and angle of attack and with $K_\beta = 3$ and $K_r = -5$. From Figure 8.3 it can be concluded that a washout time constant $T_{WO} = 5$ is more than enough to assure a dutch roll damping above the minimum required (in red). However, such high washout time constant may impair the objective of the washout filter – to allow to turn the aircraft.

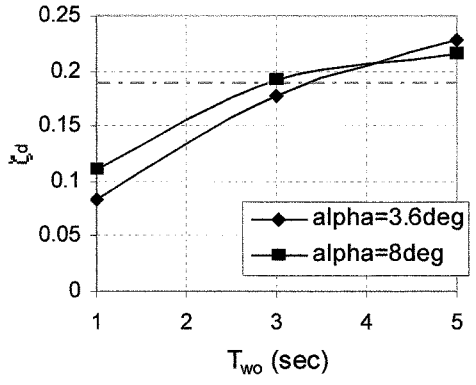

Figure 8.3 Dutch roll damping variation with T_{WO}

8.3.3.3 Aileron to rudder interconnection

In Figure 8.4 the lateral-directional response of the augmented aircraft to –1 deg aileron for the first 10seconds is presented for a flight condition of $\alpha = 8.0\,\text{deg}$ and $V_o = 100\,m/s$, and gains $K_\beta = 3$, $K_r = -5$ and $T_{WO} = 3$. Although the response is improved, the sideslip angle generated during the aileron deflection is still high, and the roll and yaw rate responses are still not ideal. On the other hand, the feedback gains used are already too high, and further increase is not desirable.

Thus, it is necessary to improve further the lateral and directional flying and handling qualities by some other means. McLean[108] and Stevens and Lewis[109] suggest an

interconnect between the aileron and rudder, i.e., to deflect automatically the rudder by a determined amount when the ailerons are deflected. In this way the sideslip angle is decreased and the yaw rate response improved further. Figure 8.4 shows the flight control system including an aileron to rudder interconnection (ARI).

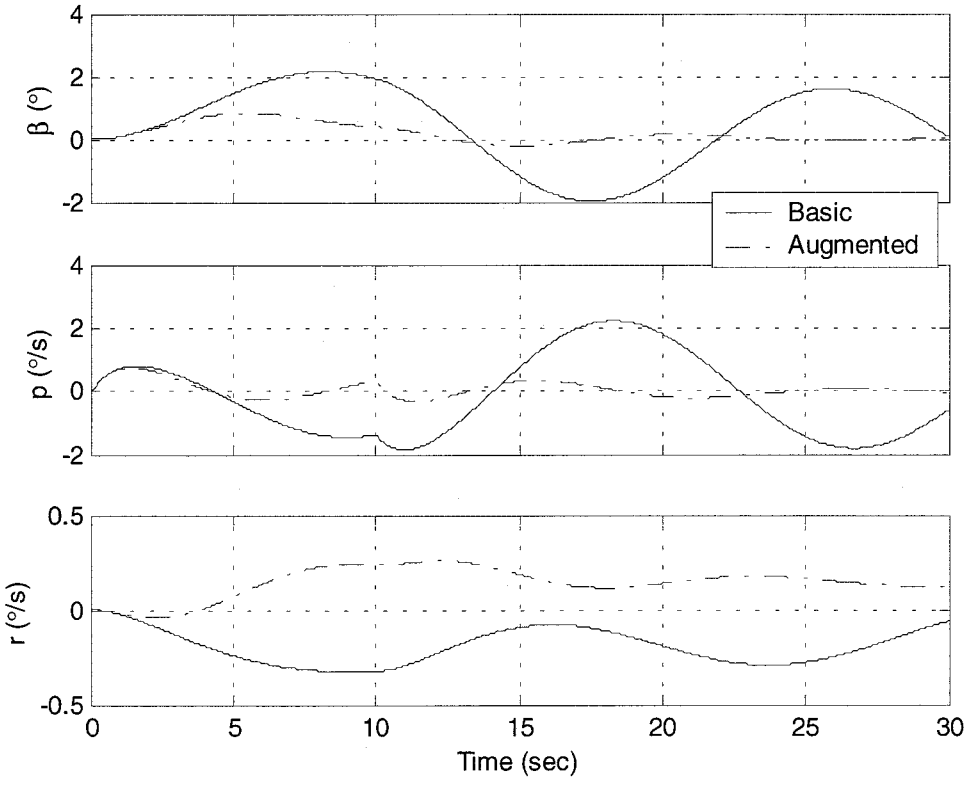

Figure 8.4 Lateral-directional response to –1 deg aileron for 10 seconds

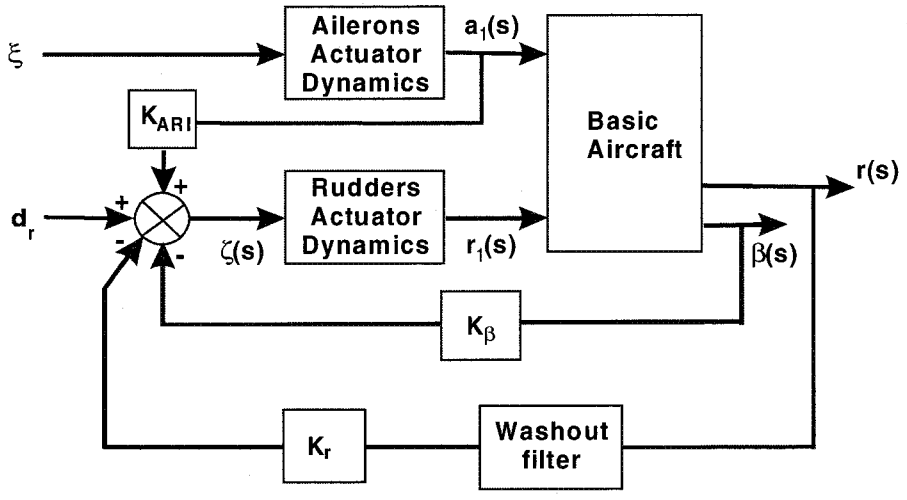

Figure 8.5 Inclusion of an aileron to rudder interconnected (ARI)

The control law now becomes that of equation (8.11) where a_1 is the actual aileron deflection. Substituting equation (8.11) in the open-loop state equation (8.8) the closed-loop state equation results, as presented in equation (8.12).

$$\varsigma = d_r - K_\beta \beta - K_r r_{WO} + K_{ARI} a_1 \tag{8.11}$$

$$\begin{bmatrix} \dot{\beta} \\ \dot{p} \\ \dot{r} \\ \dot{\phi} \\ \dot{\psi} \\ \dot{a}_1 \\ \dot{a}_2 \\ \dot{r}_1 \\ \dot{r}_2 \\ \dot{r}_{WO} \end{bmatrix} = \begin{bmatrix} y_\beta & y_p/V_o & y_r/V_o & y_\phi/V_o & 0 & y_\xi/V_o & 0 & y_\varsigma/V_o & 0 & 0 \\ l_v V_o & l_p & l_r & 0 & 0 & l_\xi & 0 & l_\varsigma & 0 & 0 \\ n_v V_o & n_p & n_r & 0 & 0 & n_\xi & 0 & n_\varsigma & 0 & 0 \\ 0 & 1 & 0 & 0 & 0 & 0 & 0 & 0 & 0 & 0 \\ 0 & 0 & 1 & 0 & 0 & 0 & 0 & 0 & 0 & 0 \\ 0 & 0 & 0 & 0 & 0 & 0 & 1 & 0 & 0 & 0 \\ 0 & 0 & 0 & 0 & 0 & -\omega_a^2 & -2\zeta_a\omega_a & 0 & 0 & 0 \\ 0 & 0 & 0 & 0 & 0 & 0 & 0 & 0 & 1 & 0 \\ -K_\beta\omega_r^2 & 0 & 0 & 0 & 0 & K_{ARI}\omega_r^2 & 0 & -\omega_r^2 & -2\zeta_r\omega_r & -K_r\omega_r^2 \\ n_v V_o & n_p & n_r & 0 & 0 & n_\xi & 0 & n_\varsigma & 0 & -1/T_{WO} \end{bmatrix} \begin{bmatrix} \beta \\ p \\ r \\ \phi \\ \psi \\ a_1 \\ a_2 \\ r_1 \\ r_2 \\ r_{WO} \end{bmatrix} + \begin{bmatrix} 0 & 0 \\ 0 & 0 \\ 0 & 0 \\ 0 & 0 \\ 0 & 0 \\ 0 & 0 \\ \omega_a^2 & 0 \\ 0 & 0 \\ 0 & \omega_r^2 \\ 0 & 0 \end{bmatrix} \begin{bmatrix} \xi \\ d_r \end{bmatrix} \tag{8.12}$$

The aileron to rudder interconnected gain, K_{ARI}, was calculated as a function of angle of incidence and is presented in Figure 8.6. It can be seen that the required K_{ARI} gain increases rapidly with increasing angle of attack. Figure 8.7 shows the reduction in the adverse sideslip generation when the aileron to rudder interconnection is included in the FCS.

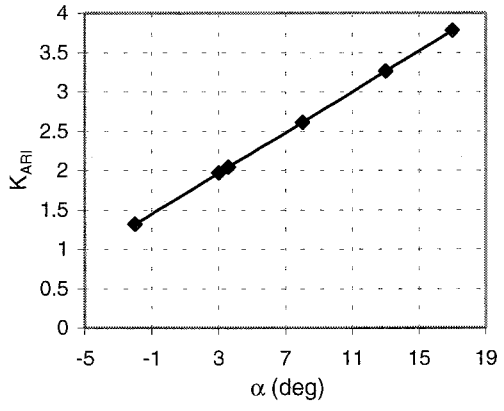

Figure 8.6 K_{ARI} gain scheduling with angle of attack

In Figures 8.7 and 8.8 a comparison between the unaugmented and the augmented aircraft is shown. The flight control system in the "Aug1" response includes a sideslip angle and washed yaw rate feedback to rudder, whilst "Aug2" includes further an aileron to rudder interconnection. Figure 8.7 shows that the sideslip response to an aileron pulse of –1 deg for 10 seconds is least for the "Aug 2" plot, which includes the aileron to rudder interconnection. It can be seen in Figure 8.7 that in the first few seconds the sideslip generated is null and it is kept to a minimum after the input is removed. Moreover, Figure 8.7 shows a significant improvement in the roll and yaw rate responses to the aileron pulse.

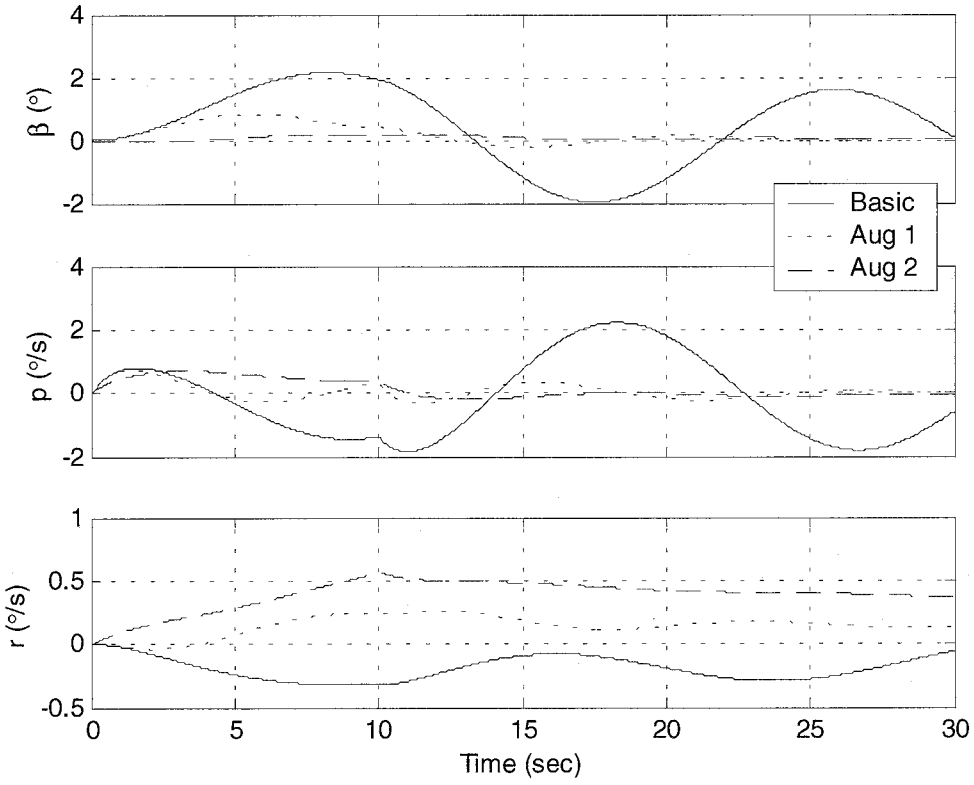

Figure 8.7 Lateral-directional response to –1 deg aileron for 10 seconds

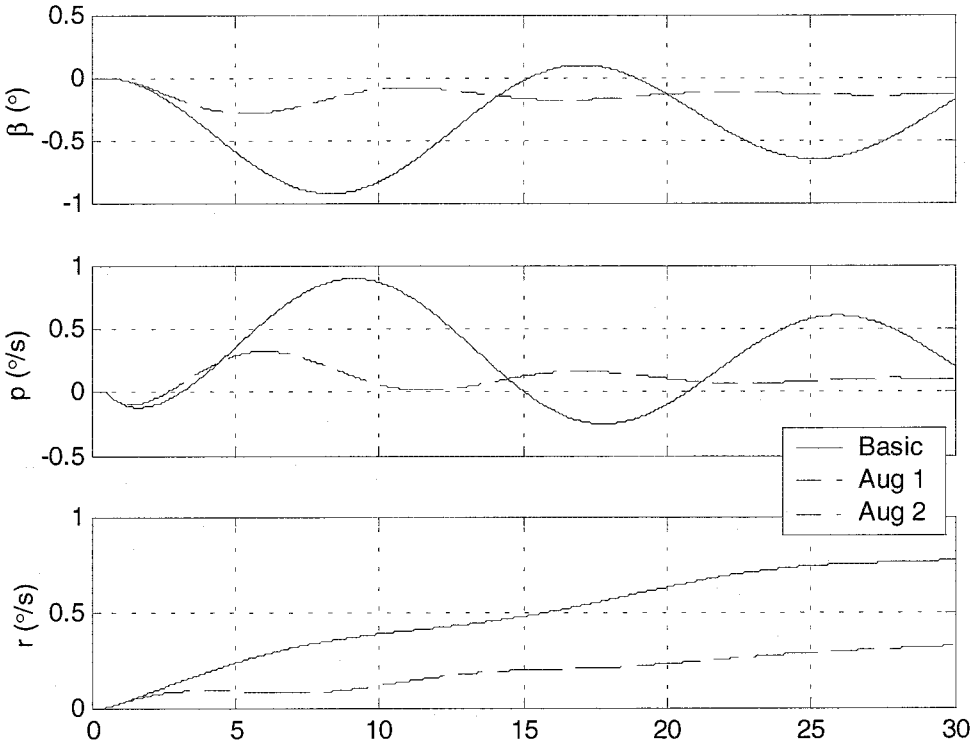

Figure 8.8 Lateral-directional response to a step rudder of –1 deg

On the other hand, the aileron to rudder interconnection does not affect the response to rudder inputs. This is shown in Figure 8.8 where "Aug 1" and "Aug 2" response plots are coincident. However, it can also be seen from Figure 8.8 that the directional flight control system greatly decreases the efficiency of the rudder. If the rudder aerodynamic control power could be significantly increased, this decrease in efficiency would not be a problem. Although the rudders are used only in a few cases, such as crosswind and engine failure, these are critical situations for safety, and it is when the pilot's workload is higher. Thus, it must be proven that these tasks can still be accomplished safely with the present rudder control power.

8.3.3.4 Inclusion of sideslip reference

Most of the flight control system test, verification and improvement were done using the flight simulator. It was when executing tasks where it was necessary to sideslip the aircraft, as in a crosswind, that it was discovered that it was not possible to maintain sideslip for a long time. It was thought that, in the same way as a yaw damper tends to null yaw rate in a steady turn, the sideslip feedback loop would try to minimise any sideslip angle. However, the introduction of a washout filter in the sideslip path did not solve this problem. The solution was found by introducing a sideslip angle reference proportional to the pilot's demand. This can be seen in Figure 8.9.

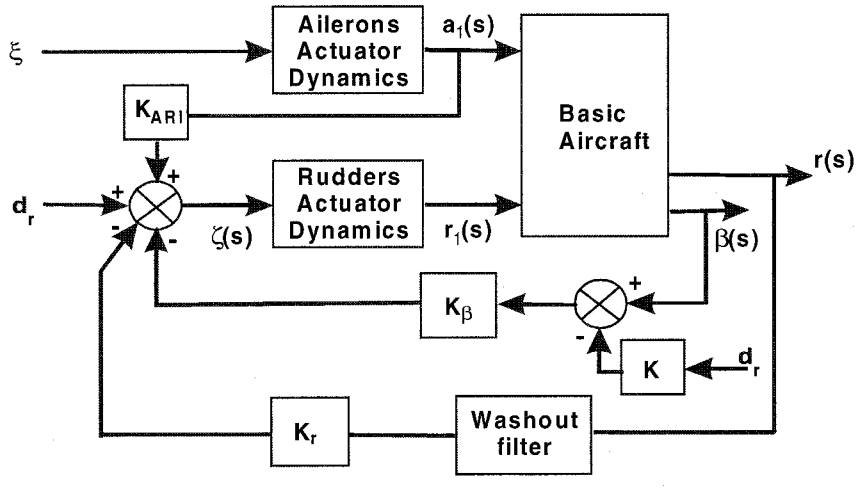

Figure 8.9 Final directional flight control system

K was made equal to the maximum sideslip achievable per maximum rudder pedal ratio. The maximum rudder pedal deflection from the simulator data is 25 deg. The maximum sideslip achievable was supposed to be 15 deg, thus giving a $K = 0.6$. However, from later tests in the simulator K was changed to 0.5, giving a 12.5 deg of maximum sideslip achievable.

8.3.4 Lateral axis controller design

In paragraph 8.3.3 a directional flight control system design is described and Figure 8.7 already shows a great improvement to the unaugmented BWB aircraft. However, for tracking purposes high precision is required and for the lateral-directional motion the aileron is the most used for control therefore, the aircraft response to aileron input must present high accuracy. Therefore, and in the same way as it was done for the longitudinal mode, a roll rate command system was designed for the lateral axis so as to give optimal response. The roll rate command system is as shown in Figure 8.10. Due to the presence of the integral the roll rate error is defined by equation (8.13). Augmenting the state equation as given in equation (8.12) to account for the roll rate error, results in the state equation (8.14).

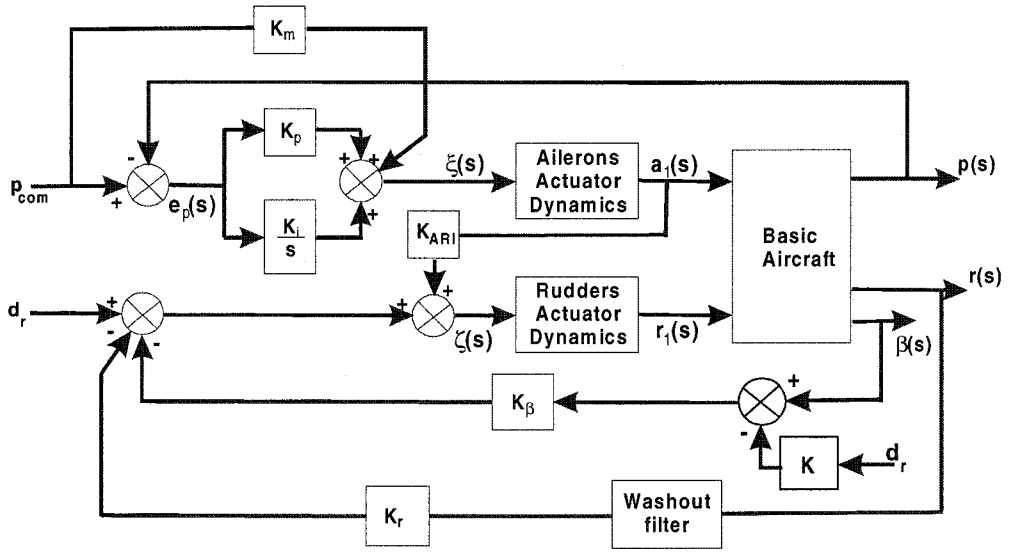

Figure 8.10 Roll command and directional stability augmentation system

$$\dot{\varepsilon}_p = (p - p_{com}) \tag{8.13}$$

$$\begin{bmatrix} \dot{\beta} \\ \dot{p} \\ \dot{r} \\ \dot{\phi} \\ \dot{\psi} \\ \dot{a}_1 \\ \dot{a}_2 \\ \dot{r}_1 \\ \dot{r}_2 \\ \dot{r}_{WO} \\ \dot{\varepsilon}_p \end{bmatrix} = \begin{bmatrix} y_\beta & y_p/V_o & y_r/V_o & y_\phi/V_o & 0 & y_\xi/V_o & 0 & y_\varsigma/V_o & 0 & 0 & 0 \\ l_v V_o & l_p & l_r & 0 & 0 & l_\xi & 0 & l_\varsigma & 0 & 0 & 0 \\ n_v V_o & n_p & n_r & 0 & 0 & n_\xi & 0 & n_\varsigma & 0 & 0 & 0 \\ 0 & 1 & 0 & 0 & 0 & 0 & 0 & 0 & 0 & 0 & 0 \\ 0 & 0 & 1 & 0 & 0 & 0 & 0 & 0 & 0 & 0 & 0 \\ 0 & 0 & 0 & 0 & 0 & 0 & 1 & 0 & 0 & 0 & 0 \\ 0 & 0 & 0 & 0 & 0 & -\omega_a^2 & -2\zeta_a\omega_a & 0 & 0 & 0 & 0 \\ 0 & 0 & 0 & 0 & 0 & 0 & 0 & 0 & 1 & 0 & 0 \\ -K_\beta\omega_r^2 & 0 & 0 & 0 & 0 & K_{ARI}\omega_r^2 & 0 & -\omega_r^2 & -2\zeta_r\omega_r & -K_r\omega_r^2 & 0 \\ n_v V_o & n_p & n_r & 0 & 0 & n_\xi & 0 & n_\varsigma & 0 & -1/T_{WO} & 0 \\ 0 & 1 & 0 & 0 & 0 & 0 & 0 & 0 & 0 & 0 & 0 \end{bmatrix} \begin{bmatrix} \beta \\ p \\ r \\ \phi \\ \psi \\ a_1 \\ a_2 \\ r_1 \\ r_2 \\ r_{WO} \\ \varepsilon_p \end{bmatrix} + \begin{bmatrix} 0 & 0 \\ 0 & 0 \\ 0 & 0 \\ 0 & 0 \\ 0 & 0 \\ 0 & 0 \\ \omega^2 & 0 \\ 0 & 0 \\ 0 & \omega_r^2 \\ 0 & 0 \\ 0 & 0 \end{bmatrix} \begin{bmatrix} \xi \\ d_r \end{bmatrix} + \begin{bmatrix} 0 \\ 0 \\ 0 \\ 0 \\ 0 \\ 0 \\ 0 \\ 0 \\ 0 \\ 0 \\ -1 \end{bmatrix} p_{con} \tag{8.14}$$

The lateral control law is given by equation (8.15). Substituting equation (8.15) into equation (8.14) and rearranging the closed-loop lateral-directional state equation results, as presented in equation (8.16).

$$\xi = -K_i e_p - K_p p + K_m p_{com} \tag{8.15}$$

$$\begin{bmatrix} \dot{\beta} \\ \dot{p} \\ \dot{r} \\ \dot{\phi} \\ \dot{\psi} \\ \dot{a}_1 \\ \dot{a}_2 \\ \dot{r}_1 \\ \dot{r}_2 \\ \dot{r}_{WO} \\ \dot{\varepsilon}_p \end{bmatrix} = \begin{bmatrix} y_\beta & y_p/V_o & y_r/V_o & y_\phi/V_o & 0 & y_\xi/V_o & 0 & y_\varsigma/V_o & 0 & 0 & 0 \\ l_v V_o & l_p & l_r & 0 & 0 & l_\xi & 0 & l_\varsigma & 0 & 0 & 0 \\ n_v V_o & n_p & n_r & 0 & 0 & n_\xi & 0 & n_\varsigma & 0 & 0 & 0 \\ 0 & 1 & 0 & 0 & 0 & 0 & 0 & 0 & 0 & 0 & 0 \\ 0 & 0 & 1 & 0 & 0 & 0 & 0 & 0 & 0 & 0 & 0 \\ 0 & 0 & 0 & 0 & 0 & 0 & 1 & 0 & 0 & 0 & 0 \\ 0 & -K_p\omega_a^2 & 0 & 0 & 0 & -\omega_a^2 & -2\zeta_a\omega_a & 0 & 0 & 0 & -K_i\omega_a^2 \\ 0 & 0 & 0 & 0 & 0 & 0 & 0 & 0 & 1 & 0 & 0 \\ -K_\beta\omega_r^2 & 0 & 0 & 0 & 0 & K_{ARI}\omega_r^2 & 0 & -\omega_r^2 & -2\zeta_r\omega_r & -K_r\omega_r^2 & 0 \\ n_v V_o & n_p & n_r & 0 & 0 & n_\xi & 0 & n_\varsigma & 0 & -1/T_{WO} & 0 \\ 0 & 1 & 0 & 0 & 0 & 0 & 0 & 0 & 0 & 0 & 0 \end{bmatrix} \begin{bmatrix} \beta \\ p \\ r \\ \phi \\ \psi \\ a_1 \\ a_2 \\ r_1 \\ r_2 \\ r_{WO} \\ \varepsilon_p \end{bmatrix} + \begin{bmatrix} 0 & 0 \\ 0 & 0 \\ 0 & 0 \\ 0 & 0 \\ 0 & 0 \\ 0 & 0 \\ K_m\omega^2 & 0 \\ 0 & 0 \\ 0 & \omega_r^2 \\ 0 & 0 \\ -1 & 0 \end{bmatrix} \begin{bmatrix} p_{com} \\ d_r \end{bmatrix} \tag{8.16}$$

The lateral-directional characteristic modes are presented in Table 8.3, as a function of the roll CSAS gains. K_m is not presented since it was made equal to $-K_i/3$ in a similar way as for the longitudinal case. From Table 8.3 it is seen that the roll mode time constant decreases with increasing negative values of K_P, but increases with increasing negative K_i values. However for the two K_i values presented the roll mode time constant is better than when $K_i = 0$. On the other hand, the spiral mode time constant decreases with increasing negative K_i and increases with increasing negative K_P. Nevertheless, since the spiral mode is stable the larger the time constant the better (slow motion). At last, the dutch roll mode frequency and damping ratio increase for increased gain magnitudes. The time response to aileron and rudder inputs is presented in Figures 8.11 and 8.12, respectively, where the gains are $K_\beta = 3$, $K_r = -5$, $T_{WO} = 3$ and $K_{ARI} = 2.6$, $K_i = -1.5$ and $K_p = -1.0$, the speed is $V_o = 100 m/s$ and $\alpha = 8.0 \deg$.

K_i	K_P	T_r (sec)	T_s (sec)	ζ_d	ω_d (rad/sec)
0	0	0.87	64.5	0.192	0.582
-0.5	-1	0.66	5.21	0.257	0.630
	-2	0.46	7.09	0.304	0.619
-1	-1	0.8	1.80	0.275	0.666
	-2	0.5	1.93	0.312	0.638

Table 8.3 Lateral-directional characteristic modes variation with gain K_i and K_P

In Figure 8.11 it is seen that the roll rate is constant, at approximately 1 deg/sec, while the command of 1 deg/sec is being applied. Once the command is removed the roll rate returns to zero. Thus, similar to the longitudinal command and stability augmentation system, the roll attitude increases linearly while an input is applied, and it is held constant when the input is removed. Furthermore, Figure 8.11 shows that with a roll CSAS the yaw rate increases at a higher rate than for the simple directional FCS. Besides, another result of the zero roll rate when the input is removed, is the constant yaw rate achieved. Thus, while the aircraft is banked the yaw angle will change steadily, for this case at a rate of almost 1 deg/sec, performing a coordinated turning flight. Although the roll CSAS seems a great improvement, it may not be so whence looking into the sideslip angle response. Figure 8.11 shows a greater sideslip angle when the roll CSAS flight control system is present. Furthermore, once the input is removed the sideslip angle remains constant with time.

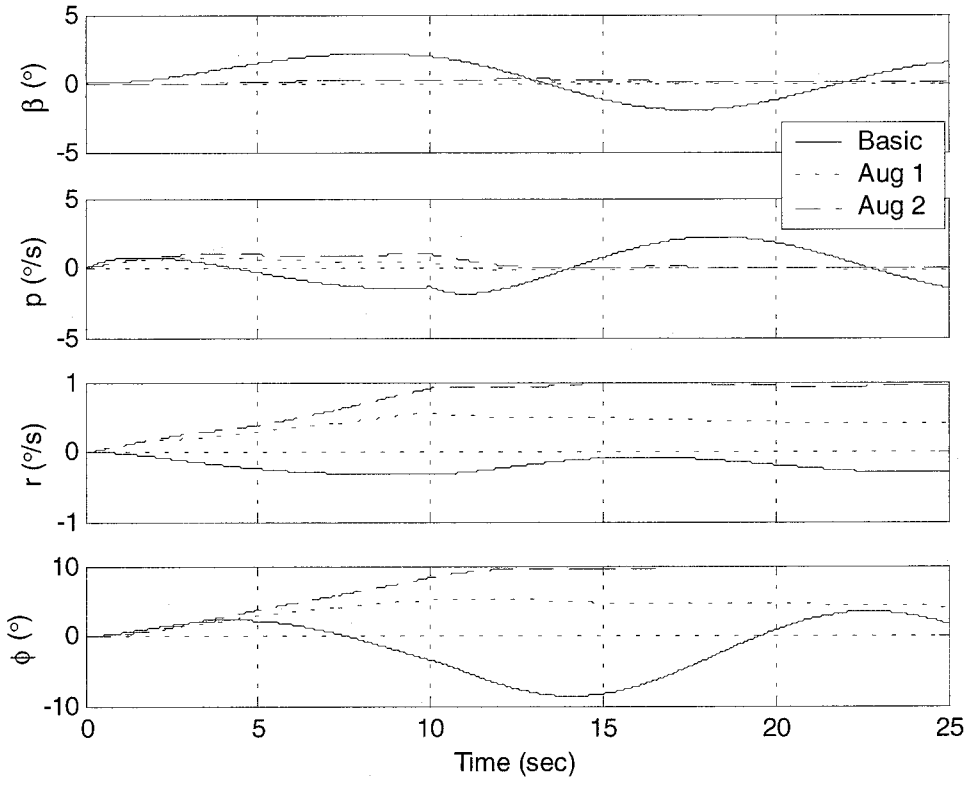

Figure 8.11 Lateral-directional response to 1 deg/sec aileron for 10 seconds

As before, Figure 8.12 shows the decrease in rudder efficiency in the presence of the directional FCS, and furthermore when the roll CSAS is added. On the other hand, and as similar to Figure 8.11, the sideslip angle generated is higher for the directional FCS plus the roll CSAS than for the directional FCS alone. A last aspect worth mentioning is the effective aileron and rudder controls surface deflection in response to –1 deg aileron, or to 1 deg/sec of roll rate demand, as shown in Figure 8.13.

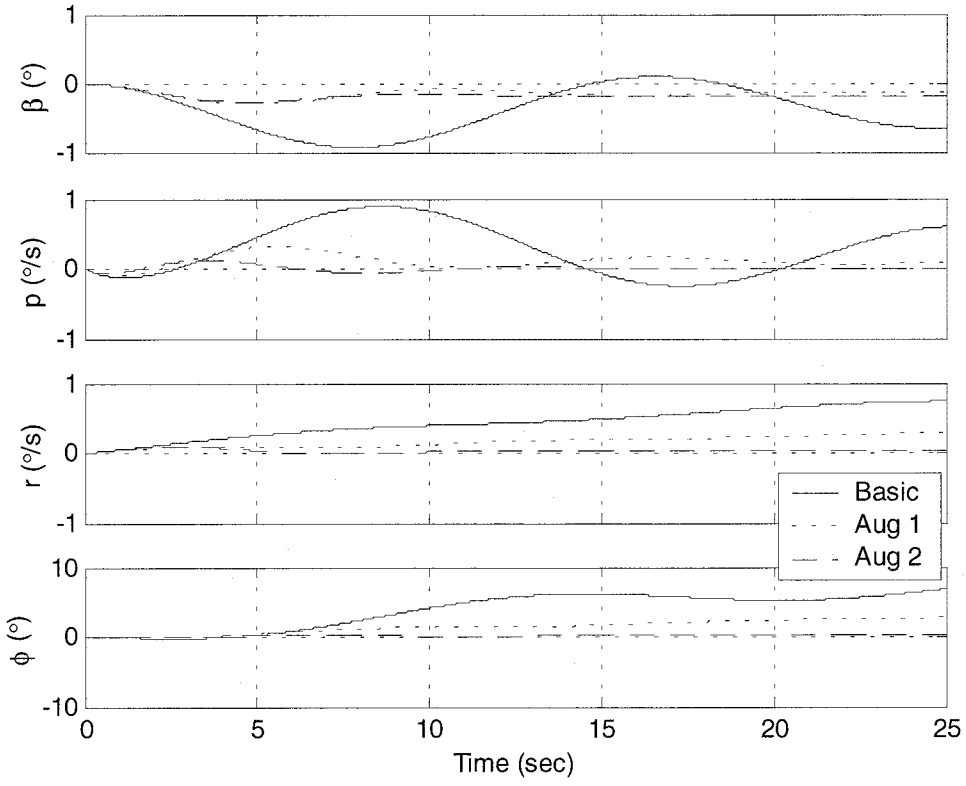

Figure 8.12 Lateral-directional time responses to a step rudder of –1 deg

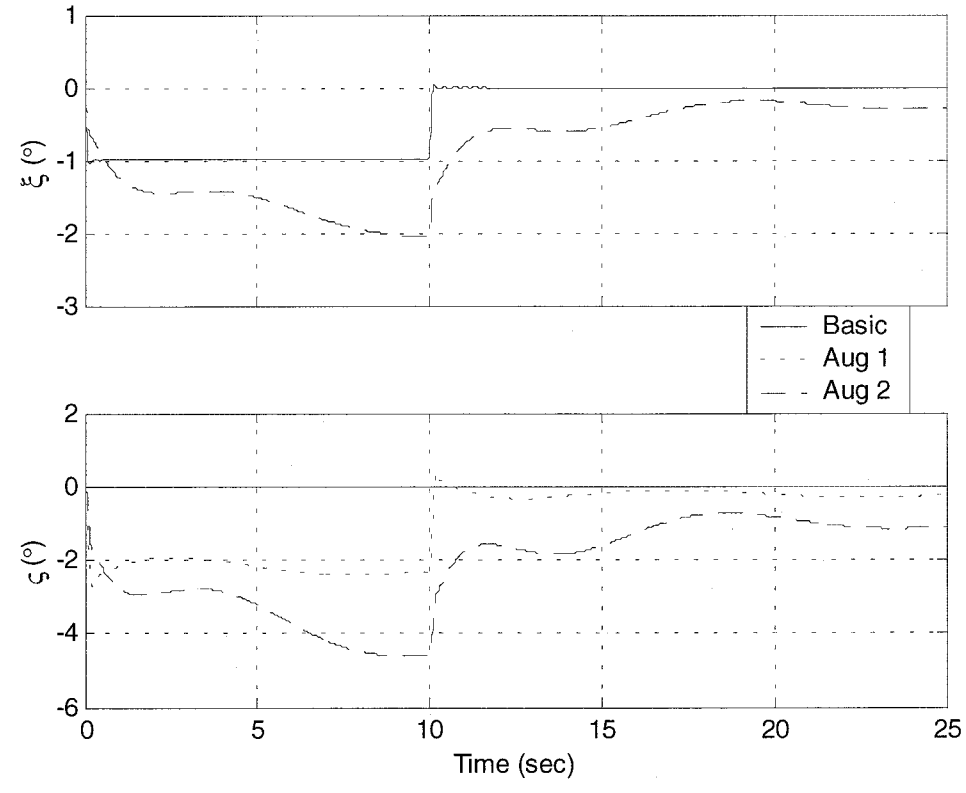

Figure 8.13 Actual aileron and rudder deflection responses to aileron input

As expected, for the basic aircraft only the aileron is deflected the amount demanded, while the rudder remains at zero. However, for the directional FCS and for the roll CSAS, the rudder is also deflected due to the aileron to rudder interconnection. Furthermore, while for the directional FCS alone the rudder deflects –2 deg, when the roll CSAS is also present, the rudder deflects more than –4 deg. Now, if the pilot's demand increases this by a factor of 10, or even 20, the rudder will saturate leaving no directional control. While this is possible for the basic and the directional FCS configurations, when the roll CSAS is present, less than 10deg/sec of roll rate is probably the maximum likely pilot demand. Therefore, the roll CSAS may actually require less rudder deflection than what is suggested by Figure 8.13.

8.3.5 Pitch rate compensation when banking

When the aircraft is rolled into a bank angle part of the lift generated is used to turn the aircraft. Therefore, less lift exists to compensate for the aircraft weight. Thus, if the angle of attack is not increased, the aircraft will loose altitude. Usually, when a pilot banks an aircraft he has also to apply back pressure on the control stick, so that the angle of attack will increase proportionally to keep the aircraft flying level. In a steady turn, the required pitch rate is given by equation (8.17), as taken from Stevens and Lewis[109].

$$q = r + \tan(p) \tag{8.17}$$

In a fly-by-wire era, however, this can be done automatically by implementing a pitch rate compensator into the flight control system for when the aircraft is rolled. Since for this aircraft a pitch rate CSAS is used, it is sufficient to add the additional pitch rate resulting from equation (8.17) to that demanded by the pilot.

8.4 Assessment of the augmented aircraft flying and handling qualities

Two different flight control systems were used to assess the lateral-directional flying and handling qualities of the augmented BWB4 configuration. The first FCS includes the directional stability augmentation system, as given in Figure 8.9, and whose gains are $K_\beta = 3.0$, $K_r = -5.0$, $T_{WO} = 1.0$ and K_{ARI} as given in Figure 8.6. The second FCS also includes the roll CSAS in the lateral axis as presented in Figure 8.10, and whose gains are as presented in Figure 8.14. For the remainder of this assessment the first flight control system will be denoted FCS 1, while the second as FCS 2. Although some of the FCS 1 and FCS 2 gains are different to those designed in the previous

paragraphs, and therefore may not represent the best flight control system design, they were used in the following flying and handling qualities assessment since these were the gains actually used in the simulator.

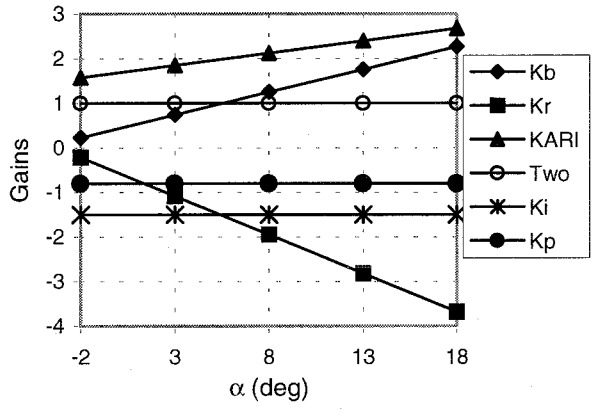

Figure 8.14 FCS 2 directional gains

In the same way as it was done for the longitudinal motion in Chapter 7, criteria have to be assessed, not just for one flight condition, but for several flight conditions representative of the mission tasks to be performed. Thus, a range of speeds and angles of attack, similar to those of Chapter 7 and repeated here in inequalities (8.2) and (8.3), were considered as representative of the variation of the mission tasks.

$$-2^{o} \leq \alpha \leq 18^{o} \tag{8.2}$$

$$80\,m/s \leq V_{o} \leq 200\,m/s \tag{8.3}$$

8.4.1 Lateral-directional characteristic modes

The lateral-directional requirements chosen in Chapter 2, MIL-F-8785C[46], impose limits to the usable roll and spiral modes time constants, as well as to the dutch roll mode damping and frequency. For Level 1, Category C and Class III aircraft these limits are as presented in Table 8.4.

	Roll mode	Spiral mode	Roll/Spiral coupling	Dutch roll mode		
	T_r (sec)	T_s (sec)	$\zeta_{rs}\omega_{rs}$ *(rad/sec)*	ζ_d	ω_d *(rad/sec)*	$\zeta_d\omega_d$ *(rad/sec)*
Upper limit	1.4	-	-	0.7	-	-
Lower limit	0.33	$T_2 > 20$ *	0.5	0.08	0.4	0.10
* T_2: time to double amplitude						

Table 8.4 Lateral-directional characteristic mode limits

The characteristic modes identification is not easy for the two flight control systems considered. High coupling between some of the modes exist for some or all combinations of speed and angle of attack. Usually the aileron and rudder actuator modes, as well as the yaw angle mode, are very visible. While the actuator modes are usually of higher frequency than the remaining modes, the yaw angle is characterised by a pole at the origin, at all times. To identify the remaining poles use of the eigenvectors magnitude was made where necessary.

8.4.1.1 BWB4 augmented with FCS 1

For FCS 1 the spiral mode is characterised, as usual, by a lag of large time constant, (slow mode). This is shown in Figure 8.15 where it is seen that for the speed and angle of attack ranges considered, the spiral time constant is always positive and increases with increasing speed (becomes a slower mode). The spiral mode time constant decreases for low angles of attack, increasing then for higher angles of attack. From Figure 8.15 it is concluded that the requirement is fulfilled since the spiral mode is stable for all combinations of angle of attack and speed.

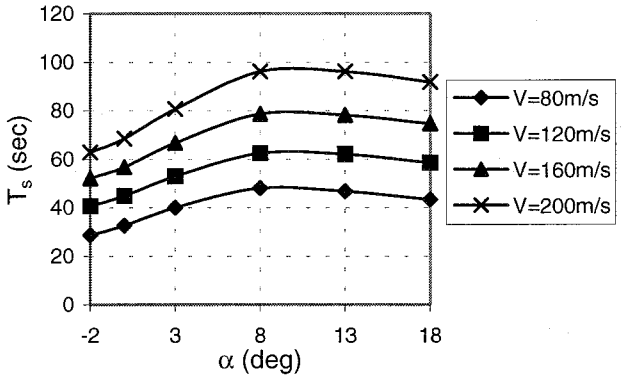

Figure 8.15 FCS 1 spiral mode time constant variation

The roll mode time constant is very clearly discernible for low angles of attack and high speeds. However, for moderate angles of attack and low to moderate speeds the roll mode couples with the washout filter time constant. As shown in Figure 8.16, the roll mode time constant has a lower time constant (faster mode) than the spiral mode which increases for increasing angles of attack and, it decreases for increasing speeds. On the other hand, at high angles of attack and low speeds, when the roll mode time constant increases, approaching 1 sec, it seems to couple with the washout time constant, which was given a value of 1 sec, as well. This coupling, as shown in Figure 8.16, generates another pair of complex roots, which is well separated from the dutch roll mode, due to the higher frequencies and damping values.

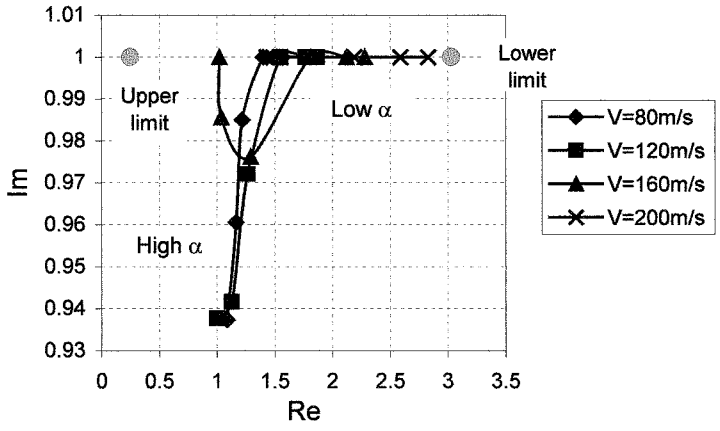

Figure 8.16 FCS 1 roll mode pole variation

From Figure 8.16 it is seen that the roll mode time constant is well within the boundaries presented in Table 8.4. However, there is no information to assess the coupling between the roll mode and the yaw rate washout filter, although this occurrence indicates that flying and handling qualities problems may occur.

The dutch roll mode frequency and damping are presented in Figures 8.17 and 8.18, for several values of speed and angle of attack. The figures show that in general the frequency and period increase with increasing speed. Furthermore, Figure 8.17 shows that the dutch roll mode frequency first decreases with increasing low angles of attack, but then increases for further increase of angles of attack. The damping also oscillates with angle of attack as seen in Figure 8.18.

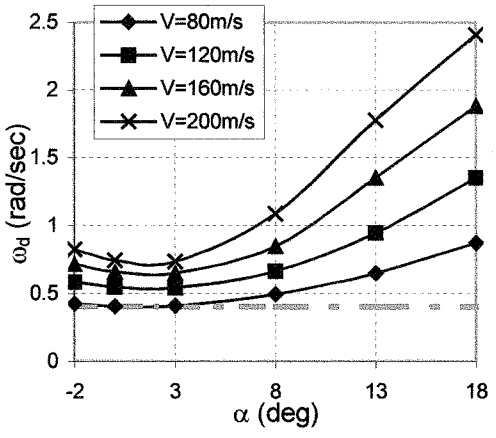

Figure 8.17 FCS 1 Dutch roll mode frequency variation

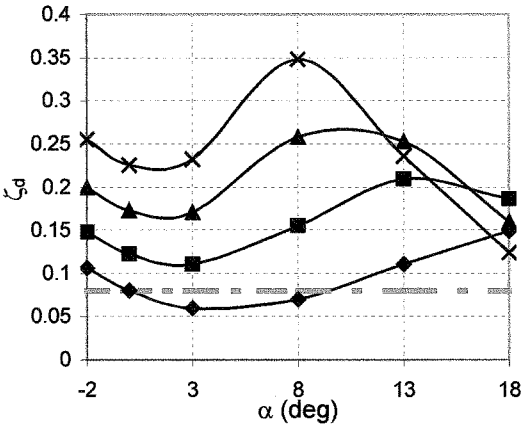

Figure 8.18 FCS 1 Dutch roll mode damping variation

Shown in Figures 8.17 and 8.18 are the required flying and handling qualities limits (in red). Whilst the dutch roll mode frequency is Level 1 for all combinations of speed and angle of attack, the dutch roll mode damping does not fulfil the requirement for the lower speed and moderate angles of attack.

8.4.1.2 BWB4 augmented with FCS 2

For FCS 2, there is a further pole at the origin due to the introduction of the integrator. Furthermore, the washout filter time constant is for FCS 2 well discernible since the roll mode couples this time with the spiral mode. To better identify all poles extensive use of the eigenvectors magnitude was made. However, this was still a difficult task, since the two pair of complex roots, roll-spiral and dutch roll mode, came close to each other for high angles of attack and low speed combinations.

Figure 8.19 shows the roll-spiral coupling mode frequency and damping variation with angle of attack and speed. It is seen from Figure 8.19 that except for the lowest speed value, the roll-spiral damping varies almost only with angle of attack, while the frequency varies almost only with speed. For the lower speed value few variation in damping is seen. Nevertheless, it is to note that for all angles of attack and speed combinations the frequency and damping are well within the Level 1 limits.

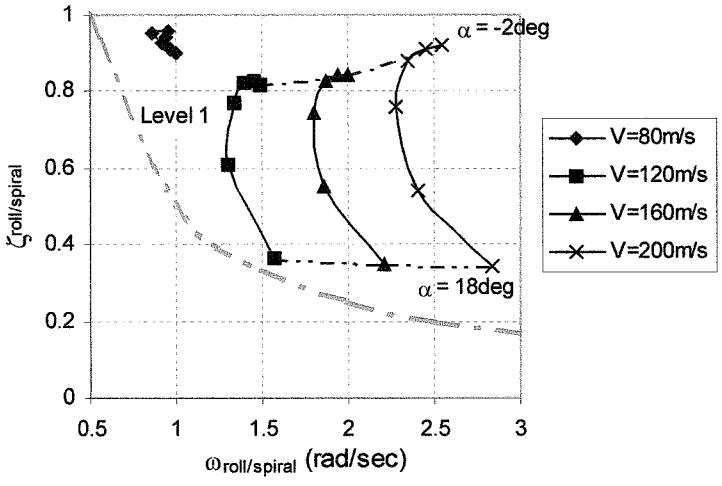

Figure 8.19 FCS 2 roll-spiral modes frequency versus damping variation

The dutch roll mode frequency and damping variation with angle of attack and speed are shown in Figures 8.20 and 8.21. In Figure 8.20 it can be seen that the dutch roll mode frequency increases with increasing speed and angles of attack, although decreasing slightly for the higher angles of attack. In the same way as the roll-spiral coupling mode, the dutch roll mode damping changes almost solely with angle of attack. Comparatively with the flying and handling qualities limits Figures 8.20 and 8.21 show that for low angles of attack the dutch roll frequency is Level 2 for the lower speed while the dutch roll damping is Level 2 for all speeds.

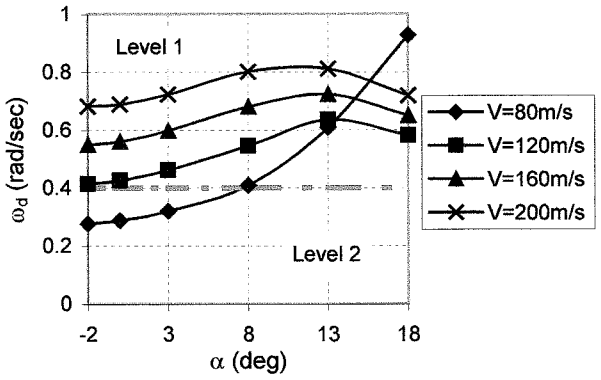

Figure 8.20 FCS 2 dutch roll mode frequency variation

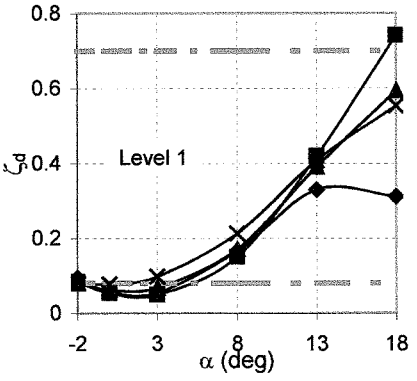

Figure 8.21 FCS 2 dutch roll mode damping variation

In conclusion, the BWB4 configuration is not completely Level 1 neither whith FCS 1 nor with FCS 2. The reason for this is the lower washout time constant, $T_{WO} = 1\text{sec}$ used in both flight control systems, FCS 1 and FCS 2, as shown in Figure 8.3 the influence of T_{WO} in the dutch roll damping. Since a T_{WO} between 1 to 2 seconds is usual in conventional aircraft it was decided to use a $T_{WO} = 1\text{sec}$. When the error was found the piloted handling trials were already done without possibility to run them again. For a question of fair comparison it was decided to use in these flying and handling qualities assessment the same gains as in the simulator.

8.4.2 Roll axis control power

One of the BWB configuration most concerning problems already demonstrated in previous chapters is the control power. The roll control being the most used for the lateral-directional motion needs to be assessed. MIL-F-8785C[46] about the roll axis control power to roll control requires for Level 1 flying and handling qualities that the time to reach 30 deg bank angle, $t_{\phi=30\,\text{deg}}$, for low speeds and with full roll control input be as shown in Table 8.5.

$t_{\phi=30\,\text{deg}}$ (sec)	Cat A	Cat B	Cat C
Upper limit	1.8	2.3	2.5

Table 8.5 Time to reach 30 deg bank angle Level 1 limits

However, since in this research the concern is mainly with the approach and landing only the limit for Category C was taken into account. Besides it was shown in paragraph 2.3.3.3 of Chapter 2 that Sweyk and Rossitto suggest more relaxed requirements for large transport aircraft. Figures 8.22 and 8.23 show respectively the time to roll 30 deg for FCS 1 and FCS 2. As it would be expected the time to roll over

30 deg bank angle decreases with increasing speed and decrease angles of attack. However, the limit for Category C is not always met for both FCS 1 and FCS 2 as shown in the Figures 8.22 and 8.23, thus for the higher limits of Category A and Category B the situation is even worse.

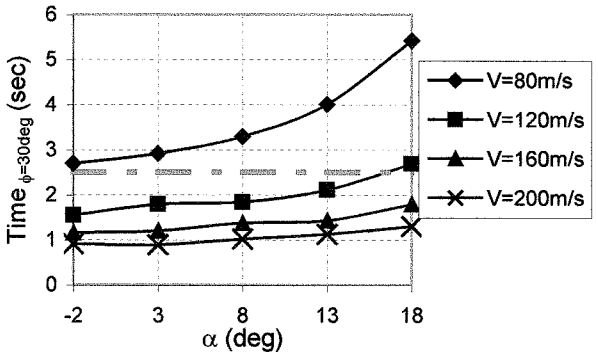

Figure 8.22 FCS 1 time to reach 30deg bank angle

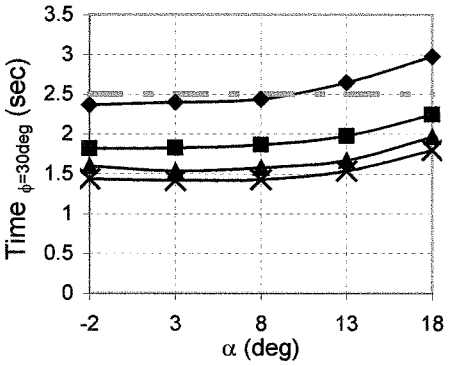

Figure 8.23 FCS 2 time to reach 30deg bank angle

8.4.3 Roll oscillations to step roll control command

An important aspect of the approach and landing task is the need for precision as seen in Chapter 2. Roll rate or attitude oscillations to roll commands are not desirable and must be limited. Configurations with a moderate to high $|\phi/\beta|_d$ response ratio and marginally low dutch roll damping, as for the basic BWB4 airframe, may present unacceptable roll oscillation characteristics. The MIL-F-8785C[46] roll oscillations to step roll control command requirement is divided in three parts as follow.

Firstly, MIL-F-8785C[46] states that following a step roll control command, the roll rate at the first minimum following the first peak shall be of the same sign and not less than 60% for Level 1 Categories A and C. The ratio between the first overshoot peak and the following first minimum, $p_{\min 1}/p_{\max 1}$ as shown in Figure 8.24, was calculated. Figures 8.25 and 8.26 shows the results for FCS 1 and FCS 2 respectively.

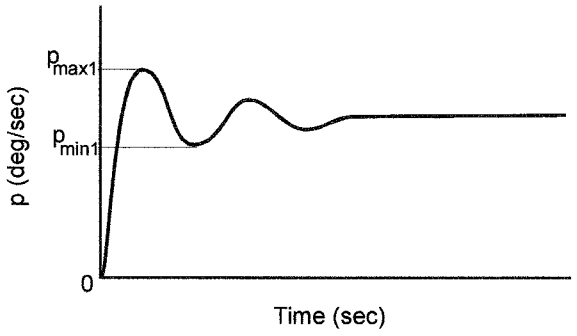

Figure 8.24 First peak and first minimum definition

Comparing Figure 8.25 and Figure 8.26 it can be seen that FCS 2 presents lower $p_{\min 1}/p_{\max 1}$ than FCS 1. This is not surprising since FCS 2 is a roll rate command system which optimises the roll rate response. Furthermore, FCS 2 presents all $p_{\min 1}/p_{\max 1}$ within Level 1 boundaries while FCS 1 does not for at least one flight condition.

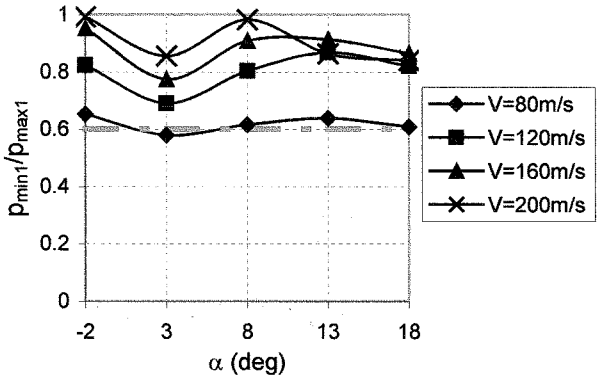

Figure 8.25 FCS 1 first minimum to first maximum ratio

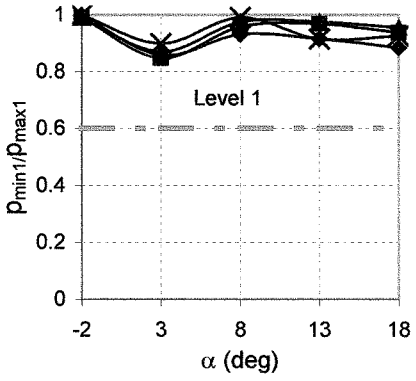

Figure 8.26 FCS 2 first minimum to first maximum ratio

Secondly, MIL-F-8785C[46] states that for step roll control commands up to the magnitude which causes a 60 deg bank angle change in $1.7T_d$ seconds, where T_d is the damped period of the dutch roll, the value of the parameter p_{osc}/p_{av} shall be within the limits given as in Figures 8.27 and 8.28. Also in Figures 8.27 and 8.28 are the results of the measurements for FCS 1 and FCS 2 respectively. The two scales in the x-axis of Figures 8.27 and 8.28 are related to the flying qualities dihedral, which refers to the phasing of roll and sideslip motion in the dutch roll mode. If the aircraft possess positive dihedral use is made of the first scale (p leads β by 45 deg to 225 deg), otherwise the second scale must be used (p leads β by 225 deg through 360 deg to 45 deg). The present BWB4 configuration has positive dihedral, thus use was made only of the first scale.

From Figure 8.27 it is seen that the FCS 1 phase angle, ψ_β, increases for increasing speeds, and decreases for low angles of attack, but then increases again for higher angles of attack. The FCS 1 measure of the roll rate oscillations, p_{osc}/p_{av}, is very lower, however, for low speeds and low angles p_{osc}/p_{av} is outside of the Level 1 region. For the FCS 2, Figure 8.28 shows that ψ_β increases with increasing speeds and angles of attack. The FCS 2 p_{osc}/p_{av} values are even lower than those for FCS 1, as it would be expected since FCS 2 includes a roll rate command system. Although for the lower angle of attack and low speeds p_{osc}/p_{av} values are outside the Level 1 boundary, in general FCS 2 met this part of the requirement better than FCS 1.

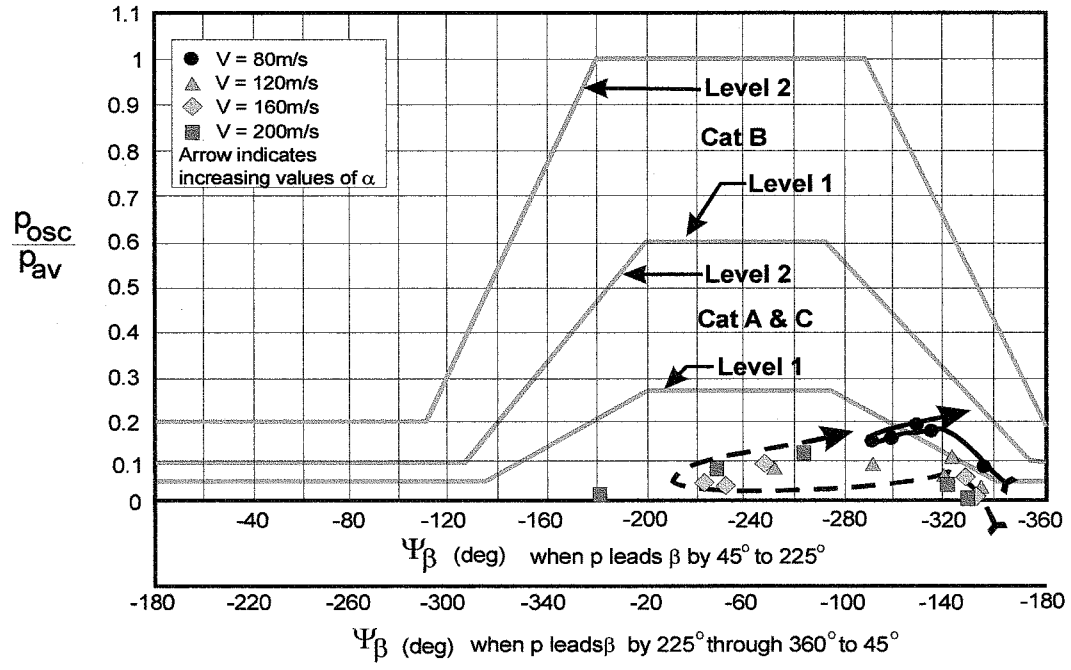

Figure 8.27 FCS 1 roll rate oscillations (Ref. 46)

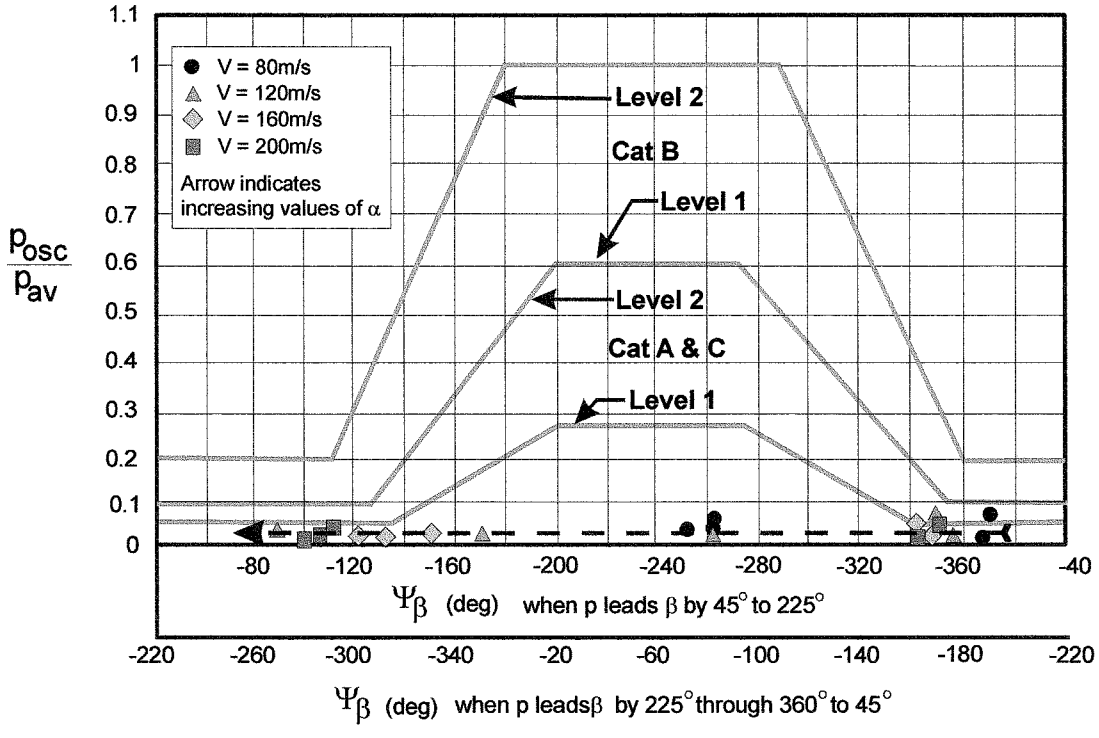

Figure 8.28 FCS 2 roll rate oscillations (Ref. 46)

Thirdly, MIL-F-8785C[46] states that following an impulse roll command the value of the parameter ϕ_{osc}/ϕ_{av} shall be within the limits as given in the requirements. However, an inspection to the roll attitude response to aileron input, as presented in Figure 8.12, for all angle of attack and speed combinations reveal that the BWB4

configuration has no roll attitude oscillations either with FCS 1 or with FCS 2. Thus, this part of the requirement is completely fulfilled.

8.4.4 Lateral acceleration at pilot's station

MIL-F-8785C[46] states that when the pilot is well forward of the centre of gravity or well above the roll axis, turn entries with zero sideslip are accompanied by large lateral accelerations at the cockpit and entries with a centred ball may be impossible. The present BWB configurations are very long and the pilot is really well forward of the centre of gravity. Therefore, a requirement to assess the lateral acceleration at the pilot's station was used. The MIL-F-8785C[46] lateral acceleration requirement states that with yaw control free and with it used to coordinate turn entry, the ratio of maximum lateral acceleration at the pilot station to maximum roll rate, $n_{y_{max}}/p_{max}$, measured for the first 2.5 seconds following a step roll control input shall not exceed the values given in Table 8.6. The value of $n_{y_{max}}$ is calculated taking in account equations (8.18) and (8.19), where g is the gravity acceleration and, the coordinates (x,z) give the distance from the point of interest to the *cg*. For the present BWB4 configuration, the pilot's station is located at (-33.22m, -1.8m).

$$a_y = \dot{v} + ru - pw - z\dot{p} + x\dot{r} \tag{8.18}$$

$$n_y = -\frac{a_y}{g} \tag{8.19}$$

$n_{y_{max}}/p_{max}$ (g/deg/sec)	Level 1	Level 2	Level 3
	0.012	0.035	0.058

Table 8.6 Maximum lateral acceleration

Figures 8.29 and 8.30 present the results for BWB4 when using FCS 1 and FCS 2, respectively, as a function of angle of attack and speed. Figure 8.29 shows that the FCS 1 $n_{y_{max}}/p_{max}$ decreases with increasing angles of attack and with decreasing speed values. However, except for the higher angle of attack where it reaches Level 1, FCS 1 is within the Level 2 boundaries. On the same way, Figure 8.30 shows that the FCS 2 $n_{y_{max}}/p_{max}$ values also decrease with increasing angles of attack and decreased speed values. However, the FCS 2 $n_{y_{max}}/p_{max}$ values are sparser, with values reaching Level 3 boundaries for high speeds and low angles of attack. Although for some flight conditions the Level 1 boundary is also reached, most of the FCS 2 $n_{y_{max}}/p_{max}$ values lay on the Level 2 region.

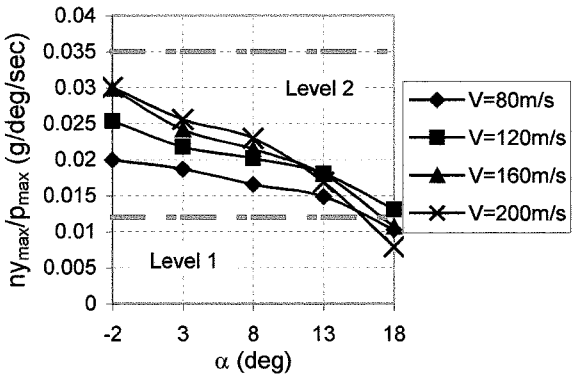

Figure 8.29 FCS 1 lateral acceleration at the pilot's station

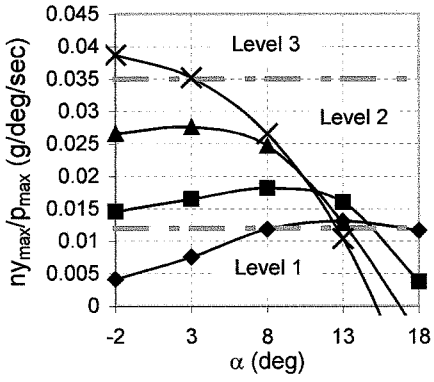

Figure 8.30 FCS 2 lateral acceleration at the pilot's station

8.4.5 Yaw axis response to roll controller

Until now the concern of this flying and handling qualities assessment has been on the roll axis response to roll controller. However, one of the drivers for the lateral-directional flight control system design was to decrease the sideslip excursions excessively high, as shown in Chapter 6. MIL-F-8785C[46] presents a requirement to insure that any yaw control needed to coordinate turn entries and recoveries/reversals is not objectionable to the pilot.

The yaw axis response to roll controller requirement of MIL-F-8785C[46] states that the amount of sideslip following a step roll control command up to the magnitude that causes a 60 deg bank angle change within T_d or 2 seconds, whichever is longer, shall be within the limits as given in Figures 8.31 and 8.32. Furthermore, following larger step roll commands, holding it fixed until the bank angle has changed at least 90 deg, the ratio of sideslip increment, $\Delta\beta$, to the parameter k should be less, for Level 1, than those values given in Table 8.7.

$\Delta\beta/k$	**Adverse sideslip**	**Proverse sideslip**
Cat A	6 deg	2 deg
Cat B & C	10 deg	3 deg

Table 8.7 Level 1 recommended maximum sideslip excursions for large roll control commands (Ref. 46)

The parameter k is defined as the ratio of commanded roll performed to applicable roll required, $k = (\phi_t)_{performed} / (\phi_t)_{required}$. Furthermore, since the approach and landing task is of concern in this research only the boundaries for Cat C were considered.

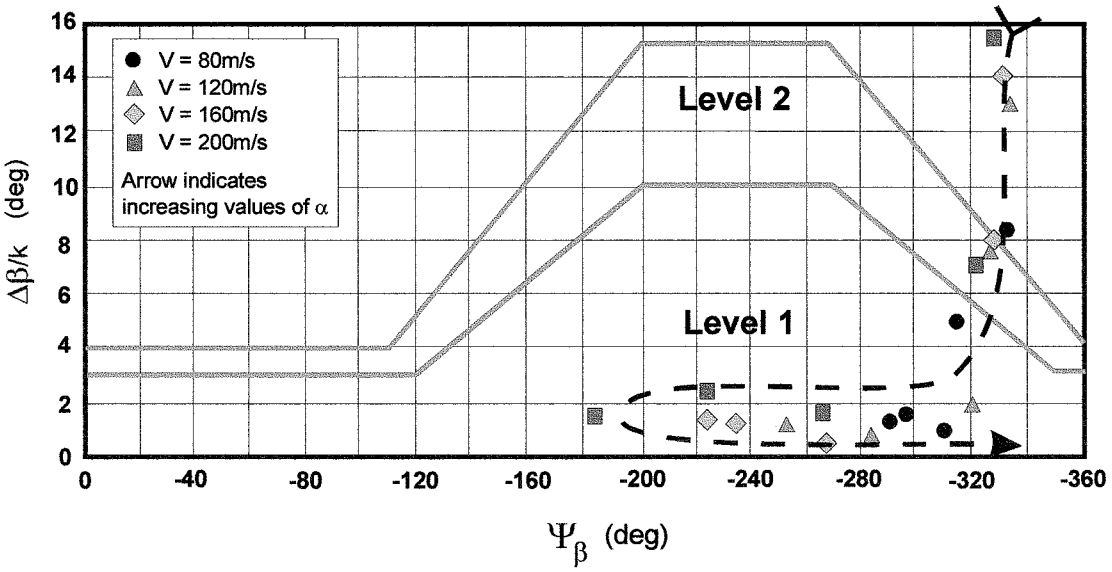

Figure 8.31 FCS 1 sideslip excursion limitations for small roll inputs (Ref. 46)

From Figures 8.31 and 8.32 it is seen that the sideslip excursions decrease for increasing values of angle of attack. In Figure 8.32 the symbols outside the plot area indicate much larger values than the maximum in the plot. Furthermore, Figure 8.31 shows that except for the low angles of attack, the FCS 1 sideslip excursions are within Level 1 boundary, whilst Figure 8.32 shows that except for a few values, around $\alpha = 8\,\text{deg}$, the FCS 2 sideslip excursions are outside the Level 1 boundary and even the majority is outside Level 2 boundary as well.

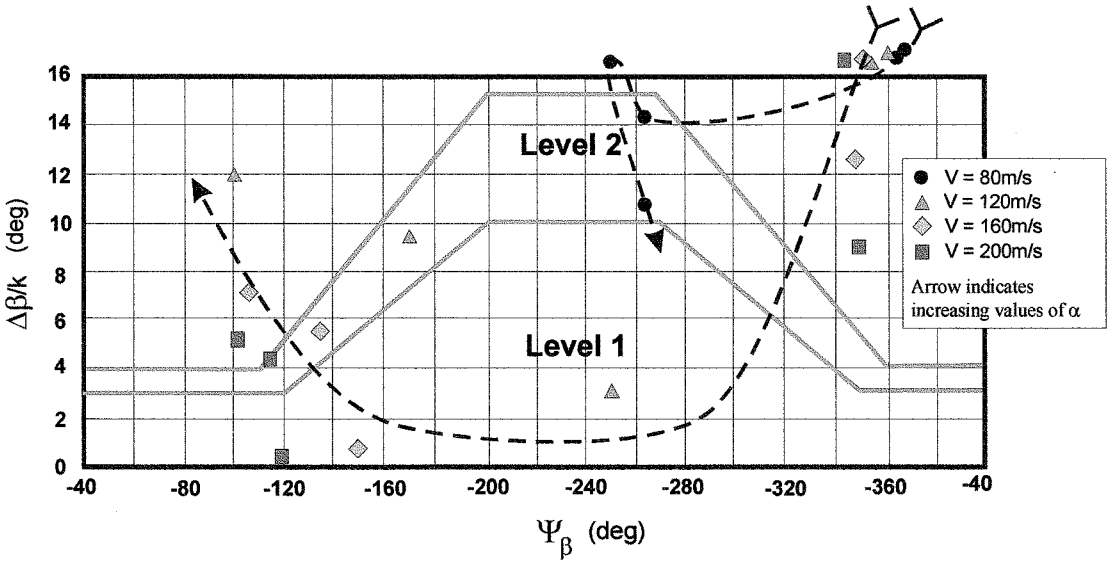

Figure 8.32 FCS 2 sideslip excursion limitations for small roll inputs (Ref. 46)

Figure 8.33 and 8.34 present the sideslip excursion of FCS 1 and FCS 2 for larger roll inputs. The flying and handling qualities limits (in red) are presented in this way in both Figures 8.33 and 8.34, because inspecting the sideslip response to a negative aileron input for the FCS 1 and FCS 2 for the several flight conditions used, it was found that for low angles of attack until $\alpha = 8\,\text{deg}$ proverse sideslip exist, i.e., negative

sideslip when rolling positively, while for higher values of angles of attack adverse sideslip existed, positive sideslip with positive rolling. The boundary between proverse and adverse sideslip is speed dependent in some extent for FCS 1.

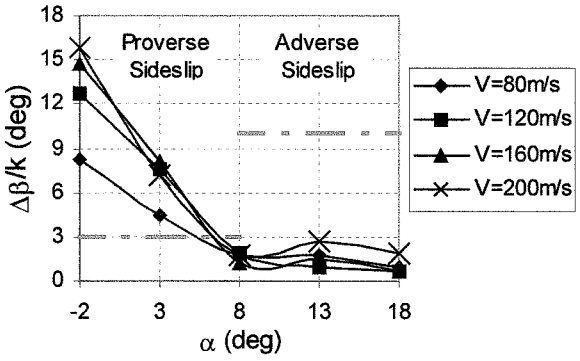

Figure 8.33 FCS 1 sideslip excursions for large roll inputs

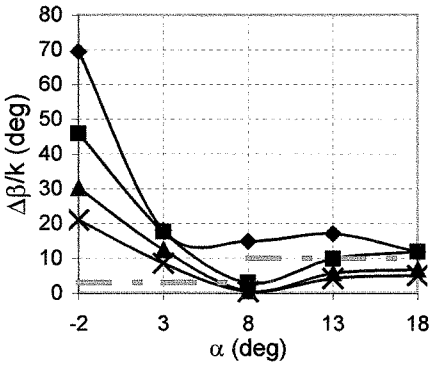

Figure 8.34 FCS 2 sideslip excursions for large roll inputs

Comparing Figures 8.33 and 8.34 it is concluded that FCS 1 presents lower sideslip excursions for larger roll inputs than FCS 2, similar for the small roll inputs. Furthermore, for high angles of attack, in the region of adverse sideslip, FCS 1 met the requirement for all speeds with very low sideslip excursions, whilst FCS 2 does not met the requirement for the lower speed and it has higher sideslip excursions for the remaining speeds. For small angles of attack, or the proverse region, neither FCS 1 nor FCS 2 fulfils the requirement. However, FCS 1 presents lower sideslip excursions than FCS 2.

8.4.6 Flying and handling qualities assessment conclusions

From the flying and handling qualities assessment of the previous paragraphs it can be concluded that the BWB4 augmented aircraft with FCS 1 and with FCS 2 presents better characteristics than the unaugmented aircraft. The flying and handling qualities of the augmented aircraft have reached Level 1 for several characteristics, however, there are still some characteristics not acceptable. These are as follow,

- The existence of coupling between modes, namely the roll mode and washout time constant coupling for FCS 1 may reveal not acceptable.
- The dutch roll mode it is not completely satisfactory at low speeds for either FCS 1 or FCS 2.
- Also the roll control power is also not satisfactory at the lower speed and low angles of attack for FCS 2, but for all angles of attack for FCS 1.

- In what the roll oscillations are concerned, FCS 2 present better characteristics than FCS 1 which does not have satisfactory characteristics for some flight conditions.

- However, when considering sideslip excursions FCS 2 presents much larger sideslip excursions than FCS 1.

- About the lateral acceleration at the pilot's station FCS 2 presents also slightly worse accelerations than FCS 1, probably due to the larger sideslip excursions.

During the introducing and tuning of the flight control system in the flight simulator, the pilot has flown the BWB4 configuration augmented with both FCS 1 and FCS 2. It was the pilot's opinion that with FCS 2 the flying and handling qualities were degraded when compared to that of FCS 1 due to the sideslip excursions. Even the improved roll oscillation characteristics were not enough improvement to accept the augmentation with FCS 2. Therefore, the piloted handling trials realised and presented in Chapter 9 only used FCS 1 has the lateral-directional flight control system.

CHAPTER 9
Piloted handling trials

"...let handling qualities be briefly defined as those dynamic and static properties of a vehicle that permit the pilot to exploit its performance and other potential in a variety of missions and roles."

Irving L. Ashkenas

9.1 Overview

As stated before, in Chapter 2, flying and handling qualities are subjective definitions, rather difficult to quantify and even sometimes to define. Attempts to define these terms always end up in matters of an evaluation in flight made by an individual when performing a specific task. Cook[99] distinguishes between flying qualities and handling qualities. He considers the pilot's perception of flying qualities to comprise a qualitative description of how well the aeroplane carries out a commanded task. On the other hand, Cook[99] considers that the pilot's perception of handling qualities is a qualitative description of the adequacy of the short term dynamic response to controls in the execution of the flight task. The author summarizes by stating that the flying qualities may be regarded as being task related, whereas the handling qualities may be regarded as being response related.

Piloted handling trials, whether in a simulator or in a real aeroplane, are the ultimate means to evaluate flying and handling qualities. Bihrle[61] states that the precision control problem can best be described by referring to the pilot comments obtained during a handling qualities investigation. In this research programme a similar procedure is followed. But before piloted handling trials can be performed several tasks have to be completed. Firstly, the objectives for such trials must be defined and, secondly, a methodology to achieve them must be designed.

In the literature a great number of experiments in flying and handling qualities can be found, with several methodologies described. These are usually separated into longitudinal and lateral evaluations, where several variations of an aircraft configuration are evaluated during the handling trials. These variations are introduced in terms of defined parameters that are believed to be key factors defining the relationship between stability and aircraft characteristics. It is then possible for these parameters to be mathematically defined to represent the more subjective handling and flying qualities description.

However, in this work such an approach was not taken, since the aircraft design was at an early stage and even the knowledge of the basic stability parameters was not right. The aircraft design is still evolving and there are many unanswered questions about the blended-wing-body configuration. Thus, the usual approach of looking for the stability characteristics that give good handling and flying was not taken. Instead, the approach was to find out whether the rather general known characteristics endow good flying and handling characteristics or not. Or rather, will this blended-wing-body configuration be able to perform the same tasks as the conventional civil aircraft of today?

The definition of flying and handling qualities is rather subjective and knowledge of it has evolved during the last 100 years of flying. Also, methods for evaluating these qualities have changed, as presented in Chapter 2 when describing the flying qualities requirements. Thus, the goal of "performing the same tasks" has the implication of evaluating the aeroplane for a required mission task, to answer whether this can, or cannot, be performed.

The simulator characteristics are also important when carrying on piloted handling trials. For more information on the simulator used the reader is referred to paragraph D.1 of Appendix D. Also presented are the modifications made to the basic simulator program to accommodate the BWB and FCS characteristics. Finally, in paragraph D.2 a transcription of the simulator code is presented.

9.2 Experiment description

9.2.1 Pilots briefing

To inform the pilots what the flying trials were about, a pilot's briefing was designed and is presented in Appendix E. This consists of 4 fields,

1) Purpose of experiment;
2) Simulator description;
3) Experiment description; and
4) Method of evaluation.

The first field gives a brief overview of what the research is for. The second field gives information about the simulator facilities. Then, the third field describes what the pilot has to do and the last one gives the parameters for handling and flying qualities evaluation during the experiment.

The most important fields are the description of the tasks to be accomplished together with the evaluation process. After each task description follows a space for the pilots to rate the evaluation and to comment. Thus, since the pilots evaluate the aircraft while accomplishing the tasks following the directions given, the choice and definition of the task has to be made carefully, and that is presented in the next paragraph.

9.2.1.1 Which tasks to choose?

The goal of simulation was to evaluate whether the BWB aircraft can perform typical tasks that civil aircraft usually perform. Thus, the tasks were chosen to be representative of civil aircraft missions. Since an extensive and complete set of tasks performed by civil aircraft would not be interesting, or even feasible, only the most demanding and representative were chosen. Furthermore, the possibilities offered by the simulator and the models implemented there, as discussed already in the previous chapter, were also taken into account when choosing the tasks to perform.

The first task that any aircraft performs is the takeoff. Then, once flying it is of interest that it can also land. Thus, since these are the most demanding "normal" tasks for a civil aircraft, they were chosen for the experiment. Furthermore, it was interesting to simulate tasks such as takeoff and landing with engine failure and subject to crosswind. The reason for this is that a civil aircraft needs to be certified as able to perform these "abnormal" or emergency tasks with a minimum threat to safety, and good flying and handling qualities are synonymous with safety. Introduction of turbulence also increases the pilots' workload and stress, helping to expose hidden problems. Thus, it is also important to be included.

Lastly, a factor to take into account is that usually the flying and handling qualities are evaluated separately for the longitudinal and lateral-directional characteristics. This

separation should be retain, in order to help the pilot in the evaluation. Nevertheless, tasks always include a mix of both longitudinal and lateral characteristics. Thus, special tasks to evaluate each of these characteristics separately are desirable. Taking in account everything discussed so far, it was decided to evaluate the following tasks with and without turbulence.

- Normal takeoff
- Crosswind takeoff
- Takeoff with engine failure
- Normal land
- Crosswind land
- Land with engine failure
- Longitudinal offset during approach
- Lateral offset during approach

However, during the preparation of the simulator for the piloted handling trials, it was found that the wind model was not included in the ground model. Thus, during the ground run in the crosswind takeoff there was no wind effect. However, as soon as the aircraft would liftoff the flight models would change, suddenly putting the aircraft into crosswind. Thus, this sudden discontinuity in the simulation made the "Crosswind Takeoff" simulation quite unrealistic so it was then abandoned. About the "Crosswind land", since the pilot could evaluate the task only until the touchdown point, it was decided to go ahead with it.

Later, during the first simulation trials, it was found that the turbulence only affected the speed magnitude, making sudden continuous changes within a range of ± 10 knots maximum. Such variation was felt, however, not to be a large disturbance as might be expected in a real turbulent environment. Thus, the trials with turbulence were also abandoned.

The remaining tasks were then detailed further and specified in terms of smaller subtasks, or steps, for the pilot to accomplish. The way of evaluation of each task was also defined and these are presented next. The main objective of this sub-definition was to have a task flow representative of what civil airliners have, though enabling the flying and handling qualities to be evaluated at the same time.

9.2.1.2 Task 1 – Normal takeoff

Task 1 aimed to represent the usual civil aircraft takeoff, climb and acceleration segments and trimming for cruise. This was defined as: rotation at V_r, liftoff and

climb to 50 ft at V_2. The aircraft should then continue to climb until a determined altitude was reached and then levelled off while accelerating to cruise speed. Lastly, the aircraft should be "trimmed" for this altitude and speed, to represent the beginning of the cruise. The flying and handling qualities evaluated in this task were:

1) How well the aircraft attitude could be established and maintained – pitch attitude tracking.
2) How well the altitude could be established and maintained while the aircraft accelerated – altitude maintenance.
3) How well the altitude and speed could be kept constant – "trim" maintenance

It is not correct to talk about trim with the present pitch rate/attitude hold command flight control system, since such system suppresses the longitudinal phugoid motion and thus the usual idea of trim. Nevertheless, as the task was to keep the speed and altitude constant, this can be considered as trimming the aircraft. However, the method of trim in this case is different to that in an aircraft with classical commands, as explained in Chapter 2.

	Desirable	**Acceptable**
Pitch attitude, θ	±2°	±5°
Altitude	±100 ft	±200 ft
Speed	±5 kts	±10 kts

Table 9.1 Definition of desirable and acceptable limits for Task 1

Moreover, since the aerodynamic data is limited to low speeds, the trim speed was not representative of the initial cruise speed, neither was the altitude. This was done to avoid the long periods of constant climbing and acceleration that a normal civil aircraft performs. The range of desirable and acceptable limits was defined as shown in Table 9.1.

9.2.1.3 Task 2 – Engine failure during takeoff

This task was to be accomplished in the same way as the previous task. However, it includes the complication of one of the outside engines failing while still running on the runway. The program would, at a pre-determined speed, automatically fail the engine. Pilot A performed this task with the engine failure speed set up for 120 kts. However, it became clear that a failure at this low speed encouraged the pilot to choose to stop the aircraft instead of continuing the takeoff. Thus, the speed at which the engine was failed was raised to 160 kts in order to obligate the pilot to continue the takeoff. The pilot who flew with the engine failed at 120 kts continued the takeoff

for the evaluation, the only difference was the time taken to accelerate the aircraft to rotation speed.

In Figure 4.8 of Chapter 4 it was shown that configuration BWB4 had no enough control power to compensate for an engine failure at low speeds. Therefore, a decrease of about a factor of three on the engine moments was done, as explained on paragraph D.1.3.3 of Appendix D. The new rudder and aileron to trim the new moments are equal to that given on Figure 4.8 reduced by the same factor of three.

	Desirable	**Acceptable**
Offset from centreline	±25% of rnw width	±50% of rnw width
Heading, ψ	±5°	±10°
Bank angle, ϕ	±5°	±10°

Table 9.2 Definition of desirable and acceptable limits for Task 2

Although the pilot's task looks similar to Task 1, there was the additional stress and workload of having to compensate for the failed engine this time and maintaining the aircraft on the initial heading. Thus, the qualities evaluated with this task were defined differently, as were the desirable and acceptable parameter limits, as presented in Table 9.2. The assessed qualities were defined as,

1) How well the heading could be re-established parallel to the centre line after the engine failure
2) How well the heading could be maintained within a reasonable bank angle for wings levelled, once in the air.

9.2.1.4 Task 3 – Normal approach and landing

After the takeoff, climbing, acceleration and cruise, the next segment a civil aircraft would accomplish is the descent and deceleration, followed by approach and land. Since descending and decelerating are also included in the approach, only the approach and landing were simulated. Similar to climbing and accelerating, the simulation of a real descent and decelerating task would make the evaluation too long. Besides, not enough data was available to simulate the high speeds encountered at the beginning of the descent and decelerating segments. This task was divided in two parts,

1) Approach until 200 ft – assessed qualities defined as how well the 1st segment was accomplished in terms of acquiring and maintaining the glide slope, as well as decelerating until and then maintaining the landing speed of 180 kts.

2) Landing itself constituted by the final approach, flare and touchdown – assessed qualities defined as how well the flare and touchdown were accomplished.

The desirable and acceptable parameter limits are presented in Table 9.3. The longitudinal and lateral displacements from the runway centreline can better be seen from the figure attached to the pilots briefing, as presented in Appendix E.

	Desirable	**Acceptable**
PAPIs for glideslope guidance	2w/2r	3w/1r or 1w/3r
Raw ILS	± ½ dot	± 1 dot
Speed	±5 kts	±10 kts

Table 9.3 Definition of desirable and acceptable limits for Task 3

9.2.1.5 Task 4 – Crosswind approach and landing

This task was the same as Task 3, except for the additional effect of a crosswind component. Thus, this task makes it possible to evaluate whether the aircraft possesses enough lateral control power to compensate for the lateral wind, or not. The pilots were first asked to fly two different approach techniques, "wing-down/crab" or "kick-off drift", to decide which they would prefer. The evaluation in this task was concerned with the landing, not with the pilot control technique.

Pilots where asked to fly the task to the touchdown point ignoring all events after touchdown, due to the lack of crosswind in the ground model. However, the touchdown is very important for the definition of desirable and acceptable limits for this task. Furthermore, during the definition of these values the pilots felt that further details were not consistent with real crosswinds. The visual system update rate was one of the details not working well. Thus, it was not possible to define precise limits for this task. Later, during the piloted handling trials this task was abandoned.

9.2.1.6 Task 5 – Engine failure during approach and landing

This task is the same as Task 3 except for the increased complication of an outside engine failure. The goal is to decide how this complication might affect the blended-wing-body flying and handling qualities. As for the takeoff task, the program automatically fails the engine, in this case once the aircraft flies below 1700ft. The pilot flying a normal approach has then to compensate for the failed engine while

continuing the approach to land. The desirable and acceptable parameter limits were established as shown in Table 9.4. The task was subdivided into two sub-tasks as follows.

1) How well the heading could be re-established and maintained together with wings level bank angle immediately after the engine failure.
2) Landing, constituted by the flare and touchdown, as previously.

	Desirable	**Acceptable**
Heading, ψ	±5°	±10°
Bank angle, ϕ	±5°	±10°
Flare and touchdown as defined for task 3		

Table 9.4 Definition of desirable and acceptable limits for Task 5

9.2.1.7 Task 6 – Approach and landing with longitudinal offset correction

This task was designed to better evaluate the longitudinal handling and flying qualities. This was achieved by evaluating the pilot action required to correct a longitudinal offset in a limited time. In other words, it aimed to evaluate the longitudinal control precision during corrective manoeuvres. This was also a way of evaluating the effect of increasing the pilot workload and stress, since it was not possible to use turbulence.

The task is described as follows; the pilot was supposed to fly the approach 1 dot high, using the ILS glideslope indicator to simulate the longitudinal offset. At 600ft effective height above the runway, the pilot reverts to fly visual, following the PAPIs indication and correcting for the longitudinal offset while maintaining a speed of 180kts. The desirable and acceptable parameter limits were the same as defined for Task 3. For precise evaluation this task was divided in two sub-tasks as follows.

1) How well the aircraft regains 2white/2red (2w/2r) spots on the PAPIs while maintaining the speed at 180kts.
2) Landing constituted by flare and touchdown.

9.2.1.8 Task 7 – Approach and landing with lateral offset correction

In the same way as the previous task, this task aimed to evaluate the pilot action required to correct a lateral offset within a limited time, or height. Thus, it aimed to evaluate the precision of lateral tracking while manoeuvring on to the runway centreline. This task also aimed to evaluate the increase in pilot workload and stress,

and how the pilot would judge the lateral flying and handling qualities in such a stressed situation. For this task the pilot was asked to fly the approach 1 dot to the right (or to the left) using the ILS glideslope indication. At 600ft *Radar Altitude* (RA), he then corrects for the lateral offset to within 200ft height and land as usual. The desirable and acceptable parameter limits were the same as defined for Task 3. The task evaluation was divided in two sub-tasks as follows.

1) How well the lateral offset could be corrected to within 200 ft height and the centreline could be tracked again.
2) Final approach, flare and touchdown as before.

9.2.1.9 Last comments

The values for the desirable and acceptable parameter limits, as well as the takeoff, landing and manoeuvring control speeds, throttle settings and attitudes required for the climb and the approach were defined with the help of a pilot. This was the same test pilot who helped to develop the flight control systems and to debug the simulator modifications, as well as validate the blended-wing-body aircraft model.

The parameter limits may seem rather relaxed, but they are thought to be representative of civil aircraft. This, of course, will lead to better *Cooper-Harper* and *Bedford Workload* opinion ratings. If these limits were tightened the pilot might feel it more difficult to achieve and keep the aircraft within limits, and would therefore rate the aircraft worse. Nevertheless, there is no obvious reason to tighten the parameter limits when the flight instruments do not have sufficient definition and precision for the pilot's guidance and evaluation.

The availability of the test pilots for the flying qualities evaluation trials partially overlapped the briefing development. Thus, some changes to the briefing were made afterwards, partly as a consequence of the way the trials ran, and partly from the pilots' comments. Thus, some differences exist between the trials, and how they were recorded for each pilot. An important difference is that pilot A and pilot B, flew the experiment without the sub-definition of each task and evaluated them in a more generic way. Pilot C and pilot D had more stringent limits to follow, which obviously influenced their ratings, as evidenced by the results.

9.2.2 Pilots' details

Four test pilots flew piloted handling trials for this research. The pilots are identified as pilot A through D. The pilots' details are presented in Appendix E paragraph E.2. However, it is useful to comment on the constitution of the group.

Pilot A, C and D are, or have been, flying test pilots. Thereby, they are used to the *Cooper-Harper* and *Bedford Workload Scales*. Moreover, their background in fighter aircraft make them used to augmented aircrafts, as well as with non-classical command stability augmentation systems, as the present configuration.

Due to the lack of available flying test pilots, it was thought that pilot B could make a valuable contribution with his knowledge of civil aircraft, although he has never been a test pilot. Therefore, pilot B lacks the knowledge of the *Cooper-Harper* and other flying and handling scale ratings, besides of being inexperienced with flying augmented aircraft having non-classical command stability augmentation systems. Although such differences might influenced his ratings, it was also found that the pilot rapidly adapted himself to this new situation and configuration. He quickly learned to use the *Cooper-Harper* and *Bedford Workload scales* so it did not represent a problem. Furthermore, being a civil pilot and used to work in team, pilot B felt he needed some help for the simulation trials. As so, a third person, simulating a co-pilot, was present calling at pre-determined crucial moments as the rotation speed, altitude to level, engine failure, threshold altitude, etc. This co-pilot also helped in tasks as recovering or deploying the undercarriage, as would usually happen in a civil aircraft. This team work in a civil cockpit increases the awareness of the pilots of the surrounded situation and of anything that may happen.

Pilot D used to be a test pilot, but, in the same way as pilot B, he is currently a civil airline pilot flying Boeing 777 aircraft. He made, therefore, a valuable contribution for this simulator model, in evaluating whether the inertias and rate of responses are representative of such large aircraft. His evaluations were influenced as well by his actual knowledge of civil aircraft procedures. Lastly, pilot C was the one who helped to improve the aircraft model flying and handling qualities, by fine tuning the flying control systems.

9.2.3 Experiment description

The piloted handling trials began with the pilots being briefed in the tasks to be performed. Some pilots had access to the briefing longer before the simulation trials

than others. However, that seemed to make no difference to the exercise. Once in the simulator the cockpit was introduced to the pilot by a presentation of the position of the controls, screens, etc. The pilot was then allowed to fly the aircraft around, to get a feeling of the controls and the characteristics of the aircraft in general. After the pilot was familiar enough with the cockpit and aircraft characteristics, the evaluation was initiated.

Each pilot flew a task at least 2 or 3 times before evaluating it. However, for some tasks the pilot was allowed to fly it more times, until confident time permitting. After flying each task, the pilot was asked to rate and comment on the task before continuing with the next task. However, the pilot was able to write further comments at the conclusion of the handling trial. The entire piloted handling trial required around 2 hours to be accomplished.

9.3 Presentation and discussion of results

9.3.1 Presentation of results

The pilot's comments from the piloted handling trials, as well as the *Cooper-Harper ratings* (CHR) and *Bedford Workload ratings* (BWR) are presented in Appendix E. The results for each task are presented in the following paragraphs. Since pilot C and pilot D assessed the blended-wing-body flying and handling qualities in more detail, in the following paragraphs the results from these pilots are presented first. Only then the assessment of pilot A and pilot B are discussed, since they assessed the flying and handling qualities in a more qualitative way, i.e., without the subtask division, although the pilots were fully aware of the parameter limits given in the pilot's briefing of Appendix E, paragraph E.1.

9.3.1.1 Task 1 – Normal takeoff

Pilot C and pilot D reported satisfactory characteristics (CHR=3) on establishing and maintaining the required pitch attitude, although there were still some mildly unpleasant variations in pitch which would not allow complete hands free flying. The workload was low enough to allow for spare activities (BWR=3).

Also satisfactory characteristics were reported (CHR=3) when changing from the climb to accelerated level flight, although pilot C complained about the high

acceleration. This introduced some workload to adjust it and was the reason for the slight increase in the average Bedford workload rating (BWR=3.5).

To maintain the speed and altitude at the required values, pilot D reported the need to continuously adjust the EPR setting with changes in speed. This contributed to an increase of the Cooper-Harper rating (CHR=3.5), as well as for the increase in the workload rating (BWR=3.5).

In general, and taking into account only the ratings of pilot A, pilot C and pilot D, the aircraft configuration was appropriate for the normal takeoff task. Pilot B, however, did report acceptable, but not satisfactory characteristics (CHR=5). This was mainly due to the difficulty of achieving and maintaining the desired speed, as pilot D also commented.

9.3.1.2 Task 2 – Engine failure during takeoff

The pilots found it very easy to maintain heading parallel to the centreline whilst on the ground after engine failure. So much so that, if it had not been for the sound of the engine running down the pilots did not, at first, notice the engine failure. Thus, the flying and handling characteristics where rated satisfactory (CHR=3) as well as the workload (BWR=3).

Once in the air the situation was different. Pilot D reported satisfactory characteristics on holding the heading, CHR=3, but only acceptable on maintaining wings level, CHR=4. Pilot C rated no satisfactory qualities (CHR=5 and BWR=6) on holding both the heading and bank angle. This rating degradation was mainly due to the presence of the dutch roll.

In general there was an increase in the workload and CHR as a result of the engine failure, especially in the air. However, this increase was not as much as initially expected. An example of this is the fact that pilot B, who was less familiar with the aircraft and test flying and even improved his ratings from a CHR = 5 to CHR = 4 comparatively to the easiest task of takeoff. Due to the hazardous character of the task the workload increased, as might be expected, or was kept at the same high value as before, which was not expected. Pilot B commented furthermore, that it felt easier to fly with just two engines than with the usual three engines.

9.3.1.3 Task 3 – Normal approach and landing

The approach down to 200ft was rated acceptable but not satisfactory, CHR=4, by both pilot C and D. This was mainly due to the lateral activity, which was distracting. This lateral activity also required more work from the pilots, and thus a slightly higher rating than would be expected was given, BWR=4.5.

The actual landing task, flare and touchdown, was rated with the same unsatisfactory CHR. This was due not only to the same lateral activity, but also to the extra work of putting the aircraft on the PAPIs glide slope indication once visual, since this was not coincident with the actual ILS glide slope indication. Furthermore, the flare required is smaller than usual, and as mentioned in paragraph D.1.3.4 of Appendix D the ground model also feels unnatural. All these influences gave extra work to the pilots. Even so, the average Cooper-Harper was rated acceptable but not satisfactory, CHR=4, while the average workload was increased, BWR=5.

Considering the overall task qualitatively, pilot A found the flying and handling qualities satisfactory, while pilot B felt that some improvement was necessary, mainly due to the speed variations and to the high landing speed as he reported. Pilot C and pilot D also require more improvement to the flying and handling qualities, although for different reasons to those stated above. Pilot A and pilot B actually rated the workload as being low in contrast to pilots C and D.

9.3.1.4 Task 4 – Crosswind approach and landing

This was a difficult task mainly due to the ground model that caused an unnatural feel once the aircraft touched down. Only pilot A and pilot B evaluated this task. In general, pilot A preferred the "wing-down/crab" technique although he felt that it was not possible to completely set up the aircraft in the "pre-flare" attitude for a good landing. Pilot B understood that the poor ground model made it difficult to assess the controllability of the aircraft in flare, and reported good roll authority for correction in "flare", previous to the touchdown. Pilot B also preferred the "wing down/crab" technique to the "kick-off-drift" technique.

9.3.1.5 Task 5 – Engine failure during approach and landing

The pilots found no problems to maintain the aircraft heading and wings level after an engine failure. Again, pilot C and pilot D commented on the fact that the engine failure is not obvious. The aircraft does not yaw, as would be expected once an

outside engine is failed. Actually, the only clue to the engine failure was a decrease in the aircraft speed. However, the high ratings, CHR=5 and BWR=6, from pilot C was due to the lack of excess thrust for reliable flight path control as reported. This was seen when pilot C tried to do a touchdown and go-around and he realised there was not enough thrust to establish a minimum climb gradient for obstacle clearance.

For the remaining part of the task, flare and touchdown, pilot D rated it equal to Task 3, since the flying qualities are nominally the same. However, due to the drop of speed and the lack of excess power to control the flight path, pilot C felt the task more difficult, consequently rating it worse.

Looking at the task as a whole, and just from a qualitative point of view, the remaining two pilots, pilot A and pilot B, rated the aircraft satisfactory, CHR = 3 with a low workload, BWR = 2. This contrasts with the ratings of pilot C and pilot D as reported above. However, pilot A reported that the task may be difficult "in the last 100 ft when a slight deviation from the centreline is difficult to correct without making the situation worse", as was already felt for the normal approach. Pilot A also comments that a lot more thrust is required, since the aircraft lands with engines almost in full power. However, pilot A considered that the aircraft remained easily controllable.

9.3.1.6 Task 6 – Approach and landing with longitudinal offset correction

In regaining the 2white/2red (2w/2r) PAPI lights at 600ft RA and 180kts speed, pilot D achieved the task without difficulty giving a satisfactory rating, CHR=3. On the other hand, pilot C reported on a small flight path PIO trend after the longitudinal offset correction. This obviously degraded his Cooper-Harper rating, CHR=5, but with a still moderate workload, BWR=4. The remaining part of the task, flare and touchdown, was similar to the normal landing of Task 3. Thus, the ratings were the same except for pilot D, who considered a decrease in workload as a result of the knowledge and skills accumulated during the trial flights.

For the more qualitative evaluations of pilots A and B, the task was considered possible leading to a satisfactory rating, CHR$\leq$3, with comments "easy to correct" and "no over control or PIO". This, again, contrasts significantly with the ratings of pilot C.

9.3.1.7 Task 7 – Approach and landing with lateral offset correction

The lateral offset correction at 600ft RA, regaining centreline by 200ft height, appeared to be possible for pilot C with an almost satisfactory rating, CHR=4, and moderate workload, BWR=4. However, pilot D felt it was difficult to correct the offset within 200ft height. Actually, he was not able to correct and land at all for the first two attempts. Pilot D reported a "reduced lateral/directional controllability" as the reason for it. On the third attempt pilot D was able to land. He rated the aircraft as acceptable, CHR=6, since he never lost control of the aircraft, being always able to perform go-arounds. On the other hand the workload was rated high, BWR=7.

For the remaining task, flare and touchdown, due to the difficulty in correcting the lateral offset, the ratings for this trial were also degraded. However, as pilot C was successful with the lateral offset correction, the flare and touchdown did not feel more difficult and so the rates were the same as for Task 3.

Pilots A and B also reported on the general task of correcting the lateral offset and landing the aircraft. Pilot A reported there was enough room to manoeuvre to control flight path to achieve the desired touchdown point. Thus, he gave acceptable Cooper-Harper and moderate workload rates, CHR=4 and BWR=4. On the other hand, although pilot A felt his correction worked, he reported there was still a small residual heading error difficult to correct in the last 100ft. Due to this difficulty the Cooper Harper rate was increase by one unity, CHR=5.

9.3.1.8 Other results

All pre-planned simulation trials were performed using the central wheel in the cockpit. However, the simulator also has a side stick which was used for some experiments. Therefore, pilot B and pilot D experimented using the side stick. Pilot B flew with side stick at his own request for a general fly-around circuit (take-off, downwind, base leg, final and land) reporting that flying while using the side stick felt much better. Pilot D, however, flew and re-evaluated Task 7 using the side stick. Pilot D, on his first attempt with the side stick, and after three hard landings using the normal centre wheel, reported that the side stick control felt more precise and he was more successful in acquiring the centreline. Thus, the ratings were immediately improved to a CHR=4 and a lower workload, BWR=5 for the approach, and BWR=3 in final landing.

Actually, the height decision when breaking out through clouds is 200ft, i.e., the minimum height at which the runway must be visible for the pilot to decide whether to land or not is 200ft. Thus, pilot A tried to accomplish Task 7 correcting the lateral offset only after 200ft RA was passed. The pilot was still able to land the aircraft although the task seemed more difficult. The pilot commented further "the easiest strategy is to fly straight at threshold and kick-off a little drift at the last few feet, well into flare".

Pilot B, not used to such a high landing speed, would allow the aircraft to drop speed easily. Sometimes the speed would decrease below the limits, which activated the speed protection. Then, the flight control system would change the longitudinal control law from the pitch rate command to a conventional rate command, causing the aircraft to automatically decrease angle of attack to regain speed. The pilot considered this aircraft behaviour strange and dangerous. The reason for this is that at low speed a great deal of lateral-directional control is lost.

9.3.2 Discussion of results

9.3.2.1 Summary of trial results

CHR		Pilots		Aver	Dev
		C	D		
Task 1	1.1	3	3	3	0
	1.2	3	3	3	0
	1.3	3	4	3.5	0.5
Task 2	2.1	3	3	3	0
	2.2	5	4	4.5	0.5
Task 3	3.1	4	4	4	0
	3.2	4	4	4	0
Task 4	-	-	-	-	-
Task 5	5.1	5	3	4	1
	5.2	4	4	4	0
Task 6	6.1	5	3	4	1
	6.2	4	4	4	0
Task 7	7.1	4	6	5	1
	7.2	4	6	5	1

Table 9.5 Pilot C and D Cooper-Harper ratings

BWR		Pilots		Aver	Dev
		C	D		
Task 1	1.1	3	3	3	0
	1.2	4	3	3.5	0.5
	1.3	3	4	3.5	0.5
Task 2	2.1	5	3	4	1
	2.2	6	4	5	1
Task 3	3.1	4	5	4.5	0.5
	3.2	4	6	5	1
Task 4		-	-	-	-
Task 5	5.1	6	3	4.5	1.5
	5.2	4	5	4.5	0.5
Task 6	6.1	4	3	3.5	0.5
	6.2	4	3	3.5	0.5
Task 7	7.1	4	7	5.5	1.5
	7.2	5	7	6	1

Table 9.6 Pilot C and D Bedford Workload ratings

The results of the piloted handling trial are gathered in Tables 9.5 to 9.8. Tables 9.5 and 9.6 show the result for Pilot C and pilot D while Tables 9.7 and 9.8 show the

result for all pilots. The rating of the complete task presented in Tables 9.7 and 9.8 for pilot C and pilot D are calculated as the maximum subtask rating of each pilot. The average and mean deviation for each task, or subtask, was calculated and is also presented in the Tables, however, this is better seen in Figures 9.1 and 9.2 for pilot C and pilot D, and in Figures 9.3 and 9.4 for all pilots.

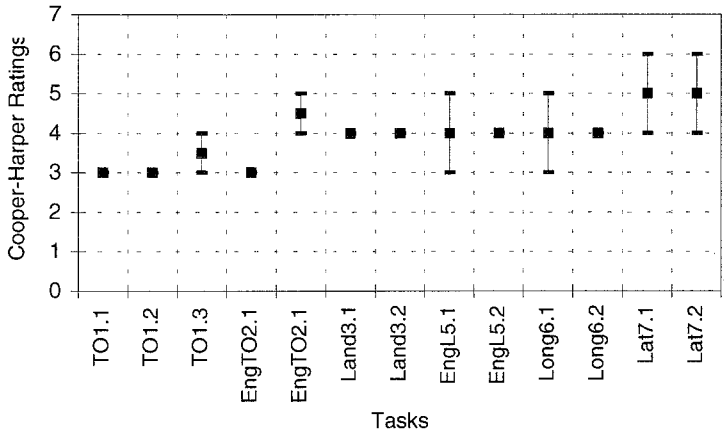

Figure 9.1 Cooper-Harper ratings for pilot C and D

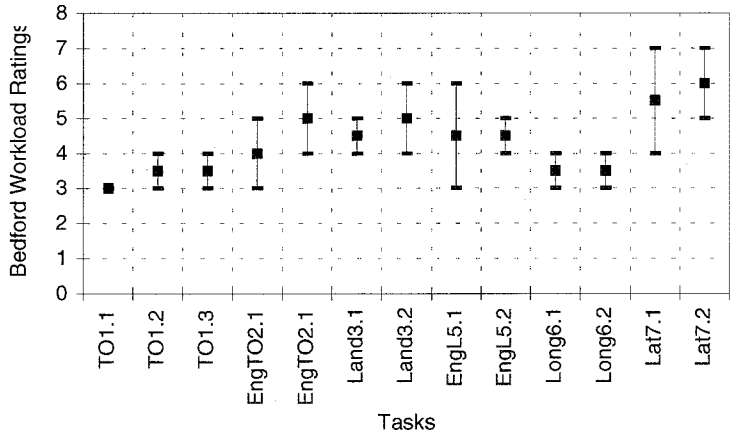

Figure 9.2 Bedford workload ratings for pilots C and D

CHR	Pilots				Aver	Dev
	A	B	C	D		
Task 1	2	5	3	4	3.5	1
Task 2	-	4	5	4	4.33	0.44
Task 3	3	4	4	4	3.75	0.375
Task 4	5	3	-	-	4	1
Task 5	3	3	5	4	3.75	0.75
Task 6	2	3	5	4	3.5	1
Task 7	5	4	4	6	4.75	0.75

Table 9.7 Cooper-Harper rates for all pilots

BWR	Pilots				Aver	Dev
	A	B	C	D		
Task 1	2	5	4	4	3.75	0.875
Task 2	-	5	6	4	5	0.67
Task 3	2	2	4	6	3.5	1.5
Task 4	4	2	-	-	3	1
Task 5	2	2	6	5	3.75	1.75
Task 6	2	2	4	3	2.75	0.75
Task 7	4	4	5	7	5	1

Table 9.8 Bedford Workload ratings of all pilots

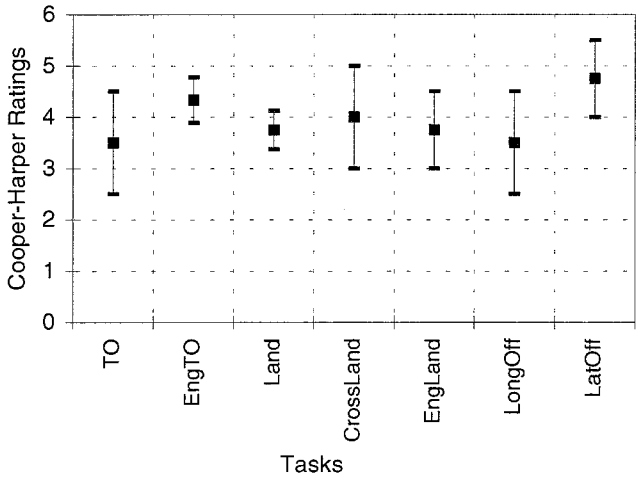

Figure 9.3 Cooper-Harper ratings for all pilots

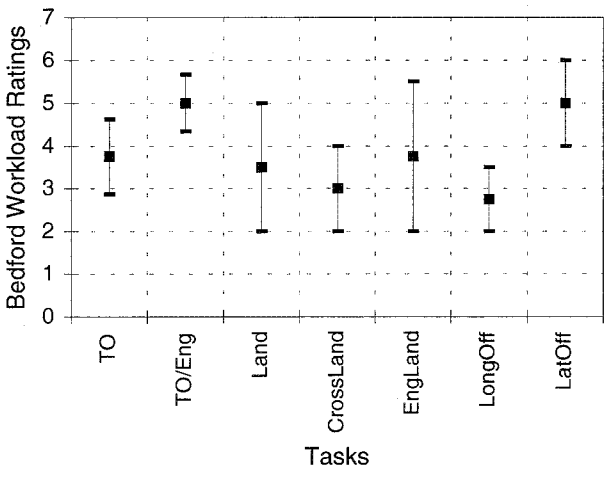

Figure 9.4 Bedford Workload ratings for all pilots

9.3.2.2 Task 1 – Normal takeoff

The reason for the poor ratings seems to be the speed fluctuation with throttle input, and its influence on altitude and pitch attitude. As pilot D commented, the throttles felt hard to move for fine adjustment to EPR, actually EPR ±0.02. Thus making it difficult to acquire the exact thrust necessary to maintain a required speed. If this required power is changed for some reason, not only the speed changes, but also the pitch attitude and altitude. However, this is a characteristic of the flight control system used, pitch rate command system. To improve this situation, an auto-throttle may be required to better control the speed. Nevertheless, this feature is only necessary in situations where speed should be exactly constant, such as cruise. However, autopilots are usually implemented for these situations.

9.3.2.3 Task 2 – Engine failure during takeoff

In general, the aircraft flying and handling qualities were rated acceptable, but not satisfactory, CHR=4.33 or Level 2. The workload was considered as increased with a reduced spare capacity, BWR=5. Since an engine failure during takeoff is an emergency case, these rates would be acceptable, however some comments follow.

The lack of relevant yaw response once the engine failed was one of the first facts noticed by the pilots. The explanation for this may be the higher moment of inertia comparatively to the moment generated by the failed engine, and thus, lower yaw acceleration. Furthermore, on the ground the explanation may be the simple ground model used, as described in Appendix D. Once in the air the reason for lack of yaw response may be due to the directional flight control system, which minimises the sideslip, thus keeping the pilot workload low.

Although it seems that the lack of yawing moment is good, the lack of clear and fast natural cues that an engine has failed can also be hazardous. The pilot may only become aware of the engine failure through a decrease in speed. This speed decrease, if noticed too late, may impair the controllability of the aircraft. The lack of adequate lateral-directional control was noticed in several flight simulations as soon as the speed was allowed to go below 160kts.

Finally, pilot B declared that it was easier to fly with two engines than with three, the reason was again, the speed control. With two engines there is less excess power and less acceleration, and thus smaller speed changes. With three engines, more power is available and less throttle movement is needed for fine tuning, which is not possible with the present simulator throttle lever installation.

9.3.2.4 Task 3 – Normal approach and landing

The normal approach, flare and touchdown, got an average CHR of 3.75 and a workload rate of 3.5, revealing acceptable but not satisfactory, or Level 2, flying and handling qualities. The reasons given for these ratings, are the light lateral activity, the unnatural flare and the difference between the PAPIs and the ILS glide slope indication.

The difference between the PAPIs and the ILS glide slope indication by itself does not constitute a problem. It may feel strange to the pilot that, although closely following the ILS indication, he found the aircraft not in the right place with respect to the

PAPIs. However, this only requires some understanding and mechanization to correct for this difference.

The unnatural flare is due to the pitch rate command attitude hold flight control system. When approaching the runway the pilot pulls the stick back to rotate and achieve a soft touchdown. However, if the stick is kept back, due to the nature of the control system the pitch attitude will keep on increasing, as well as the angle of attack. In this situation, the pilot is forced to push the stick forward, which feels unnatural compared with what he is used to in a more conventional aircraft. This is the reason why the Airbus A320 and the Boeing B777 have different control laws implemented for the flare and touchdown, as explained in Chapter 1. In Chapter 2 it was also stated that the pitch rate command attitude hold characteristic might be a good flight control system for tracking, but has unconventional flare characteristics. Moreover, since blended-wing-body configurations have a large span and wing area, once in ground effect there is an effective increase in lift. This also requires less stick pull back than usual. Furthermore, the high landing speed and flying on the "back side of the drag curve", with a higher power setting, may also help to this effect. This different control technique during the flare requires a learning process from the pilot, after which the ratings may improve, as actually happened.

Finally, the last and perhaps most important problem of this configuration is the lateral activity reported by the pilots during the approach. In the literature review of Chapter 1, it was seen that if small or no vertical tails are present, it is difficult to accurately fly such aircraft in the lateral-directional sense. As was seen in the stability analysis of this research, the blended-wing-body configurations used have a low directional static stability and rather lightly damped, or even unstable dutch roll mode. Moreover, as seen in Chapter 7, even after the introduction of a directional flight control system, there were still some problems of light dutch roll, roll rate oscillations, sideslip angle generation and adverse yaw rate response to aileron input.

9.3.2.5 Task 4 – Crosswind approach and landing

Due to the low rudder power control, the crosswind approach and landing task was intended to evaluate whether the aircraft possesses enough lateral-directional control power. However, due to several factors presented above in paragraph 9.2.1.2, this task was only flown and evaluated by two pilots before being abandoned. Some comments can be made about it.

One of the crosswind simulation problems was the lack of a crosswind in the ground model. Thus, the crosswind exists while the aircraft is airborne, but not once the wheels touch the ground. This has the effect that, as soon as the wheels touch the ground all the compensation for the crosswind is suddenly the *"Tracking Make Good"* of the aircraft. So, the pilots were asked to evaluate the tasks only until immediately before touchdown. However, it is on the flare just before the touchdown that the pilot corrects for the crosswind. It is then during the touchdown that the pilot actually evaluate the complete task. Although difficult, pilots tried to evaluate the aircraft flying and handling qualities under this condition.

Actually, one pilot noticed a problem which made the validity of the crosswind task simulation questionable. Some pilots complained that even with the aircraft in the air it seemed there was no crosswind. As the effect was more apparent when near to the ground, it seemed to be related to the wind model once more. However, it was not due to the proximity of the ground, but to the existence of better visual references that the apparent lack of crosswind was noticed. This pilot feeling of inexistence of crosswind when it is actually there is thought to be related to the blended-wing-body configuration, actually the inexistent of vertical surfaces, and so of lateral forces. This characteristic was already mentioned in Chapter 1. Northrop[6] comments that the Northrop XB-35 large bomber was not influenced by lateral winds, even presenting the characteristic as an advantage especially in turbulence during long flights. To cross check this theory, one pilot flew the original B747 model, but the same problem seemed to exist. Thus, it was concluded that these problems may be related to the visual system refresh rate.

Nevertheless, two qualitative flight evaluations were completed, as pilot A and pilot B seemed not to be aware of the lack of crosswind. This task was also flown during the development of the flight control systems. In the early stage of development the lack of lateral power control seemed to be the problem. However, once the directional flight control system was implemented it was possible to land, even with satisfactory flying qualities, according to pilot A. Furthermore, as shown in Chapter 4, pilots reported that for the last final correction almost all available directional control was being used which is undesirable.

9.3.2.6 Task 5 – Engine failure during approach and landing

As presented in the results of this task, the lack of yawing moment, which turns the aircraft into the direction of the failed engine, or other noticeable cues, is the main problem. As commented for Task 2, paragraph 9.3.2.3, this lack of yawing moment

may be a coupling of low directional acceleration due to large inertia, with the automatic compensation from the lateral-directional flight control system.

On one hand, this seems to remove a great deal of workload from the pilot giving rise to low or moderate workload ratings, and acceptable in the limit of satisfactory (CHR=3.75) flying qualities. On the other hand, the unawareness of the pilot that an engine has failed can actually be a more serious problem. If the pilot is busy with other tasks and he does not notice the engine failure, the speed will begin to decay due to the action of the pitch rate command/attitude hold system. Furthermore, if the speed decreases below the minimum control speed (160kts) lateral-directional control may be impaired. Moreover, as shown by pilot C a decision to abort the land and go-around at a late stage, may not be possible due to lack of thrust. Therefore, a possible solution is the inclusion of an engine failure warning and protection system to augment the pilot's awareness, and to increase the overall engine thrust delivery. Of course, this last point has other implications, if the directional control power is not good for the actual thrust power delivered, it will be degraded if the thrust is increased following loss of an engine.

9.3.2.6 Task 6 – Approach and landing with longitudinal offset correction

All except pilot C reported satisfactory qualities, CHR less than 3, on the completion of this task. Pilots commented the task to be "straightforward" and "easy" to correct for the longitudinal offset. Pilot D emphasized the usefulness of the trend vector in the speed window to keep speed on the desirable value and pilot B reported enough longitudinal control left for manoeuvre. However, the fact that pilot C has encountered a PIO may indicate problems that, although hidden, do exist. PIO problems tend to appear mainly in times of higher stress or workload, such as in the presence of turbulence, making control even more dangerous.

9.3.2.7 Task 7 – Approach and landing with lateral offset correction

This seemed to be the task that all pilots had more problems with, resulting in high workload ratings, and where the flying and handling qualities were worse leading to the highest CHR. Nevertheless, except for pilot D, all were able to perform the task after one or two attempts. From the comments of pilot D who also did the experiment using the side stick, it seems that the lack of control sensitivity and ability for precision lateral flight was the main problem in this task. Moreover, knowledge of the aircraft lateral-directional behaviour might also be important, since pilot C

accomplished the task faster and better – he was the one with more hours flying the simulator.

9.4 Conclusions

Limited piloted handling trials were performed to assess the flying and handling qualities of an augmented blended-wing-body configuration. Limited piloted handling trials since the fixed simulator enables also to simulate only limited reality, as it simulates no motion cues. The proper limitations of the aircraft model (low speed and linear flow) limits further the reality possible to be simulated. Nevertheless, within all these assumptions the results obtained are considered valid and possible to correlate with the analytical flying and handling qualities assessment.

The piloted handling trials reveal that the selected blended-wing-body configuration has essentially Level 1 or Level 2 flying and handling qualities, depending on the task. The main contributions for the Level 2 incursions were identified as residual lateral-directional activity, unconventional flare, ground to flight model discontinuity, flight path PIO, and insufficient flight path control when one engine has failed.

At first it seemed that these results contrasted with the analytical longitudinal flying and handling qualities assessment in Chapter 7 where Level 1 characteristics were anticipated. However, the takeoff task, which includes almost only longitudinal activity was rated Level 1. Besides, it should not be forgotten that before applying the criteria, some assumptions were made. One of these concerned the adequacy of the control law for the task at hand, and for the flare it was seen that the present flight control system does not give the best control characteristics. Thus, it was not surprising that pilots rated the flare worse. Moreover, the touchdown problem that further degrades the pilot perception of the aircraft flying and handling qualities is related to the physical models used. This is actually the discontinuity between the ground model and the flying model. That the longitudinal flying and handling qualities are actually Level 1 can be seen in Figures 9.1 and 9.3 from the improving results of the longitudinal offset correction, Task 6, comparatively to the previous landing tasks.

In conclusion, if the flare control law were modified, or if the pilots could learn and accept new control characteristics, and if the ground model were improved, the ratings for the same blended-wing-body configuration in the approach and landing would improve. Only the presence of the flight path PIO completely opposes the Level 1

ratings from the requirements assessment. However, no PIO criteria were applied to try and predict it. Actually, in Chapter 7 attention is drawn to amplitude and rate saturation. Although no analytical studies were done on this subject, the control amplitude and rate of deflection were limited during the simulation, probably inducing the PIO.

Relative to the lateral-directional flying-qualities, the piloted handling trials confirmed the flying and handling qualities criteria assessment of Chapter 8 Level 1 to Level 2 flying qualities were anticipated. One of the problems related to the blended-wing-body aerodynamic characteristics, namely that degraded flying and handling qualities seems to be due to the residual lateral activity, once the lateral modes are upset by pilot inputs or external disturbances (crosswind, engine failure). This seems more pronounced at low speeds, probably due to the low dutch roll damping, shown in paragraph 8.4.1.1, as result of the low washout filter time constant used. Besides of this residual lateral activity, at low speeds the already weak lateral-directional controls become ineffective making it difficult to control the aircraft. Actually, the main limiter on choosing the blended-wing-body landing speed was not the stall speed, as it would usually be for a conventional aircraft, but was the minimum control speed, which is somewhat large around 160kts. Besides, at speeds near, or lower than, the landing speed the aircraft is flying on the back side of the drag curve due to the aircraft low drag. Thus, a decrease in speed increases the drag, which then decreases the speed further. By deploying the landing gear the aircraft drag is increased improving these qualities, but this is still not enough.

In the case of an engine failure during approach and landing, the high minimum control speed together with flying on the back side of the drag curve gives rise to a dangerous situation. The landing is actually made with the remaining engines almost at maximum thrust, which is very uncomfortable for passengers, due to noise reasons. This means that no additional thrust is available to fulfil the requirements of touchdown/go-around during an engine-failed landing. Attention is drawn to the fact that to be able to perform the engine failure task, the engine yawing moment was decreased by a factor of three due to the limited rudder control power. Thus, requirements on the rudder control power, which already needs to be increased by a factor of three, become heavier if engine thrust needs to be further increased. Also, during an engine failure, a visual and, or audible warning should exist to alert the pilot to the situation. On the other hand, the directional flight control system implemented reduces the effects of the critical engine failure, hence reducing the pilot workload.

From these conclusions it is clear that the lateral-directional control system designed needs improvement, although this also depends on the increase of aerodynamic lateral-directional control power. However, the fact that lateral offsets could not be corrected due to the centre wheel imprecision, but improved when using the side stick, may indicate problems of control sensitivity. In the same way as for the longitudinal motion, no control sensitivity was included in the requirements assessment. Thus, if the lateral-directional control sensitivity is not right, it may be the source of the Level 2 flying and handling qualities, and not only the augmented aircraft itself.

CHAPTER 10
Thesis Conclusions and Future Work

"The courage to go deeper is found by letting your desire grow larger than your fear."

Anon.

"It is a rough road that leads to the heights of greatness"

Seneca

10.1 Thesis conclusions

When investigating the next generation of commercial transport aircraft, specifically the blended-wing-body concept, a step between tailless and full flying wing, was revived. This configuration has attracted attention worldwide and Cranfield University has accepted the challenge of this configuration as well, being the subject of research under areas such as design, structures, aerodynamics and flight dynamics. The flight dynamics, flight controls and flying and handling qualities of a large transport fly-by-wire blended-wing-body aircraft were the subject of this research.

Low speed data from four different blended-wing-body configurations were gathered and a general representative model was created for flight simulation. The first step of this research was to understand the basic longitudinal and lateral-directional static stability characteristics of the BWB, whose conclusions are as follow.

- The right balance of static stability has to be found. Deviation from the optimum results in the penalty of a huge requirement for control power, or else the possibility of controlled flight becomes questionable.

- Due to the limited control power available, positive static margin might be limited to lower values than those used in conventional aircraft. Static margin may be limited further if manoeuvrability requirements are also taken into account.

- Unstable configurations, on the other hand, seem to offer a more favourable configuration for tailless aircraft.

This is so since they require lower elevator angles to trim and much lower angles of attack to trim. Also the required elevator angle per 'g' is lower, but the most significant reduction is on the angle of attack per 'g'. However, other considerations such as control power to assure stability augmentation over the full flight envelope must be taken into account when considering unstable configurations.

- Increase of control power is needed either by increasing the control surfaces area, using more powerful actuators, or by limiting the static margin to smaller values around the neutral point.

- Low levels of directional static stability were found on blended-wing-body aircrafts due to lack of vertical surfaces and aft *cg* positions. The levels of lateral static stability are the same as for conventional aircraft.

- To trim in a crosswind, low levels of directional and lateral stability need lower aileron and rudder deflections. Whilst, high levels of control power (equal to that of the BWB2 configuration) are desirable to trim out an engine failure.

- Due to the limited control power extra care is needed on designing the lateral-directional control surfaces to eliminate the adverse yaw and roll induced by the aileron and rudder deflection.

A basic understanding of the blended-wing-body flight dynamics through the use of the implementation of the equations of motion and the assessment of its flying and handling qualities was also done. The main results are as follows;

- Blended-wing-body configurations do not have radically different dynamic stability properties compared with conventional aircraft.

A conventional transport aircraft is considered to have reasonable large positive static margin to give a well stable aircraft. However, if this is changed to small or even

negative static margin the conventional aircraft also suffers from dynamic instability in the same way as the blended-wing-body aircraft. This means, that for rather stable BWB configurations the same stable short period and phugoid modes are present, and that for small or negative static margins short period and phugoid instability exist as a consequence of the small or negative static margin, in the same way as would happen in a conventional aircraft.

- In the same way as for the longitudinal motion, the difference between the BWB and conventional aircraft from the point of view of lateral-directional dynamics is the low directional stability.

- This leads to dynamic instability (the dutch roll mode is of rather low damping and frequency, or even unstable, although the stable roll and spiral modes similar to those of conventional aircraft) and high angles of sideslip that are undesirable.

- Adverse yaw response to aileron inputs exists for some of the present BWB configurations. However, this is due not only to the usual adverse yaw effect of aileron control surfaces but mainly to the cross-coupling derivatives, C_{l_r} and C_{n_p}.

These characteristics result in poor flying and handling qualities either for the longitudinal or lateral-directional motion, making it necessary to use stability augmentation. During the design of longitudinal, as well as lateral-directional, stability augmentation systems the following conclusions were reached.

- High gains are necessary to compensate for the low control power. This was found more critical for the lateral-directional motion. As a result, levels of allowed instability need to be decreased, or in other words, inherent stability needs to be increased.

- A pitch rate command/attitude hold system was the flight control system designed for the longitudinal motion. This kind of flight control system is particularly interesting for tracking tasks such as the approach and landing, although possessing some undesirable characteristics during flare.

- Longitudinal flight control system design poses few problems, mainly due to the high level of past research in this area. The same is not so for the lateral-directional flight control system design.

- The lateral-directional requirements used, actually MIL-F-8785C[46], are difficult to apply to BWB flight control system design and alternative requirements are not available.

- During the lateral-directional flight control system design it was found that due to the directional instability the directional axis must be augmented before the lateral axis.

- Although improvement was seen, the lateral-directional flying and handling qualities were still not satisfactory.

This was due mainly to the rather limited directional control power not being enough to completely improve the flying qualities. A roll rate command system together with the previous directional control system was evaluated. Although the rolling performance improved further, the sideslip angle generated became too large, being of dislike to the pilots.

- A review of the present civil and military flying and handling qualities requirements for large aircraft revealed that the civil requirements are of rather relaxed nature since they do not address flying and handling qualities explicitly.

- To allow for the low control power the longitudinal GCAP design requirement needed to be modified. Furthermore, there is still little information to assist in choosing the most adequate response-types for the civil transport role.

Limited piloted simulation trials were used to assess the blended-wing-body aircraft flying and handling qualities from the pilot's point of view. The results obtained from this ground fixed simulator were correlated with the analytical results using the flying and handling qualities requirements. Taking in account some considerations first, it can be said that these piloted handling trials do validate the requirements and criteria used. Moreover, it was concluded that for longitudinal motion the present requirements are appropriate for use in BWB configurations. For the lateral-directional motion it was found that the lateral-directional requirements need more research, even for application to conventional aircraft.

The piloted simulation trials also brought more understanding to light. Firstly, the importance of the right control sensitivity and adequacy of the response-type used as defended by some authors. This consideration is important independently of the

aircraft configuration or role. Secondly, the piloted trials also highlighted the importance of having a representative and accurate simulation model.

Differences in flying and handling qualities requirements for the blended-wing-body aircraft seems not to exist compared to conventional aircraft, although the differences found in the blended-wing-body and conventional aircraft behaviour. However, the requirements relate to minimum characteristics that still need to be fulfilled so that certain acceptable levels of flying and handling qualities are present. These minimum characteristics may change with the task or aircraft role, but as defended by the new approach to mission oriented requirements, it will not change with aircraft size or type.

10.2 Future work

Some understanding was established in the blended-wing-body configuration, however, more research must follow before a civil transport blended-wing-body aircraft is made reality. From the results of this thesis, the following research guidelines are suggested.

1) The qualitative character of the civil requirements has been addressed in the past, but no changes have been noticed so far. More research in the lateral-directional motion is needed, either in flight control system design requirements, as in advisable response-types for specific mission tasks. The military requirements boundaries for the lateral-directional motion need to be revised to allow for highly augmented aircraft types.

2) The physical limitations presented in this thesis, actually the lower control power available should be addressed. Furthermore, better aerodynamic data, more accurate and complete, should be made available for a more accurate and complete flight dynamic analysis, flight control system design and real-time simulation.

3) The aerodynamic mechanisms that affect the cross-coupling derivatives C_{l_r} and C_{n_p} should be identified and the aircraft re-designed to minimise the adverse yaw to aileron inputs of these derivatives.

4) A different longitudinal flight control system presenting better characteristics at flare while retaining the good tracking characteristics could be designed. The lateral-directional flight control system needs a readjustment of the

washout filter time constant to allow the yaw damper to damp out the dutch roll oscillations. In the future, both longitudinal and lateral-directional control sensivities need to be checked before assessing flying and handling qualities.

5) Another form of control augmentation presented by Cameron and Prince[27] as *control allocation*, may provide a different way to solve the problem of limited control. Paul and Garrard[25] have applied different lateral-directional control laws (and FCS structures) to a tailless aircraft claiming to have achieved good flying and handling qualities.

6) So far only the rigid aircraft has been taking into account. However, an aircraft of this size will have aeroelastic issues which should be taken in account. Thus, a next step could be the implementation of an aeroelastic model, application of the present flight control systems designed and assessment of the augmented aeroelastic model flying and handling qualities.

7) More complete piloted handling trials should be made, using perhaps other mission tasks which, although not representative of civil transport aircraft task are more adequate for flying and handling qualities evaluations purposes. Actually, the inclusion of turbulence and representative crosswind takeoff and landing tasks should be realized. Moving base and, or in-flight simulators should also be used to evaluate the accelerations at the pilot's station.

8) The aircraft response to a gust was not studied, however there is some literature indicating this aspect may present handling qualities problems in tailless types. Therefore, more research in this field is necessary.

REFERENCES

1. Morris, A., "*Distributed MDO: the way of the future*", Proceedings of the CEAS Conference on Multidisciplinary Aircraft Design and Optimization, Koln, Germany, pp 3-18, June 2001.
2. Chudoba, B., "*Development of a generic stability and control methodology for the conceptual design of conventional and unconventional aircraft configurations*", PhD thesis, College of Aeronautics, Cranfield University, 2001.
3. Lippisch, Alexander, "*The delta wing – history and development*", Iowa state University Press, AMES, 1981.
4. Wood, R. M. and Bauer, S. X. S., "*Flying Wings / Flying Fuselages*", AIAA 2001-0311, 39th AIAA Aerospace Sciences Meeting & Exhibit, Reno, 8-11 January 2001.
5. Castro, H. V. de, "*History of tailless aircraft*". To be published as a College of Aeronautics report.
6. Northrop, John K., "*The development of all-wing aircraft*", 35th Wilbur Wright Memorial Lecture, The Royal Aeronautical Society Journal, Vol. 51, pp.481-510, 1947.
7. Jones, Robert T., "*Notes on the stability and control of tailless airplanes*", NACA No.837, December 1941.
8. Mair, W. A., "*Notes on the relative merits of swept back and swept forward wings for tailless and high speed aircraft*", RAE TN Aero 1810, Royal Aircraft Establishment, July 1946.
9. Sears, W. R., "*Flying Wing airplanes – The XB-35/YB-49 program*", AIAA 80-3036, The evolution of the aircraft wing design, Proceedings of the Symposium, Dayton, Ohio, March 18-19, 1980.
10. Shepperd, J. A. H., "*The estimated effects of various parameters on the increments in lift and pitching moment due to flaps on tailless aircraft*", RAE Report 1861a, Royal Aircraft Establishment, Farnborough, June 1944.
11. Thorpe, A. W., "*Note on the longitudinal stability and trim of tailless aircraft*", RAE TN Aero 1021, Royal Aircraft Establishment, Farnborough, August 1942.
12. Donlan, Charles J., "*An interim report on the stability and control of tailless airplanes*", NACA Report No.796, August 1944.
13. Lee, G. H., "*Tailless aircraft design problems*", The Royal Aeronautical Society Journal, Vol. 51, pp. 109-129, 1947.

14. Trouncer, J. and Wright, D. F., "*Wind tunnel tests on the effect of variable incidence tips and tip slats on tailless gliders*", RAE TN Aero 1496, Royal Aircraft Establishment, Farnborough, August 1944.
15. Seacord, C. L. and Ankenbruck, H.O., "*Effect of wing modifications on the longitudinal stability of a tailless all-wing airplane model*", NACA ACR L5G23, 1945
16. Hills, R. and Kucheman, D., "*A note on cranked sweptback wings*", RAE TN Aero 1911, Royal Aircraft Establishment, Farnborough, July 1947.
17. Bolsunovsky, A. L., Buzoverya, N. P., Gurevich, B. I., Denisov, V. E., Dunaevsky, A. I., Shkadov, L. M., Sonin, O. V., Udzhuhu, A. J. and Zhurihin, J. P., "*Flying wing – problems and decisions*", Aircraft Design 4 (2001) 193-219, Pergamon, 2001.
18. Donlan, C. J., "*Current status of longitudinal stability*", NACA RM L8A28, 1948.
19. Wilkinson, K.G., Shepperd, J.A.H. and Lyon, H. M., "*The longitudinal response of tailless aircraft*", RAE Report Aero 2060, Royal Aircraft Establishment, Farnborough, July 1945.
20. Kronfeld, R., "*Test-flying a tailless glider*", The Aeroplane Journal, pp. 367-369, April 11, 1947.
21. Fremaux, C. M., Vairo, D. M. and Whipple, R. D., "*Effect of geometry, static stability, and mass distribution on the tumbling characteristics of generic flying-wing models*", AIAA-93-3615, AIAA Atmospheric Flight Mechanics Conference, August 9-11, Monterey, California, 1993.
22. Begin, Lee, "*The Northrop flying wing prototypes*", AIAA-83-1047, AIAA Aircraft Prototype and Technology Symposium, Dayton, Ohio, March 23-24, 1983.
23. Thorpe, A.W. and Curtis, M. F., "*Lateral stability of tailless aircraft*", RAE Report No. Aero 1826 or Reports and Memoranda No. 2074, Royal Aircraft Establishment, 1943.
24. Shepperd, J.A.H., "*Effect of reducing the size of fin and rudder upon the lateral response of the General Aircraft tailless glider*", RAE TN Aero 1695, Royal Aircraft Establishment, Farnborough, October 1945.
25. Paul, R. and Garrard, W. L., "*Dynamics and control of tailless aircraft*", AIAA-97-3776, AIAA Atmospheric Flight Mechanics Conference, August 11-13, New Orleans, Louisiana, 1997.
26. Esteban, S., *"Static and dynamic analysis of an unconventional plane: flying wing"*, AIAA-2001-4010, AIAA Atmospheric Flight Mechanics Conference and Exhibit, Montreal, Canada, 6-9 August, 2001.

27. Cameron, D. and Princen, N., "*Control allocation challenges and requirements for the blended wing body*", AIAA-2000-4539, AIAA Guidance, Navigation and Control Conference and Exhibit, Denver, CO, 14-17 August 2000.
28. Neumark, S., Lyon, H. M. and Thorpe, A. W., "*British tailless and tailfirst projects*", RAE Technical Note No. Aero 1043, Royal Aeronautical Establishment, October 1942.
29. Neumark, S., "*Analysis of the longitudinal stability of tailless and tailfirst aircraft*", RAE Report Aero 1859, Royal Aircraft Establishment, Farnborough, December, 1944.
30. King, H. F. and Taylor, J. W. R, "*Milestones of the air: Jane's 100 significant aircraft, 1909-1969* ", New York: McGraw-Hill, 1969.
31. Tuck, D. A., "*Research and development of supersonic transport aircraft standards and the application to the Concorde U.S. certification*", Cockpit - the Society of Experimental Test Pilots Technical Publications, pp 5-20, January, February, March 2001.
32. Couch, R. S. and Hinds, B. J., "*B-2, advanced technology bomber, testing*", 1989 Report to the Aerospace Profession - 33rd Symposium Proceedings, The Beverly Hilton, Beverly Hills, California, pp 344-354, September 1989.
33. Birk, F. T. and Staley, C. W., "*B-2 flight test update*", 1992 Report to the Aerospace Profession – 36th Symposium Proceedings, The Beverly Hilton, Beverly Hills, California, pp 174-187, September 1992.
34. Weiss, D. L. and Dunn, J. C., "*B-2A flight test progress report*", 1995 Report to the Aerospace Profession – 39th Symposium Proceedings, The Beverly Hilton, Beverly Hills, California, pp 17-33, September 1995.
35. Crenshaw, K. and Cameron, S. E., "*B-2 safety lessons learned*", 1995 Report to the Aerospace Profession – 39th Symposium Proceedings, The Beverly Hilton, Beverly Hills, California, pp 208-223, September 1995.
36. Moss, C., "*B-2A residual pitch oscillation (RPO) investigation*", 1997 Report to the Aerospace Profession – 41st Symposium Proceedings, The Beverly Hilton, Beverly Hills, California, pp 393-410, September 1997
37. Favre, C., "Fly-by-wire for commercial aircraft: the Airbus experience", Chapter 8 of "Advances in Aircraft Flight Control", edited by Tischler, Mark B., Taylor and Francis, London, 1996.
38. Schmitt, Vernon R., Morris, James W. and Jenney, Gavin D., "*Fly-by-wire – A historical and design perspective*", SAE – Society of Automotive Engineers, Inc, 1998

39. Sankrithi, M. M. K. V. and Bryant, W. F., "*7J7 Manual flight control functions*", AIAA-87-2454, pp 905-913, 1987.
40. Cashman, J. E., "*Boeing 777 – Progress to the plan*", 1995 Report to the Aerospace Profession – 39th Symposium Proceedings, The Beverly Hilton, Beverly Hills, California, pp 4-16, September 1995.
41. Bisgood, P. L., "*A review of recent research on handling qualities, and its application to the handling problems of large aircraft*", ARC RM No 3458, Part I and II, 1967.
42. Pallett, E.H.J. and Coyle, Shawn, "*Automatic flight control*", Blackwell Science Ltd, Fourth edition, 1993.
43. Cook, M. V., "*On the design of command and stability augmentation systems for advanced technology aeroplanes*", Trans Inst MC, Vol. 21 No 2/3, pp 85-98, 1999.
44. Philipps, William H., "*Flying qualities from early airplanes to the Space Shuttle*", AIAA-88-0751, presented at the AIAA 26th Aerospace Sciences Meeting, Reno, Nevada, January 11-14, 1988.
45. Ashkenas, I. L., "*Twenty-five years of handling qualities research*", Journal of Aircraft, Vol. 21, No. 5, pp 289-301, May 1984.
46. Anon, "*Military Specification – Flying Qualities of Piloted Airplanes*", MIL-F-8785C, Department of Defense, USA, 1980.
47. Hoh, R. H., Mitchell, D.G., Ashkenas, I.L., Klein, R.H., Heffley, R.K. and Hodgkinson, J., *"Proposed MIL standard and handbook: flying qualities of air vehicles"*, AFWAL-TR-82-3081, Ohio Wright-Patterson Air Force Base, 1982.
48. Anon, "*Military Standard – Flying Qualities of Piloted Airplanes*", MIL-STD-1797A (USAF), Department of Defense, USA, 1987.
49. Mitchell, David G., Hoh, Roger H., Aponso, Bimal L and Klyde, David H., "*Proposed incorporation of mission-oriented flying qualities into MIL-STD-1797A*", WL-TR-94-3162, October, 1994.
50. Anon., "*Joint Aviation Requirements – JAR 25, Large aeroplanes*", Joint Aviation Authority.
51. Anon., "*Federal Aviation Regulations – Part 25*", Federal Aviation Administration, United States Department of Transportation.
52. Anon., "*Design and Airworthiness Requirements for Service Aircraft*", Defence Standard 00-970/Issue 1, Volume 1, Book 2, Part 6 – Aerodynamics, Flying Qualities and Performance. Ministry of Defence, UK 1983.

53. Fuller, S. G. and Potts, D. W., "*Design criteria for the future of flight controls*", AFWAL-TR-82-3064, Proceedings of Flight Dynamics Laboratory Flying Qualities and Flight Controls Symposium, March 2-5, 1982.
54. Ashkenas, I. L., "*Introduction and overview*", AGARD Lecture Series No.157, May 1988
55. Mooij, H. A., "*Low-speed longitudinal flying qualities of modern transport aircraft*", AGARD Lecture Series No.157, May 1988.
56. Woodcock, R. J., "*A second look at MIL prime flying qualities requirements*", AGARD Lecture Series No.157, May 1988.
57. Hoh, Roger H., "*Advances in flying qualities – Concepts and criteria for a Mission Oriented Flying Qualities Specification*", AGARD Lecture Series No.157, May 1988.
58. Barnes, A.G., "*The role of simulation in flying qualities and flight control system related development*", AGARD Lecture Series No.157, May 1988
59. Cook, M., "*Flying qualities and flight control – Lecture notes*", MSc Course, Module 1 and 2, College of Aeronautics, Cranfield University, January 2000.
60. Gibson, J. C., "*Development of a methodology for excellence in handling qualities design for fly by wire aircraft*", Delft University Press, 1999.
61. Bihrle, Jr., W., "*A Handling qualities theory for precise flight path control*", Technical report AFFDL-TR-65-198, Wright-Patterson Air Force Base, June 1966.
62. Anon., "*Flying qualities Conference*", AFFDL-TR-66-148, Wright-Patterson Air Force Base, 1966.
63. Stein, G. and Henke, A. H., "*A design procedure and handling qualities criteria for lateral-directional flight control system*", AFFDL-TR-70-152, Wright-Patterson Air Force Base, October 1970.
64. Booz, J. E., "*Relative evaluation of MIL-STD 1797 Longitudinal Flying qualities criteria applicable to flared landing and approach*", AIAA 88-4363, AIAA Atmospheric Flight Mechanics Conference, August 15-17, Minneapolis, Minnesota, pp. 314-329, 1988.
65. Rossitto, Ken F., Hodgkinson, John, Williams, Todd M., Leggett, Dave B., Bailey, Randall E. and Ohmit, Eric E., "*Initial results of an in-flight investigation of longitudinal flying qualities for augmented, large transports in approach and landing*", AIAA 93-3816, presented at the AIAA Guidance, Navigation, and Control Conference, August 9-11, Monterey, California, 1993.

66. Field, E J, "*Flying qualities of transport aircraft: precognitive or compensatory?*", PhD thesis, College of Aeronautics, Cranfield University, June 1995.
67. Gautrey, J. E. and Cook, M. V., "*A generic control anticipation parameter for aircraft handling qualities evaluation*", The Aeronautical Journal, Vol. 151, March 1998.
68. Gautrey, James E., "*Flying and flight control system design for fly-by-wire transport aircraft*", PhD thesis, College of Aeronautics, Cranfield University, 1998.
69. Field, E. J. and Rossitto, K. F., "*Approach and landing longitudinal flying qualities for transports based on in-flight results*", AIAA 99-4095, AIAA Atmospheric Flight Mechanics Conference, August 9-11, Portland, Oregon, USA, 1999.
70. Shweyk, K. M., Rossitto, Ken F. and Mitchel, David G., "*Applicability of pitch and flight path bandwidth criteria to transport aircraft with flight-path-rate response system*", AIAA 2000-3990, AIAA Atmospheric Flight Mechanics Conference, August 14-17, Denver, Colorado, USA, 2000.
71. Shweyk, K. M. and Rossitto, K. F., "*Proposed roll control criteria for the design of lateral control stick shapping functions in large transport aircraft*", AIAA-99-4094, AIAA Atmospheric Flight Mechanics Conference, August 9-11, Portland, California, 1999.
72. Monnich, W. and Dalldorff, L., "*A new flying qualities criterion for flying wings*", AIAA-93-3668-CP, AIAA Atmospheric Flight Mechanics Conference, Monterey, August 9-11, pp 448-451, 1993.
73. Gibson, J.C., *"Development of a methodology for excellence in handling qualities design for fly by wire aircraft"*, Delft University Press, 1999.
74. Pratt, Roger W., "*Flight Control Systems*", Volume 184, Progress in Astronautics and Aeronautics, 2000.
75. Hodgkinson, John, "*Aircraft Handling Qualities*", Oxford Blackwell Science Ltd, 1999.
76. Anon., *"Lift curve slope and aerodynamic center position of wings in inviscid subsonic flow"*, Volume 2d, Item 70011, ESDU International Ltd, London, 1970.
77. Anon, "*USAF stability and control DATCOM*", Flight Control Division Air Force Flight Dynamics Laboratory, Wright-Patterson Air Force Base, Ohio, 1960.
78. Benepe, David B., Kouri, Bobby G., Webb, J. Bert and al General Dynamics Fort Worth Division, *"Aerodynamic characteristics of non-straight-taper*

wings", WP AFFDL – TR – 66 – 73, Wright – Patterson Air Force Base, Ohio, October 1966.

79. Torenbeek, Egbert, *"Synthesis of subsonic Airplane design"*, Delft University Press, Kluwer Academic Publishers, 1990.
80. Raymer, Daniel P., *"Aircraft Design: A conceptual approach"*, AIAA, Education series, 1992.
81. Kruger, W., *"Six-component measurements on a cranked swept-back wing (for Ar 234)"*, Volkenrode MAP - VG 66 - 816T, 1947.
82. Lamar, John E., and Alford Jr., William J., "*Aerodynamic center considerations of wings and wing-body combinations*", NASA TN D-3581, Langley Research center, October 1966.
83. Hancock, G. J., *"An introduction to the flight dynamics of rigid aeroplanes"*, Ellis Horwood Limited, 1995.
84. Smith, H., Howe, D. and Fielding, J. P., "*Blended-wing-body high capacity airliner BW-98 Project Specification*", AVD 9800/1, College of Aeronautics, Cranfield University, September 1998.
85. Smith, H., "*Blended wing body airliner advanced technology integration study BW-01 Project Specification*", AVD 0100/1, Aerospace Engineering Group, School of Engineering, Cranfield University, October 2001.
86. Holdcroft, D. P., *"Group design project – Blended Wing Body study: final thesis – project co-ordination, cost control, flight dynamics & wind tunnel data"*, Group Design Project of the Aeronautical Engineering course, College of Aeronautics, 2000.
87. Beet, P.D., *"Blended wing body airliner, initial stability & control estimate, aerodynamic design & detail design of a sub-scale demonstrator vehicle"*, Group Design Project of the Aeronautical Engineering course, College of Aeronautics, 2000.
88. Bennett, P.R., *"The performance analysis and mass control of a subscale demonstrator for a blended wing body airliner"*, Group Design Project of the Aeronautical Engineering course, College of Aeronautics, 2000.
89. Hobson, Nathan R., "*Kestrel Blended Wing Body sub-scale demonstrator – General systems and avionics design*", MSc Thesis, College of Aeronautics, Cranfield University, 2001.
90. Robinson, P. H., "*Concept design of a blended wing body airliner and design plus build of the sub-scale demonstrator vehicle 'Kestrel'*", MSc Thesis, College of Aeronautics, Cranfield University, 2001.
91. Youngren, H. H., Bouchard, E. E., Coopersmith, R. M. and Miranda, L. R, "*Comparison of Panel Method Formulations and its influence on the*

development of QUADPAN, an advanced low-order method", AIAA Paper 83-1827, 1983.

92. Anon., "*MOB – A computational design engine incorporating multi-disciplinary design and optimisation for blended-wing-body configurations*", EU Contract: 01/03/2000-G4RD-CT-1999-00172.
93. Smith, H. and Yarf-Abbasi, A., "*The MOB Blended Wing Body reference aircraft*", MOB/4/CU/TReport/004, Issue 3, G4RD-CT1999-0172, July 2001.
94. Qin, N, Vavalle, A. and LeMoigne, A., "*A study of spanwise lift distribution for blended wing body*", CEAS Aerodynamics Research Conference, Cambridge, June 2002.
95. LeMoigne, A. and Qin, N., "*A discrete adjoint method for aerodynamic sensitivities for Navier-Stokes flows*", CEAS Aerodynamics Research Conference, Cambridge, June 2002.
96. LaRocca, G., Krakers and Tooren, M. J. L. van, "Development of an ICAD generative model for a blended-wing-body aircraft design", AIAA paper
97. Castro, H. V. de, "*The longitudinal static stability of tailless aircraft*", CoA report No. 0018/1, Cranfield University, 2001.
98. Cook, M. V. and Castro, H. V. de, "*The longitudinal flying qualities of a Blended-Wing-Body civil transport aircraft*". Paper no2804 to be published in the Aeronautical Journal of the Royal Aeronautical Society early 2004.
99. Cook, MV, "*Flight dynamics principles*", Arnold publishers, 1997.
100. Etkin, B., "*Dynamics of flight: stability and control*", New York, Wiley, 1996.
101. Babister, A. W., "*Aircraft dynamic stability and response*", Oxford New York, Pergamon Press, 1961.
102. Dickinson, B., "*Aircraft stability and control for pilots and engineers*", London, Pitman, 1968
103. McRuer, Duane, Ashkenas, Irving and Graham, Dustan, "*Aircraft dynamics and automatic control*", Princeton University Press, Princeton, New Jersey, 1973.
104. Bishop, R.H., "*Modern control systems analysis and design: using MATLAB and SIMULINK*", Menlo Park, CA, Addison Wesley, 1997.
105. Ogata, Katsuhiko, "*Modern control engineering*", 4th edition, Prentice Hall, 2002.
106. Shinners, S. M., "*Modern control system theory and design*", John Wiley and Sons, USA, 1998.
107. Roskam, Jan, "*Airplane flight dynamics and automatic flight controls*", DARcorporation, Vol. I and II, 1995.

108. McLean, D., "*Automatic flight control systems*", Prentice-Hall, New York, 1990.
109. Stevens, B.L. and Lewis, F.L., "*Aircraft control and simulation*", New York, John Wiley, 1992.
110. Rolfe, J.M. and Staples, K.J., "*Flight Simulation*", Cambridge University Press, 1986.
111. Allerton, D. J., "*Engineering flight simulation at Cranfield*", Aerogram – Journal of College of Aeronautics, Cranfield University, Volume 9, Number 4, December 1999.
112. Cooling, J.E., "*MODULA-2 for microcomputer systems*", Chapman & Hall, London, 1988.
113. Neeson, D. E., "*A simulation of the engines and landing gear of the jetstream aircraft*", MSc Thesis, College of Aeronautics, Cranfield University, 1994.
114. Cooper, G.E. and Harper, Jr., R.P., "*The use of pilot rating in the evaluation of aircraft handling qualities*", AGARD-R-567, 1969.

WEB SITES REFERENCES

W1. http://northrop.host.sk/northrop_x4.htm
W2. http://www.wing.cranfield.ac.uk/avt-4.htm
W3. www.centennialofflight.gov/essay/Evolution_of_Technology/Lifting_bodies
W4. http://www.iss.northropgrumman.com/gallery/usaf/b2.htm
W5. http://www.jaapteeuwen.speedlinq.nl/pictures/thumbs/index.htm
W6. http://www.ctie.monash.edu.au/hargrave/northrop.html
W7. http://www.nurflugel.com/Nurflugel/Northrop/northrop.html
W8. http://www.concordeSST.com/
W9. http://www.allstar.fiu.edu/aero/TO&Land.htm

Appendix A
REQUIREMENTS

A.1 Civil JAR-25 regulations

The JAR-25 is subdivided in three sections: the regulations section, the section where acceptable means of compliance and interpretation of the requirements is presented and, lastly, the section containing advisory material. The first section has the plain description of each requirement, while the second section has an understanding of what each requirement means and how it shall be used and proved, just like a handbook. Section 1 and 2 are then divided in several parts as follow,

1) Subpart A – General,
2) Subpart B – Flight,
3) Subpart C – Structure,
4) Subpart D – Design and construction,
5) Subpart E – Powerplant,
6) Subpart F – Equipment,
7) Subpart G – Operating limitations and information,
8) Subpart J – Gas turbine auxiliary power unit installations, and
9) Appendices.

The subpart that is of use in this research is subpart B, which called Flight. This part is then divided in several main subjects, already more sounding as: General, Performance, Controllability and Manoeuvrability, Trim, Stability, Stalls, Ground Handling Characteristics and Miscellaneous Flight Requirements.

This subpart composed by the above main subjects contains all the civil requirements related to flight and thus flying and handling qualities. These were analysed and the main requirements that seem relevant for this thesis are presented next. This section does not pretend to be an extensive copy of the civil requirements, but will present in simple the requirements somehow relevant to flying and handling qualities assessment. Thus, for more information the reader is referred to the main document of the JARs-25[50].

A.1.1 Subpart B – Flight

A.1.1.1 Controllability and Manoeuvrability

General (JAR 25.143)

The aeroplane must be safely controllable and manoeuvrable during takeoff, climb, level flight, descent and landing.

It must be possible to make a smooth transition from one flight condition without exceptional pilot skill, alertness, or strength, and without danger of exceeding the aeroplane limit-load factor under any probable operating conditions, including: a) the sudden failure of a critical engine, b) the sudden failure of the second critical engine, in case of three or more engines, and c) configuration changes.

Furthermore, when manoeuvring at a constant air speed, the stick forces and the gradient of the curve stick force versus manoeuvring load factor must lie within satisfactory limits. The stick forces must not be so great as to make excessive demands on the pilot's strength when manoeuvring the aeroplane, and must not be so low that the aeroplane can easily be overstressed inadvertently. Changes of gradient which occur with changes of load factor must not cause undue difficulty in maintaining control of the aeroplane, and local gradients must not be so low as to result in a danger of over-controlling.

Longitudinal control (JAR 25.145)

It must be possible at any speed (within a described range) to pitch the nose downward so that the acceleration to this selected trim speed is prompt. This shall be accomplished with: the aeroplane at the trim, the landing gear extended, the wings flaps retracted and extended, and power off and at maximum continuous power.

With the landing gear extended, no change in trim control, or exertion of more than 50 pounds control force, may be required for the manoeuvres described.

It must be possible, without exceptional piloting skill, to prevent loss of altitude when complete retraction of the high lift devices from any position is begun during steady straight level flight at 1.2 V_s with simultaneous application of not more than take-off power, the landing gear extended and the critical combinations of landing weights and altitudes.

During the climb after take-off with one engine inoperative and landing gear retracted, it must be possible in conditions of moderate atmospheric turbulence, to manoeuvre the aeroplane in a manner appropriate to the phase of flight without encountering natural or artificial stall warning.

Directional and lateral control (JAR 25.147)

It must be possible, with the wings level, to yaw into the operative engine and to safely make a reasonably sudden change in heading of up to 15 deg in the direction of the critical inoperative engine.

This must be shown at $1.4V_{s1}$, for heading changes up to 15 deg, and with the critical engine inoperative and its propeller in the minimum drag position, the power required for level flight at $1.4V_{s1}$, but not more than maximum continuous power, the most unfavourable centre of gravity, landing gear retracted, wing flaps in the approach position and maximum landing weight.

For lateral control the requirement says that it must be possible to make 20 deg banked turns with and against the inoperative engine, from steady flight at a speed equal to $1.4V_{s1}$, with the critical engine inoperative, the remaining engines at maximum continuous power, the most unfavourable *cg* position, landing gear both retracted and extended, wing-flaps in the most favourable climb position and maximum take-off weight.

Furthermore, with the critical engine inoperative, roll response must allow normal manoeuvres. Lateral control must be sufficient at the speeds likely to be used with one engine inoperative for climb, cruise, descent and landing approach, to provide a peak roll rate necessary for safety without excessive control forces or travel.

With all engines operating, roll response must allow normal manoeuvres (recoveries from upset gusts and initiate evasive manoeuvres). There must be enough excess lateral control sideslips, to allow a limited amount of manoeuvring and to correct for gusts. Lateral control must be enough at any speed to provide a peak roll rate necessary for safety, without excessive control forces or travel.

Minimum control speed (JAR 25.149)

V_{MC} is the calibrated speed, at which, when the critical engine is suddenly made inoperative, it is possible to maintain control of the aeroplane with that engine still inoperative, and maintain a straight flight with an angle of bank of not more than 5 deg.

VM_{CG}, the minimum control speed on the ground, is the calibrated airspeed during the takeoff run at which, when the critical engine is suddenly made inoperative it is possible to maintain control of the aeroplane with the use of the primary aerodynamic controls alone, to enable the takeoff to be safely continued using normal piloting skill.

VM_{CL}, the minimum control speed during landing approach with all engines operating, must be established with the aeroplane in the most critical configuration for approach and landing.

A.1.1.2 Trim

Trim (JAR 25.161)

The aeroplane must maintain lateral and directional trim with the most adverse lateral displacement of the centre of gravity within the relevant operating limitations, during normally expected conditions of operation.

Further, the aeroplane must maintain longitudinal trim during a climb, either a glide or an approach, and level flight at any speed.

The aeroplane must maintain longitudinal, directional, and lateral trim at $1.4V_{s1}$, during the climbing flight with the critical engine inoperative, the remaining at maximum continuous power and landing gear and wing-flaps retracted.

A.1.1.3 Stability

General (JAR 25.171)

The aeroplane must be longitudinally, directionally and laterally stable in accordance with JAR 25.137 to 25.177. In addition, suitable stability and control feel (static stability) is required in any condition normally encountered in service.

Static longitudinal stability (JAR 25.173)

The characteristics of the elevator control forces must be as follow: a pull must be required to obtain and maintain speeds below the specified trim speed, and a push must be required to obtain and maintain speeds above the specified trim speed. Further, the airspeed must return to within 10% of the original trim speed for the climb, approach and landing conditions, and within 7.5% for the cruising condition, when the control force is slowly released from any speed. Moreover, the average gradient of the stable slope of the stick force versus speed curve may not be less than 1 pound for each 6 knots. Lastly, it is permissible for the aeroplane, without control forces, to stabilise on speeds above or below the desired trim speeds if exceptional attention of the part of the pilot is not required to return and maintain the desired trim speed and altitude.

Demonstration of static longitudinal stability (JAR 25.175)

Static longitudinal stability must be shown in climb, cruise, approach and landing.

Static directional and lateral stability (JAR 25.177)

The static directional stability must be positive or any landing gear and flap position and symmetrical power conditions.

The static lateral stability for any landing gear and wing-flap and symmetric power condition, may not be negative at any airspeed.

Lastly, in straight steady sideslips the aileron and rudder control movements and forces must be substantially proportional to the angle of sideslip. At greater angles the rudder pedal forces may not reverse and increased rudder deflection must produce increased angles of sideslip.

And, unless the aeroplane has a yaw indicator, there must be enough bank accompanying side slipping to clearly indicate any departure from steady unyawed flight.

Dynamic stability (JAR 25.181)
Any short period oscillation, not including combined lateral-directional oscillations must be heavily damped with the primary controls free and in a fixed position.

Any combined lateral-directional oscillations, dutch-roll, occurring between $1.2V_S$ and maximum allowable speed appropriate to the configuration of the aeroplane, must be positively damped with controls free, and must be controllable with normal use of the primary controls without requiring exceptional pilot skill.

A.1.1.4 Ground handling characteristics

Longitudinal stability and control (JAR 25.231)
Aeroplanes may have no uncontrollable tendency to nose over in any reasonable expected operating condition or when rebound occurs during landing or take-off.

Directional stability and control (JAR 25.233)
There may be no uncontrollable ground-looping tendency in 90 deg crosswinds. Aeroplanes must be satisfactorily controllable, without exceptional piloting skill or alertness, in power-off landings at normal landing speed, without using brakes or engine power to maintain straight path. Furthermore, the aeroplane must have adequate directional control during taxying.

A.1.1.5 Miscellaneous flight requirements

Out-of-trim characteristics (JAR 25.255)
From an initial condition with the aeroplane trimmed at cruise speeds, the aeroplane must have satisfactory manoeuvring stability and controllability with the degree of

out-of-trim in both the aeroplane nose-up and nose-down directions, which results from the greater of a three-second movement of the longitudinal trim system for the particular flight condition or the maximum mistrim that can be sustained by the autopilot while maintaining level flight in the high speed cruising condition.

A.1.2 Subpart D – Design and construction

In subpart D, design and construction, there is reference to the flight control systems under the subject control systems. These are presented next.

A.1.2.1 Control systems

General (JAR 25.671)
Each control and control system must operate with the ease, smoothness, and positiveness appropriate to its function.

The aeroplane must be shown by analysis, test, or both, to be capable of continued safe flight and landing after any of the following failures or jamming in the flight control system and surfaces within the normal flight envelope, without requiring exceptional piloting skill or strength: 1) any single failure not shown to be extremely improbable, excluding jamming, 2) any combination of failures not shown to be extremely improbable, excluding jamming, and 3) any jam in a control position normally encountered during takeoff, climb, cruise, normal turns, descent and landing unless the jam is shown to be extremely improbable or alleviated.

The aeroplane must be designed so that it is controllable if all engines fail.

Stability augmentation and automatic and power-operated systems (JAR 25.672)
It must be shown that after any single failure of the stability augmentation system or any other automatic or power-operated system, the aeroplane is safely controllable when the failure or malfunction occurs, the controllability and manoeuvrability requirements of this JAR-25 are met within a practical operational flight envelope, and the trim, stability, and stall characteristics are not impaired below a level needed to permit continued safe flight and landing.

Appendix B
BWB DATA

B.1 BWB1 configuration data

This part presents the data set of the first blended-wing-body configuration studied in this research. Figure B.1 presents the general arrangement of configuration BWB1.

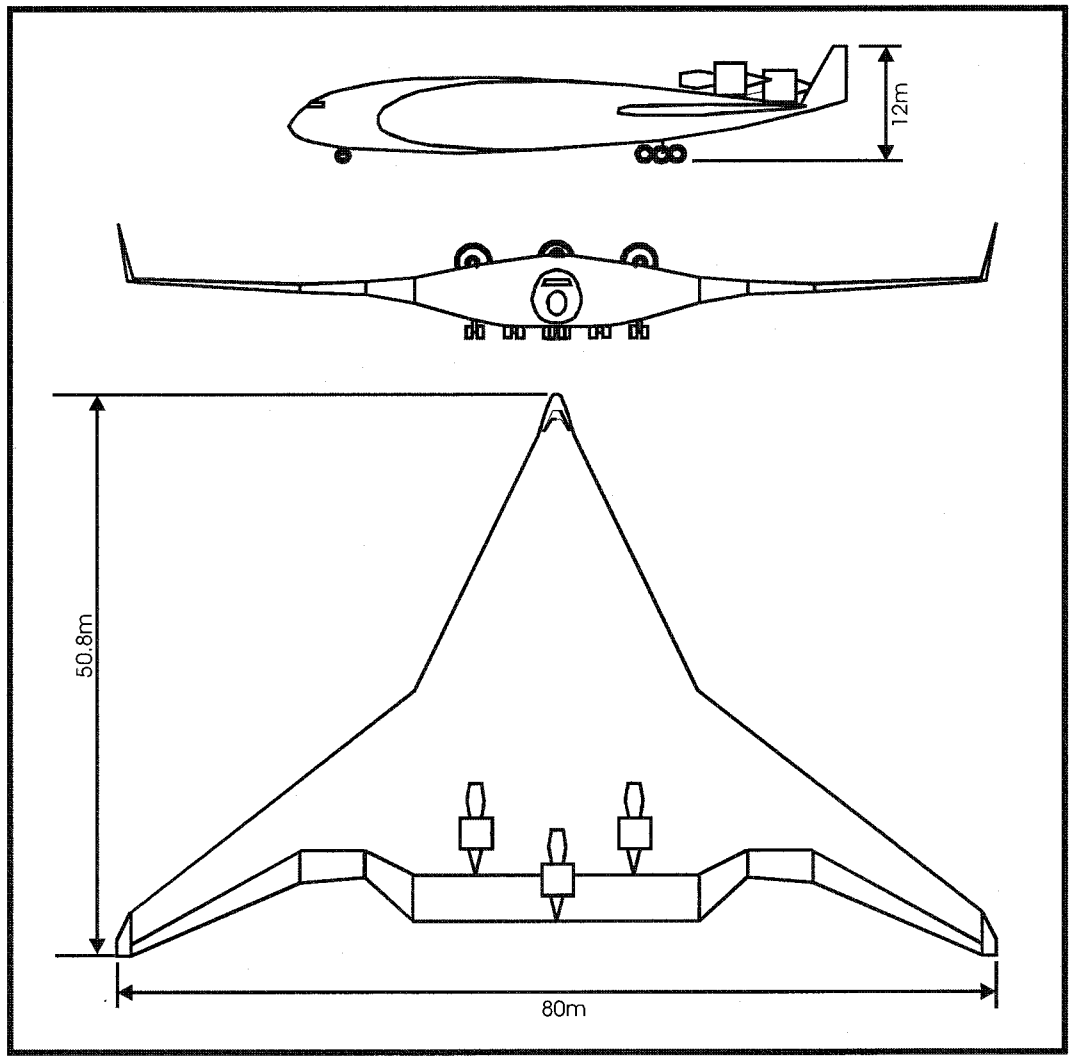

Figure B.1 3-view drawing of configuration BWB1, BWB3 and BWB4

	Weight Kg	$\bar{X}$ m	$\bar{Z}$ m	I_{XX} $(\times 10^6)$ $Kg.m^2$	I_{YY} $(\times 10^6)$ $Kg.m^2$	I_{ZZ} $(\times 10^6)$ $Kg.m^2$
MTOW	480,072	31.88	0.082	108.702	47.128	155.830
LG down	480,072	31.83	-0.014	108.802	47.282	155.984
Start Cruise	443,680	31.03	0.088	77.032	42.702	119.734
OEW	210,469	31.36	0.365	28.347	24.307	52.655
LG down	210,469	31.25	0.147	28.348	24.509	25.857

Table B.1 Mass, centre of gravity position and moments of inertia for several *cg*

Gross area S_{gross}	1390.6 m^2
Trapezoidal area S_{trap}	841.7 m^2
Span b	80.0 m
Trapezoidal AR	7.14
Gross root chord $c_{r_{gross}}$	48.0 m
Trapezoidal root chord $c_{r_{trap}}$	17.72 m
Tip chord c_t	4.0 m
Gross wing *mac* $\bar{\bar{c}}_{gross}$	27.28 m
Trapezoidal wing *mac* $\bar{\bar{c}}_{trap}$	12.31 m
LE sweepback	
- Body Λ_{LE_B}	52.3 deg
- Trapezoidal wing $\Lambda_{LE_{trap}}$	38.3 deg
Thickness centre t/c	16.5%
- Maximum	18%
- Outboard	8%
Dihedral at centre Γ	0 deg
At crank	1.5 deg
At outer wing	3 deg

Table B.2 General BWB1 geometric data

The general geometric and mass data are shown in Tables B.1 to B.3. The most forward and afterward *cg* positions are shown in Figure B.2, together with the neutral point position and the mean aerodynamic chord position for the trapezoidal wing.

Mass Information	(Kg)
Operating empty Weight (OEW)	212,869
Maximum Takeoff Weight (MTOW)	480,072
Max Landing Weight (MLW)	322,599

Table B.3 General BWB1 mass information

Based in figure B.2 the centre of gravity range for this aircraft was estimated to be between $h = 0.336$ and $h = 0.468$ of the *mac* gross wing. This gives a range of 13.2% *mac* gross wing range, which looks a rather small number comparatively to conventional configurations. However, one should remember that the *mac* gross wing for the BWB concept is bigger than that of a conventional aircraft. Actually, 13.2% *mac* for this configuration gives a range in meters equal to 3.6 meters.

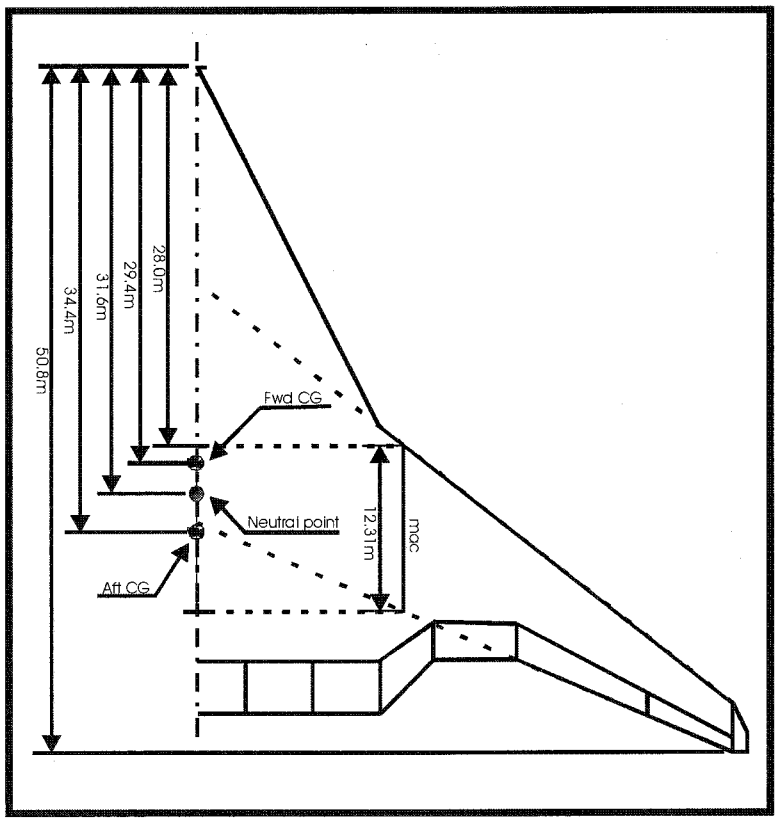

Figure B.2 BWB1, BWB3 and BWB4 planform

	Approach Case	Cruise Case
Speed/Mach, *V/Ma*	150 kts	0.85
Altitude, *h*	Sea Level	10,059 m
Mass, *m*	322,599 Kg	443,680 Kg
Static Margin, K_n	1.5% gross *mac*	1.9% gross *mac*
	3.3% trap *mac*	4.2% trap *mac*
***cg* position,** X_{cg}	31.23 m	31.9 m
Neutral point position, X_n	31.638 m	32.42 m

Table B.4 Definition of two representative flight conditions: approach and cruise

Aerodynamic information is presented in Tables B.5 to B.7 for two different flight conditions: a low subsonic speed and low altitude case referent to an approach flight condition, and a high subsonic speed and high altitude case referent to a cruise flight condition. The values of the two flight conditions are presented in Table B.4.

From the value of the lift coefficient given in Table B.5 and the flight condition values given in Table B.4, it was possible to discover that the gross wing area of 1390m^2 was the reference area used. This is therefore the reason why the lift slope coefficient is low for this kind of configuration when compared to values of conventional aircrafts.

Aerodynamic data	Approach	Cruise
C_L	1.054	0.236
C_{L_α}	3.327	5.382
ΔC_{L_η}	0.0247	0.0
C_m	0.0	0.0
C_{m_o}	0.0047	0.0044
ΔC_{m_η}	-0.0067	0.0
$\Delta C_{m_{LE}}$	0.0178	0.0
C_{D_o}	0.0139	0.0142
K_n	0.0566	0.0591
$\Delta C_{D_{LG}}$	0.03	0.0

Table B.5 Aerodynamic data for an approach and cruise representative flight conditions

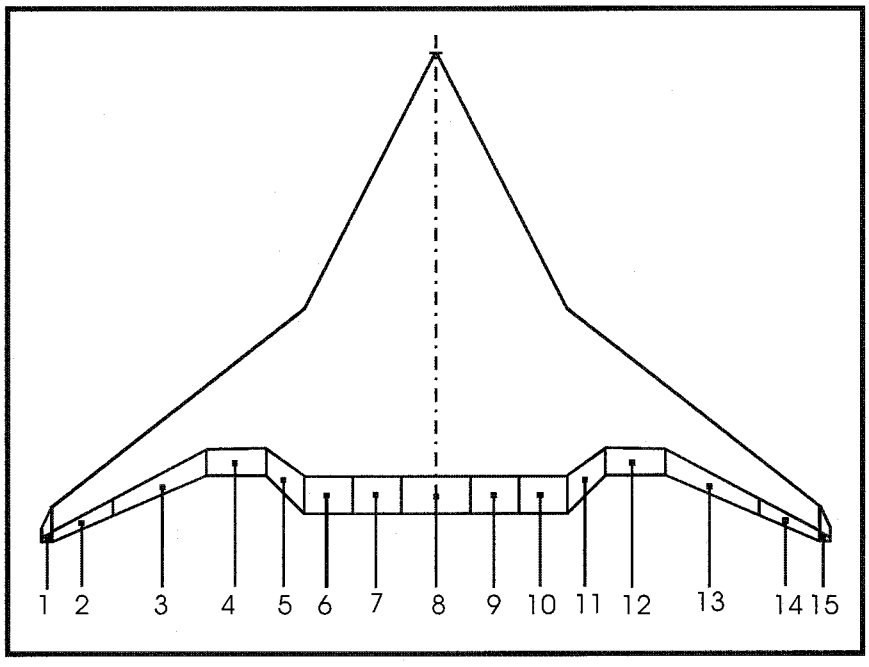

Figure B.3 BWB1, BWB3 and BWB4 control surfaces

From Figure B.3 it can be seen that BWB1 has 7 control surfaces on the trailing edge of the wing-body. The maximum deflections allowed are –5/+15 degrees deflection for the inboard surfaces, -20/+20 degrees deflection for surface number 4 and –25/+25 degrees deflection for the outboard control surfaces. There are two fins at the tip of the wings with rudders incorporated. The deflection of these is -37/+37 degrees of maximum control deflection.

The longitudinal control surfaces data as well as the lateral-directional data is given in Tables B.6 and B.7. The longitudinal control stability coefficients are given for all 7 trailing edge surfaces, suggesting that any of them can be used for pitch control. For lateral control, only one control stability coefficient is given, correspondent to the trailing edge surfaces number 6 and 7. From this it is concluded that surface 6 and 7 can work either as elevons or just as ailerons.

	Approach	Cruise
C_{l_p}	-0.1854	-0.2180
C_{l_r}	0.1744	0.0731
C_{l_v}	-0.4325	-0.3630
C_{l_ξ}	-0.0963	-0.1642
C_{l_ς}	0.0012	0.0021
C_{n_p}	-0.0906	-0.0328
C_{n_r}	-0.0157	-0.0116
C_{n_v}	0.0070	0.0105
C_{n_ξ}	0.0093	0.0089
C_{n_ς}	-0.0087	-0.0148
C_{Y_p}	0.3855	0.1321
C_{Y_r}	0.0223	0.0258
C_{Y_v}	-0.2783	-0.2933
C_{Y_ξ}	0.0	0.0
C_{Y_ς}	0.0376	0.0638

Table B.6 Lateral-directional aerodynamic and control stability derivatives

η	Approach		Cruise	
	C_{L_η}	C_{m_η}	C_{L_η}	C_{m_η}
1	0.1797	-0.0469	0.2518	-0.0728
2	0.2754	-0.0745	0.3606	-0.1058
3	0.2595	-0.0682	0.3225	-0.0911
4	0.2447	-0.0544	0.3189	-0.0733
5	0.3369	-0.0746	0.4835	-0.1030
6	0.3405	-0.1097	0.4726	-0.1394
7	0.1224	-0.0581	0.1528	-0.0678

Table B.7 Longitudinal control stability coefficients for all 7 trailing edge surfaces

Lastly, one more valuable piece of information in this data set is the specification of the powerplant for this configuration. Thus, designers are previewing that turbo-engines with a delivering of static thrust at sea level around 418.4 kN will be necessary.

B.2 BWB2 configuration data

This section presents the geometric, aerodynamic and mass properties data for the BWB2 configuration. The general arrangement of configuration BWB2 is given in Figure B.4.

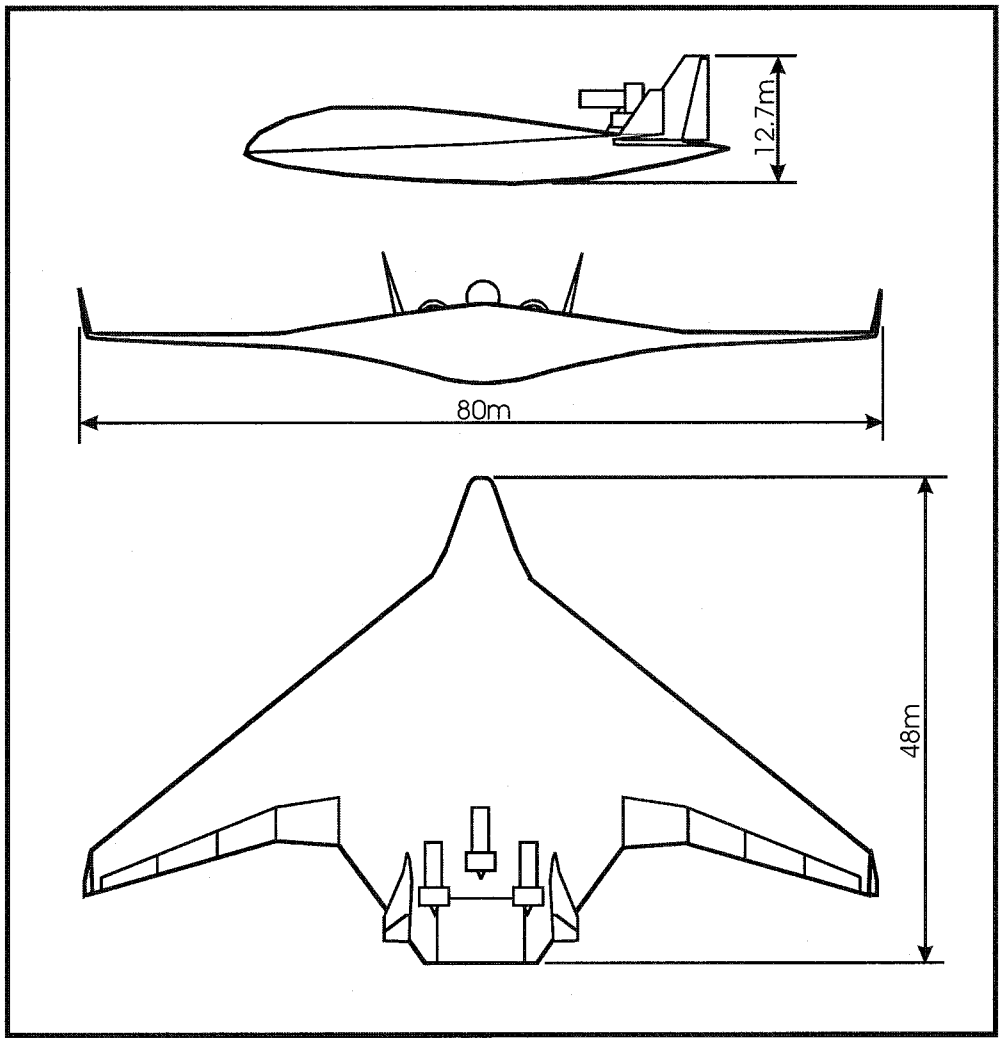

Figure B.4 BWB2 3D-view drawing

In the geometric data presented on Table B.8, the mean aerodynamic chord for the trapezoidal wing is not given. Thus, it was concluded that the gross wing *mac* and area were used as the reference measures, and the trapezoidal wing *mac* was not considered necessary.

Gross area S_{gross}	1515.0 m^2
Trapezoidal area S	692 m^2
Span b	80.0 m
Gross AR	4.22
Trapezoidal AR	9.25
Gross root chord $c_{r_{gross}}$	40.0 m
Trapezoidal root chord c_r	13.0 m
Tip chord c_t	4.3 m
Gross wing *mac*, $\bar{\bar{c}}_{gross}$	26.264 m
Trapezoidal wing *mac*, $\bar{\bar{c}}$	-
LE sweepback Λ_{LE}	38.0 deg
Dihedral Γ	2 deg

Table B.8 Geometric information of the BWB2 configuration

The mass and moments of inertia are presented in Table B.9 for just one condition. Although the units for the moments of inertia are presented as $Kg.m^2$, no units were found with the values on the aircraft design reports, thus, there is no certainty that these values are right. When compared with the BWB1 moments of inertia, the BWB2 moments of inertia are a factor of 10^3 bigger, what seems a large difference. Later, during the flight dynamic analysis, it was found that moments of inertia of this magnitude are not advisable and smaller moments of inertia were used, as shown.

	Weight Kg	I_{XX} $Kg.m^2$	I_{YY} $Kg.m^2$	I_{ZZ} $Kg.m^2$
Original	460,869	4.832×10^{11}	5.283×10^{10}	2.517×10^{11}
Used	460,869	4.832×10^{8}	5.283×10^{7}	2.517×10^{8}

Table B.9 BWB2 mass and moments of inertia

Wind tunnel test experiments were done for a sub-scale demonstrator, Krestel[86]. The stability derivatives calculated from the wind tunnel data are presented in Table B.10. The tests were performed for a low speed of 90 m/s and just one *cg* position, which was not given with the data but it can be calculated from the aerodynamic data.

The pitching moment derivative due to lift is by definition the symmetric of the aircraft static margin. Thus, using this definition and the data given in Table B.10 follows the aircraft *cg* position for this experiment.

$$\frac{dC_m}{dC_L} = -K_n \Rightarrow K_n = 0.0322 \qquad \text{(B.1)}$$

Aerodynamic data	
C_{L_o}	0.0322
C_{L_α}	3.306
C_{D_o}	0.0117
k_1	-0.02
k_2	0.12
C_{m_o}	0.0227
$C_{m_{CL}}$	-0.0322
C_{l_v}	-0.1948
C_{n_v}	0.086
C_{Y_v}	-0.2005

Table B.10 Aerodynamic data obtained for the sub-model Kestrel

The result of equation (B.1) means that this configuration had a stable static margin of $K_n = 0.322\bar{\bar{c}}$ or in other words that the cg is at $h = 0.322$, forward of the neutral point or aerodynamic centre. The more general value of pitching moment due to angle of attack can be calculated using the following relationship.

$$C_{m_\alpha} = \frac{dC_m}{dC_L} \times \frac{\partial C_L}{\partial \alpha} \Rightarrow C_{m_\alpha} = -0.1065\left(rad^{-1}\right) \tag{B.2}$$

The lift plot versus angle of attack presented an unusual characteristic of having the curve slope presented in the table above, until only an angle of incidence of 10 deg and having a different curve slope of $C_{L_\alpha} = 0.2177\left(rad^{-1}\right)$ for angle of attack values greater than 10 deg, as can also be seen from Figure B.5.

Once more, due to the low value of the lift curve slope it is concluded that probably the gross wing area was taken as the reference area, although no real clear indication is given elsewhere in the aircraft reports. Considering the trapezoidal wing area as reference area, the lift curve slope values would be as presented in equation (B.3)

$$C_{L_{\alpha 1}} = 7.233\left(rad^{-1}\right) \text{ and } C_{L_{\alpha 2}} = 0.4766\left(rad^{-1}\right) \tag{B.3}$$

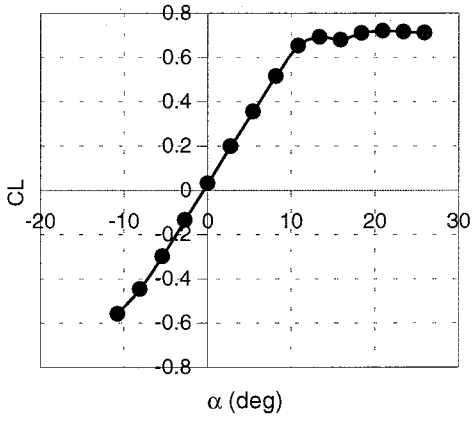

Figure B.5 BWB2 Lift coefficient versus angle of attack

The drag polar given is only valid for values of lift coefficient between $-4 < C_L < 0.6$. These wind tunnel tests only measured static aerodynamic derivatives and control derivatives, where two kinds of controls were tested for efficiency, actually the usual plain flaps and split flaps. The results for the control surfaces are given in Table B.11 and the controls general arrangement is shown in Figure B.6.

	C_{L_δ}	C_{m_δ}	C_{Y_δ}	C_{l_δ}	C_{n_δ}
1	0.1490	-0.0630	-0.0057	-0.0630	0.0
2	0.3266	-0.0802	0.0	-0.0917	0.0
3	0.3667	-0.0802	-0.0057	-0.0630	0.0
4	0.1547	-0.0286	-0.0115	-0.0172	0.0
5	0.1834	-0.0630	-0.0023	0.0	0.0
P1-2	0.4870	-0.4011	0.0	0.0	0.0
A1-2	-0.0115	0.005	-0.0286	-0.3323	0.0017
P3-4	0.4985	-0.0917	0.0	0.0	0.0
S – 1	-0.0745	0.0286	0.0115	0.0516	-0.0057
S – 2	-0.1375	0.0344	0.0057	0.0630	-0.0057
S – 3	-0.1490	0.0229	-0.0046		-0.0017
R – P	0.0	0.0057	0.0802	0.0172	-0.0290
R – D	0.0974	-0.0458	0.0017	0.0	0.0

Table B.11 Control stability derivatives for BWB2

P1-2 means deflecting surfaces 1 and 2 simultaneously and proportionally in both sides of the wing, either both down or both up. The same follows for P3-4, but deflecting surfaces 3 and 4 instead. A1-2 means that surfaces 1 and 2 are simultaneously deflected, but asymmetrically on each side of the wing, i.e., if on the right side surfaces 1 and 2 go up, on the left side these go down. S-1, S-2 and S-3 means that surfaces 1, 2 or 3 are split flaps. R – P stands for rudder deflected proportionally while R – D stands for rudder deflected differentially on each fin, one

deflecting right and the other left. From the values of Table B.11 the following conclusions were drawn.

- Surfaces 2 and 3 generate the highest lift per degree deflected and so they are best as high lift surfaces. However, they also generate the largest pitching moment when deflecting each surface individually.
- When considering pairs of adjacent surfaces simultaneously deflected, the pair 3 and 4, P3-4, generates more lift and less pitching moment than pair 1 and 2. Thus, pair 1-2 will be the best for pitching control, while pair 3-4 could work as a high lift surface.
- Although surfaces 1 to 5 present some lateral-directional effects when deflected proportionally, these are not of great magnitude and may be neglected.
- The pair 1-2 when deflected asymmetrically on each side of the wing present the biggest rolling moment per degree of control surface deflected, being, therefore, the best for roll control. Deflecting the pair 1-2 asymmetrically also generates an adverse yaw.
- For yaw control the rudders deflected proportionally in each vertical surface present the best option since they produce the larger yawing moment.
- If using split flaps, per degree of split flap open, there is no great effect, but independent of the degree they are open they generate considerable yawing moment. However, they also generate rolling moment, which may not be desirable, as well as considerable lift loss and pitching moment.

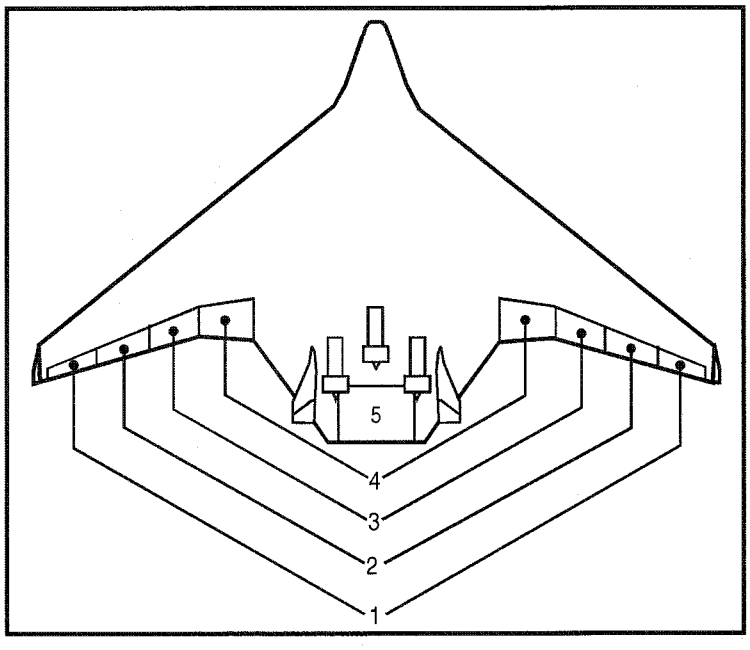

Figure B.6 BWB2 control surfaces arrangement

B.3 BWB3 configuration data

This appendix presents the geometric, mass properties and aerodynamic data for the BWB3 configuration. Actually, the geometric data is equal to that given for the BWB1 configuration in Table B.2. In the same way, the general configuration is the same as given in Figures B.1, B.2 and B.3. In this section only the BWB3 data different from that of BWB1will be presented. The aircraft mass for several conditions is as given in Table B.12.

Maximum Takeoff Weight (MTOW)	371280Kg
Maximum Landing Weight (MLW)	322599Kg
Operation Empty Weight (OEW)	136995Kg
Maximum payload	115000Kg

Table B.12 BWB3 configuration masses

B.3.1 Aerodynamic stability derivatives

The longitudinal aerodynamic stability derivatives obtained from CFD data is given in Table B.13 as function of *cg* position. It can be noted that not all stability derivatives are actually *cg* dependent, as some are constant for all different *cg* positions.

X_{CG} (m)	29.4	30.4	31.4	32.4	33.4	34.4
C_{Z_o}	-0.0217	-0.0217	-0.0217	-0.0217	-0.0217	-0.0217
C_{Z_α}	5.4868	5.4868	5.4868	5.4868	5.4868	5.4868
C_{Z_q}	1.0787	0.9678	0.8568	0.7459	0.6351	0.5243
C_{m_o}	-0.0370	-0.0388	-0.0405	-0.0423	-0.0441	-0.0458
C_{m_α}	-0.9950	-0.5493	-0.1036	0.3422	0.7879	1.2336
C_{m_q}	-0.8799	-0.7809	-0.7001	-0.6374	-0.5929	-0.5665

Table B.13 Aerodynamic Stability derivatives function of *cg* position

In Table B.14 the values of the normal force coefficient slope and pitching moment coefficient slope are retained to calculate the static stability margin. Knowing that when the *cg* is at the neutral point the static margin is zero, by definition of neutral point, it is then possible to calculate the location of the neutral point, h_n.

X_{CG} (m)	29.4	30.4	31.4	32.4	33.4	34.4
C_{Z_α}	5.4868	5.4868	5.4868	5.4868	5.4868	5.4868
C_{m_α}	-0.9950	-0.5493	-0.1036	0.3422	0.7879	1.2336
$K_n \approx -\frac{C_{m_\alpha}}{C_{Z_\alpha}}$	0.181 $(18.1\%\bar{\bar{c}})$	0.100 $(10.0\%\bar{\bar{c}})$	0.019 $(1.9\%\bar{\bar{c}})$	-0.062 $(-6.2\%\bar{\bar{c}})$	-0.144 $(-14.4\%\bar{\bar{c}})$	-0.225 $(-22.5\%\bar{\bar{c}})$

Table B.14 Static margin calculation for each *cg* position

In Figure B.7 the static margin is plotted against the *cg* position. From the plot it can be seen that the neutral point lays between 31 and 32 (m), which is where the curve crosses the axis of zero static margin. Doing an interpolation with the values of Table B.14, the neutral point is found to be at $X_{h_n} = 31.65m$.

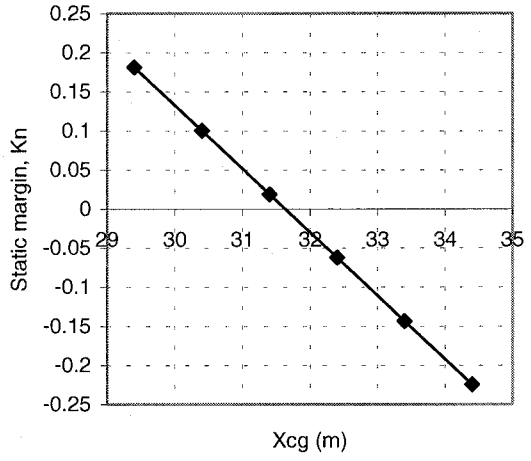

Figure B.7 BWB3 static stability margin versus *cg* position

The lateral stability derivatives are angle of attack dependent, as well as sideslip angle dependent. Table B.15 shows the side force and rolling moment coefficients due to roll rate and sideslip angle as function of angle of attack.

	Basic	α
C_{Y_β}	-0.3086	0.4879
C_{Y_p}	-0.0814	2.0667
C_{l_β}	-0.0465	-0.3007
C_{l_p}	-0.3562	0.0735

Table B.15 BWB3 lateral-directional derivatives

The "basic" column is the value of the derivative for zero angle of attack, and the "α" column is the variation of the derivative with angle of attack. When there is no "α" column, there is no dependence on angle of attack. This holds for all the remaining

tables. The side force and rolling moment coefficients due to the yaw rate shown in Table B.16 as function also of the *cg* position. The yawing moment coefficients are all dependent on *cg* position, besides its variation with sideslip angle and angle of attack. This is shown in table B.17.

X_{cg} (m)	C_{Y_r}	C_{l_r}	
	Basic	Basic	α
29.4	-0.1555	0.0272	0.5867
30.4	-0.1655	0.0261	0.5797
31.4	-0.1675	0.0250	0.5727
32.4	-0.175	0.0239	0.5658
33.4	-0.18	0.0229	0.5588
34.4	-0.194	0.0218	0.5518

Table B.16 BWB3 C_{Y_r} and C_{l_r} derivatives

XCG	C_{n_β}		C_{n_p}		C_{n_r}	
	Basic	α	Basic	α	Basic	α
29.4	0.0152	-0.2787	0.0134	-0.8733	-0.0315	0.0867
30.4	0.0114	-0.2726	0.0124	-0.8475	-0.0332	0.0805
31.4	0.0075	-0.2665	0.0114	-0.8217	-0.0351	0.0746
32.4	0.0037	-0.2604	0.0103	-0.7958	-0.0372	0.0690
33.4	-0.0002	-0.2543	0.0093	-0.7700	-0.0394	0.0637
34.4	-0.0041	-0.2482	0.0083	-0.7442	-0.0419	0.0587

Table B.17 BWB3 yawing moment coefficient derivatives

B.3.2 Control stability derivatives

The BWB3 configuration possesses 15 control surfaces, taking into account the rudder controls in the vertical surfaces as well, as shown in Figure B.3. The surfaces are numerated from the left to the right where the first surface is the left winglet rudder, the next surface the most outboard wing flap, the surface number 8 the middle wing flap, and the last surface, surface 15th, is the right winglet rudder.

On Table B.18 the control stability derivatives side force, normal force and rolling moment coefficients due to the control surfaces deflection, C_{Y_δ}, C_{Z_δ} and C_{l_δ}, are presented for each of the fifteen surfaces. The control stability derivatives C_{m_δ} and C_{n_δ}, the pitching moment and yawing moment due to the control surfaces deflection, are shown in Tables B.19 and B.20 respectively for each surface and as function of the *cg* position. The axial force coefficients, equal to drag for small angles of attack,

are not presented because the CFD code used is an inviscid one, so the effect due to the profile is not present, and the effect induced by lift is negligible.

Flap #	C_{Y_δ}	C_{Z_δ}	C_{l_δ}
1	-0.0230	-0.0120	0.0059
2	-0.0092	-0.0521	0.0198
3	-0.0077	-0.1137	0.0322
4	-0.0044	-0.1111	0.0221
5	-0.0030	-0.0801	0.0115
6	-0.0028	-0.0906	0.0089
7	-0.0018	-0.0935	0.0048
8	0.0	-0.1184	0.0
9	0.0018	-0.0935	-0.0048
10	0.0028	-0.0906	-0.0089
11	0.0030	-0.0801	-0.0115
12	0.0044	-0.1111	-0.0221
13	0.0077	-0.1137	-0.0322
14	0.0092	-0.0521	-0.0198
15	-0.0237	0.0164	0.0078

Table B.18 BWB3 control stability derivatives independent of *cg* position

X_{CG} (m)	**29.4**	**30.4**	**31.4**	**32.4**	**33.4**	**34.4**
Flap 1	-0.0151	-0.0142	-0.0132	-0.0122	-0.0112	-0.0103
Flap 2	-0.0619	-0.0577	-0.0534	-0.0492	-0.0450	-0.0407
Flap 3	-0.0972	-0.0880	-0.0787	-0.0695	-0.0603	-0.0510
Flap 4	-0.0716	-0.0626	-0.0535	-0.0445	-0.0355	-0.0265
Flap 5	-0.0523	-0.0458	-0.0393	-0.0328	-0.0263	-0.0198
Flap 6	-0.0659	-0.0586	-0.0512	-0.0438	-0.0365	-0.0291
Flap 7	-0.0685	-0.0609	-0.0533	-0.0457	-0.0381	-0.0305
Flap 8	-0.0874	-0.0778	-0.0681	-0.0585	-0.0489	-0.0393
Flap 9	-0.0685	-0.0609	-0.0533	-0.0457	-0.0381	-0.0305
Flap 10	-0.0659	-0.0586	-0.0512	-0.0438	-0.0365	-0.0291
Flap 11	-0.0523	-0.0458	-0.0393	-0.0328	-0.0263	-0.0198
Flap 12	-0.0716	-0.0626	-0.0535	-0.0445	-0.0355	-0.0265
Flap 13	-0.0972	-0.0880	-0.0787	-0.0695	-0.0603	-0.0510
Flap 14	-0.0619	-0.0577	-0.0534	-0.0492	-0.0450	-0.0407
Flap 15	0.0212	0.0198	0.0185	0.0172	0.0158	0.0145

Table B.19 BWB3 C_{m_δ} stability derivative versus *cg* position

X_{CG} (m)	29.4	30.4	31.4	32.4	33.4	34.4
Flap 1	-0.0057	-0.0054	-0.0051	-0.0048	-0.0045	-0.0042
Flap 2	-0.0021	-0.0020	-0.0019	-0.0018	-0.0016	-0.0015
Flap 3	-0.0014	-0.0013	-0.0012	-0.0011	-0.0010	-0.0009
Flap 4	-0.0007	-0.0006	-0.0006	-0.0005	-0.0005	-0.0004
Flap 5	-0.0006	-0.0005	-0.0005	-0.0005	-0.0004	-0.0004
Flap 6	-0.0005	-0.0004	-0.0004	-0.0004	-0.0003	-0.0003
Flap 7	-0.0003	-0.0003	-0.0003	-0.0002	-0.0002	-0.0002
Flap 8	0.0	0.0	0.0	0.0	0.0	0.0
Flap 9	0.0003	0.0003	0.0003	0.0002	0.0002	0.0002
Flap 10	0.0005	0.0004	0.0004	0.0004	0.0003	0.0003
Flap 11	0.0006	0.0005	0.0005	0.0005	0.0004	0.0004
Flap 12	0.0007	0.0006	0.0006	0.0005	0.0005	0.0004
Flap 13	0.0014	0.0013	0.0012	0.0011	0.0010	0.0009
Flap 14	0.0021	0.0020	0.0019	0.0018	0.0016	0.0015
Flap 15	-0.0058	-0.0055	-0.0053	-0.0050	-0.0047	-0.0044

Table B.20 BWB3 C_{n_δ} stability derivative as a function of *cg* position

Once knowing the result of deflecting a control surface it is possible to allocate each surface to control the three axes, pitch, roll and yaw axis. This distribution changed during the research due to knowledge being acquired with the research. The evolution for each control axis is presented next.

B.3.3 Control of the pitch axis

To control the pitch axis, initially the control surface was chosen with the highest pitching moment per degree of control surface deflected. After the static calculations were done, it was clear that just one surface was not enough to trim and control the pitch axis principally at low speed flight conditions. Thus, a sum of the several control surfaces in the wing trailing edge was used instead. However, not all surfaces had the same range of deflection. The surfaces that were used to control the roll axis as well were deflected less to allow for this.

	$\Delta\eta_{max}$ (deg)	C_{Z_η}	C_{m_η}					
			29.4	30.4	31.4	32.4	33.4	34.4
# 3	+/-30	-0.2274	-0.1944	-0.1760	-0.1574	-0.1390	-0.1206	-0.1020
#5-8	+/-30	-0.6468	-0.4614	-0.4166	-0.3712	-0.3264	-0.2816	-0.2364
#2-4	+/-15	-0.5538	-0.4608	-0.4084	-0.3557	-0.3031	-0.2507	-0.1981

Table B.21 Control surfaces chosen to control the pitch axis

B.3.4 Control of the roll axis

To control the roll axis, initially the control surface was used with the largest rolling moment generated per degree of control deflected. Later, also a sum of control surfaces was used and in a last stage due to the results during the flight control system design, a combination of control surfaces was used which would give the highest rolling moment per degree deflected and the lowest adverse yaw generated.

	$\Delta\xi_{max}$ (deg)	C_{Y_ξ}	C_{l_ξ}	C_{n_ξ}					
				29.4	30.4	31.4	32.4	33.4	34.4
# 3	+/-30	-0.0154	-0.0644	0.0028	0.0026	0.0024	0.0022	0.0020	0.0018
#2-4	+/-15	-0.0426	-0.1482	0.0084	0.0078	0.0074	0.0068	0.0062	0.0056
# 4	+/-15	-0.0088	-0.0442	0.0014	0.0012	0.0012	0.0010	0.0010	0.0008

Table B.22 BWB3 control surfaces chosen to control the roll axis

B.3.5 Control of the yaw axis

There was no alternative for the control of the yaw axis. However the basic values of the control surfaces were multiplied by a factor of 5, as shown in table B.23, at some stage of the research, simulating an increase of the directional control power in some way: or by augmenting the rudders surface area, or by using alternative stronger yawing moments generator surfaces, such as split rudders or drag rudders.

	$\Delta\varsigma_{max}$ (deg)	C_{Y_ς}	C_{l_ς}	C_{n_ς}					
				29.4	30.4	31.4	32.4	33.4	34.4
#1	+/-30	-0.0460	0.0118	-0.0114	-0.0108	-0.0102	-0.0096	-0.0090	-0.0084
1*5	+/-30	-0.2300	0.0590	-0.0570	-0.0540	-0.0510	-0.0192	-0.0180	-0.0168

Table B.23 BWB3 control surfaces chosen to control the yaw axis

B.4 BWB4 configuration data

Since the BWB4 configuration is geometrically, and relatively to the masses and inertias equal to the BWB3 configuration, these values are not repeated here, but can be found in sections B.1 and B.3. The aerodynamic data was obtained for only one *cg* position located at $X_{cg} = 33.22m$ and for values of alpha equal to 0/10/20 deg. The neutral point was calculated to be at $X_{h_n} = 31.6m$. Thus, the present *cg* position used renders the basic airframe unstable.

	C_L	C_m
Basic	0.3204	-0.040
α	5.8347	0.7412
$q\bar{\bar{c}}/V$	4.3815	-3.5739
η	2.2575	-0.7162

Table B.24 BWB4 longitudinal aerodynamic and control stability derivatives

The longitudinal aerodynamic derivatives, given in Table B.24, were calculated in a wind-axes system while the lateral-directional derivatives, given in Table B.25, are represented in body axes. Taking into account Figure B.3 for the control surfaces, the longitudinal controls are defined as being surfaces 2 to 14, while the lateral controls are the control surfaces 2 and 14 (the most outboard flaps), and, 3 and 13 (the following inboard flaps) referred to respectively as "1" and "2" by the indices used on Table B.25. The rudder controls are referent to the control surfaces on the vertical surfaces in the wingtips, surfaces 1 and 15 of Figure B.3.

	C_Y		C_l		C_n	
	Basic	α	Basic	α	Basic	α
β	-0.1398	0	-0.0104	-1.1233	0.0213	-0.2584
p	-0.372	2.5356	-0.4641	0.1255	0.0631	-0.8337
r	-0.2888	0.485	-0.0787	0.7612	-0.0349	0.0037
ξ_1	-0.0621	0.2134	-0.0710	0	0.0014	-0.0957
ξ_2	-0.041	0.0819	-0.1500	0	0.0041	-0.0504
ς	0.097	-0.0656	0.0253	0.0178	-0.0158	0.0352

Table B.25 BWB4 lateral aerodynamic and control stability derivatives

Appendix C
ROOT LOCUS PLOTS

C.1 BWB4 configuration root locus plots

C.1.1 Roll rate feedback to aileron input

When roll rate is fed back as shown in Figure C.1, the control law is as given in equation (C.1). Introducing this equation into the basic lateral-directional state space matrix equation, given by equation (5.23) of chapter 5, equation (C.2) results.

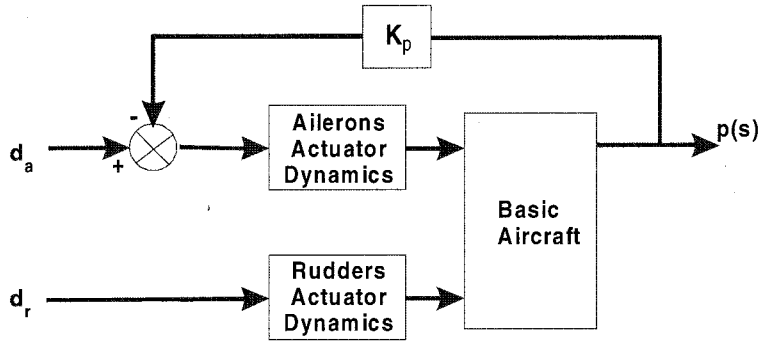

Figure C.1 Roll rate feedback to aileron input

$$u = -K_p p \tag{C.1}$$

$$\begin{bmatrix} \dot{\beta} \\ \dot{p} \\ \dot{r} \\ \dot{\phi} \end{bmatrix} = \begin{bmatrix} y_\beta & (y_p - y_\xi K_p) & y_r & y_\phi \\ l_\beta & (l_p - l_\xi K_p) & l_r & 0 \\ n_\beta & (n_p - n_\xi K_p) & n_r & 0 \\ 0 & 1 & 0 & 0 \end{bmatrix} \begin{bmatrix} \beta \\ p \\ r \\ \phi \end{bmatrix} + \begin{bmatrix} y_\xi & y_\varsigma \\ l_\xi & l_\varsigma \\ n_\xi & n_\varsigma \\ 0 & 0 \end{bmatrix} [\xi \quad \varsigma] \tag{C.2}$$

As it can be seen from equation (C.2) the fed back terms introduced are going to modify the basic aerodynamic derivatives due to the roll rate. If the feedback gain, K_p, is well chosen it is possible to directly influence the roll time constant through the term $(l_p - l_\xi K_p)$ based on the results of Chapter 5. However, as it can be seen from Figure C.2, feeding back roll rate to aileron input influences the remaining lateral-directional characteristic modes.

From Figure C.2, for increasing negative values of the K_p gain, the roll mode time constant decreases, as it would be expect. A reasonably low value of K_p around –0.5, augments significantly this mode. Moreover, increasing negative values of K_p also decreases the spiral mode time constant. This decrease is however smaller for the spiral mode than for the roll mode, when low K_p values are considered. On the other hand, increasing negative K_p values decrease the dutch roll frequency, quite rapidly. So that, for a K_p around –1.5, the dutch roll mode becomes unstable.

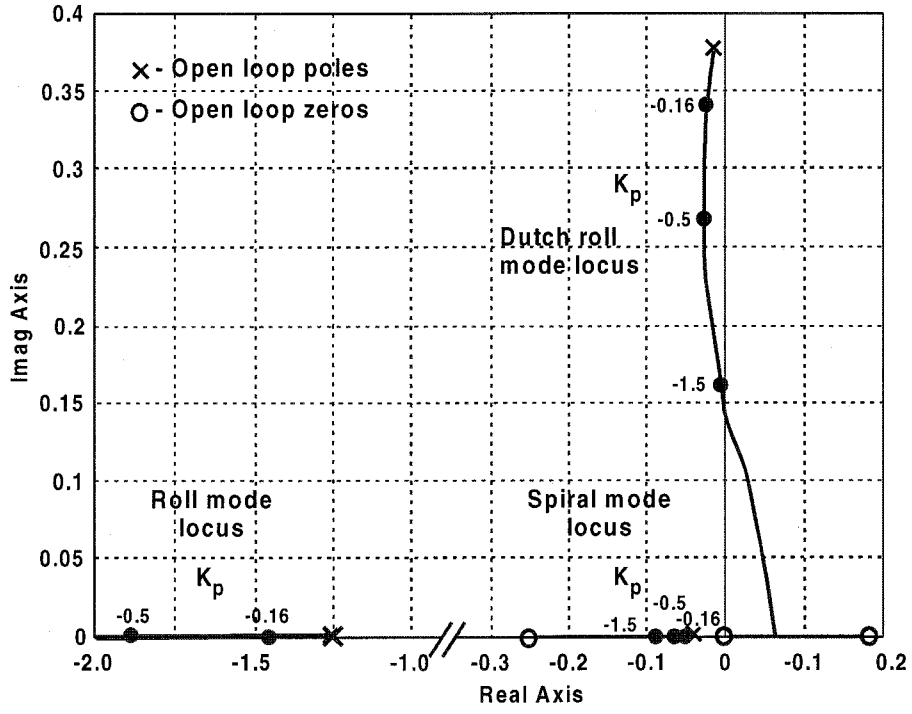

Figure C.2 BWB4 root locus plot – roll rate feedback to aileron input

C.1.2 Sideslip angle feedback to rudder input

For the sideslip angle feedback to rudder input, as shown in Figure C.3, the control law is given by equation (C.3). On substituting the control law into the state space matrix of equation (5.23), equation (C.4) results.

$$u = -K_\beta \beta \tag{C.3}$$

$$\begin{bmatrix} \dot{\beta} \\ \dot{p} \\ \dot{r} \\ \dot{\phi} \end{bmatrix} = \begin{bmatrix} (y_\beta - y_\varsigma K_\beta) & y_p & y_r & y_\phi \\ (l_\beta - l_\varsigma K_\beta) & l_p & l_r & 0 \\ (n_\beta - n_\varsigma K_\beta) & n_p & n_r & 0 \\ 0 & 1 & 0 & 0 \end{bmatrix} \begin{bmatrix} \beta \\ p \\ r \\ \phi \end{bmatrix} + \begin{bmatrix} y_\xi & y_\varsigma \\ l_\xi & l_\varsigma \\ n_\xi & n_\varsigma \\ 0 & 0 \end{bmatrix} [\xi \quad \varsigma] \tag{C.4}$$

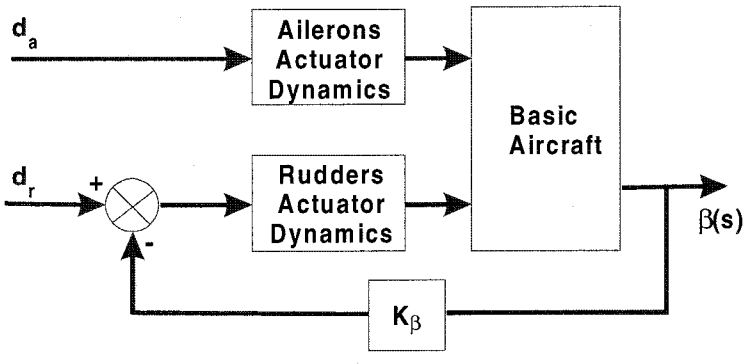

Figure C.3 Sideslip angle feedback to rudder input

From equation (C.4) it can be seen that a well chosen K_β value will increase the term related with the directional static stability, actually $(n_\beta - n_\varsigma K_\beta)$. On the other hand, it will also influence the lateral static stability term, $(l_\beta - l_\varsigma K_\beta)$. As usually n_β and l_β have opposite signs, a favourable augmentation for the directional static stability will also be favourable for the lateral static stability, depending on the values of n_ς and l_ς.

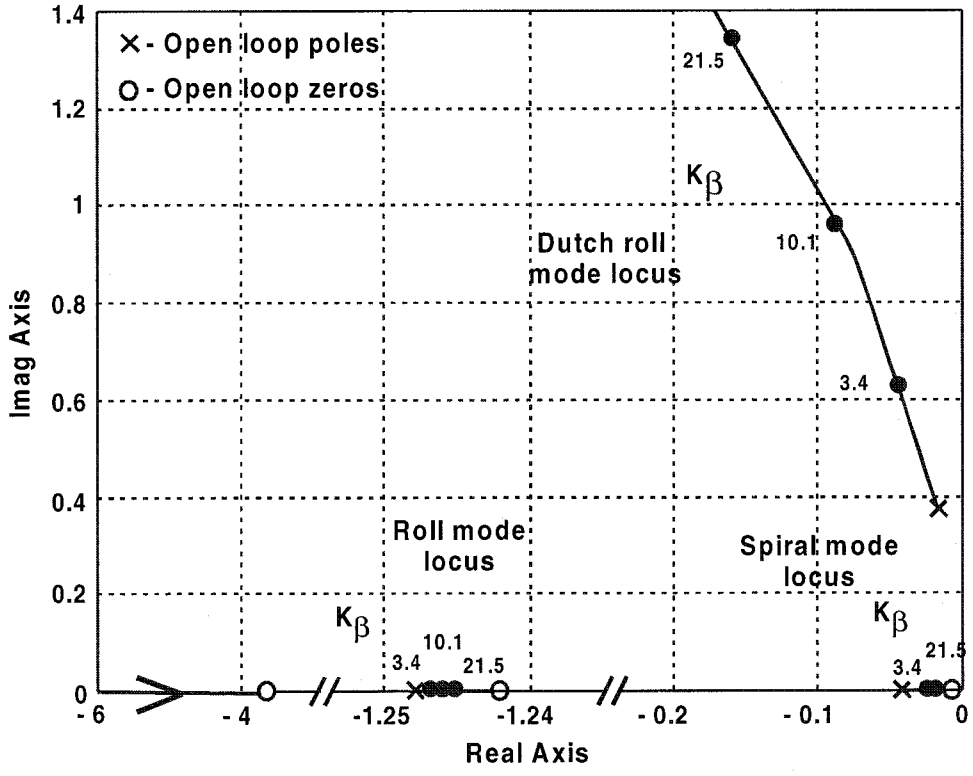

Figure C.4 BWB4 root locus plot – sideslip angle feedback to rudder input

From the root locus plot of Figure C.4, the variation of the lateral-directional characteristic modes can be seen. When increasing the K_β values positively, Figure C.4 shows that the dutch roll mode frequency increases greatly, without almost no change in the roll and spiral modes. However, relatively large values of K_β are necessary, probably higher than 2 or 3, to increase the dutch roll mode frequency to desirable values. On the other hand, the dutch roll mode damping almost do not change.

C.1.3 Yaw rate feedback to rudder input

The yaw rate feedback control law for the feedback shown in Figure C.5 is as given in equation (C.5). When introducing this equation into the state space matrix equation, equation (5.23) of Chapter 5, the matrix equation, as given in (C.6), results.

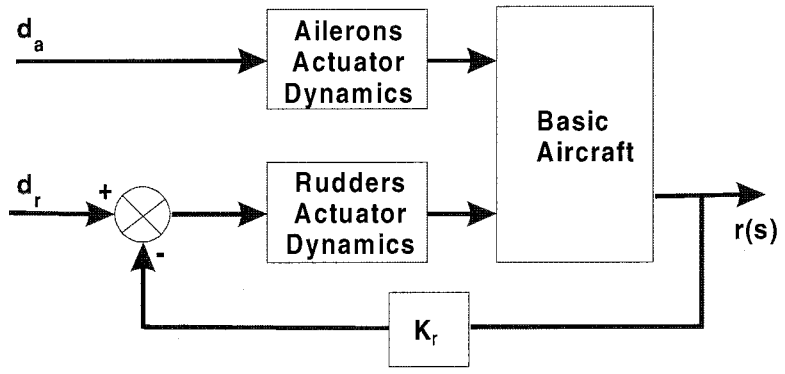

Figure C.5 Yaw rate feedback to rudder input

$$u = -K_r r \tag{C.5}$$

$$\begin{bmatrix} \dot{\beta} \\ \dot{p} \\ \dot{r} \\ \dot{\phi} \end{bmatrix} = \begin{bmatrix} y_\beta & y_p & (y_r - y_\varsigma K_r) & y_\phi \\ l_\beta & l_p & (l_r - l_\varsigma K_r) & 0 \\ n_\beta & n_p & (n_r - n_\varsigma K_r) & 0 \\ 0 & 1 & 0 & 0 \end{bmatrix} \begin{bmatrix} \beta \\ p \\ r \\ \phi \end{bmatrix} + \begin{bmatrix} y_\xi & y_\varsigma \\ l_\xi & l_\varsigma \\ n_\xi & n_\varsigma \\ 0 & 0 \end{bmatrix} [\xi \quad \varsigma] \tag{C.6}$$

From the reduced order models presented on Chapter 5, it was concluded that the dutch roll and spiral modes are complex motions, governed by more than just a single stability derivative. It was seen, however, that the y_r term is considered as dominant in the spiral mode for conventional aircrafts. This was considered also true for some blended wing body configurations. Through this feedback, this term can be changed as shown in equation (C.6). However, the directional stiffness, n_r, is the main parameter to be influenced in this feedback since it is related with the dutch roll damping.

In Figure C.5 the root locus is presented negative values of K_r are used in the yaw rate feedback to rudder input. From Figure C.5 it is seen that the dutch roll mode variation with increasing K_r is smaller than what would be expected. Nevertheless, increasing negative values of K_r increase the dutch roll mode damping, without changing the dutch roll mode frequency significantly. On the other hand, within this K_r variation the roll mode time constant increases, while the spiral mode time constant decreases. This happens until a value of $K_r = -11.1$, when the roll and spiral mode combine originating a second oscillatory mode. Since a K_r value of –11.1 is somehow large for feedback, this second oscillatory mode will never appear. However, relatively large values of K_r are necessary to change the dutch roll mode damping to desirable values.

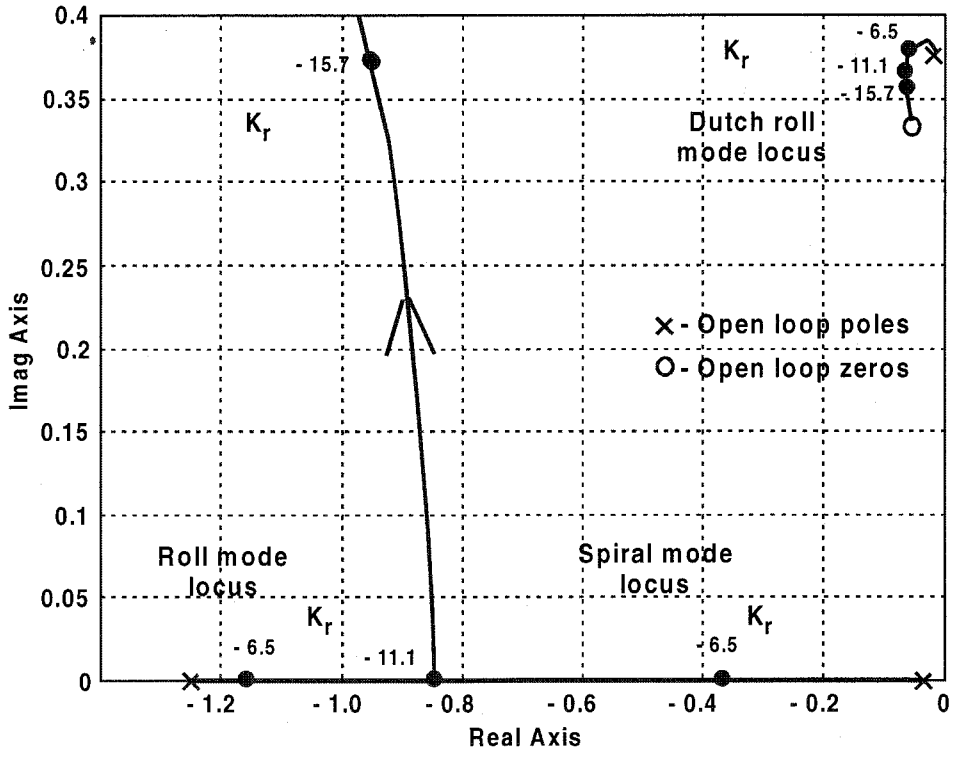

Figure C.6 BWB4 root locus plot – yaw rate feedback to rudder input (negative K_r)

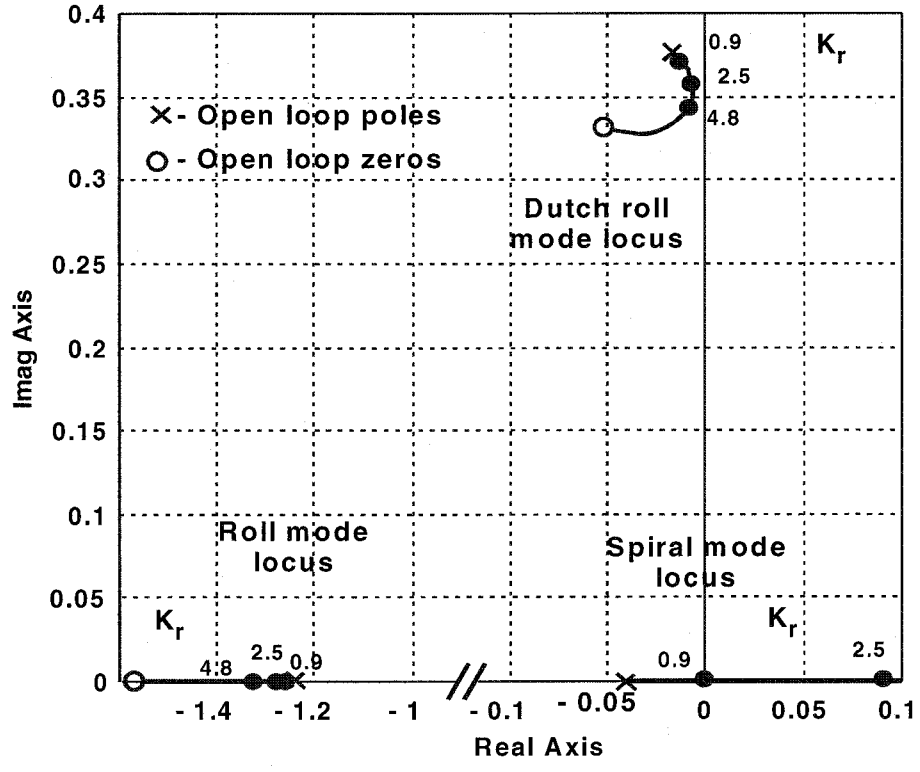

Figure C.7 BWB4 root locus plot – yaw rate feedback to rudder input (positive K_r)

Figure C.7 presents the root locus plot when positive K_r values are considered. From this figure it is seen that the dutch roll mode damping first decreases with increasing K_r values. Only for K_r values higher than 4.8 thus the dutch roll damping increases with further increases of K_r. Furthermore, although the spiral mode time constant initially increases with increasing K_r values, it becomes unstable for a low K_r value, around 0.9. And, although the roll mode time constant decreases its value for increasing K_r, this variation is almost insignificant. Thus, from this analysis it is concluded that positive values of K_r are not interesting for feedback.

C.1.4 Lateral acceleration to rudder input

Lateral acceleration is very easily obtainable by using accelerometers, which are widely used in aeronautic applications. Although not present in the state space matrix as a state variable, lateral acceleration can still be used as a control law. Figure C.8 shows the feedback of lateral acceleration to rudder input, throughout the control law can be deduced, as shown in equation (C.7).

$$u = -K_{a_y} a_y \tag{C.7}$$

$$a_y = \dot{v} - pW_e + rU_e \tag{C.8}$$

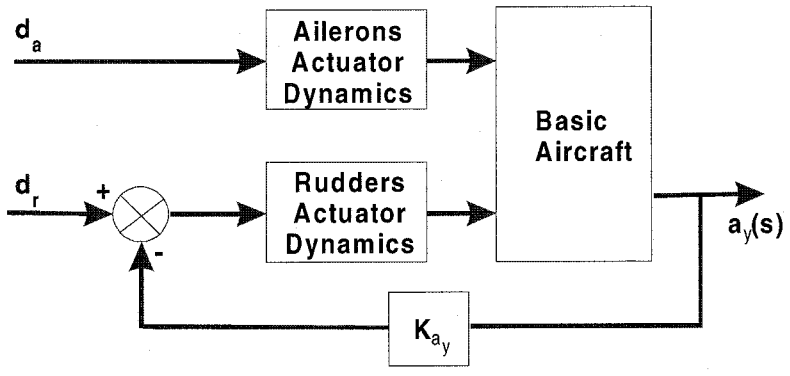

Figure C.8 Lateral acceleration feedback to rudder input

From Cook[99] the lateral acceleration for small perturbations was taken, as given in equation (C.8). From the first row of the matrix equation (5.23), the value of $\dot{v}$ is obtained. Substituting this value in equation (C.8) and substituting the result in equation (C.7), the control law becomes as shown in equation (C.9). Therefore, the result is no more simpler when substituting equation (C.9) in the matrix equation (5.23). Since all terms of the augmented state space matrix are modified with this control law, no previous conclusions can be drawn.

$$u = -K_{a_y}\left[y_\beta \beta + (y_p - W_e)p + (y_r + U_e)r + y_\phi \phi + y_\xi \xi + y_\varsigma \varsigma\right] \qquad \text{(C.9)}$$

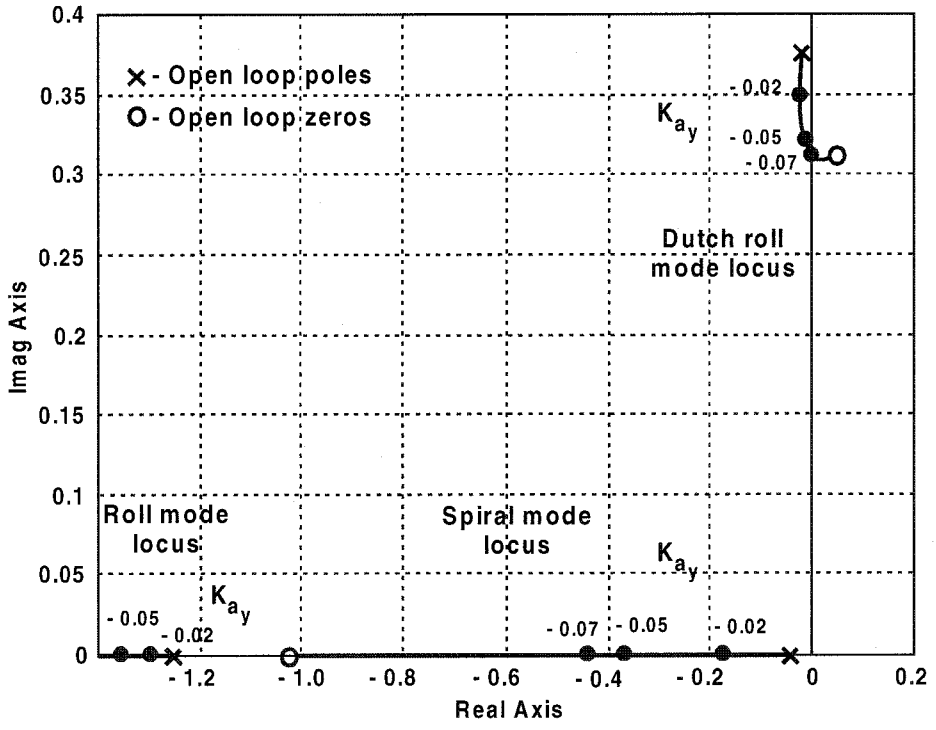

Figure C.9 BWB4 root locus plot – lateral acceleration feedback to rudder input

In Figure C.9 the root locus of BWB4 configuration when using lateral acceleration to rudder input is presented. From the figure it is seen that an increase of negative K_{a_y} values decrease the roll and spiral mode time constants. However, the dutch roll mode frequency and damping decrease, becoming eventually unstable. Furthermore, the sensibility of the spiral and dutch roll modes to K_{a_y} variations is higher than that of the roll mode. As a conclusion, although lateral acceleration is an easily measurable variable and the K_{a_y} gains are of lower value, there is no real interest in feeding this variable back to rudder input.

Appendix D
SIMULATOR

D.1 Flight simulation

D.1.1 Overview

In the early days of aviation, few or no calculation was done before constructing an aircraft. Some drawings were the only planning necessary to construct a flying machine, and any problem would be solved once the machine was ready. As knowledge increased, limited theoretical studies became the practice to confirm what might be expected. However, even after this effort, only when a flying machine was constructed, was total confirmation of its flying and handling qualities achieved.

Aircraft performance increased over time, enabling flight at faster speeds and higher altitudes. Furthermore, aircraft technology has continued to increase in complexity. As presented in Chapter 2, requirements have been developed of aiming to understand which parameters influence flying and handling qualities. Then, wind tunnel tests have been used to evaluate some aerodynamic characteristics, which would then be confirmed and validated, through the construction and flight of a prototype. However, today in the development of high performance aircraft, it is not permitted to construct prototypes without a high degree of certainty that its flying and handling qualities will be acceptable.

The flying and handling qualities specifications that have been developed in the meanwhile, attempt to constrain aircraft designs to satisfactory flying and handling qualities. Through analysis it is possible to conclude that satisfactory flying and handling qualities are present, as long as the aircraft characteristics are within the limits dictated by the requirements. However, due to the complexity and diversity of flying and handling qualities, this has not always been true. History has shown examples of aircraft that turned out to be a disaster when the requirements indicated satisfactory flying and handling qualities, and aircraft which turned out to have pleasant flying characteristic when the requirements have pointed to defective flying and handling qualities.

Another tool to complement flying and handling qualities requirements was necessary, and flight simulation has been playing an important role in flying and handling qualities development for some time now. Early mechanical simulators, such as the Link Trainer, were used for "some" pilot-navigation training. However, computer based simulators were firstly developed for engineering development. As its technology grew in complexity and better levels of fidelity were achieved, the use of simulation as a research and design tool in the development of new aircraft has

increased. Flight simulation appears here as a tool to bring all aircraft aspects together: the basic airframe and the flight control system, the cockpit and the pilot.

Many authors, for example Barnes[58], argue that simulation is a good tool to design aircraft with good flying and handling qualities. Barnes[58] claims that flight simulation makes a vital contribution to the understanding of flying quality requirements and to the clearance of modern aircraft flight controls. Philipps[44] states further that the widespread use of simulators to design satisfactory control systems may make the reliance on written handling-qualities specifications less important than previously. However, Woodcock[56] argues that simulators should not be used independently of written specifications, since it is not possible to simulate all flight phases as encountered in service.

Besides, simulators still have their pitfalls, such as lags in the motion shown by the visual display comparatively to that shown on instruments, non-linear response characteristics, lack of precision cues and others that make such devices misleading for highly accurate research studies, or even for development tests. Following this idea, in the past, and sometimes still today, there have been doubts about the validity of results from ground-based simulator experiments. However, Barnes[58] states that the situation today is that all simulators have a part to play and simulators have been proving their value. One example is the development of the Northrop-Grumman B-2 aircraft where simulation tools were a key factor, as emphasised by Couch and Hinds[32], and Birk and Staley[33].

In this research a similar opinion is shared: flying and handling qualities requirements were already used in the design of flight control systems, and in the analytical assessment of the augmented aircraft flying and handling qualities. Thus, now is the time for real time flight simulation, bringing all aircraft knowledge together and including a pilot in the loop. This way, it is possible to confirm the results reached so far or to find out whether and where more research may be necessary.

D.1.2 Flight simulator description

During this research, three different simulators were used: a small simulator in Delft University of Technology (TU Delft), and the small ground based "AEROSOFT" and the main large ground based simulators in the Cranfield University College of Aeronautics. However, since the TU Delft simulator was only used to test an initial design of the longitudinal flight control system for a short time, it will not be described here. On the other hand, both fixed ground based simulators in Cranfield

University are similar. Due to this similarity the small simulator was used only to modify the basic model, develop new models and to verify all changes made. In the end, it was on the main simulator that final adjustments to the flight control system were made and the flight simulation trials actually took place. Therefore, only this main simulator, which is shown in Figure D.1, is described.

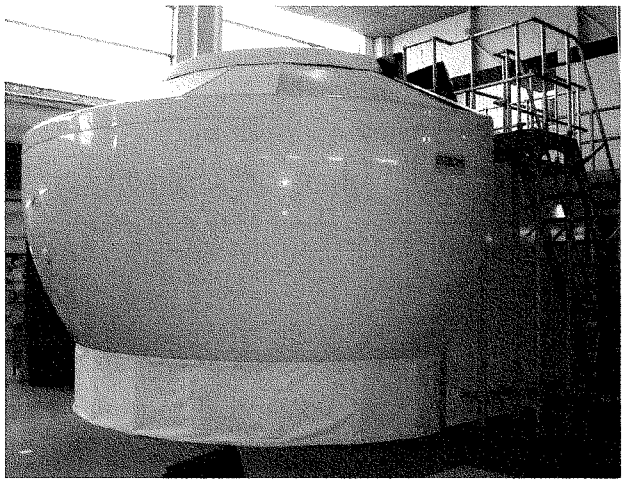

Figure D.1 Cranfield University flight simulator

Barnes[58] states that a research simulator breaks down into several components: the cockpit, the stick feel, the modelling (or physical models), the visual display, the motion system and an architecture bringing all the previous components together.

D.1.2.1 Simulator structure

Allerton[111] comments that computing power is no longer a restriction on the complexity of the aircraft model and flight control system. Models used for flying qualities work must have a high iteration rate, better than 300 solutions per second is desirable. In these circumstances, ground based simulators have the advantage over airborne simulators, because more comprehensive computing facilities can be provided in a ground installation.

The main ground based fixed Cranfield University simulator structure is made up of four PCs, as shown in Figure D.2, and a Silicon Graphics Onyx-II workstation connected to a local dedicated Ethernet. Between the four PCs, one provides the airframe flight model and the primary flight display. A second PC provides the engine model and the engine displays. A third PC emulates the navigation system and the navigation displays. The fourth PC is used as an instructor station system, having a Windows-like user interface. It also provides standard instructor station functions to

enable simulator sessions to be monitored and controlled. The instructor station is furthermore used to provide a flight data recording facility.

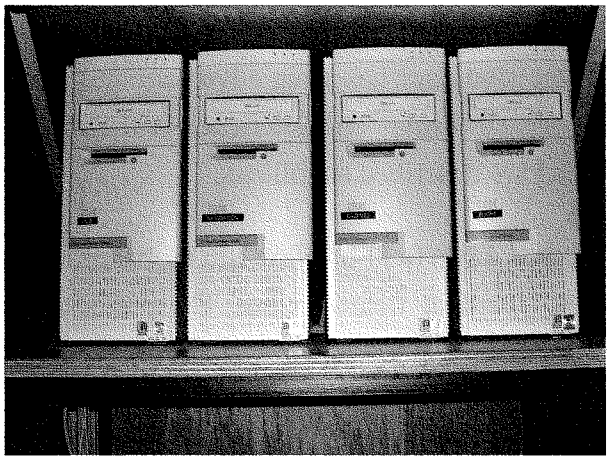

Figure D.2 Cranfield University flight simulator PCs

The Ethernet packets contain aerodynamic data, engine data and avionics data and this information can be displayed on-line, as well as stored for off-line analysis and to replay simulator events. Ethernet is used since it provides a means of high-speed communication between computers, with the advantages of being a mature, reliable and low cost technology. Allerton[111] states that with a simple protocol the delays due to being designed to cope with concurrent transmissions, can be minimised. Furthermore, since there are five processors, one in each PC plus the workstation, less than 10% of the 20ms frame is dedicated to inter-processor data transfers, for each processor.

The simulator is based on a modular concept in order to achieve real-time performance. This means, the computation of the flight model and associated aircraft displays is accomplished at an iteration rate of at least 50Hz, thus ensuring the fidelity of the models and displays. This modular approach, where modules are partitioned across several PCs, makes it easy to develop, integrate and test each module. The modules can be assembled from software libraries and combined and integrated for specific research applications. Specific flight and aircraft models, engine models, aircraft displays, sensors and even weather modules can easily be used. By this means, it was possible and easy to make the necessary changes to simulate the blended-wing-body aircraft. The changes made to some modules of the basic program are presented later in this appendix.

D.1.2.2 Visual display

Barnes[58] states that the type of work determines the display requirement. Again, display deficiencies, such as time delay or resolution can affect flying qualities assessments. An airborne simulator has a big advantage in this respect. Nevertheless, from Allerton[111], the visual display characteristics of the main Cranfield University simulator were taken and are described as follows.

The projection system is a 180° field-of-view SEOS Panorama providing full cross-cockpit viewing and 40° vertical field-of-view. The projection system provides the flight crew with an out-of-the-window view with natural depth and distance and this specific system is used in many airline flight simulators, as shown in Figure D.3. A Silicon Graphics Onyx-II image generator providing three 60° channels at 50 Hz is the responsible for the generation of the visual. This state-of-the-art visual system is used in many large-scale simulators and provides a fully textured image with anti-aliasing to eliminate the jagged edges found on lower fidelity visual systems.

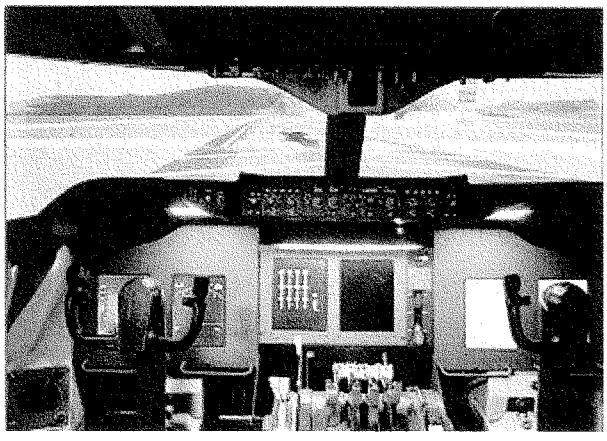

Figure D.3 Visual image in the cockpit' simulator (Ref. 111)

D.1.2.3 Cockpit

Barnes[58] is of the opinion that for flying and handling qualities research, there is no need to use a cockpit representing a particular aircraft. The transport aircraft should utilise a cockpit representative of a transport aircraft, whilst the seating position for a fighter should correspond in terms of geometric location relative to stick, controls, and displays.

The Cranfield University simulator, as Allerton[111] says, has been designed as a generic future advanced flight deck. An original British Airways flight deck, used as a

cockpit procedures trainer for the Boeing 747/100, has been completely refurbished. The analogue instruments have been replaced by six LCDs, the centre pedestal and flight controls have been overhauled and the navigation, communications and flight control panels have been replaced by modern simulated aircraft equipment, manufactured by Elan Informatique. Views of the simulator cockpit interior are shown in Figures D.3 and D.4. The displays can be re-programmed to accommodate a range of aircraft instruments and the flight deck contains a mixture of Boeing and Airbus flight control panels and flight control systems, including both conventional control columns and side-sticks. In this way, any military or civil aircraft modelled can be readily integrated. For the present research, the flight deck configuration used was that representative of a civil transport aircraft.

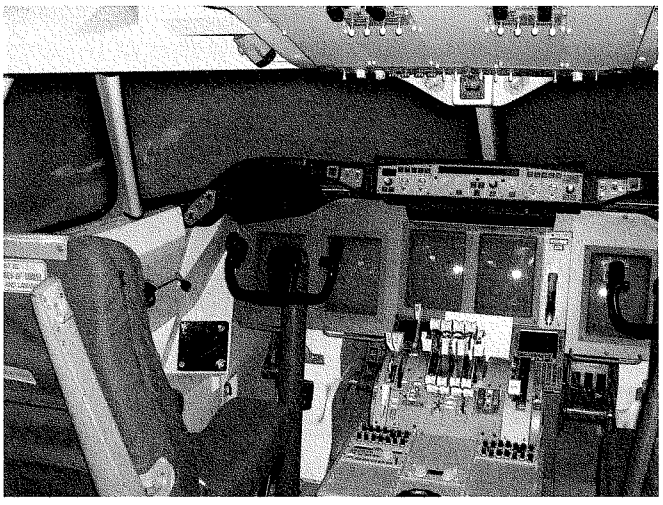

Figure D.4 Simulator cockpit disposition

Modern Electronic Flight Instrument Systems (EFIS) displays are used, where the information and symbology on the display is generated in the form of computer graphics. EFIS displays contain sliding scales, compass segments and attitude information. A real-time graphics library has been implemented to provide the set of graphical primitives found in modern aircraft EFIS displays. The displays are actually generated in the flight simulator using a standard Pentium PC with a standard SVGA graphics card. The real-time graphics library is compliant with the VESA graphics standard.

The performance of the real-time graphics display library has been analysed to ensure that it maintains a 50 Hz update, even with maximum graphical change between consecutive frames. In practice, update rates of over 300 Hz have been demonstrated for an emulation of the Boeing-747 *primary flight display* (PFD) and navigation displays.

As seen in Figure D.3, the front panel comprises CRT screens which show the primary, secondary and engine flight instruments. The primary flight display contains the *Horizon Indicator* (HI) with *Instrument Landing System* (ILS) and glide slope indication incorporated, the *Speed Indicator* (SI) in tape format with a speed trend indicator incorporated, the altitude indicator also in tape format with *Radio Altitude* (RA) indicator at the bottom. At the right of this display, from the pilot view, is the secondary flight display with possibility for several representation modes such as position of the aircraft relatively to the runway, ILS guides, etc. The knob to switch between these several modes of the secondary flight display is on the top of the front panel, with the navigation aids and communication displays. To the right of the primary and secondary displays, at the centre of the panel, is the engine systems display, which also shows information about other systems, such as the landing gear, flap and spoiler position. The engine information consists of the engine EPR, etc.

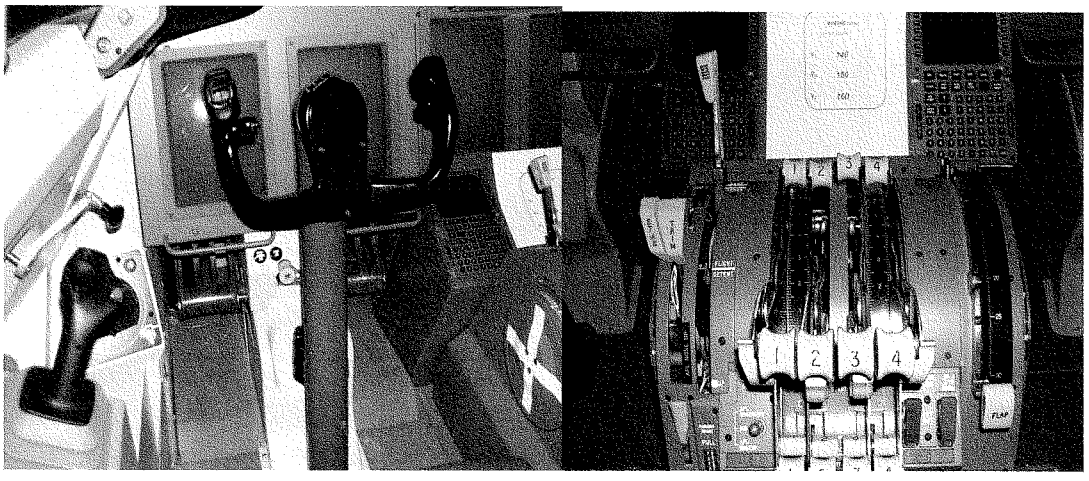

Figure D.5 Simulator control wheel, sidestick and throttle system

The pilot control is a centre pedestal wheel, which has a stall shaker included. Thus, instead of an audible stall warning, the pilot feels the control wheel shaking when entering the stall. A side stick is also available to the pilot on the left, as shown in Figure D.5. On the centre pedestal there are four throttle levers, with possibility to couple them two by two. On the left side of the levers is the longitudinal control wheel trim, and on the right side is the flaps lever. Behind the throttle levers is the rudder trim and small buttons to trim the ailerons. On the overhead panel there are a many knobs and buttons. Included in these, are the engine starter knobs localized right up and between the pilots. These knobs have to be tilted and maintained tilted until a certain rpm value has passed to start the engines.

D.1.2.4 Stick feel

For handling qualities work an accurate representation of the stick force gradient, friction, travel, non-linear gearing and other relationships between the pilot's input and control surface deflection is essential. In spite of the recommendation of Barnes[58], measures of the stick force gradient, friction and travel was not available. The only available information already included in the simulator model was the stick and pedals gearing to control surface deflections.

D.1.2.5 General

The components described above are all important and are linked together to provide an engineering research tool. Furthermore, Barnes[58] comments that the choice of the operating system for easy operation is important as well. Successful investigations require the ability to repeat cases and to change parameters quickly, and to record qualitative and quantitative results. Each of the four Cranfield University simulator PCs has Microsoft Windows operating system, and uses MODULA-2[112] as the programming language for the simulation software.

Furthermore, Allerton[111] explains that aerodynamic, engine and avionics data are broadcasted by three PCs as Ethernet packets. These packets are assembled by the instructor station computer and stored either in memory or copied to disk as raw Ethernet packets. Typically, these packets contain 512 bytes of flight test data, so that 1.5 Mbytes of data is stored per minute. A windows based data analysis package has been developed to record and display flight data. Any of the flight variables can be plotted at any phase of a simulator session in appropriate units and scaling.

In effect, a full flight data recording and replay system has been developed, based around the capture and storage of Ethernet packets and standard PCs. Data stored on disk can be retrieved off-line. Because the stored packets have the same format as run-time packets, the same software is re-used for off-line display of recorded data. In addition, stored data can also be replayed through the simulator.

An additional package, termed *Script*, has been developed to support research in the simulator. Script allows a complex simulator session to be defined as a simple description of simulator conditions and events and also to define the sequencing of data recording and the format and presentation of recorded data. The recorded output can be imported directly into an Excel spreadsheet.

The Script program is implemented as a parallel process running on the instructor station. The specific Script program is selected, automatically compiled and then executed in real-time. The flight conditions and events are detected from inspection of the incoming Ethernet packets. Flight situations are invoked by instructor station commands, added to the Ethernet packet transmitted by the instructor station, for example to set the visibility or to fail a sub-system.

D.1.3 Software module changes for BWB simulation

As stated in the simulator description, the computation is partitioned through four PCs,

1) the FLIGHT MODEL computer containing the flight model and the primary flight display,
2) the ENGINE computer containing the engine model and engine displays,
3) the NAVIGATION computer which emulates the navigation system and navigation displays, and
4) the IOS computer containing the instructors station.

Thus, each computer has part of the simulation program, which comprises several modules and procedures assembled using MODULA-2 libraries constitute each module. The basic flight model presented in the simulator was that of the Boeing 747-400 with respective engines for the engine model. Since in this research a BWB aircraft was being used some changes were required, though only to the aircraft flight model and engines model. However, in the end the only modifications made were limited to the FLIGHT MODEL. The ENGINE, NAVIGATION and IOS computer software were retained as is.

D.1.3.1 *Model* module

At first it was thought that, in order to set up the simulator for a blended-wing-body configuration, only the substitution of aerodynamic data would be necessary. Thus, only the file with the aerodynamic data stored within the FLIGHT MODEL computer would be changed. However, all blended-wing-body aerodynamic data for configurations BWB3 and BWB4 was referenced to a body axis system. On the other hand, in the case of the B747-400 configuration the aerodynamic data is referred to a wind, or stability, axis system as usual. With aerodynamic data referred to wind axes, the aerodynamic forces are calculated first in wind reference axes, and then

transformed to body reference axes. In the case of the blended-wing-body, the aerodynamic forces are automatically calculated with respect to body axes, without the need for this extra calculation step.

The aerodynamic data for the B747-400 configuration is given for one point of reference only; the aerodynamic centre. However, during simulation, forces are calculated relative to the centre of gravity. Thus, extra moments are calculated due to the translation of aerodynamic forces from the aerodynamic centre to the centre of gravity. However, as explained in Chapter 3, the blended-wing-body forces and moments are already given relative to the centre of gravity. Furthermore, for the BWB3 configuration different sets of data exist for different *cg* positions. Therefore, the algorithms used to calculate the aerodynamic forces and moments are different for the B747-400 and the blended-wing-body applications.

Thus, the task of modifying the simulator program was not to simply to substitute aerodynamic data. Deeper changes were necessary in several modules. Actually, the *Model* and *Aero* modules, where the aerodynamic forces and moments are calculated and the aerodynamic data is stored, were modified. In the end the entire structure of the module *Model* was changed, since the procedures that constitute the module were found to be rather large. Thus, these larger procedures were split into smaller new procedures, although the code was kept the same. This was done to give better visibility of the functionality of the flight simulation.

In Table D.1 the relations between the few procedures existent on the initial B747-400 *Model* module and the more numerous procedures of the final BWB *Model* module are presented. The actual simulator code for this module is presented in paragraph D.2.1 and D.2.2 of this appendix. As can be seen, almost all new procedures have a direct relation with parts of code of the old *FlightModel* procedure. Furthermore, the new *FlightModel* procedure is only a list of procedures to be called to accomplish the flight simulation, showing clearly the simulation sequence.

Special attention is drawn to the procedures *AeroCall* and *BodyToStab*. The *AeroCall* procedure, as the name suggests, calls other procedures within the *Aero* module, that calculate the aerodynamic derivatives for the present flight condition. With this information, *AeroCall* then calculates the aerodynamic forces and moments already in body reference axes. The *BodyToStab* procedure transforms the aerodynamic Normal, Axial and Side forces in body reference axes to the stability reference axes. In other words, it calculates the Lift and Drag forces. Although not necessary in the *Model* module itself or for the FLIGHT MODEL computer, the Lift and Drag information

was necessary to calculate information for modules within other computers, e.g., the NAVIGATION computer. The flexibility for changing modules at will is possible as long as variables and relations between other modules are maintained.

B747-400 Model Procedures	Procedure description	Correspondence with BWB Model Procedures
SetDCM	Transformation matrix from body to earth axis	**SetDCM**
SetQuaternions	Calculate the quaternions from the Euler angles	**SetQuaternions**
Signx	Change sign	**Signx**
FlightModel	Read inputs from pilot's commands	**ReadInputs**
	Transform the inputs read	**TransformInputs**
	Stall warning	**CallStall**
	Calculate speed, Mach number, alpha and beta angles	**SpeedAlphaBeta**
	Alpha maximum and stall warning	**CallStall**
	Aerodynamic coefficient derivatives	**AeroCall**
	Calculate thrust	**EngineModel**
	Drag and Lift	**BodyToStab**
	Calculate G number	**GsForces**
	Friction coefficients	**Friction**
	Compute total forces	**TotalForces**
	Calculate linear accelerations	**LinearAccelerations**
	Calculate linear velocities	**LinearVelocities**
	Introduce turbulence in the speed and change to earth reference axis	**SpeedToEarth**
	Calculate aircraft position	**Position**
	Call ground model or transform roll and yaw moments to stability axis	**GroundForces**
	Compute total moments	**TotalMoments**
	Angular accelerations	**AngularAccelerations**
	Angular velocities	**AngularVelocities**
	Ground handling	**Included in the FlightModel procedure**
	Compute quaternions values	**IntQuaternions**
	Attitude	**Attitude**
GroundModel	Calculate ground moments	**GroundModel**
No procedure correspondence with the B747-400	Load the aircraft model data	**LoadModel**
	Calculate the aircraft inertias	**Inertias**
	Calculate the gravity forces	**GravityForces**
	Introduce lag in the engine response	**EngineLag**
	Transformation matrix from body to stability axis	**SetDCMStab**
	Call all the above functions in the appropriate order	**FlightModel**

Table D.1 Procedures from the B747-400 and the BWB *Model* modules

Thus, *SetDCMStab* procedure was created to transform vectors between the body reference axes and the stability reference axes. Since this operation was not done on the initial B747-400 simulation, there is no direct correspondence with any previous module, procedure or part of code. The new *EngineLag* procedure also has no

correspondence to the B747-400 code. This procedure will be presented later in this chapter. Other procedures were created due to specific conditions of the blended-wing-body data and the way it was stored. For example, the *LoadModel*, *Inertias* and *GravityForces* procedures presented next.

LoadModel is a procedure created to load data between different BWB models, including different *cg* positions, or between different flight control systems. A variable from the old B747-400 code, *CgPosition*, was used with a different function, namely that of defining the aerodynamic and flight control system data to load. Since this variable can be defined through the instructor station, the blended-wing-body model configuration and flight control system could be changed during flight simulation trials without the need to edit, change and compile the code again.

Inertias is a procedure which calculates inertial and mass quantities for use in other procedures. It was created with the idea to update the inertial and mass values, in case mass was allowed to vary during a simulation run. However, data related with mass and inertia changes have not been available during the research program, therefore, the procedure never worked the way it was originally meant to do. In the same way, *GravityForces* is a procedure created to calculate the aircraft weight with mass variations during a simulation run. This procedure at the same time transforms the weight force usually represented in earth reference axes to body reference axes. In the original B747-400 model this step was done when forces were summed. However, in this way more clarity seemed to be achieved.

D.1.3.2 *Aero* and *AeroData* modules

The B747-400 *Aero* module is used to calculate the aerodynamic coefficients in stability or wind reference axes, taking into account angle of attack, flap deflections and landing gear deployment. It is also in this module that mass and inertias were calculated. However, as said before, the blended-wing-body aircraft aerodynamic data is given in body reference axes. Moreover, the present blended-wing-body configurations do not possess high-lift surfaces, generally known as flaps, and the control surfaces located in the wing trailing edge, being flaps, influence the aerodynamic forces in a different way. For these reasons the *Aero* module was modified. Many of the original procedures were maintained, but they were internally modified to accommodate the particularities of the blended-wing-body aerodynamic data. This is shown in Table D.2 by the large quantity of procedures common to both modules. Table D.2 also shows that the procedures not present in the BWB *Aero* module are those related with the concepts of lift and drag coefficients, C_L and C_D. As

the BWB data is given in body axes, it makes more sense to talk about normal and axial coefficients, C_Z and C_X, and therefore the new procedures unique to the BWB model. The simulator code referent to this module is presented in paragraph D.2.3 and D.2.4.

Common Procedures	Procedures unique to B747-400	Procedures unique to BWB
AeroMaxAlpha, AeroCz0, AeroCz1, AeroCyBeta, AeroCyDr, AeroCm0, AeroCmAlpha, AeroCmDe, AeroCmQ, AeroCmAlphaDot, AeroClBeta, AeroClDr, AeroClDa, AeroClP, AeroClR, AeroCnBeta, AeroCnDr, AeroCnDa, AeroCnP, AeroCnR	AeroCl, AeroCd, AeroClTail, AeroClfw, AeroCnBetaDot, IxxMoment, IyyMoment, IzzMoment, IxzMoment	AeroCzQ, AeroCzDe, AeroCx0, AeroCxk1, AeroCxk2, AeroCyDa, AeroCyP, AeroCyR, Coefficients, NormalCoef, AxialCoef, LateralCoef, RollingMtCoef, PitchingMtCoef, YawingMtCoef.

Table D.2 Procedures of the *Aero* module for the B747 and BWB models

The procedures *AeroCx0*, *AeroCxK1* and *AeroCxK2* together with *AxialCoef,* actually do the same as the procedure *AeroCd.* The procedure *AeroClTail* has no meaning for these BWB configurations, since there is no tail. The *AeroCzDe* procedure was created, to calculate the contribution to the normal force from the control surfaces deflection, not important in the case of conventional configurations. Other differences shown in Table D.2 are due to minor differences in the present BWB data. *AeroCnBetaDot* is a good example, which was removed since no $\dot{\beta}$ data is given for the present BWB configurations.

On the other hand, procedures *AeroCyDa*, *AeroCyP* and *AeroCyR*, which do not exist for the B747-400 flight model, were created. The procedures *IxxMoment*, *IyyMoment*, *IzzMoment* and *IzzMoment* of the B747-400 program were changed into the *Inertias* procedure, and placed in the *Model* module, as explained above. The remaining procedures unique to the BWB code calculate the aerodynamic coefficient derivatives, and the forces and moments coefficients. These procedures are used by the *AeroCall* procedure within the *Model* module.

The *AeroData* module was created to store the several blended-wing-body data. For that two different RECORD structures were defined. One structure called *AircraftRecord* was created to store aerodynamic and other general aircraft data. Table D.3 shows how the *AircraftRecord* structure is organized. The other structure was created to store the flight control system, therefore its name *FCSRecord.* The organization of this structure is presented in Table D.4. Then, *BWB* was defined as a structure of the *AircraftRecord* type, while *AFCS* was defined as a structure of the *FCSRecord* type.

BWB - Aircraft Record		
Geo – Geometric data Record	**Name**	Configuration identification
	B	Aircraft span
	S	Wing reference area
	Mac	Mean aerodynamic chord
Mass – Mass properties data Record	**Mass**	Configuration mass
	Xcg, Ycg, Zcg	Centre of gravity coordinates
	Ixx, Iyy, Izz	The 3 moments of inertia
	Ixy, Ixz, Iyz	The 3 products of inertia
XF - Axial coefficient force data Record	**Cxo**	Basic axial force coefficient
	Cxk1	First parameter of the Drag Polar
	Cxk2	Second parameter of the Drag Polar
	CxFi	Derivatives due to elevators
YF – Lateral force coefficient derivatives data Record	**Cyo**	Basic lateral force coefficient
	Cybo, Cyb_a	Derivatives due to sideslip
	CyPo, CyP_a	Derivatives due to roll rate
	CyRo, CyR_a	Derivatives due to yaw rate
	CyAio, CyAi_a	Derivatives due to aileron deflection
	CydRo, CydR_a	Derivatives due to rudder deflection
ZF – Normal force coefficient data Record	**Czo**	Basic normal force coefficient
	Cza	Derivative due to angle of attack
	Czq	Derivative due to pitch rate
	CzFi	Derivative due to elevators deflection
Rmt – Rolling moment coefficients Record	**Clo**	Basic rolling moment coefficient
	Clbo, Clb_a	Derivatives due to sideslip angle
	ClPo, ClP_a	Derivatives due to roll rate
	ClRo, ClR_a	Derivatives due to yaw rate
	ClAio, ClAi_a	Derivatives due to aileron deflections, i=1…8
	CldRo, CldR_a	Derivatives due to rudder deflection
Pmt – Pitching moment coefficients Record	**Cmo**	Basic Pitching moment coefficient
	Cma	Derivative due to angle of attack
	Cmq	Derivative due to pitch rate
	CmFi	Derivatives due to elevator deflection
Ymt – Yawing moment coefficients Record	**Cno**	Basic yawing moment coefficient, i=1…8
	Cnbo, Cnb_a	Derivative due to sideslip angle
	CnPo, CnP_a	Derivative due to roll rate
	CnRo, CnR_a	Derivative due to yaw rate
	CnAio, CnAi_a	Derivatives due to aileron deflection, i=1…8
	CndRo, CndR_a	Derivatives due to rudder deflection
Point	**x, y, z**	Pilot station coordinates, or any other point
Lgear – Landing Gear Record	**MainGearCG**	Axial distance from the main gear to the CG
	NoseGearCG	Axial distance from nose gear to the CG
	CGToGround	CG normal distance to the Ground
	GearOffset	Distance between the right and left main wheels
	XoM, XoN	Main and nose gear displacement when at rest
Eng – Engine Record	**Armi, i=1…3**	Lateral distance from engine to A/C centreline
	Height	Distance from engines to ground
Note: subscript o means a basic coefficient. Subscript _a means a coefficient due to angle of attack variation. Subscript i means the number of elements of the same type existents.		

Table D.3 Aircraft Record structure and the type of data stored

AFCS – FCS Record		
LatFCS - Lateral FCS Record, feedback input to aileron	**Kp**	Roll rate feedback gain
	Kb	Sideslip gain
	Kphi	Roll attitude gain
	Ki	Integral gain for a roll rate command FCS
	Kpi	Proportional gain for a roll rate command FCS
	m	Feedforward gain for a roll rate command FCS
LongFCS - Longitudinal FCS record, feedback input to elevator	**Kq**	Pitch rate gain
	Ki	Integral gain for a pitch rate command FCS
	Kp	Proportional gain for a pitch rate command FCS
	m	Feedforward gain for a pitch rate command FCS
	Ka	Angle of attack gain
DirFCS - Directional FCS Record, feedbacks input to rudder	**Kr_i**	Yaw rate gain
	Kb_i	Sideslip angle gain
	Kari_i	Aileron to rudder interconnected gain
	Two	Washout filter time constant
	Kay	Lateral acceleration gain
PreF - Pre-Filter Record	**T2d**	Desired Ttheta2
	T2a	Actual Ttheta2
Note: subscript _i means several elements of the same type.		

Table D.4 Flight control system Record structure and type of data stored

Then, through the use of two procedures, *SetupModel* and *SetupFCS*, called by the *LoadModel* of the *Model* module the *BWB* and *AFCS* structures are loaded with the blended-wing-body configuration and flight control system as specified in the *CgPosition* variable. The *SetupModel* has stored six BWB3 sets of data corresponding to the six BWB3 *cg* positions, plus the BWB4 data set. The *SetupFCS* has stored several sets of flight control system gains for each of the seven previous blended-wing-body possibilities. The gain sets may represent different flight control systems since unwanted gain elements are set to zero. These can be seen in the simulator code presented in paragraph D.2.5 and D.2.6.

D.1.3.3 *EngineModel* and *EngineLag* procedures

With respect to the engines, the original B747-400 possesses four engines, while all of the present blended-wing-body configurations have only three. Besides, since the aircraft masses are different, the static thrust of each engine is different. Thus, it looked like it would be necessary to change the engine model. On the other hand, blended-wing-body configurations use similar engines to the B747-400 and although being different in number, or delivering a different amount of thrust, in general gas turbines behave in the same manner with altitude changes and pilot demands. Furthermore, the time for the research was limited and available data did not enable the development of a completely new engine model.

Thus, it was decided to keep the original engine module and to create simple engine procedures inside the *Model* module instead. These procedures are *EngineModel* and *EngineLag*, as already presented in Table D.1. The first solution tried was to use the throttle lever position of each engine from the *Engines* module, in the ENGINE MODEL computer, and simply multiply it by the maximum static thrust expected for blended-wing-body configurations. This resulted in the *EngineModel* procedure, which gave the immediate thrust change in response to pilot demands.

However, since the simultaneous thrust change with throttle lever change does not represent reality, the *EngineLag* procedure was created to introduce a simple lag in the engine response to the throttle levers. A simple first order lag, with a time constant of 1 second was found to give a better representation of reality. However, as a consequence the complete engine model of the original B747-400 simulation was not used.

The second attempt used directly the thrust of each engine from the B747-400 model, instead of the throttle lever position. Thus, the *EngineModel* procedure was modified to use the individual thrust from only three engines, sum them up and multiply then by a factor which would augment the total thrust to that expected for blended-wing-body configurations. Moreover, multiplying the thrust of each engine by the distance of the thrust line to the centreline, resulted in the engine moments, as modelled already in the first attempt. The engine moment was not multiplied by the augmenting factor since on Chapter 4 it was found impossible for the BWB4 configuration to trim an engine failure.

D.1.3.4 *FCS* module

As seen in Chapters 7 and 8, an important part of this research is the flight control system design to improve the basic blended-wing-body flying and handling qualities. However, the B747-400 model has only autopilot control systems incorporated in the NAVIGATION computer, and a simple yaw damper incorporated in the aerodynamic model of the *Aero* module. A new module called *FCS* was therefore created, in the FLIGHT MODEL computer, to accommodate all flight control systems. As seen above, the *AeroData* module already accounted for the flight control system gains. In Table D.5 all procedures of the *FCS* module are presented, separated into the axis to which they relate, longitudinal or pitch, lateral or roll, and directional or yaw. The simulator code for the *FCS* module can be seen in paragraph D.2.7 and D.2.8.

FCS	Procedure name
Longitudinal flight control system procedures	PreFilter, FeedForward, LongFeedBack, TurnCompensation, LongFCS
Lateral flight control system procedures	LatFeedBack, RollFeedBack, BankAngle, RollRateCmd, LatFeedFwd, LatFCS
Directional flight control system procedures	SideFeedBack, AilRudInt, KariWO, YawFeedBack, AccFeedBack, DirFCS
Others	Actuator

Table D.5 FCS module procedures

The procedures *LongFCS*, *LatFCS*, *DirFCS* and *Actuator*, although defined in the *FCS* module, are actually used in the *Model* module. The *Actuator* procedure, as the name suggests, simulates the actuator dynamics as a second order system. *LongFCS*, *LatFCS* and *DirFCS* are the main procedures that determine the response of each axis flight control system by calling other procedures. *LongFCS* is able to call four other procedures: *PreFilter*, *FeedForward*, *LongFeedBack* and *TurnCompensation*. Depending on whether each of these procedures are called or not, different longitudinal control laws result. Different flight control system structures can also be chosen through the values assigned to the different flight control system gains, as mentioned before. For example if *AFCS.PF.T2d* and *AFCS.PF.T2a*, the gains used in the *PreFilter* procedure are made equal to one, the pre-filter is "cleared" from the longitudinal flight control system, although it is still called by the code. It is as if the longitudinal flight control system of Figure 7.6 of Chapter 7 would be simulated instead of that in Figure 7.5 of the same chapter.

The *LatFCS* procedure is an even better example of the possibility to simulate different flight control system structures. *LatFCS* can call up to six other procedures, actually all the other procedures in the lateral flight control system block of Table D.5. However, these cannot all be used at the same time. To simulate the roll rate command system of Figure 8.2 of Chapter 8, only the *RollRateCmd* and *LatFeedFwd* procedures are used together. *LatFeedback*, *RollFeedBack* and *BankAngle* procedures are simple feedback loops. The variables fed back are lateral acceleration, roll rate and roll attitude respectively. These three procedures can be used either one at a time or combined. As before, the control of the flight control system structure is done either through the code, or through the flight control system gains.

In the same way, the *DirFCS* procedure can call four other different procedures, *SideFeedBack*, *AilRudInt*, *YawFeedBack* and *AccFeedBack*, to simulate several flight control system structures. Combining the *SideFeedBack*, *YawFeedBack* and *AilRudInt*

procedures the flight control systems of Figures 8.5, 8.7 and 8.9 of Chapter 8, can be simulated. The *KariWO* procedure simulates a washout filter for the aileron to rudder interconnection, and can be called within the *AilRudInt* procedure. The *AccFeedBack* procedure simulates a simple feedback back loop of lateral acceleration.

D.1.3.5 Ground module

As mentioned before in this thesis, the approach and landing tasks are the most demanding flight phases for a civil transport aircraft. Thus, they are frequently used in flight simulator trials to assess aircraft flying and handling qualities. It was intended to use these flight missions in blended-wing-body flight simulation trials from the outset of this research. In an approach and landing, the aircraft is airborne for most of the task. Only for the last seconds, during the flare and touchdown, the aircraft touches the runway and rolls on the ground. Although lasting only a few seconds within all mission this transition is important, since it is the flight culmination where success or otherwise is determined.

The ground model is, therefore, an important part of the flight model since it determines the forces and moments at the moment the wheels touch the ground and during ground roll. Thus, the ground model should be as accurate and representative of reality as possible. However, an inspection of the B747-400 ground model revealed a very simple and discontinuous model. The B747-400 ground model determines the aircraft distance to the ground, and if this value is equal to or less than, zero the aircraft is considered to be on the ground. Thus, there are only two possibilities, in the air, or completely with all wheels in the ground. Such a ground model represents a large discontinuity in simulating touchdown of the aircraft.

Although Rolfe and Staples[110] argue that too much detail in simulation is sometimes not desirable, and a simple but representative physical model is best, some improvement to the ground model would give a rather more realistic simulation. Thus, an attempt was made to implement a different ground model, actually only for the longitudinal axis. In this ground model the wheels were considered damped springs and independent of each other. However, after implementing and correcting this ground model the aircraft would not take off, unless the speed was largely increased, during a takeoff simulation. This was found to be due to the engines position. For all the present blended-wing-body configurations, the location of the engines at the rear-top produces a negative pitching moment difficult to overcome with the present weak longitudinal control surfaces. To solve this problem, the engine height was lowered to

the *cg* line, thus removing the engine pitching moment. After this change it was found possible to takeoff the aircraft, although large control deflections were still necessary.

At this point new problems appeared, especially during the rotation phase. When the pilot initiate un-stick, pitch attitude and angle of attack oscillations were noticed during rotation until lift-off. It seemed also that sometimes the aircraft would take longer to takeoff than at other times, with the aircraft nose going up and down during this time.

During lift-off there are large changes in forces and moments contrasting with the small changes of the landing gear displacement. These systems are known as "stiff" systems and require different, or at least smaller, integration steps to give a smoother transition. Besides, the amount of time needed for the aircraft to takeoff is directly related to the low power control surfaces. Once the nose wheel leaves the ground during rotation, the pitching moment due to the nose wheel friction force disappears. If at this time the forces due to the control surfaces are not strong enough the aircraft nose will come down again. The solution would then be, to either modify the integration model or to decrease the integration step size. However, it was not possible to modify the integration step size without changing other modules, which depend on this variable as well. Moreover, the integration procedure used is intrinsic to the language and could not easily be changed. A new integration procedure could have been created, however that was not done. Instead a different pilot technique was adopted. The pilot would keep the aircraft firmly on the ground until the speed increased above the normal take-off speed and would then pull back the stick rather decidedly.

This solution, however, led to another "unreal" situation. Once airborne the aircraft would experience a sudden increase in pitch attitude. This was due to the point of application used to calculate the aircraft moments. While on the ground, this point was the main wheels contact point with the ground. However, once in the air the centre of gravity was used, as usual. Although appearing unreal, the simulator test pilot commented that such effect happens in reality. However, in the present simulation the effect was magnified due to the high elevator deflection necessary for takeoff.

In the end, this landing gear model was abandoned. Instead, the original B747-400 ground model, modified to take into account the engine moments only was used. Although not used, the mathematical model just discussed is presented in paragraph

D.3 of this appendix, since it comprised a large part of the time for simulator development.

D.1.4 Simulator validation

After the changes done to the simulator software it was necessary to validate these changes. As Barnes[58] states, in some circumstances full validation only comes when the simulated vehicle is flown. Prior to that however, confidence has been built up, based on knowledge and experience.

However, in the case of the present BWB configurations no experience or past knowledge exists. Using the test pilots experience, minor corrections to general aircraft behaviour were made, e.g. control coupling effects. For the peculiarities of blended-wing-body aircraft behaviour, validation was done using comparisons with the linear analytical model responses as far as possible. Moreover, analysis was also used to check whether a particular behaviour observed in the simulator could be possible due to these configurations proper characteristics.

D.2 Simulator code modified

D.2.1 Model.def

```
DEFINITION MODULE Model;
(*************************************************************************)
(*                      Version 2.0                                      *)
(*                  Helena V. de Castro                                  *)
(*                      13 - 02 - 02                                     *)
(*************************************************************************)
CONST
  G               = 9.81;
  RollingFriction = 0.016;    (* was 0.015; *)
  EarthRadius     = 6378137.0;
VAR
  Latitude, Longitude : LONGREAL;
  dLatitude, dLongitude : LONGREAL;
  Pitch : REAL;               (* pitch attitude <Euler> (rads) *)
  Roll : REAL;                (* roll attitude <Euler> (rads) *)
  Yaw : REAL;                 (* yaw attitude <Euler> (rads) *)
  Vn, Ve, Vd : REAL;          (* Aircraft vel <Euler> (m/s) *)
  Pz : REAL;                  (* aircraft altitude <Euler> (m) *)
  U, V, W : REAL;             (* aircraft vel <aircraft> (m/s) *)
  UDot, VDot, WDot : REAL;    (* aircraft accn, <aircraft> (m/s/s) *)
  P, Q, R : REAL;             (* angular rates <aircraft> (rad/s) *)
  PDot, QDot, RDot : REAL;    (* angular accns <aircraft> (rad/s/s *)
  Pmt, Rmt, Ymt : REAL;       (* moments <aircraft> (Nm) *)
  Alpha, Beta : REAL;         (* angles of attack, sideslip (rads) *)
  AlphaWing : REAL;           (* wing angle of attack (rads) -- Not in use --*)
  AlphaDot, BetaDot : REAL;   (* alpha rate, beta rates (rads/s) *)
  Cl : REAL;                    (* -- Lift coefficient for print -- *)
(*  ClTail : REAL;              (* -- NOT IN USE -- for print -- *)
  Clfw : REAL;                  (* -- NOT IN USE -- for print -- *) *)
  Cd : REAL;                    (* -- Drag coefficient for print -- *)
(*  CyBeta : REAL;              (* -- NOT IN USE -- for print -- *)
  CyDr : REAL;                  (* -- NOT IN USE -- for print -- *)
  Cz0 : REAL;                   (* -- NOT IN USE -- for print -- *)
  Cz1 : REAL;                   (* -- NOT IN USE -- for print -- *)
  Cm0 : REAL;                   (* -- NOT IN USE -- for print -- *)
  CmAlpha : REAL;               (* -- NOT IN USE -- for print -- *)
  CmDe : REAL;                  (* -- NOT IN USE -- for print -- *)
  CmQ : REAL;                   (* -- NOT IN USE -- for print -- *)
  CmAlphaDot : REAL;            (* -- NOT IN USE -- for print -- *)
  ClBeta : REAL;                (* -- NOT IN USE -- for print -- *)
  ClDr : REAL;                  (* -- NOT IN USE -- for print -- *)
  ClDa : REAL;                  (* -- NOT IN USE -- for print -- *)
  ClP : REAL;                   (* -- NOT IN USE -- for print -- *)
  ClR : REAL;                   (* -- NOT IN USE -- for print -- *)
  CnBeta : REAL;                (* -- NOT IN USE -- for print -- *)
  CnBetaDot : REAL;             (* -- NOT IN USE -- for print -- *)
  CnDr : REAL;                  (* -- NOT IN USE -- for print -- *)
  CnDa : REAL;                  (* -- NOT IN USE -- for print -- *)
  CnP : REAL;                   (* -- NOT IN USE -- for print -- *)
  CnR : REAL;                   (* -- NOT IN USE -- for print -- *) *)
  Lift          : REAL;         (* Lift force for print *)
  Drag          : REAL;         (* Drag force for print *)
  SideForce     : REAL;         (* Sideforce for print *)
  OneG : REAL;                  (* mass * gravity acc *)
  Thrust        : REAL;         (* Engine force for print *)
  DiffBraking : REAL;
  GForce, GMin, GMax : REAL; (* units of load factor *)
  XFg, YFg, ZFg : REAL;         (* Gravity forces *)
  XForce, YForce, ZForce : REAL;  (* Newtons *)
  XAero, YAero, ZAero   : REAL;
  lAero, mAero, nAero : REAL; (* Aerodynamic moments *)
  GroundX, GroundY, GroundZ : REAL;   (* Ground forces *)
  Groundl, Groundm, Groundn : REAL;   (* Ground moments *)
  A11, A12, A13 : REAL;       (* DCM elements *)
  A21, A22, A23 : REAL;
  A31, A32, A33 : REAL;
  Vc, VcDot : REAL;           (* True aircraft vel (m/s) *)
  MachNumber : REAL;
  Elevator : REAL;            (* inceptors (rads) *)
  Aileron : REAL;
```

```
  Rudder : REAL;
  ElevatorTrim : REAL;       (* inceptor trims (rads) *)
  AileronTrim : REAL;
  RudderTrim : REAL;
  ElevAcSpeed, ElevAcPos : REAL;      (* Actuator variables *)
  AlrAcSpeed, AlrAcPos : REAL;
  RdrAcSpeed, RdrAcPos : REAL;
  LeftBrake, RightBrake : REAL; (* 0.0 -> 1.0 *)
  Wheel : REAL;                 (* 0.0 -> 1.0 *)
  Flaps : REAL;                   (* 0.0 -> 1.0 *)
  Gear : REAL;                    (* 0.0 -> 1.0 (UP -> DOWN) *)
  Stalling : BOOLEAN;
  OnTheGround : BOOLEAN;
  e0, e1, e2, e3 : REAL;
  DeFCS, DaFCS, DrFCS : REAL;
  Elev, Alr, Rdr : REAL;
  Aircraft, FlightControl : CARDINAL;
(* ----------- Procedures ------------- *)
   PROCEDURE FlightModel();
   PROCEDURE SetDCM();
   PROCEDURE SetQuarternions();
   PROCEDURE LoadModel;
   PROCEDURE Inertias;
   PROCEDURE ReadInputs;
   PROCEDURE AeroCall;
   PROCEDURE BodyToStab;
   PROCEDURE Friction(U : REAL): REAL;
   PROCEDURE GroundForces;
   PROCEDURE GravityForces;
   PROCEDURE TotalForces;
   PROCEDURE TotalMoments;
   PROCEDURE AngularAccelerations;
   PROCEDURE LinearAccelerations;
   PROCEDURE AngularVelocities;
   PROCEDURE LinearVelocities;
   PROCEDURE GroundModel;
   PROCEDURE IntQuaternions;
   PROCEDURE SpeedToEarth;
   PROCEDURE GsForces;
   PROCEDURE Position;
   PROCEDURE Attitude;
   PROCEDURE SpeedAlphaBeta;
   PROCEDURE SetDCMStab;
   PROCEDURE TransformInputs;
   PROCEDURE EngineModel;
   PROCEDURE EngineLag(VAR Tau : REAL; Throttle : REAL);
END Model.
```

D.2.2 Model.mod

```
IMPLEMENTATION MODULE Model;
(*****************************************************************)
(*                      Helena V. de Castro                      *)
(*                          11 - 07 - 02                         *)
(*                            version 1.0                        *)
(*  This module contains the most complete spring model for the  *)
(* landing gear. But still misses the engine contribution on TO or *)
(* when flying assymetric (one side engine failed).              *)
(*****************************************************************)
FROM MathLib0 IMPORT
  sin, cos, arcsin, arctan, sqrt;
IMPORT LongMathLib0;
FROM Weather IMPORT
  Rho, PressureAltitude, DensityRatio, SpeedOfSound, Turbulence,
  ISADeviation, WindX, WindY, UTurb, VTurb, WTurb;
FROM Maths IMPORT
  Integrate, LongIntegrate, Normalise, Limit, PI, PIBY2, arctanXY, ONERAD;
FROM IOLib IMPORT
  GetLeftBrake, GetRightBrake, GetElevator, GetAileron, GetRudder,
  GetElevatorTrim, GetAileronTrim, GetRudderTrim, GetParkBrake,
  GetLeftWheel, GetRightWheel, Freezing, StickShaker;
FROM Aero IMPORT
  AeroMaxAlpha, AeroCm0, AeroCmAlpha, AeroCmDe,
  AcHeight, CGHeight, EyeZStation, ElevatorGain, AileronGain, RudderGain,
```

```
  ElevatorTrimGain, AileronTrimGain, RudderTrimGain, WingIncidence,
  CgPosition, AxialCoef, LateralCoef, NormalCoef, RollingMtCoef,
  PitchingMtCoef,YawingMtCoef, Coefficients, Mass, Ixx, Iyy, Izz,
  Ixy, Ixz, Iyz;
FROM AeroData IMPORT
   BWB, AFCS, SetupModel, SetupFCS;
FROM Clocks IMPORT
  SysTicks;
FROM Systems IMPORT
  GetFlapPosition, GetGearPosition;
FROM AeroDefn IMPORT
  SwitchPosition;
FROM FCS IMPORT
  LongFCS, LatFCS, DirFCS, Actuator;
FROM AeroLink IMPORT
   NavPkt, EngPkt;
(* -------------- Constants for the new model ----------------- *)
CONST
   MaxThrust = 550000.0; (* Maximum thrust of each engine*)
                         (* as there is 3 the total maximum thrust is*)
                         (* 1500000N or 1500kN*)
   Te = 1.0;    (* Engine time constant *)
VAR
   e0Dot, e1Dot, e2Dot, e3Dot : REAL;
   Pstab, Rstab : REAL;       (* Roll and pitch in stability axis -- NOT IN USE -- *)
   Irr, Ppq, Pqr, Pn, Pl, Qpp, Qpr, Qrr, Qm, Rpq, Rqr, Rn, Rl : REAL;
   Da, De, Dr : REAL;         (* pilot inputs for aileron, elevator and rudder *)
   DeTrim, DaTrim, DrTrim : REAL;     (* Pilot trim inputs, from trim wheels *)
   Fn, Fm                 : REAL;     (* Nose gear and main gear forces *)
   Vc2 : REAL;
   BS11, BS12, BS13 : REAL;
   BS21, BS22, BS23 : REAL;
   BS31, BS32, BS33 : REAL;
   Engine : ARRAY [1..3] OF REAL;
   PowerMoment : REAL;
(* Calculation of DCM ------------------------ *)
PROCEDURE SetDCM;
VAR
  e00, e11, e22, e33 : REAL;
BEGIN
  e00 := e0 * e0;
  e11 := e1 * e1;
  e22 := e2 * e2;
  e33 := e3 * e3;
  A11 := e00 + e11 - e22 - e33;
  A12 := 2.0 * (e1 * e2 - e0 * e3);
  A13 := 2.0 * (e0 * e2 + e1 * e3);
  A21 := 2.0 * (e1 * e2 + e0 * e3);
  A22 := e00 - e11 + e22 - e33;
  A23 := 2.0 * (e2 * e3 - e0 * e1);
  A31 := 2.0 * (e1 * e3 - e0 * e2);
  A32 := 2.0 * (e2 * e3 + e0 * e1);
  A33 := e00 - e11 - e22 + e33;
END SetDCM;
(* ------------------------------------------------------ *)
PROCEDURE SetQuarternions();
VAR
  p, r, y : REAL;
  sp, cp, sr, cr, sy, cy : REAL;
BEGIN
  p := Pitch * 0.5;
  r := Roll * 0.5;
  y := Yaw * 0.5;
  sp := sin(p);
  cp := cos(p);
  sr := sin(r);
  cr := cos(r);
  sy := sin(y);
  cy := cos(y);
  e0 := cr * cp * cy + sr * sp * sy;
  e1 := sr * cp * cy - cr * sp * sy;
  e2 := cr * sp * cy + sr * cp * sy;
  e3 := cr * cp * sy - sr * sp * cy;
END SetQuarternions;
(* ------------------------------------------------------ *)
PROCEDURE Sign(x : REAL) : REAL;
```

```
BEGIN
  IF x >= 0.001 THEN
    RETURN 1.0
  ELSIF x <= -0.001 THEN
    RETURN -1.0
  ELSE
    RETURN 0.0
  END;
END Sign;
(*------------------------------------------------------- *)
PROCEDURE LoadModel;
VAR
  dec, cent : REAL;
BEGIN
  dec := CgPosition * 10.0;
  cent := CgPosition * 100.0;
  Aircraft := TRUNC(dec);
  FlightControl := TRUNC(cent);
  SetupModel(Aircraft);
  SetupFCS(FlightControl);
  Mass := BWB.Mass.Mass;
  Ixx := BWB.Mass.Ixx;
  Iyy := BWB.Mass.Iyy;
  Izz := BWB.Mass.Izz;
  Ixy := BWB.Mass.Ixy;
  Ixz := BWB.Mass.Ixz;
  Iyz := BWB.Mass.Iyz;
  CGHeight := BWB.LGear.CGToGround;
  EyeZStation := AcHeight - CGHeight;
END LoadModel;
(* ------------------------------------------------------- *)
PROCEDURE Inertias;
BEGIN
   Irr := Ixx * Izz - Ixz * Ixz;
   Ppq := ((Ixx - Iyy + Izz) * Ixz) / Irr;
   Pqr := ((Iyy - Izz) * Izz - Ixz * Ixz) / Irr;
   Pn  := Ixz / Irr;
   Pl  := Izz / Irr;
   Qpp := -Ixz / Iyy;
   Qpr := (Izz - Ixx) / Iyy;
   Qrr := Ixz / Iyy;
   Qm  := 1.0 / Iyy;
   Rpq := ((Ixx - Iyy) * Ixx + Ixz * Ixz) / Irr;
   Rqr := ((Iyy - Izz - Ixx) * Ixz) / Irr;
   Rn  := Ixx / Irr;
   Rl  := Ixz / Irr;
   OneG := Mass * G;
END Inertias;
(* ------------------------------------------------------- *)
PROCEDURE ReadInputs;  (* Read pilot's inputs *)
BEGIN
   Elevator := GetElevator();
   Aileron  := GetAileron();
   Rudder   := GetRudder();
   ElevatorTrim := GetElevatorTrim();
   AileronTrim  := GetAileronTrim();
   RudderTrim   := GetRudderTrim();
   Flaps := GetFlapPosition();
   Gear  := GetGearPosition();
   LeftBrake  := GetLeftBrake();
   RightBrake := GetRightBrake();
   IF GetParkBrake() = On THEN
      LeftBrake  := 1.0;
      RightBrake := 1.0;
   END;
   Wheel := GetLeftWheel() + GetRightWheel();
   IF Vc > 15.0 THEN (*ineffective above 30kts *)
      Wheel := 0.0;
   END;
END ReadInputs;
(* ------------------------------------------------------- *)
PROCEDURE TransformInputs;
BEGIN
   De := Elevator * ElevatorGain;
   Dr := Rudder * RudderGain;
   Da := -Aileron * AileronGain; (* negative sign was added since
```

```
                                    a positive pilot wheel input corresponds
                                    to a negative aileron deflection *)
   DeTrim := -ElevatorTrim * ElevatorTrimGain;
   DaTrim := -AileronTrim * AileronTrimGain;
   DrTrim := -RudderTrim * RudderTrimGain;
   DeFCS := LongFCS(-De/4.0); (* De;*)
   DeTrim := 0.0;      (* because the FCS is a pitch rate command *)
   Elev := Actuator(ElevAcPos, ElevAcSpeed, DeFCS + DeTrim);
   IF (Elev >= (30.0 / ONERAD)) THEN
      Elev := 30.0/ONERAD;
   ELSIF (Elev <= (-30.0 / ONERAD)) THEN
      Elev := -30.0/ONERAD;
   END;
   DaFCS := LatFCS(Da/1.4);
   Alr := Actuator(AlrAcPos, AlrAcSpeed, DaFCS + DaTrim);
   IF (Alr >= (30.0 / ONERAD)) THEN
      Alr := 30.0/ONERAD;
   ELSIF (Alr <= (-30.0 / ONERAD)) THEN
      Alr := -30.0/ONERAD;
   END;
   DrFCS := DirFCS(Dr, -Alr);
   Rdr := Actuator(RdrAcPos, RdrAcSpeed, DrFCS + DrTrim);
   IF (Rdr >= (30.0 / ONERAD)) THEN
      Rdr := 30.0/ONERAD;
   ELSIF (Rdr <= (-30.0 / ONERAD)) THEN
      Rdr := -30.0/ONERAD;
   END;
(*   Elevator := Elev/ElevatorGain;  (* To really achieve the desired output *)
   Aileron := Alr/AileronGain;
   Rudder := Rdr/RudderGain; *)
END TransformInputs;
(* ------------------------------------------------------- *)
PROCEDURE GravityForces;
VAR
   Fg : REAL;
BEGIN
   Fg := G * BWB.Mass.Mass;
   XFg := A31 * Fg;
   YFg := A32 * Fg;
   ZFg := A33 * Fg;
END GravityForces;
(* ------------------------------------------------------- *)
PROCEDURE AeroCall;    (* Aerodynamic forces and moments in body axis *)
BEGIN
   Coefficients;
   ZAero := 0.5 * Rho * Vc2 * BWB.Geo.S * NormalCoef(Elev);
   XAero := 0.5 * Rho * Vc2 * BWB.Geo.S * AxialCoef();
   YAero := 0.5 * Rho * Vc2 * BWB.Geo.S * LateralCoef(Alr, Rdr);
   lAero := 0.5 * Rho * Vc2 * BWB.Geo.S * BWB.Geo.b * RollingMtCoef(Alr, Rdr);
   mAero := 0.5 * Rho * Vc2 * BWB.Geo.S * BWB.Geo.mac * PitchingMtCoef(Elev);
   nAero := 0.5 * Rho * Vc2 * BWB.Geo.S * BWB.Geo.b * YawingMtCoef(Alr, Rdr);
END AeroCall;
(* ------------------------------------------------------- *)
(* Procedure to calculate aerodynamic forces and moments in stability axis *)
PROCEDURE BodyToStab;
BEGIN
   Drag :=     -(BS11 * XAero + BS12 * YAero + BS13 * ZAero);
   SideForce := BS21 * XAero + BS22 * YAero + BS23 * ZAero;
   Lift :=     -(BS31 * XAero + BS32 * YAero + BS33 * ZAero);
   IF (Vc2 <= 0.0) THEN
      Cl := 0.0;
      Cd := 0.0;
   ELSE
      Cl := Lift / (0.5 * Rho * Vc2 * BWB.Geo.S);
      Cd := Drag / (0.5 * Rho * Vc2 * BWB.Geo.S);
   END;
END BodyToStab;
(* ------------------------------------------------------- *)
PROCEDURE Friction(U : REAL): REAL;
VAR
   BrakingFriction : REAL;
   BreakoutFriction : REAL;
BEGIN
   BrakingFriction := (LeftBrake + RightBrake) * 0.263;
   IF U < 7.0 THEN
      BreakoutFriction := (7.0 - U)/500.0
```

```
   ELSE
      BreakoutFriction := 0.0
   END;
   RETURN (RollingFriction + BreakoutFriction + BrakingFriction)
END Friction;
(* ------------------------------------------------------- *)
PROCEDURE GroundForces;
VAR
   FrictionCoef : REAL;
BEGIN
   IF (OnTheGround) THEN
      FrictionCoef := Friction(U);
      GroundX := -FrictionCoef * (ZAero + ZFg);
   ELSE
      GroundX := 0.0;
   END;
   GroundY := 0.0;
   GroundZ := 0.0;
END GroundForces;
(* ------------------------------------------------------- *)
PROCEDURE TotalForces;
BEGIN
   XForce := XFg + XAero + GroundX + Thrust;
   YForce := YFg + YAero + GroundY;
   ZForce := ZFg + ZAero + GroundZ;
END TotalForces;
(* ------------------------------------------------------- *)
PROCEDURE TotalMoments;       (* Total forces and moments *)
BEGIN
   Rmt := lAero;
   Pmt := mAero;
   Ymt := nAero + PowerMoment;
END TotalMoments;
(* ------------------------------------------------------- *)
PROCEDURE AngularAccelerations;
BEGIN
   PDot := Ppq * P * Q + Pqr * Q * R + Pn * Ymt + Pl * Rmt;
   QDot := Qpp * P * P + Qpr * P * R + Qrr * R * R + Qm * Pmt;
   RDot := Rpq * P * Q + Rqr * Q * R + Rn * Ymt + Rl * Rmt;
END AngularAccelerations;
(* ------------------------------------------------------- *)
PROCEDURE LinearAccelerations;       (* Calculation of linear accelerations *)
BEGIN
   UDot := XForce / BWB.Mass.Mass - Q * W + R * V;
   VDot := YForce / BWB.Mass.Mass - R * U + P * W;
   WDot := ZForce / BWB.Mass.Mass - P * V + Q * U;
END LinearAccelerations;
(* ------------------------------------------------------- *)
PROCEDURE AngularVelocities;  (* Integration of aircraft accelerations *)
BEGIN
   Integrate(P, PDot);
   Limit(P, -PI, PI);
   Normalise(P);
   Integrate(Q, QDot);
   Normalise(Q);
   Integrate(R, RDot);
   Normalise(R);
END AngularVelocities;
(* ------------------------------------------------------- *)
PROCEDURE LinearVelocities;
BEGIN
   Integrate(U, UDot);
   Integrate(V, VDot);
   Integrate(W, WDot);
END LinearVelocities;
(* ------------------------------------------------------- *)
PROCEDURE GroundModel;
VAR
   Vc2 : REAL;
   dYmt : REAL;
   WheelYaw : REAL;
BEGIN
   Vc2 := Vc * Vc;
   Pmt := mAero - (ZFg + ZAero) * BWB.LGear.MainGearCG
          + (Thrust + XAero) * BWB.Eng.Height;
   Integrate(Q, Pmt/BWB.Mass.Iyy);
```

```
   Integrate(Pitch, Q);
   IF Pitch < 0.0 THEN
      Pitch := 0.0;
      Q := 0.0;
   END;
   Rmt := -BWB.Mass.Mass * 9.81 * Sign(Roll) * BWB.LGear.GearOffset + lAero;
   IF ABS(Roll) > 0.2 THEN
      Integrate(P, Rmt / BWB.Mass.Ixx);
      Integrate(Roll, P);
   ELSE
      Rmt := lAero;    (* rolls about u/c not cg *)
      Integrate(P, Rmt / BWB.Mass.Ixx - 157.9 * Roll);
      Integrate(Roll, P - 17.59 * Roll);
   END;
(* Jim - modified rudder to yaw moment gain - originally 0.4 *)
   WheelYaw := U * Wheel * 0.01;
   IF U > 15.0 THEN    (* ignore after 30kts *)
      WheelYaw := 0.0;
   END;
   Ymt := ((RightBrake - LeftBrake) * 2.0 - Dr * 1.0) * U * 0.005 + WheelYaw;
   dYmt := PowerMoment / BWB.Mass.Izz * (2.0 - LeftBrake - RightBrake) * 0.5;
   IF ABS(dYmt) > 0.02 THEN
      Ymt := Ymt + dYmt;
   END;
   IF Vc < 2.5 THEN
      dYmt := dYmt + Thrust * BWB.LGear.GearOffset / BWB.Mass.Izz * (RightBrake -
LeftBrake);
      IF ABS(dYmt) > 0.02 THEN
        Ymt := Ymt + dYmt;
      END;
   END;
   Integrate(R, 0.8 * (Ymt - R));
   Integrate(Yaw, R);
END GroundModel;
(* ------------------------------------------------------- *)
PROCEDURE IntQuaternions;
VAR
   Lambda : REAL;
BEGIN
   Lambda := 25.0 * (1.0 - (e0 * e0 + e1 * e1 + e2 * e2 + e3 * e3));
   e0Dot := -0.5 * (e1 * P + e2 * Q + e3 * R) + Lambda * e0;
   e1Dot :=  0.5 * (e0 * P + e2 * R - e3 * Q) + Lambda * e1;
   e2Dot :=  0.5 * (e0 * Q + e3 * P - e1 * R) + Lambda * e2;
   e3Dot :=  0.5 * (e0 * R + e1 * Q - e2 * P) + Lambda * e3;
   Integrate(e0, e0Dot);
   Integrate(e1, e1Dot);
   Integrate(e2, e2Dot);
   Integrate(e3, e3Dot);
END IntQuaternions;
(* ------------------------------------------------------- *)
PROCEDURE GsForces;
BEGIN
   GForce := Lift / OneG;      (* NOTE: CHECK THIS VALUE, the GForce = Lift?  *)
   Limit(GForce, -6.0, 10.0);
   IF GForce > GMax THEN
      GMax := GForce
   ELSIF GForce < GMin THEN
      GMin := GForce
   END;
END GsForces;
(* ------------------------------------------------------- *)
PROCEDURE SpeedToEarth;
BEGIN
   U := U + UTurb * A11 + VTurb * A21 + WTurb * A31;
   V := V + UTurb * A12 + VTurb * A22 + WTurb * A32;
   W := W + UTurb * A13 + VTurb * A23 + WTurb * A33;
   IF U < 0.0 THEN
      U := 0.0;
   END;
   Vn := U * A11 + V * A12 + W * A13;
   Ve := U * A21 + V * A22 + W * A23;
   IF (OnTheGround) AND (ZFg + ZAero > 0.0) THEN
      Pz := CGHeight + NavPkt.GroundLevel;
      Vd := 0.0;
   ELSE
      Vn := Vn - WindX;
```

```
      Ve := Ve - WindY;
      Vd := U * A31 + V * A32 + W * A33;
   END;
END SpeedToEarth;
(* ------------------------------------------------------- *)
PROCEDURE Position;
BEGIN
   IF NOT Freezing THEN
      dLongitude := LONG(Ve) / ((EarthRadius - LONG(Pz)) *
                    LongMathLib0.cos(Latitude));
      dLatitude := LONG(Vn) / (EarthRadius - LONG(Pz));
      LongIntegrate(Latitude, dLatitude);
      LongIntegrate(Longitude, dLongitude);
      Integrate(Pz, Vd);
   END;
END Position;
(* ------------------------------------------------------- *)
PROCEDURE Attitude;
VAR
   t : REAL;
BEGIN
   t := -A31;
   Limit(t, -1.0, 1.0);
   Pitch := arcsin(t);
   Roll := arctanXY(A33, A32);
   Yaw := arctanXY(A11, A21);
END Attitude;
(* ------------------------------------------------------- *)
PROCEDURE SpeedAlphaBeta;
BEGIN
   Vc2 := U * U + V * V + W * W;
   Vc  := sqrt(Vc2);
   MachNumber := Vc / SpeedOfSound;
   IF Vc < 10.0 THEN
      Alpha    := 0.0;
      Beta     := 0.0;
      AlphaDot := 0.0;
      BetaDot  := 0.0;
   ELSE
      Alpha    := arctan(W / U);
      Beta     := arcsin(V / Vc);
      AlphaDot := WDot / Vc;
      BetaDot  := VDot / Vc;
      IF OnTheGround THEN
         Alpha := Pitch;
      END;
   END;
END SpeedAlphaBeta;
(* ------------------------------------------------------- *)
PROCEDURE SetDCMStab;
VAR
   cosalpha, sinalpha, cosbeta, sinbeta : REAL;
BEGIN
   cosalpha := cos(Alpha);
   sinalpha := sin(Alpha);
   cosbeta := cos(Beta);
   sinbeta := sin(Beta);
   BS11 := cosalpha * cosbeta;
   BS12 := sinbeta;
   BS13 := sinalpha * cosbeta;
   BS21 := -cosalpha * sinbeta;
   BS22 := cosbeta;
   BS23 := -sinalpha * sinbeta;
   BS31 := - sinalpha;
   BS32 := 0.0;
   BS33 := cosalpha;
END SetDCMStab;
(* ------------------------------------------------------- *)
PROCEDURE EngineLag(VAR Tau : REAL; Throttle : REAL);
VAR
   dTau : REAL;
BEGIN
   dTau := MaxThrust/Te * Throttle - 1.0/Te * Tau;
   Integrate(Tau, dTau);
END EngineLag;
(* ------------------------------------------------------- *)
```

```
PROCEDURE EngineModel;
VAR
   i : CARDINAL;
BEGIN
(*   FOR i := 1 TO 3 DO
       EngineLag(Engine[i],EngPkt.EngineLevers[i]);
   END;*)
   Thrust := 3.5 * (EngPkt.Engines[1].Thrust
                  + EngPkt.Engines[2].Thrust
                  + EngPkt.Engines[3].Thrust);
   PowerMoment := - EngPkt.Engines[1].Thrust * BWB.Eng.Arm1
                  - EngPkt.Engines[2].Thrust * BWB.Eng.Arm2
                  - EngPkt.Engines[3].Thrust * BWB.Eng.Arm3;
(*   Thrust := Engine[1] + Engine[2] + Engine[3];
   PowerMoment := - Engine[1] * BWB.Eng.Arm1 - Engine[2] * BWB.Eng.Arm2
                  - Engine[3] * BWB.Eng.Arm3; *)
END EngineModel;
(* ------------------------------------------------------- *)
PROCEDURE CallStall;
CONST
   MaxAlpha = 27.0/ONERAD;
BEGIN
   IF (ABS (Alpha) > (MaxAlpha - 0.05)) THEN (* stall warning activated *)
      Stalling := TRUE;                              (* at 3deg below max alpha*)
      StickShaker(Stalling);
   END;
END CallStall;
(* ------------------------------------------------------- *)
PROCEDURE FlightModel;
BEGIN
   LoadModel;
   OnTheGround := Pz >= (CGHeight + NavPkt.GroundLevel - 0.001);
   Inertias;
   ReadInputs;
   TransformInputs;
   GravityForces;
   EngineModel;
   AeroCall;
   BodyToStab;
   GsForces;
   GroundForces;
   TotalForces;
   TotalMoments;
   LinearAccelerations;
   LinearVelocities;
   IF OnTheGround THEN
      GroundModel;
      IF (ZFg + ZAero > 0.0) THEN
         V := 0.0;
         Beta := 0.0;
         BetaDot := 0.0;
         W := 0.0;
         GForce := 1.0;
         SetQuarternions;
      END;
   ELSE
      AngularAccelerations;
      AngularVelocities;
   END;
   IntQuaternions();
   SetDCM;
   Attitude;
   SpeedToEarth;
   Position;
   Stalling := FALSE;
   StickShaker(Stalling);
   SpeedAlphaBeta;
   CallStall;
   SetDCMStab;
END FlightModel;
(* ------------------------------------------------------- *)
BEGIN
  CgPosition := 0.10; (*Possibilities: 0.10,0.11,0.20,0.30,0.31,0.40,0.50,0.60,0.70*)
  LoadModel;
  Inertias;
  Vc := 0.0; (* 120.0; *)
```

```
  MachNumber := 0.0; (* 0.356;*)
  Alpha := 0.0; (* 0.149;*)    (* 8.51deg *)
  Beta := 0.0;
  Pitch := 0.0; (* Alpha;*)
  Roll := 0.0;
  Yaw := 0.0;
  Latitude := 0.0;
  Longitude := 0.0;
  Pz := BWB.LGear.CGToGround + NavPkt.GroundLevel; (*- 5.0;*) (* -914.4;*) (* 2,000
feet *)
  U := Vc * cos(Alpha) * cos(Beta);   (* U := 0.0; *)
  V := Vc * sin(Beta);                (* V := 0.0; *)
  W := Vc * sin(Alpha) * cos(Beta);   (* W := 0.0; *)
  Vc2 := U * U + V * V + W * W;
  SetDCMStab;
  UDot := 0.0;
  VDot := 0.0;
  WDot := 0.0;
  P := 0.0;
  Q := 0.0;
  R := 0.0;
  PDot := 0.0;
  QDot := 0.0;
  RDot := 0.0;
  SetQuarternions();
  SetDCM();
  Vn := U * A11 + V * A12 + W * A13;  (* Vn := 0.0; *)
  Ve := U * A21 + V * A22 + W * A23;  (* Ve := 0.0; *)
  Vd := U * A31 + V * A32 + W * A33;  (* Vd := 0.0; *)
  GMin := 1.0;
  GMax := 1.0;
  Flaps := 0.0;
  Gear := 0.0;
  OnTheGround := TRUE; (* FALSE;*)
  Stalling := FALSE;
  ElevAcPos     := 0.0; (*0.149;*)    (* -14.14deg to trim Vc = 120m/s and h = 914m *)
  ElevAcSpeed   := 0.0;
  AlrAcPos      := 0.0;
  AlrAcSpeed    := 0.0;
  RdrAcPos      := 0.0;
  RdrAcSpeed    := 0.0;
  Engine[1] := (*400000.0;*) 0.0;
  Engine[2] := (*400000.0;*) 0.0;
  Engine[3] := (*400000.0;*) 0.0;
  Elev := 0.0;
  Alr := 0.0;
  Rdr := 0.0;
END Model.
```

D.2.3 Aero.def

```
DEFINITION MODULE Aero;
(*********************************************************************)
FROM Maths IMPORT
 ONERAD;
CONST
 OuterEngineArm = 0.0;
 InnerEngineArm = 7.5;
  AcHeight = -5.739; (* Eye Height over lowest wheel (m) *)
 AerialHeight = -3.3; (* Aerial Height over lowest wheel (m) *)
 EyeXStation = 24.4; (* Pilot Station to a/c CG (m) *)
 EyeYStation = -0.5; (* Pilot Station to a/c CG (minus sign for left seat) (m) *)
  WingIncidence   = 0.0; (*---------- Not used --------*)
 ElevatorGain    = (23.0 / ONERAD); (* +-1.0 -> 23 degs *)
 AileronGain     = (40.0 / ONERAD); (* +-1.0 -> 40 degs *)
 RudderGain      = (25.0 / ONERAD); (* +-1.0 -> 25 degs *)
 ElevatorTrimGain = (30.0 / ONERAD);
 AileronTrimGain  = (30.0 / ONERAD);
 RudderTrimGain   = (25.0 / ONERAD);
  FlapsUpRate = 0.0015;  (* 2.2 deg/sec *)
 FlapsDownRate = 0.0015;
 GearUpRate = 0.004;    (* 5 secs transit *)
 GearDownRate = 0.004;
VAR
```

```
  CgPosition : REAL;
  s, b, CBar          : REAL;
  Mass     : REAL;
  Ixx,Iyy,Izz,Ixz, Ixy, Iyz          : REAL;
  Cx0, k1, k2, CxDe : REAL;
  Cz0, Cza1, CzQ, CzDe : REAL;
  Cyb, CyP, CyR, CyDa, CyDr : REAL;
  Clb, ClP, ClR, ClDa, ClDr : REAL;
  Cm0, Cma, CmQ, CmDe : REAL;
  Cnb, CnP, CnR, CnDa, CnDr : REAL;
  CoefNorm : REAL;
  MainGearCG, NoseGearCG, CGToGround, GearOffset : REAL;
  CGHeight, EyeZStation : REAL;
PROCEDURE AeroMaxAlpha() : REAL;
PROCEDURE AeroCz0() : REAL;
PROCEDURE AeroCz1() : REAL;
PROCEDURE AeroCzDe() : REAL;
(*PROCEDURE AeroCl() : REAL;*)
(*PROCEDURE AeroClTail() : REAL;*)
(*PROCEDURE AeroClfw() : REAL; *)
PROCEDURE AeroCx0() : REAL;
PROCEDURE AeroCxK1() : REAL;
PROCEDURE AeroCxK2() : REAL;
PROCEDURE AeroCyBeta() : REAL;
PROCEDURE AeroCyDr() : REAL;
PROCEDURE AeroCyDa() : REAL;
PROCEDURE AeroCyP() : REAL;
PROCEDURE AeroCyR() : REAL;
PROCEDURE AeroCm0() : REAL;
PROCEDURE AeroCmAlpha() : REAL;
PROCEDURE AeroCmDe() : REAL;
PROCEDURE AeroCmQ() : REAL;
PROCEDURE AeroCmAlphaDot() : REAL;
PROCEDURE AeroClBeta() : REAL;
PROCEDURE AeroClDr() : REAL;
PROCEDURE AeroClDa() : REAL;
PROCEDURE AeroClP() : REAL;
PROCEDURE AeroClR() : REAL;
PROCEDURE AeroCnBeta() : REAL;
PROCEDURE AeroCnBetaDot() : REAL;
PROCEDURE AeroCnDr() : REAL;
PROCEDURE AeroCnDa() : REAL;
PROCEDURE AeroCnP() : REAL;
PROCEDURE AeroCnR() : REAL;
PROCEDURE Coefficients;
PROCEDURE NormalCoef(De : REAL) : REAL;
PROCEDURE AxialCoef() : REAL;
PROCEDURE LateralCoef(Da, Dr : REAL) : REAL;
PROCEDURE RollingMtCoef(Da, Dr : REAL) : REAL;
PROCEDURE PitchingMtCoef(De : REAL) : REAL;
PROCEDURE YawingMtCoef(Da, Dr : REAL) : REAL;
END Aero.
```

D.2.4 Aero.mod

```
IMPLEMENTATION MODULE Aero;
(*****************************************************************)
(*     This module calculates the aerodynamic forces and moments    *)
(*     from the aircraft characteristics.                           *)
(*     The original module was changed for a new source of data,    *)
(*     actually aerodynamic data already in body axis reference!    *)
(*                          Version 2.0                             *)
(*                      Helena V. de Castro                         *)
(*                          12 - 02 - 02                            *)
(*****************************************************************)
FROM IOLib IMPORT
  DigitalDataC;
FROM Model IMPORT
  Alpha, AlphaWing, Gear, Flaps, MachNumber, Pz, Beta, Vc, P, Q, R,
  Aircraft;
FROM AeroData IMPORT
   BWB;
FROM AeroLink IMPORT
   NavPkt;
```

```
(* ------------------------------------------------------------ *)
(*      Implementation of the original program procedures       *)
(* ------------------------------------------------------------ *)
PROCEDURE AeroMaxAlpha() : REAL;
BEGIN
  RETURN 0.262 + Flaps * 0.0;
END AeroMaxAlpha;
(* ------------------------------------------------------------ *)
PROCEDURE AeroCz0() : REAL;
BEGIN
  RETURN BWB.ZF.CZo;
END AeroCz0;
(* ------------------------------------------------------------ *)
PROCEDURE AeroCz1() : REAL;
VAR
   h : REAL;
BEGIN
   h := -(Pz - NavPkt.GroundLevel);
   IF h< 0.0 THEN
      h := 0.0;
      RETURN -7.495;
   ELSIF (h>=0.0) AND (h<=5.0) THEN
      RETURN 0.1454*h - 7.495;
   ELSIF (h>5.0) AND (h<15.0) THEN
      RETURN 0.0397*h - 6.4388;
   ELSIF (h>=15.0) AND (h<110.0) THEN
      RETURN 0.00375*h - 5.8993;
   ELSE
      RETURN BWB.ZF.CZa;
   END;
END AeroCz1;
(* ------------------------------------------------------------ *)
PROCEDURE AeroCzQ() : REAL;
BEGIN
   RETURN BWB.ZF.CZq;
END AeroCzQ;
(* ------------------------------------------------------------ *)
(*PROCEDURE AeroCl() : REAL;
VAR
  Cz0, Cz1, MaxAlpha : REAL;
  Cl, DeltaAlpha, DeltaCl, AbsAlpha : REAL;
BEGIN
  Cz0 := AeroCz0();
  Cz1 := AeroCz1();
  MaxAlpha := AeroMaxAlpha();
  Cl := Cz0 + Cz1 * Alpha;
  AbsAlpha := ABS (Alpha);
  IF (AbsAlpha > MaxAlpha) THEN  (* above max.alpha, limit lift *)
    DeltaAlpha := AbsAlpha - MaxAlpha;
    DeltaCl := 20.0 * DeltaAlpha * DeltaAlpha;
    IF AlphaWing > 0.0 THEN
      DeltaCl := -DeltaCl
    END;
    Cl := Cl + DeltaCl
  END;
  RETURN Cl;
END AeroCl; *)
(* ------------------------------------------------------------ *)
PROCEDURE AeroCzDe() : REAL;
BEGIN
  RETURN BWB.ZF.CZF8;
END AeroCzDe;
(* ------------------------------------------------------------ *)
PROCEDURE AeroCx0() : REAL;
BEGIN
  RETURN BWB.XF.CXo + 0.028*Gear;
END AeroCx0;
(* ------------------------------------------------------------ *)
PROCEDURE AeroCxK1() : REAL;
BEGIN
   RETURN BWB.XF.CXk1;
END AeroCxK1;
(* ------------------------------------------------------------ *)
PROCEDURE AeroCxK2() : REAL;
BEGIN
   RETURN BWB.XF.CXk2;
```

```
END AeroCxK2;
(* ------------------------------------------------------------ *)
PROCEDURE AeroCyBeta() : REAL;
BEGIN
  RETURN BWB.YF.CYbo + BWB.YF.CYb_a * Alpha;
END AeroCyBeta;
(* ------------------------------------------------------------ *)
PROCEDURE AeroCyDr() : REAL;
BEGIN
  RETURN BWB.YF.CYdRo + BWB.YF.CYdR_a * Alpha;
END AeroCyDr;
(* ------------------------------------------------------------ *)
PROCEDURE AeroCyDa() : REAL;
BEGIN
   RETURN BWB.YF.CYA8o + BWB.YF.CYA8_a * Alpha;
END AeroCyDa;
(* ------------------------------------------------------------ *)
PROCEDURE AeroCyP() : REAL;
VAR
   CYp : REAL;
BEGIN
   CYp := BWB.YF.CYPo + BWB.YF.CYP_a * Alpha;
   IF ((Aircraft = 7) AND (Vc > 0.0)) THEN
      CYp := CYp * BWB.Geo.b / (2.0 * Vc);
   END;
   RETURN CYp;
END AeroCyP;
(* ------------------------------------------------------------ *)
PROCEDURE AeroCyR() : REAL;
VAR
   CYr : REAL;
BEGIN
   CYr := BWB.YF.CYRo + BWB.YF.CYR_a * Alpha;
   IF ((Aircraft = 7) AND (Vc > 0.0)) THEN
      CYr := CYr * BWB.Geo.b / (2.0 * Vc);
   END;
   RETURN CYr;
END AeroCyR;
(* ------------------------------------------------------------ *)
PROCEDURE AeroCm0() : REAL;
BEGIN
  RETURN BWB.Pmt.Cmo;
END AeroCm0;
(* ------------------------------------------------------------ *)
PROCEDURE AeroCmAlpha() : REAL;
BEGIN
  RETURN BWB.Pmt.Cma;
END AeroCmAlpha;
(* ------------------------------------------------------------ *)
PROCEDURE AeroCmDe() : REAL;
BEGIN
  RETURN BWB.Pmt.CmF8;
END AeroCmDe;
(* ------------------------------------------------------------ *)
PROCEDURE AeroCmQ() : REAL;
BEGIN
  RETURN BWB.Pmt.Cmq;
END AeroCmQ;
(* ------------------------------------------------------------ *)
PROCEDURE AeroCmAlphaDot() : REAL;
BEGIN
  RETURN 0.0;
END AeroCmAlphaDot;
(* ------------------------------------------------------------ *)
PROCEDURE AeroClBeta() : REAL;
BEGIN
  RETURN BWB.Rmt.Clbo + BWB.Rmt.Clb_a * Alpha;
END AeroClBeta;
(* ------------------------------------------------------------ *)
PROCEDURE AeroClDr() : REAL;
BEGIN
  RETURN BWB.Rmt.CldRo + BWB.Rmt.CldR_a * Alpha;
END AeroClDr;
(* ------------------------------------------------------------ *)
PROCEDURE AeroClDa() : REAL;
BEGIN
```

```
  RETURN BWB.Rmt.ClA8o + BWB.Rmt.ClA8_a * Alpha;
END AeroClDa;
(* ------------------------------------------------------------ *)
PROCEDURE AeroClP() : REAL;
VAR
   Clp : REAL;
BEGIN
  Clp := BWB.Rmt.ClPo + BWB.Rmt.ClP_a * Alpha;
  IF ((Aircraft = 7) AND (Vc > 0.0)) THEN
      Clp := Clp * BWB.Geo.b / (2.0 * Vc);
  END;
  RETURN Clp;
END AeroClP;
(* ------------------------------------------------------------ *)
PROCEDURE AeroClR() : REAL;
VAR
   Clr : REAL;
BEGIN
  Clr := BWB.Rmt.ClRo + BWB.Rmt.ClR_a * Alpha;
  IF ((Aircraft = 7) AND (Vc > 0.0)) THEN
      Clr := Clr * BWB.Geo.b / (2.0 * Vc);
  END;
  RETURN Clr;
END AeroClR;
(* ------------------------------------------------------------ *)
PROCEDURE AeroCnBeta() : REAL;
BEGIN
  RETURN BWB.Ymt.Cnbo + BWB.Ymt.Cnb_a * Alpha;
END AeroCnBeta;
(* ------------------------------------------------------------ *)
PROCEDURE AeroCnBetaDot() : REAL;
BEGIN
  RETURN 0.0;
END AeroCnBetaDot;
(* ------------------------------------------------------------ *)
PROCEDURE AeroCnDr() : REAL;
BEGIN
  RETURN BWB.Ymt.CndRo + BWB.Ymt.CndR_a * Alpha;
END AeroCnDr;
(* ------------------------------------------------------------ *)
PROCEDURE AeroCnDa() : REAL;
BEGIN
  RETURN BWB.Ymt.CnA8o + BWB.Ymt.CnA8_a * Alpha;
END AeroCnDa;
(* ------------------------------------------------------------ *)
PROCEDURE AeroCnP() : REAL;
VAR
   Cnp : REAL;
BEGIN
  Cnp := BWB.Ymt.CnPo + BWB.Ymt.CnP_a * Alpha;
  IF ((Aircraft = 7) AND (Vc > 0.0)) THEN
      Cnp := Cnp * BWB.Geo.b / (2.0 * Vc);
  END;
  RETURN Cnp;
END AeroCnP;
(* ------------------------------------------------------------ *)
PROCEDURE AeroCnR() : REAL;
VAR
   Cnr : REAL;
BEGIN
  Cnr := BWB.Ymt.CnRo + BWB.Ymt.CnR_a * Alpha;
  IF ((Aircraft = 7) AND (Vc > 0.0)) THEN
      Cnr := Cnr * BWB.Geo.b / (2.0 * Vc);
  END;
  RETURN Cnr;
END AeroCnR;
(* ------------------- New procedures ------------------ *)
PROCEDURE Coefficients;
BEGIN
   Cz0 := AeroCz0();
   Cza1 := AeroCz1();
   CzQ := AeroCzQ();
   CzDe := AeroCzDe();
   Cx0 := AeroCx0();
   k1 := AeroCxK1();
   k2 := AeroCxK2();
```

```
   Cyb := AeroCyBeta();
   CyP := AeroCyP();
   CyR := AeroCyR();
   CyDa := AeroCyDa();
   CyDr := AeroCyDr();
   Cm0 := AeroCm0();
   Cma := AeroCmAlpha();
   CmQ := AeroCmQ();
   CmDe := AeroCmDe();
   Clb := AeroClBeta();
   ClP := AeroClP();
   ClR := AeroClR();
   ClDa:= AeroClDa();
   ClDr:= AeroClDr();
   Cnb := AeroCnBeta();
   CnP := AeroCnP();
   CnR := AeroCnR();
   CnDa:= AeroCnDa();
   CnDr:= AeroCnDr();
END Coefficients;
(* ------------------------------------------------------ *)
PROCEDURE NormalCoef(De : REAL) : REAL;
BEGIN
   CoefNorm := Cz0 + Cza1 * Alpha + CzQ * Q + CzDe * De;
   RETURN CoefNorm;
END NormalCoef;
(* ------------------------------------------------------ *)
PROCEDURE AxialCoef() : REAL;
BEGIN
   RETURN -(Cx0 + k1 * (-CoefNorm) + k2 * CoefNorm * CoefNorm);
END AxialCoef;
(* ------------------------------------------------------ *)
PROCEDURE LateralCoef(Da, Dr : REAL) : REAL;
BEGIN
   RETURN Cyb * Beta + CyP * P + CyR * R + CyDa * Da + CyDr * Dr;
END LateralCoef;
(* ------------------------------------------------------ *)
PROCEDURE RollingMtCoef(Da, Dr : REAL) : REAL;
BEGIN
   RETURN Clb * Beta + ClP * P + ClR * R + ClDa * Da + ClDr * Dr;
END RollingMtCoef;
(* ------------------------------------------------------ *)
PROCEDURE PitchingMtCoef(De : REAL) : REAL;
BEGIN
   RETURN Cm0 + Cma * Alpha + CmQ * Q + CmDe * De;
END PitchingMtCoef;
(* ------------------------------------------------------ *)
PROCEDURE YawingMtCoef(Da, Dr : REAL) : REAL;
BEGIN
   RETURN Cnb * Beta + CnP * P + CnR * R + CnDa * Da + CnDr * Dr;
END YawingMtCoef;
(* ------------------------------------------------------------ *)
BEGIN
END Aero.
```

D.2.5 AeroData.def

```
DEFINITION MODULE AeroData;
(* Aerodynamic data for several different aircrafts or configurations *)
(* ------------------------------------------------------------ *)
TYPE
  GeometricPropertiesRecord = RECORD
    Name : ARRAY [1..5] OF CHAR;
    b              : REAL;
    S              : REAL;
    mac    : REAL;
  END;
(* ------------------------------------------------------------ *)
  MassPropertiesRecord = RECORD
    Mass           : REAL;
    Xcg            : REAL;
    Ycg            : REAL;
    Zcg            : REAL;
    Ixx            : REAL;
    Iyy            : REAL;
```

```
    Izz             : REAL;
    Ixz             : REAL;
    Iyz             : REAL;
    Ixy             : REAL;
  END;
  (* ------------------------------------------------------------ *)
  ZForceRecord = RECORD
    CZo    : REAL;
    CZa    : REAL;
    CZq    : REAL;
    CZF1   : REAL;
    CZF2   : REAL;
    CZF3   : REAL;
    CZF4   : REAL;
    CZF5   : REAL;
    CZF6   : REAL;
    CZF7   : REAL;
    CZF8   : REAL;
  END;
  (* ------------------------------------------------------------ *)
  XForceRecord = RECORD
    CXo    : REAL;
    CXk1   : REAL;
    CXk2   : REAL;
    CXF1   : REAL;
    CXF2   : REAL;
    CXF3   : REAL;
    CXF4   : REAL;
    CXF5   : REAL;
    CXF6   : REAL;
    CXF7   : REAL;
    CXF8   : REAL;
  END;
  (* ------------------------------------------------------------ *)
  SideRecord = RECORD
    CYo    : REAL;
    CYbo   : REAL;
    CYb_a  : REAL;
    CYPo   : REAL;
    CYP_a  : REAL;
    CYRo   : REAL;
    CYR_a  : REAL;
    CYA1o  : REAL;
    CYA1_a          : REAL;
    CYA2o  : REAL;
    CYA2_a          : REAL;
    CYA3   : REAL;
    CYA4   : REAL;
    CYA5   : REAL;
    CYA6   : REAL;
    CYA7   : REAL;
    CYA8o  : REAL;
    CYA8_a          : REAL;
    CYdRo  : REAL;
    CYdR_a          : REAL;
  END;
  (* ------------------------------------------------------------ *)
  RollRecord = RECORD
    Clo    : REAL;
    Clbo   : REAL;
    Clb_a  : REAL;
    ClPo   : REAL;
    ClP_a  : REAL;
    ClRo   : REAL;
    ClR_a  : REAL;
    ClA1o  : REAL;
    ClA1_a : REAL;
    ClA2o  : REAL;
    ClA2_a : REAL;
    ClA3   : REAL;
    ClA4   : REAL;
    ClA5   : REAL;
    ClA6   : REAL;
    ClA7   : REAL;
    ClA8o  : REAL;
```

```
  ClA8_a: REAL;
  CldRo  : REAL;
  CldR_a: REAL;
END;
(* ------------------------------------------------------------ *)
PitchRecord = RECORD
  Cmo    : REAL;
  Cma    : REAL;
  Cmq    : REAL;
  CmF1   : REAL;
  CmF2   : REAL;
  CmF3   : REAL;
  CmF4   : REAL;
  CmF5   : REAL;
  CmF6   : REAL;
  CmF7   : REAL;
  CmF8   : REAL;
END;
(* ------------------------------------------------------------ *)
YawRecord = RECORD
  Cno    : REAL;
  Cnbo   : REAL;
  Cnb_a  : REAL;
  CnPo   : REAL;
  CnP_a  : REAL;
  CnRo   : REAL;
  CnR_a  : REAL;
  CnA1o  : REAL;
  CnA1_a         : REAL;
  CnA2o  : REAL;
  CnA2_a         : REAL;
  CnA3   : REAL;
  CnA4   : REAL;
  CnA5   : REAL;
  CnA6   : REAL;
  CnA7   : REAL;
  CnA8o  : REAL;
  CnA8_a         : REAL;
  CndRo  : REAL;
  CndR_a         : REAL;
END;
(* ------------------------------------------------------------ *)
AccelerationPointRecord = RECORD
  x              : REAL;
  y              : REAL;
  z              : REAL;
END;
(* ------------------------------------------------------------ *)
GearRecord = RECORD
  MainGearCG : REAL;
  NoseGearCG : REAL;
  CGToGround : REAL;
  GearOffset : REAL;
  XoM    : REAL;
  XoN    : REAL;
END;
(* ------------------------------------------------------------ *)
EngineRecord = RECORD
  Arm1   : REAL;
  Arm2   : REAL;
  Arm3   : REAL;
  Height : REAL;
END;
(* ------------------------------------------------------------ *)
AircraftRecord = RECORD
  Geo    : GeometricPropertiesRecord;
  Mass   : MassPropertiesRecord;
  XF             : XForceRecord;
  YF             : SideRecord;
  ZF             : ZForceRecord;
  Rmt    : RollRecord;
  Pmt    : PitchRecord;
  Ymt    : YawRecord;
  Point  : AccelerationPointRecord;
  LGear  : GearRecord;
```

```
  Eng     : EngineRecord;
 END;
(* ------------------------------------------------------------- *)
 LateralFCSRecord = RECORD
  Kp              :REAL;
  Kb              :REAL;
  Kphi    :REAL;
  Ki              :REAL;
  Kpi     :REAL;
  m               :REAL;
 END;
 (* ------------------------------------------------------------- *)
 LongitudinalFCSRecord = RECORD
  Kq              :REAL;
  Kp              :REAL;
  Ki              :REAL;
  Ka              :REAL;
  m               :REAL;
 END;
 (* ------------------------------------------------------------- *)
 DirectionalFCSRecord = RECORD
  Kr0     :REAL; (*Yaw rate gain*)
  Kr1     :REAL;
  Kr2     :REAL;
  Kr3     :REAL;
  Kb0     :REAL; (*Sideslip gain*)
  Kb1     :REAL;
  Kb2     :REAL;
  Kb3     :REAL;
  Kari0   :REAL; (*Aileron-rudder interconnect*)
  Kari1   :REAL;
  Kari2   :REAL;
  Kari3   :REAL;
  Two     :REAL; (*WashOut gain*)
  Kay     :REAL;
 END;
 (* ------------------------------------------------------------- *)
 PreFilterFCSRecord = RECORD
  T2d     :REAL;
  T2a     :REAL;
 END;
 (* ------------------------------------------------------------- *)
 FCSRecord = RECORD
  LatFCS :LateralFCSRecord;
  LongFCS         :LongitudinalFCSRecord;
  DirFCS :DirectionalFCSRecord;
  PreF    :PreFilterFCSRecord;
 END;
(* ------------------------------------------------------------- *)
VAR
 BWB : AircraftRecord;
 AFCS : FCSRecord;
PROCEDURE SetupModel(Identifier1 : CARDINAL);
PROCEDURE SetupFCS(Identifier2 : CARDINAL);
END AeroData.
```

D.2.6 AeroData.mod

```
IMPLEMENTATION MODULE AeroData;
(*********************************************************************)
(*      This module calculates the aerodynamic forces and moments    *)
(*      from the aircraft characteristics.                           *)
(*      The original module was changed for a new source of data,    *)
(*      actually aerodynamic data already in body axis reference!    *)
(*                          Version 2.0                              *)
(*                      Helena V. de Castro                          *)
(*                          27 - 04 - 02                             *)
(*********************************************************************)
PROCEDURE SetupModel(Identifier1 : CARDINAL);
BEGIN
   CASE Identifier1 OF
     1: BWB.Geo.Name   := 'BWB21';
        BWB.Geo.S      := 841.7;
        BWB.Geo.b      := 80.0;
```

```
BWB.Geo.mac   := 12.31;
BWB.Mass.Mass := 3.7128E5;
BWB.Mass.Ixx  := 4.7032E7;
BWB.Mass.Iyy  := 2.506977E7;          (* principal MoI along y-axis, Kg.m2 *)
BWB.Mass.Izz  := 9.9734E7;            (* principal MoI along z-axis, Kg.m2 *)
BWB.Mass.Ixz  := 0.0;                 (* Product of inertia *)
BWB.Mass.Ixy  := 0.0;
BWB.Mass.Iyz  := 0.0;
BWB.XF.CXo    := 0.0117;
BWB.XF.CXk1:= -0.02;
BWB.XF.CXk2:= 0.12;
BWB.XF.CXF1:= 0.0;
BWB.XF.CXF2:= 0.0;
BWB.XF.CXF3:= 0.0;
BWB.XF.CXF4:= 0.0;
BWB.XF.CXF5:= 0.0;
BWB.XF.CXF6:= 0.0;
BWB.XF.CXF7:= 0.0;
BWB.XF.CXF8:= BWB.XF.CXF2 + BWB.XF.CXF3 +
              BWB.XF.CXF4 + BWB.XF.CXF5 +
              BWB.XF.CXF6 + BWB.XF.CXF7;
BWB.YF.CYo    := 0.0;
BWB.YF.CYbo   := -0.3086;
BWB.YF.CYb_a  := 0.4879;
BWB.YF.CYPo   := -0.0814;
BWB.YF.CYP_a  := 2.0666;
BWB.YF.CYRo   := -0.1584;
BWB.YF.CYR_a  := 0.0;
BWB.YF.CYA1o := -0.0184;
BWB.YF.CYA1_a := 0.0;
BWB.YF.CYA2o := -0.0154;
BWB.YF.CYA2_a := 0.0;
BWB.YF.CYA3:= -0.0088;
BWB.YF.CYA4:= -0.0060;
BWB.YF.CYA5:= -0.0056;
BWB.YF.CYA6:= -0.0036;
BWB.YF.CYA7:= 0.0;
BWB.YF.CYA8o := BWB.YF.CYA3; (* + BWB.YF.CYA2;   *)
BWB.YF.CYA8_a := 0.0;
BWB.YF.CYdRo := 0.0467*5.0;
BWB.YF.CYdR_a := 0.0;
BWB.ZF.CZo    := 0.0217;
BWB.ZF.CZa    := -5.4868;
BWB.ZF.CZq    := -1.0787;     (* -4.3815; *)(* q*c/Vc *)
BWB.ZF.CZF1:= -0.1042;
BWB.ZF.CZF2:= -0.2274;
BWB.ZF.CZF3:= -0.2222;
BWB.ZF.CZF4:= -0.1602;
BWB.ZF.CZF5:= -0.1812;
BWB.ZF.CZF6:= -0.1870;
BWB.ZF.CZF7:= -0.1184;
BWB.ZF.CZF8:= BWB.ZF.CZF1 + BWB.ZF.CZF2 + BWB.ZF.CZF3 +
              BWB.ZF.CZF4 + BWB.ZF.CZF5 +
              BWB.ZF.CZF6 + BWB.ZF.CZF7;
BWB.Rmt.Clo := 0.0;
BWB.Rmt.Clbo:= -0.0465;
BWB.Rmt.Clb_a:= -0.3007;
BWB.Rmt.ClPo:= -0.3562;
BWB.Rmt.ClP_a:= 0.0735;
BWB.Rmt.ClRo:= 0.0272;
BWB.Rmt.ClR_a:= 0.5867;
BWB.Rmt.ClA1o := -0.0396;
BWB.Rmt.ClA1_a := 0.0;
BWB.Rmt.ClA2o := -0.0644;
BWB.Rmt.ClA2_a := 0.0;
BWB.Rmt.ClA3 := -0.0442;
BWB.Rmt.ClA4 := -0.023;
BWB.Rmt.ClA5 := -0.0178;
BWB.Rmt.ClA6 := -0.0096;
BWB.Rmt.ClA7 := 0.0;
BWB.Rmt.ClA8o := BWB.Rmt.ClA3; (* + BWB.Rmt.ClA2;*)
BWB.Rmt.ClA8_a := 0.0;
BWB.Rmt.CldRo := 0.0156*5.0;
BWB.Rmt.CldR_a := 0.0;
BWB.Pmt.Cmo := -0.0370;
BWB.Pmt.Cma := -0.9950;
```

```
BWB.Pmt.Cmq := -0.8799;       (* -3.5739; *)(* q*c/Vc *)
BWB.Pmt.CmF1 := -0.1272;
BWB.Pmt.CmF2 := -0.1980;
BWB.Pmt.CmF3 := -0.1414;
BWB.Pmt.CmF4 := -0.0984;
BWB.Pmt.CmF5 := -0.1198;
BWB.Pmt.CmF6 := -0.1198;
BWB.Pmt.CmF7 := -0.0712;
BWB.Pmt.CmF8 := BWB.Pmt.CmF1 + BWB.Pmt.CmF2 + BWB.Pmt.CmF3 +
                BWB.Pmt.CmF4 + BWB.Pmt.CmF5 +
                BWB.Pmt.CmF6 + BWB.Pmt.CmF7;
BWB.Ymt.Cno := 0.0;
BWB.Ymt.Cnbo:= 0.0152;
BWB.Ymt.Cnb_a:= -0.2787;
BWB.Ymt.CnPo:= 0.0134;
BWB.Ymt.CnP_a:= -0.8733;
BWB.Ymt.CnRo:= -0.0315;
BWB.Ymt.CnR_a:= 0.0867;
BWB.Ymt.CnA1o := 0.0046;
BWB.Ymt.CnA1_a := 0.0;
BWB.Ymt.CnA2o := 0.0028;
BWB.Ymt.CnA2_a := 0.0;
BWB.Ymt.CnA3 := 0.0014;
BWB.Ymt.CnA4 := 0.0010;
BWB.Ymt.CnA5 := 0.0008;
BWB.Ymt.CnA6 := 0.0006;
BWB.Ymt.CnA7 := 0.0;
BWB.Ymt.CnA8o := BWB.Ymt.CnA3; (* + BWB.Ymt.CnA2;*)
BWB.Ymt.CnA8_a := 0.0;
BWB.Ymt.CndRo := -0.0115*5.0;
BWB.Ymt.CndR_a := 0.0;
BWB.Point.x := 0.0;
BWB.Point.y := 0.0;
BWB.Point.z := 0.0;
BWB.LGear.MainGearCG := 5.0;
BWB.LGear.NoseGearCG := 24.3;
BWB.LGear.CGToGround := (*-3.826;*) -2.0;
BWB.LGear.GearOffset := 0.0;
BWB.LGear.XoM := -0.0762;
BWB.LGear.XoN := -0.05;
BWB.Eng.Arm1 := -7.5;         (* Left engine *)
BWB.Eng.Arm2 := 0.0;          (* Middle engine *)
BWB.Eng.Arm3 := 7.5;          (* Right engine *)
BWB.Eng.Height := 0.0;|
```

```
7: BWB.Geo.Name   := 'MOB';              (* Values from MOB project *)
   BWB.Geo.S      := 841.7;
   BWB.Geo.b      := 80.0;
   BWB.Geo.mac    := 12.31;
   BWB.Mass.Mass := 3.7128E5;
   BWB.Mass.Ixx   := 4.7032E7;
   BWB.Mass.Iyy   := 2.506977E7;         (* principal MoI along y-axis, Kg.m2 *)
   BWB.Mass.Izz   := 9.9734E7;           (* principal MoI along z-axis, Kg.m2 *)
   BWB.Mass.Ixz   := 0.0;                (* Product of inertia *)
   BWB.Mass.Ixy   := 0.0;
   BWB.Mass.Iyz   := 0.0;
   BWB.XF.CXo     := 0.0117;
   BWB.XF.CXk1:= -0.02;
   BWB.XF.CXk2:= 0.12;
   BWB.XF.CXF1:= 0.0;
   BWB.XF.CXF2:= 0.0;
   BWB.XF.CXF3:= 0.0;
   BWB.XF.CXF4:= 0.0;
   BWB.XF.CXF5:= 0.0;
   BWB.XF.CXF6:= 0.0;
   BWB.XF.CXF7:= 0.0;
   BWB.XF.CXF8:= 0.0;
   BWB.YF.CYo     := 0.0;
   BWB.YF.CYbo    := -0.1398;
   BWB.YF.CYb_a   := 0.0;
   BWB.YF.CYPo    := -0.372;
   BWB.YF.CYP_a   := 2.5356;
   BWB.YF.CYRo    := -0.2888;
```

```
BWB.YF.CYR_a  := 0.485;
BWB.YF.CYA1o:= -0.0621;
BWB.YF.CYA1_a:= 0.2134;
BWB.YF.CYA2o := -0.041;
BWB.YF.CYA2_a:= 0.0819;
BWB.YF.CYA3 := 0.0;
BWB.YF.CYA4 := 0.0;
BWB.YF.CYA5 := 0.0;
BWB.YF.CYA6 := 0.0;
BWB.YF.CYA7 := 0.0;
BWB.YF.CYA8o := BWB.YF.CYA2o;        (* + BWB.YF.CYA1; *)
BWB.YF.CYA8_a:= BWB.YF.CYA2_a;
BWB.YF.CYdRo := 0.0917;
BWB.YF.CYdR_a:= -0.0656;
BWB.ZF.CZo    := -0.3204;
BWB.ZF.CZa    := -5.8347;
BWB.ZF.CZq    := -1.0787;            (* -4.3815; *)(* q*c/Vc *)
BWB.ZF.CZF1:= 0.0;
BWB.ZF.CZF2:= 0.0;
BWB.ZF.CZF3:= 0.0;
BWB.ZF.CZF4:= 0.0;
BWB.ZF.CZF5:= 0.0;
BWB.ZF.CZF6:= 0.0;
BWB.ZF.CZF7:= 0.0;
BWB.ZF.CZF8:= -2.2575;
BWB.Rmt.Clo := 0.0;
BWB.Rmt.Clbo:= -0.0104;
BWB.Rmt.Clb_a:= -1.1233;
BWB.Rmt.ClPo:= -0.4641;
BWB.Rmt.ClP_a:= 0.1255;
BWB.Rmt.ClRo:= -0.0787;
BWB.Rmt.ClR_a:= 0.7612;
BWB.Rmt.ClA1o := -0.071;
BWB.Rmt.ClA1_a:= 0.0;
BWB.Rmt.ClA2o := -0.1500;
BWB.Rmt.ClA2_a:= 0.0;
BWB.Rmt.ClA3 := 0.0;
BWB.Rmt.ClA4 := 0.0;
BWB.Rmt.ClA5 := 0.0;
BWB.Rmt.ClA6 := 0.0;
BWB.Rmt.ClA7 := 0.0;
BWB.Rmt.ClA8o := BWB.Rmt.ClA2o;      (* + BWB.Rmt.ClA1;*)
BWB.Rmt.ClA8_a:= BWB.Rmt.ClA2_a;
BWB.Rmt.CldRo := 0.0253;
BWB.Rmt.CldR_a:= 0.0178;
BWB.Pmt.Cmo := -0.040;
BWB.Pmt.Cma := 0.7412;
BWB.Pmt.Cmq := -0.8799;      (* -3.5739; *)(* q*c/Vc *)
BWB.Pmt.CmF1 := 0.0;
BWB.Pmt.CmF2 := 0.0;
BWB.Pmt.CmF3 := 0.0;
BWB.Pmt.CmF4 := 0.0;
BWB.Pmt.CmF5 := 0.0;
BWB.Pmt.CmF6 := 0.0;
BWB.Pmt.CmF7 := 0.0;
BWB.Pmt.CmF8 := -0.7162;
BWB.Ymt.Cno := 0.0;
BWB.Ymt.Cnbo:= 0.0213;
BWB.Ymt.Cnb_a:= -0.2584;
BWB.Ymt.CnPo:= 0.0631;
BWB.Ymt.CnP_a:= -0.8337;
BWB.Ymt.CnRo:= -0.0349;
BWB.Ymt.CnR_a:= 0.0037;
BWB.Ymt.CnA1o := 0.0014;
BWB.Ymt.CnA1_a:= -0.0957;
BWB.Ymt.CnA2o := 0.0041;
BWB.Ymt.CnA2_a:= -0.0504;
BWB.Ymt.CnA3 := 0.0;
BWB.Ymt.CnA4 := 0.0;
BWB.Ymt.CnA5 := 0.0;
BWB.Ymt.CnA6 := 0.0;
BWB.Ymt.CnA7 := 0.0;
BWB.Ymt.CnA8o := BWB.Ymt.CnA2o;       (* + BWB.Ymt.CnA1;*)
BWB.Ymt.CnA8_a:= BWB.Ymt.CnA2_a;
BWB.Ymt.CndRo := -0.0158;
BWB.Ymt.CndR_a:= 0.0352;
```

```
        BWB.Point.x := 0.0;
        BWB.Point.y := 0.0;
        BWB.Point.z := 0.0;
        BWB.LGear.MainGearCG := 1.0;
        BWB.LGear.NoseGearCG := 28.3;
        BWB.LGear.CGToGround := (*-3.826;*) -2.0;
        BWB.LGear.GearOffset := 0.0;
        BWB.LGear.XoM := -0.0762;
        BWB.LGear.XoN := -0.05;
        BWB.Eng.Arm1 := -7.5;        (* Left engine to CG *)
        BWB.Eng.Arm2 := 0.0;         (* Middle engine to CG *)
        BWB.Eng.Arm3 := 7.5;         (* Right engine to CG *)
        BWB.Eng.Height := 0.0;              (* Engine height to CG *)
   END;
END SetupModel;
(*****************************************************************)
PROCEDURE SetupFCS(Identifier2: CARDINAL);
BEGIN
   CASE Identifier2 OF
   10:   AFCS.LatFCS.Kp := 0.0;
         AFCS.LatFCS.Kb := 0.0;
         AFCS.LatFCS.Kphi := 0.0;
         AFCS.LatFCS.Ki := 0.0;
         AFCS.LatFCS.Kpi := 0.0;
         AFCS.LatFCS.m := 0.0;
         AFCS.LongFCS.Kq := 0.0;
         AFCS.LongFCS.Kp := -5.0;
         AFCS.LongFCS.Ki := 0.0;
         AFCS.LongFCS.Ka := 0.0;
         AFCS.LongFCS.m       := 1.0;
         AFCS.DirFCS.Kr0 := 0.0;
         AFCS.DirFCS.Kr1 := 0.0;
         AFCS.DirFCS.Kb0 := 0.0;
         AFCS.DirFCS.Kb1 := 0.0;
         AFCS.DirFCS.Kari0 := 0.0;
         AFCS.DirFCS.Kari1 := 0.0;
         AFCS.DirFCS.Two := 1.0;
         AFCS.DirFCS.Kay := 0.0;
         AFCS.PreF.T2d := 1.0;
         AFCS.PreF.T2a  := 1.0;|
.
.
.
.
   74:  AFCS.LatFCS.Kp := 0.0;
        AFCS.LatFCS.Kb := 0.0;
        AFCS.LatFCS.Kphi := 0.0;
        AFCS.LatFCS.Ki := 0.0;
         AFCS.LatFCS.Kpi := 0.0;
         AFCS.LatFCS.m := 0.0;
        AFCS.LongFCS.Kq := 1.0;
        AFCS.LongFCS.Kp := -1.0716;
        AFCS.LongFCS.Ki := -2.7486;
        AFCS.LongFCS.Ka := -0.5811;
        AFCS.LongFCS.m  := 2.7486/3.0;
        AFCS.DirFCS.Kr0 := -5.0;
        AFCS.DirFCS.Kr1 := 0.0;
        AFCS.DirFCS.Kb0 := 3.0;
        AFCS.DirFCS.Kb1 := 0.0;
        AFCS.DirFCS.Kari0 := 1.5783;
        AFCS.DirFCS.Kari1 := 7.4095;
         AFCS.DirFCS.Two := 1.0;
        AFCS.DirFCS.Kay := 0.0;
        AFCS.PreF.T2d := 1.646/3.01;
        AFCS.PreF.T2a  := 1.0/1.6998;|
   75:  AFCS.LatFCS.Kp := -1.0;
        AFCS.LatFCS.Kb := 0.0;
        AFCS.LatFCS.Kphi := 0.0;
        AFCS.LatFCS.Ki := -1.5;
        AFCS.LatFCS.Kpi := -0.8;
        AFCS.LatFCS.m := 0.0;
        AFCS.LongFCS.Kq := 1.0;
        AFCS.LongFCS.Kp := -1.0716;
        AFCS.LongFCS.Ki := -2.7486;
        AFCS.LongFCS.Ka := -0.5811;
        AFCS.LongFCS.m  := 2.7486/3.0;
```

```
        AFCS.DirFCS.Kr0 := -0.5602;
        AFCS.DirFCS.Kr1 := -9.9518;
        AFCS.DirFCS.Kb0 := 0.4324;
        AFCS.DirFCS.Kb1 := 5.8402;
        AFCS.DirFCS.Kari0 := 1.6815;
        AFCS.DirFCS.Kari1 := 3.1584;
         AFCS.DirFCS.Two := 1.0;
        AFCS.DirFCS.Kay := 0.0;
        AFCS.PreF.T2d := 1.646/3.01;
        AFCS.PreF.T2a  := 1.0/1.6998;
   END;
END SetupFCS;
END AeroData.
```

D.2.7 FCS.def

```
DEFINITION MODULE FCS;
(*********************************************************************)
(*   This is the declaration part of the FCS module.                 *)
(*   This module is changed to accommodate for the different         *)
(*   FCS of the BWB2 aircraft.                                       *)
(*              Version 2.0                                          *)
(*            Helena V. de Castro                                    *)
(*              13 - 02 - 02                                         *)
(*********************************************************************)
VAR
  Rwo : REAL;
  Ecf : REAL;
  PROCEDURE PreFilter(LongCmd : REAL) : REAL;
  PROCEDURE FeedForward(PFout : REAL) : REAL;
  PROCEDURE Integration(PFout : REAL) : REAL;
  PROCEDURE LongFeedBack() : REAL;
  PROCEDURE Actuator(VAR ActuatorPosition, ActuatorSpeed : REAL;   Input : REAL) : REAL;
  PROCEDURE TurnCompensation() : REAL;
  PROCEDURE LongFCS(LongCmd : REAL) : REAL;
  PROCEDURE LatFeedBack() : REAL;
  PROCEDURE RollFeedBack() : REAL;
  PROCEDURE BankAngle() : REAL;
  PROCEDURE RollRateCmd(Lat : REAL) : REAL;
  PROCEDURE LatFeedFwd(Lat : REAL) : REAL;
  PROCEDURE LatFCS(LatCmd : REAL) : REAL;
  PROCEDURE SideFeedBack(DirCmd : REAL) : REAL;
  PROCEDURE AilRudInt(Lat : REAL) : REAL;
  PROCEDURE KariWO(Tcf, Kari : REAL) : REAL;
  PROCEDURE YawFeedBack(dR : REAL) : REAL;
  PROCEDURE AccFeedBack() : REAL;
  PROCEDURE DirFCS(DirCmd, LatCmd : REAL) : REAL;
END FCS.
```

D.2.8 FCS.mod

```
IMPLEMENTATION MODULE FCS;
(*********************************************************************)
(*     This is changed from the B747 original to account for the     *)
(*     different FCS used in the BWB2.                               *)
(*     This module contains the flight control systems for           *)
(*     longitudinal and lateral-directional motions.                 *)
(*     For longitudinal a commanded stability augmentation system    *)
(*     is used, for lateral and directional (more directional)       *)
(*     a yaw damper is implemented.                                  *)
(*                         Version 2.0                               *)
(*                      Helena V. de Castro                          *)
(*                         13 - 02 - 02                              *)
(*********************************************************************)
FROM Maths IMPORT
   Rads, Limit, Normalise, Integrate, ONERAD;
FROM MathLib0 IMPORT
   tan, cos;
FROM Aero IMPORT
   CGHeight, Cza1, AeroMaxAlpha;
FROM AeroData IMPORT
```

```
   AFCS, BWB;
FROM Model IMPORT
   Pitch, Roll, Yaw, Pz, Vd, U, UDot, P, Q, Alpha, R, RDot, PDot, Beta,
   AlrAcSpeed, FlightControl, VDot, GForce, OneG, Vc, OnTheGround;
FROM Weather IMPORT
   Rho;
CONST
  wn = 30.0;           (* actuator frequency *)
  damp = 0.7;          (* actuator damping *)
VAR
   PF, LongIntg, LatIntg : REAL;   (* state for pre-filter and Integrals *)
(* ------------------ Pocedures ---------------------- *)
PROCEDURE PreFilter(LongCmd : REAL) : REAL;
VAR
 PFDot : REAL;
BEGIN
   PFDot := (1.0 - AFCS.PreF.T2d / AFCS.PreF.T2a) * LongCmd -
            (1.0 / AFCS.PreF.T2a) * PF;
   Integrate(PF, PFDot);
   RETURN 1.0 / AFCS.PreF.T2a * PF + AFCS.PreF.T2d / AFCS.PreF.T2a * LongCmd;
END PreFilter;
(* ---------------------------------------------------------- *)
PROCEDURE FeedForward(PFout : REAL) : REAL;
BEGIN
  RETURN AFCS.LongFCS.Kp * (AFCS.LongFCS.m - 1.0) * PFout;
END FeedForward;
(* ---------------------------------------------------------- *)
PROCEDURE Integration(PFout : REAL) : REAL;
VAR
   Err : REAL;
BEGIN
   Err := PFout - Q*AFCS.LongFCS.Kq;
   Integrate(LongIntg, Err);
   RETURN AFCS.LongFCS.Ki * LongIntg  + AFCS.LongFCS.Kp * Err;
END Integration;
(* ---------------------------------------------------------- *)
PROCEDURE LongFeedBack() : REAL;
BEGIN
   RETURN -AFCS.LongFCS.Ka * Alpha;   (*-Ka * Alpha;*)
END LongFeedBack;
(* ---------------------------------------------------------- *)
PROCEDURE TurnCompensation() : REAL;
BEGIN
   RETURN R * tan(Roll);
END TurnCompensation;
(* ---------------------------------------------------------- *)
PROCEDURE LongFCS(LongCmd : REAL) : REAL;
CONST
   AlphaMax = 0.32;
   VLim = 80.0;
VAR
   PFout : REAL;
   Asw : REAL;
BEGIN
   IF (FlightControl = 74) THEN
      IF ( (Alpha > AlphaMax) OR (Vc < VLim) ) THEN
         IF ((Alpha > AlphaMax) AND (LongCmd < 0.0)) THEN
           LongCmd := 0.0;
        END;
        Asw := -LongCmd + 1.3*Alpha;
      ELSE
         PFout := PreFilter(LongCmd);
        Asw := FeedForward(PFout) + LongFeedBack() + Integration(PFout);
      END;
   ELSE
      PFout := PreFilter(LongCmd);
      Asw := FeedForward(PFout) + LongFeedBack() + Integration(PFout);
   END;
   RETURN Asw;
END LongFCS;
(* ---------------------------------------------------------- *)
PROCEDURE LatFeedBack() : REAL;
BEGIN
   RETURN AFCS.LatFCS.Kb * Beta;      (*Kb * Beta;*)
END LatFeedBack;
(* ---------------------------------------------------------- *)
```

```
PROCEDURE RollFeedBack() : REAL;
BEGIN
   RETURN -AFCS.LatFCS.Kp * P;
END RollFeedBack;
(* ---------------------------------------------------------- *)
PROCEDURE BankAngle() : REAL;
BEGIN
   RETURN -AFCS.LatFCS.Kphi * Roll;
END BankAngle;
(* ---------------------------------------------------------- *)
PROCEDURE RollRateCmd(Lat : REAL) : REAL;
VAR
   Err : REAL;
BEGIN
   Err := Lat - P*AFCS.LatFCS.Kp;
   Integrate(LatIntg, Err);
   RETURN AFCS.LatFCS.Ki * LatIntg + AFCS.LatFCS.Kpi * Err;
END RollRateCmd;
(* ---------------------------------------------------------- *)
PROCEDURE LatFeedFwd(Lat : REAL) : REAL;
BEGIN
   RETURN Lat * AFCS.LatFCS.m * AFCS.LatFCS.Kp;
END LatFeedFwd;
(* ---------------------------------------------------------- *)
PROCEDURE LatFCS(LatCmd : REAL) : REAL;
VAR
   Asw : REAL;
BEGIN
   IF (FlightControl = 76) THEN
      Asw := RollRateCmd(-LatCmd/2.0) + LatFeedFwd(-LatCmd/2.0);
   ELSE
      Asw := LatCmd + LatFeedBack() + RollFeedBack() + BankAngle();
   END;
   RETURN Asw;
END LatFCS;
(* ---------------------------------------------------------- *)
PROCEDURE SideFeedBack(DirCmd: REAL) : REAL;
VAR
   Kb : REAL;
   Asw : REAL;
BEGIN
   Kb := AFCS.DirFCS.Kb0 + AFCS.DirFCS.Kb1 * Alpha;
   IF ((FlightControl = 74) OR (FlightControl = 62)) THEN
      Asw := -Kb * (Beta - 10.0/20.0 * DirCmd);
   ELSE
      Asw :=  -Kb * Beta;
   END;
   RETURN Asw;
END SideFeedBack;
(* ---------------------------------------------------------- *)
PROCEDURE AilRudInt(Lat : REAL) : REAL;
VAR
   Kari : REAL;
   Tcf : REAL;
   Asw : REAL;
BEGIN
   Kari :=  AFCS.DirFCS.Kari0 + AFCS.DirFCS.Kari1 * Alpha;
   CASE FlightControl OF
   61:
      Tcf := 0.05;
      Asw := KariWO(Tcf,Kari);|
   62:
      Tcf := 0.05;
      Asw := KariWO(Tcf,Kari);|
   74:
      Tcf := 0.05;
      Asw := KariWO(Tcf,Kari);|
   75:
      Tcf := 3.0;
      Asw := KariWO(Tcf,Kari);|
   ELSE
      Asw := Kari*Lat;
   END;
   RETURN Asw;
END AilRudInt;
(* ---------------------------------------------------------- *)
```

```
PROCEDURE KariWO(Tcf, Kari: REAL): REAL;
VAR
   dEcf : REAL;
BEGIN
   dEcf := -1.0/Tcf*Ecf - Kari*AlrAcSpeed;
   Integrate(Ecf,dEcf);
   RETURN Ecf;
END KariWO;
(* ------------------------------------------------------- *)
PROCEDURE YawFeedBack(dR : REAL) : REAL;
VAR
   dRwo : REAL;
   Kr   : REAL;
BEGIN
   Kr :=  AFCS.DirFCS.Kr0 + AFCS.DirFCS.Kr1 * Alpha;
   dRwo := dR - Rwo * 1.0/AFCS.DirFCS.Two;
   Integrate(Rwo, dRwo);
   RETURN -Kr * Rwo;
END YawFeedBack;
(* ------------------------------------------------------- *)
PROCEDURE AccFeedBack() : REAL;
BEGIN
   RETURN -AFCS.DirFCS.Kay * VDot;
END AccFeedBack;
(* ------------------------------------------------------- *)
PROCEDURE DirFCS(DirCmd, LatCmd : REAL) : REAL;
BEGIN
   RETURN DirCmd + SideFeedBack(DirCmd) + AilRudInt(LatCmd)
                 + YawFeedBack(RDot);
END DirFCS;
(* ------------------------------------------------------- *)
PROCEDURE Actuator(VAR ActuatorPosition, ActuatorSpeed : REAL;
                   Input : REAL) : REAL;
VAR
   APDot, ASDot : REAL;
BEGIN
   APDot := ActuatorSpeed;
   ASDot := - wn * wn * ActuatorPosition - 2.0 * damp * wn * ActuatorSpeed +
            wn * wn * Input;
   Integrate(ActuatorPosition, APDot);
   Integrate(ActuatorSpeed, ASDot);
   RETURN ActuatorPosition;
END Actuator;
(* ------------------------------------------------ *)
BEGIN
  PF := 0.0;
  LongIntg := 0.0;
  LatIntg := 0.0;
  Rwo := 0.0;
  Ecf := 0.0;
END FCS.
```

D.3 Landing gear model

A reasonably representative ground model is important to perform flight-simulated landings. In this section, a relatively simple longitudinal ground model is presented. Firstly, the nose and main landing gears are considered independent from each other. Secondly, the landing gear wheels are approached to damped springs (second order system). Before the landing gear model is presented a diagram of forces and moments acting on the aircraft during the ground roll must be considered. Figure D.6 shows the forces and moments acting on the aircraft for the particular case of straight runway, and pitch attitude equal to angle of attack.

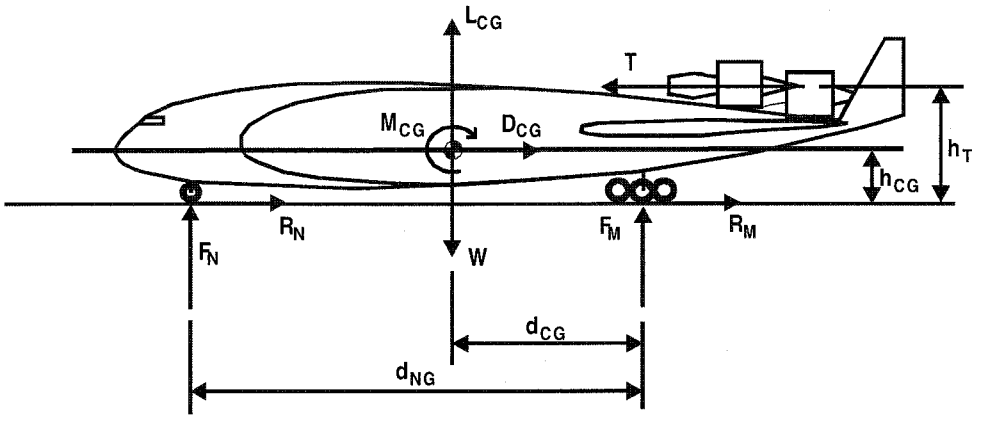

Figure D.6 Forces diagram of aircraft on ground rolling

If the aircraft is in equilibrium the forces and moments sum up to zero. Otherwise, they sum up in a resultant force and moment responsible for the movement of the aircraft. While the aircraft rolls on the ground the instantaneous centre of rotation is near to the main gear contact point with the ground, and not the *cg*. Hence this point is considered for the moment's point of reference. For the diagram present in figure D.6 the total forces and moments on the longitudinal plane are those given by equations (D.1) to (D.3).

$$\sum F_x = T - D_{CG} - R_N - R_M \tag{D.1}$$

$$\sum F_z = W - L_{CG} - F_N - F_M \tag{D.2}$$

$$\sum M_{MG} = M_{CG} + F_N d_{NG} - (W - L_{CG}) d_{CG} + D_{CG} h_{CG} - T h_T \tag{D.3}$$

Except for the normal and axial landing gear friction forces, all other forces and moments are already calculated in the present flight model. These four new forces, F_N, F_M, R_N and R_M, become just two when taking in account that the normal and axial forces are related as shown in equations (D.4) and (D.5), where μ_f is the ground friction coefficient.

$$R_N = \mu_f F_N \tag{D.4}$$

$$R_M = \mu_f F_M \tag{D.5}$$

Different physical models found in the literature can be used to calculate the normal friction forces, F_N and F_M. The more complex model each one of the landing gear components, such as wheels, struts etc, in great detail. A simple landing gear model[113] was used here instead. This model considers each landing gear, main and nose, as a whole structure behaving as a damped spring, i.e., as a second order like system.

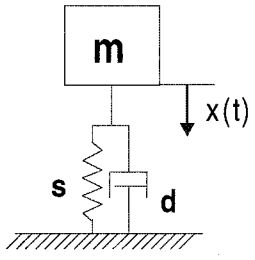

$$m\frac{d^2x(t)}{dt^2} + B\frac{dx(t)}{dt} + kx(t) = F(t)$$

where

B is the damping
k is the spring constant

Figure D.7 Mass-spring-damper or second order like system

Figure D.7 shows that the resultant of forces exerted on an aircraft landing gear induces a displacement in the landing gear. Equations (D.6) and (D.7) present the situations for the nose and main landing gears. The displacement is then related to the normal force that the landing gear exerts on the aircraft. Equations (D.8) and (D.9) present the relation between the nose and main landing gear forces and displacements.

$$m\frac{d^2x(t)}{dt^2} + B_N\frac{dx(t)}{dt} + k_N x(t) = R_N(t) \tag{D.6}$$

$$m\frac{d^2x(t)}{dt^2} + B_M\frac{dx(t)}{dt} + k_M x(t) = R_M(t) \tag{D.7}$$

$$F_N(t) = B_N\frac{dx(t)}{dt} + k_N x(t) \tag{D.8}$$

$$F_M(t) = B_M\frac{dx(t)}{dt} + k_M x(t) \tag{D.9}$$

Where B_N and B_M are the nose and main landing gear damping constants, and k_N and k_M are the nose and main landing gear spring constants. Comparing equation (D.10), the free force system, to equation (D.11), the general second order system characteristic equation, the values of B_N and B_M are calculated by making the damping of the system in equation (D.12) equal or higher to 0.7.

$$\ddot{x} + \frac{B}{m}\dot{x} + \frac{k}{m}x = 0 \tag{D.10}$$

$$s^2 + 2\xi\omega_n s + \omega_n{}^2 = 0 \tag{D.11}$$

$$B = 2\xi\sqrt{mk} \tag{D.12}$$

The values of k_N and k_M are calculated from static equilibrium conditions, so that the landing gear deflections will have determined value known as landing gear static deflections. From literature it was found that characteristic values for the nose and main landing gear static deflections, x_{o_N} and x_{o_M}, are around 0.5 and 0.7m.

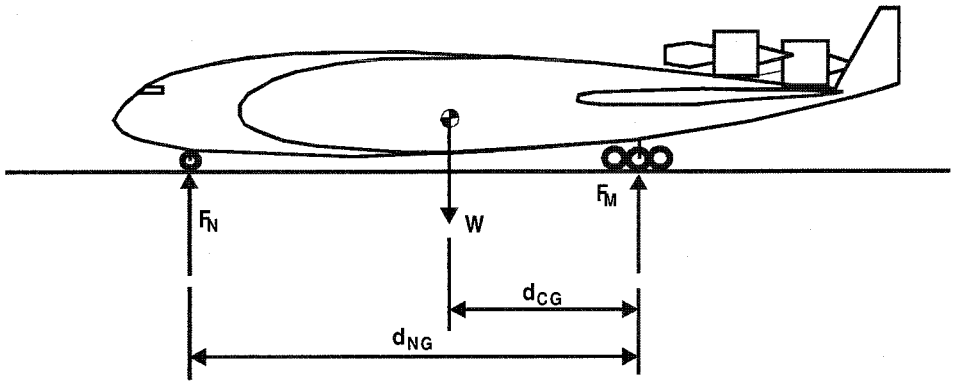

Figure D.8 Free forces diagram for an equilibrium static condition

$$W = F_N + F_M \tag{D.13}$$

$$F_N d_{NG} = W d_{CG} \tag{D.14}$$

$$F_N = k_N x_{o_N} \tag{D.15}$$

$$F_M = k_M x_{o_M} \tag{D.16}$$

Thus, from the static equilibrium diagram of figure D.8, equations (D.13) and (D.14) result. Since there is static equilibrium, the landing gear forces induced on the aircraft, equations (D.8) and (D.9) are reduced to equations (D.15) and (D.16). Combining equations (D.13) to (D.16), the nose and main landing gear spring constants, k_N and k_M, result in equations (D.17) and (D.18).

$$k_N = \frac{W}{x_{o_N}} \frac{d_{CG}}{d_{NG}} \tag{D.17}$$

$$k_M = \frac{W}{x_{o_M}} \left(1 - \frac{d_{CG}}{d_{NG}}\right) \tag{D.18}$$

Thus, the only values that need to be calculated to finally get the normal friction forces at any moment are the nose and main landing gear displacements, $x_N(t)$ and $x_M(t)$, and speeds, $\dot{x}_N(t)$ and $\dot{x}_M(t)$ of equations (D.8) and (D.9). These values are calculated taking in account Figure (D.4).

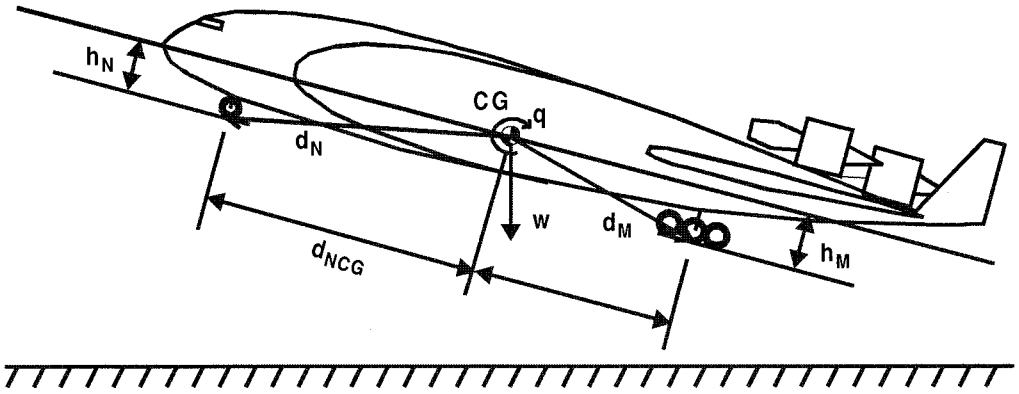

Figure D.9 Takeoff or approach situation

From figure D.9 it is seen that the nose and main landing gear speeds, $\dot{x}_N(t)$ and $\dot{x}_M(t)$, are equal to the down velocity of the centre of gravity, w, plus the contribution from the pitch rate rotation due to the distance from the *cg* of the nose and main landing gear, d_N and d_M. These are given by equations (D.19) and (D.20). In the same way, the nose and main landing gear actual displacements, $x_N(t)$ and $x_M(t)$, can be calculated as given in equations (D.21) and (D.22).

$$\dot{x}_N(t) = -d_N q + w \tag{D.19}$$

$$\dot{x}_M(t) = d_M q + w \tag{D.20}$$

where $d_N = \sqrt{h_N{}^2 + d_{NCG}{}^2}$ and $d_M = \sqrt{h_M{}^2 + d_{MCG}{}^2}$

$$x_N(t) = (h_{CG} - d_{NCG}\sin(\theta)) - (h_N + x_{Next} + GL)\cos(\theta) \tag{D.21}$$

$$x_M(t) = (h_{CG} - d_{MCG}\sin(\theta)) - (h_M + x_{Mext} + GL)\cos(\theta) \tag{D.22}$$

Where h_{CG} is the *cg* height to the ground, GL is the ground level, and x_{Next} and x_{Mext} are the displacements of the nose and main landing gear when these are completely extended. The first terms in equations (D.21) and (D.22), $(h_{CG} - d_{NCG}\sin(\theta))$ and $(h_{CG} - d_{MCG}\sin(\theta))$, represent the height of the wheels point contact to the ground. The second terms, $(h_N + x_{Next} + GL)\cos(\theta)$ and $(h_M + x_{Mext} + GL)\cos(\theta)$ represent the distance of that same point when the nose and main landing gears are completely extended, i.e., no forces act over the landing gear as the aircraft is airborne.

Appendix E
FLIGHT SIMULATION TRIALS

E.1 Pilots briefing

Large commercial Blended wing body (BWB) transport aircraft

Trial specification

Nov 2002

1 Introduction

The principle objective of this work is to develop flight control concepts and control law specifications or criteria for the next generation of large commercial blended wing body (BWB) aircraft.

A BWB aircraft has been mathematically modelled as a baseline configuration with elevons (trailing edge flaps combining aileron and elevator functionality) and rudder. Complete engine and partial undercarriage models are also included.

2 Background

The aerodynamic mathematical model has been used to address controllability issues in the low speed flight regime. Pure control power has been assessed through piloted simulation in all three axes. There are no high lift devices, e.g. flaps. A minimum takeoff and approach speed of 180kts was achieved for a longitudinal unstable configuration.

This configuration is flown in the backside of the drag curve, thus it is not possible to effectively reduce the engine thrust and hence the noise generated maybe an issue. Piloted simulation indicates that flight path stability on the approach is improved with the landing gear extended for the low approach speeds.

3 Trial objectives

The trial aims to:

i. Assess the longitudinal handling and flying qualities of an augmented BWB aircraft configuration while performing specified tasks in calm and turbulent air.

ii. Assess the lateral-directional handling and flying qualities of an augmented BWB aircraft configuration while performing specified tasks in calm and turbulent air.

4 Aircraft model description

An augmented longitudinally neutral stable configuration will be assessed.

The Centre of Gravity (CG) is fixed and its position chosen for the tasks is at 15% mac (mean aerodynamic chord) rearward of the baseline neutral point resulting in an increasingly longitudinal unstable aircraft as well as in the degradation of the lateral-directional too.

The model includes 3 engines. The engine dynamics are modelled by a series of throttles, which replicate in full the engines of a B747.

5 Flight control system and inceptors description

Pitch rate/attitude hold command system (PRAH)
Sideslip augmentation system
Yaw damper with washout

Full-scale longitudinal stick commands +5/-5 (deg/sec) pitch rate demand response.
Full-scale lateral stick operates +20/-20 (deg/sec) of roll rate demand response.
Full rudder deflection equates to +10/-10 (deg) sideslip.

The aircraft has a 20deg incidence limit, beyond which the data is invalid.

6 Trial requirements

Mathematical model/software

1. Pitch rate/attitude hold control law
2. Sideslip and velocity vector yaw rate control law
3. Interconnection between aileron and rudder
4. Manual thrust control
5. Undercarriage selector
6. Select levels of turbulence

Inceptors

1. Central wheel control column for pitch and roll inputs.
2. Rudder pedals for yaw control
3. Centre mounted throttle box for manual engine control
4. Longitudinal trim control on a button on the left corner of the wheel.
5. Coarse - Nose wheel steering at low taxiing or run speeds (<30kts). Fine – Nose wheel steering through rudder pedals.
6. Undercarriage selection through cockpit lever.

Cockpit indication

1. Head down display (see attached diagram)
2. Engine status indication for all 3 engines
3. Undercarriage position indication:
    a. Red for unlocked and in transit
    b. Green down and locked
4. DME LED indicator (distance in NM to threshold)
5. ILS Raw Data or PFD (Primary Flight Displays)

Visuals (outside view)

- 180deg dome with three channels representation.
- High definition of runway representation and general environment
- Precision Approach Path Indicator (PAPI's) for glideslope approach.

TASK EVALUATION

The evaluation will be made by using the Bedford Workload Scale ratings to estimate workload levels and the Cooper-Harper Scale rating to assess the handling qualities.

The Bedford Workload Scale is a ten point rating scale based on the concept of spare capacity and effort. It is very similar in appearance to the more familiar Cooper-Harper Rating scale and is used in a similar manner.

Following the performance of a specified task the pilot selects a workload description, which is the best indicator of task workload and returns the numerical rating associated with this description. The workload assessed is that involving execution of the primary task, i.e. maintaining aircraft trajectory within specified limits. Additional tasks should be included as part of the pilot's spare capacity.

The flight task to be rated and the time over which the assessment is made must be well defined. Emphasis should be placed upon the need to consider the numerical values simply as a way of summarising the descriptor selected for a given task.

TRIAL SCHEDULE

TASK DESCRIPTIONS

TASK 1 – Normal Takeoff, climbing and accelerating segments

Initial conditions: aircraft at MTOW, at the runway threshold ready for the takeoff.

Start the engines with parking brake on and throttles closed. Release the brake, set full thrust and check for normal operation of engines and increase of airspeed. Control the aircraft along the runway, let speed increase and rotate at Vr=180kts. Select 10deg of pitch attitude. Recover the landing gear and climb till reaching 1000ft above the ground. At this altitude the pilot must increase the airspeed to 200kts and then climb again, with 15deg of pitch attitude, until 5,000ft is reached. Then the aircraft shall be levelled at 5000ft and accelerated to 250kts (use 2deg of pitch and 0.98EPR), maintaining then this speed and altitude.

Evaluation 1.1: Select and maintain 10deg pitch attitude

(desired: ±2deg; adequate: ±5deg)

Cooper-Harper rating: **1 2 3 4 5 6 7 8 9 10**

Bedford Workload rating: **1 2 3 4 5 6 7 8 9 10**

Evaluation 1.2: Maintain 5000ft while accelerating from 200 to 250kts

(desired: ±100ft ; adequate: ± 200ft)

Cooper-Harper rating: **1 2 3 4 5 6 7 8 9 10**

Bedford Workload rating: **1 2 3 4 5 6 7 8 9 10**

Evaluation 1.3: Maintain 250kts at 5000ft

(desired: ±5kts; adequate: ±10kts)

Cooper-Harper rating: **1 2 3 4 5 6 7 8 9 10**

Bedford Workload rating: **1 2 3 4 5 6 7 8 9 10**

Pilot Comments (continue on the back if necessary):

TASK 2 – Critical engine failure takeoff + second segment climb

Initial conditions: same as before.

Procedure: same as before till the engine is failed automatically. Recognition of which engine is failed. Keep the aircraft going straight on the runway and assess both bank and heading control and rotate at Vr. Select a pitch attitude of less than 5deg in the way that a certain rate of climb together with a slight increase of speed will be possible, so, to achieve V_2 (V_2 is around 190-200kts) and select the gear up (action to be done immediately). Fly till 1000ft. Let the speed build up till it reaches 220kts and then keep climbing with a pitch attitude till 7deg until an altitude of 5000ft is reached. Level off at this altitude and accelerate the aircraft to 250kts, maintaining then both altitude and speed constant as before.

Evaluation 2.1: Maintain heading centreline after engine failure

(desired: within ±25% of runway width; adequate: within ±50% of runway centreline)

Cooper-Harper rating: **1 2 3 4 5 6 7 8 9 10**

Bedford Workload rating: **1 2 3 4 5 6 7 8 9 10**

Evaluation 2.2: After take-off maintain straight, wings level, climb

(desired: ±5deg of Hdg / ±5deg of bank; adequate: ±10deg of Hdg / ±10deg of bank)

Cooper-Harper rating: **1 2 3 4 5 6 7 8 9 10**

Bedford Workload rating: **1 2 3 4 5 6 7 8 9 10**

Pilot Comments:

TASK 3 – Normal approach and landing

Initial conditions: aircraft at MLW, trimmed for level flight with 180kts at 2500ft at 8NM from threshold. Set throttles at 5.0.

Procedure: Bring throttles back as necessary to decelerate the aircraft, check and/or set undercarriage down, and, begin to descend to acquire the 3deg glideslope and the landing speed of 180kts (+2deg of pitch and 1.07EPR). Continue the approach by maintaining the ILS flight path till touchdown.

(For lands check desired and adequate values at the end of the tasks scheduling)

Evaluation 3.1: Approach till 200ft

Cooper-Harper rating: **1 2 3 4 5 6 7 8 9 10**

Bedford Workload rating: **1 2 3 4 5 6 7 8 9 10**

Evaluation 3.2: Landing (Flare & Touchdown)

Cooper-Harper rating: **1 2 3 4 5 6 7 8 9 10**

Bedford Workload rating: **1 2 3 4 5 6 7 8 9 10**

Pilot Comments:

TASK 4 – One engine inoperative landing

Initial conditions: same as before.

Procedure: same as for the normal landing till the point that engine 3 suddenly fails at 1700ft of altitude. Compensate for the engine failure keeping the aircraft on the glideslope continuing the approach till touchdown.

Evaluation 4.1: Maintain heading and wings level

(desired: ±5deg of Hdg / ±5deg of bank; adequate: ±10deg of Hdg / ±10deg of bank)

Cooper-Harper rating: **1 2 3 4 5 6 7 8 9 10**

Bedford Workload rating: **1 2 3 4 5 6 7 8 9 10**

Evaluation 4.2: Landing (as before)

Cooper-Harper rating: **1 2 3 4 5 6 7 8 9 10**

Bedford Workload rating: **1 2 3 4 5 6 7 8 9 10**

Pilot Comments:

TASK 5 – Approach (with longitudinal offset)

Initial condition: same as before.

Procedure: the pilot should fly a normal approach by maintaining 1dot low on the PFD till an altitude of 600ft when he should abandon the indication given by the ILS, making a visual approach, aided by the PAPIs, from this point on.

Evaluation 5.1: Regain 2Whites/2Reds on PAPI at 180kts

(desired speed: ±5kts; adequate speed: ±10kts)

Cooper-Harper rating: **1 2 3 4 5 6 7 8 9 10**

Bedford Workload rating: **1 2 3 4 5 6 7 8 9 10**

Evaluation 5.2: Landing (as before)

Cooper-Harper rating: **1 2 3 4 5 6 7 8 9 10**

Bedford Workload rating: **1 2 3 4 5 6 7 8 9 10**

Pilot Comments:

TASK 6 – Approach (with lateral offset)

Initial condition: same as before.

Procedure: the pilot should fly a normal approach using the glide slope indication as guidance but keeping 1dot to the right (line up on taxiway, as a visual reference). When at 600ft altitude the pilot should abandon the indication given by the ILS and make a visual approach correcting the lateral offset.

Evaluation 6.1: Regain centreline by 200ft height

(desired: ± ½ runway width; adequate: ±1 runway width)

Cooper-Harper rating: **1 2 3 4 5 6 7 8 9 10**

Bedford Workload rating: **1 2 3 4 5 6 7 8 9 10**

Evaluation 6.2: Landing (as before)

Cooper-Harper rating: **1 2 3 4 5 6 7 8 9 10**

Bedford Workload rating: **1 2 3 4 5 6 7 8 9 10**

Pilot Comments:

Desired values

The following performance levels refer to this sequence, and the rating is to be made on the performance between 5 and 1 miles from touchdown.

	Desired	Adequate
1. Visual approach		
a. Use PAPIs for glideslope guidance	2w, 2r	3w, 1r 1w, 3w
b. Speed	-/+ 5kts	-/+ 10kts
2. Raw ILS		
a. Glideslope:	-/+ ½ dot	-/+1dot
b. Speed:	-/+5kts	-/+10kts
3. Raw ILS with Offsets		
a) Establish 1dot above glideslope. At 2miles acquire glideslope within 1mile.		
a. Glideslope:	-/+ ½ dot	-/+1dot
b. Speed:	-/+5kts	-/+10kts
b) Visually offset approximately 50ft above glideslope by 250ft. Actively correct to re-establish correct flight path.		
a. Glideslope:	-/+ ½ dot	-/+1dot
b. Speed:	-/+5kts	-/+10kts
c) Visually offset laterally by distance and at height determined by quality of simulator visuals etc. Correct accordingly.		
a. Localiser:	-/+ ½ dot	-/+1dot
b. Speed:	-/+5kts	-/+10kts
4. Engine Out		
Using Raw ILS approach		
a. Glideslope:	-/+ ½ dot	-/+1dot
b. Speed:	-/+5kts	10kts

Landings are to be made from all above approaches.

	Desired	Adequate
a. Speed:	+5, -0kts	+10, -5kts
b. Longitudinal displacement	Refer to figure 1	
c. Lateral displacement	Refer to figure 1	

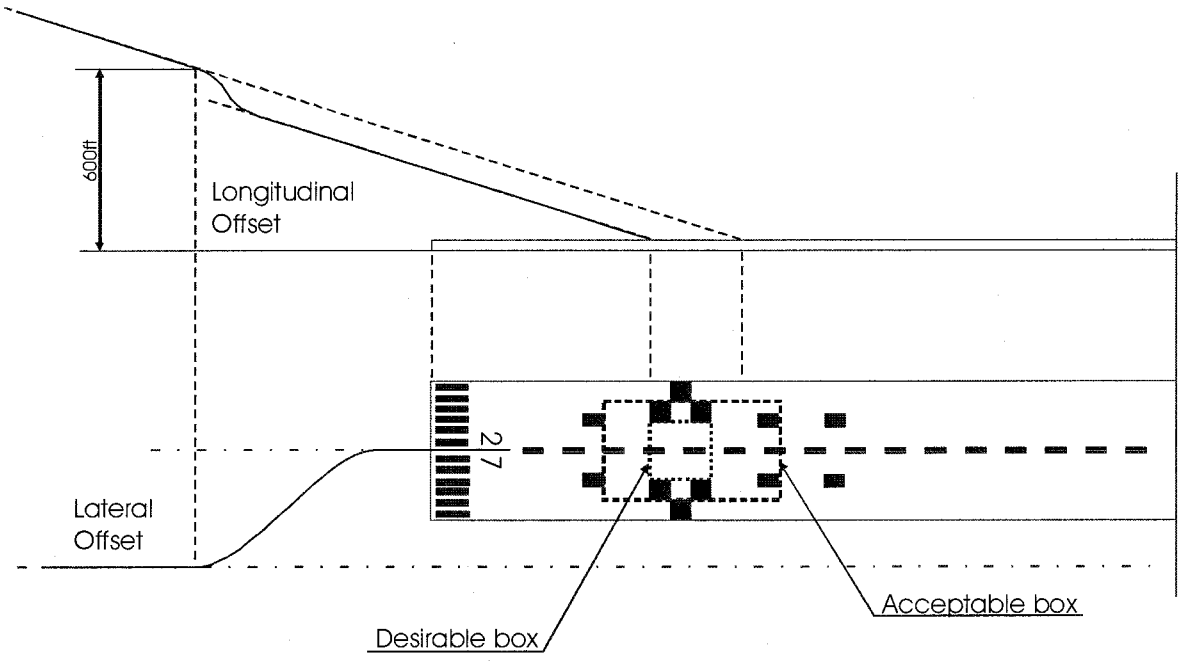

Fig.1 – Longitudinal and lateral offset during landing and desirable and acceptable touchdown box

E.2 Pilot's details

- Pilot A:
  - **Ian Burrett** has approximately 22years flying of which 14years was as test pilot. In those 22years he has flown a total of 40 thousand flight hours of which 200hours as training, 1900 hours in fast jets (Jaguar, Hawk, Buccaneer, Tornado, Hunter) and the remaining 1900hours as pilot of heavy aircraft (Tristar, VC10, C130K, C130J, BAC I-II).

- Pilot B:
  - **Jeremy Purry** is presently a civil aircraft pilot for British Midland (Bmi) flying short/medium haul in B737 type aircrafts. He has accomplished so far approximately 12,700 flying hours. He has flown other kinds of aircrafts as DC-9, F-27, HP-7, SD3-60, PA-31, PA-23 and PA-28.

- Pilot C:
  - **Roger Bailey** is the chief pilot of the Cranfield College of Aeronautics since 1990. Previously he had more than 5000 hours flying the C-130 for the RAF and 1000 hours as a flight instructor. He also graduated from the USAF TPS and afterwards spent three years at RAE Bedford as the squadron commander working on the Civil Avionics Programme, on Tornado and various Engineering Simulators. Since 1990 he has also flown the historic light aircraft of the Shuttleworth collection.

- Pilot D:
  - **Rick Pope** is presently (also) a civil aircraft pilot for the British Airways as a B777 pilot although he has flown already B757 and B767 aircrafts. He used to be a qualified flying instructor of the HAWK aircraft and a flying test pilot in aircrafts as Tornado, Harrier, F15E and Jaguar. In the approximately 8000 flying hours he accomplished so far he has flown also aircrafts as HS125, NS748, BAC1-II, King Air. At present he is also "the spare pilot" of the College of aeronautics for the Jetstream aircraft.

E.3 Pilot's comments

E.3.1 PILOT A (Simulator trials at 15 / Nov / 2002)

Task 1 – Normal Takeoff (CHR=2 / BWR=2)

"Set up - roll mode: much slugged with pitch"

Task 2 – Critical engine failure takeoff (- / -)

"Very little yaw at Vef (Engine failure speed). Pitch: initially slow to respond c. 30lb pull the rapid pilot to 10-12deg no. Roll mode felt very sluggish: frequently obtained ±30deg wheel, occasionally obtained ±45deg wheel. PIO tendency. Effect of yaw: roll wrong, wrong."

NOTE: these two evaluations were made with the pilot input demand divided by 2.5~3, which gave this sluggish feeling. The remaining evaluations were made with the pilot input demand divided by just 1.4, thus, giving a much faster aircraft response and feeling much better to the pilot.

Task 3 – Normal approach and landing (CHR=3 / BWR=2)

"With faster roll mode time constant: A/C easy to fly in pitch and airspeed control (provided pitch and throttle inceptors are used gently). Roll control adequate. Started to get difficult in last 100ft" *

Task 4 – Crosswind landing (CHR=5 / BWR=4)

"1st attempt: kick off drift – led to difficulty compensating for roll so landed with bank applied. 2nd attempt: wind down crab – still difficult to precisely set up a/c in "pre-flare" attitude → firm landing."

NOTE: the high ratings are due the final stages of the flight (see * below).

Task 5 – One engine inoperative landing (CHR=3 / BWR=2)

"Initially very slight yaw. Compensate with 30-40lbf left rudder. Then flew as per normal approach."

* *"Still observe difficult in last 50-100ft when task gain is high. Slight deviation from centreline is difficult to correct without making situation worse due to excessive bank and anticipation required to amest roll rate and level wings again."*

Task 6 – Approach for longitudinal offset (CHR=2 / BWR=2)

"Easy to correct pitch attitude. Once back on glide path, 2-3 pitch attitude corrections required but easy to perform and no overcontrol or PIO. NB: Pitch control breakout and friction may be a little high (≥ 10lb)."

Task 7 – Approach for lateral offset (CHR=5 / BWR=4)

"Correction worked but small residual heading error led to drift off centreline which was difficult to correct in last 100ft, partly because simulator fidelity (lack of motion)."

Task 8 – Normal approach with turbulence

Note: Task not interesting since the present turbulence model only affects the magnitude of longitudinal speed and as so, only the longitudinal movement being not a problem.

Task 9 – Crosswind approach and landing with lateral offset corrected at 200ft

"Decision at 200ft: easiest strategy is to fly a/c straight at threshold and kick off a little drift at last few feet (well into flare)."

Note: This task was tried since it would represent the most difficult task. It was decided to correct the offset just at 200ft because this is actually the decision altitude - the breakout cloud altitude or the minimum height decision when the runway has to become visible and the pilot decides whether to land or go-around. It was found very difficult to correct the lateral offset at or below 200ft since the offset was too large (1dot to the left or right) and would not give enough time for correction. The same task was tried again without the crosswind component without great improvements for the lateral offset.

E.3.2 PILOT B (Simulator trials at 21 / Nov / 2002)

Task 1 – Normal Takeoff (CHR=5 / BWR=5)

"There is limited control laterally on takeoff. A/c does not respond to rudder inputs and tends to sideslip off to side off runway. (Understand that the "model" is not very accurate in the ground regime). In flight is very slow to achieve auto trim. It is unnatural to a pilot not to have pitch trim control. Speed control. It is highly sensitive to speed excursions. It is very nearly impossible to control speed accurately with thrust as do on normal jet a/c. As briefed a/c is unstable & augmented, and on approach especially sits on the

'back side of the drag curve'. Hence, very unstable in speed and if speed decays bleeds away rapidly and it is very difficult to recover."

Task 2 – Critical engine failure takeoff (CHR=4 / BWR=5)

"In practice an engine cut was given at 120kts, suggest this to be much low for A/C to accelerate to V_r on remaining power. Works better if a V_1 is set at say 20kts, i.e. 160kts, below V_r and engine failed just after that speed. Easily controllable in yaw, in fact difficult to detect engine failure, initially no "swing" present. Very little yaw in climb out as expected for large a/c yaw decreases with increase of speed."

Task 3 – Normal approach and landing (CHR=4 / BWR=2)

"Again speed control very difficult. Slight over-sensitivity in pitch, not aided by lack of natural trim control. 180kt is a very high speed on approach. Limited opportunity to make "late" lateral corrections."

Task 4 – Crosswind landing (CHR=3 / BWR=2)

"Good roll authority for correction in 'flare'. Seems easier with the wing-down/crab technique due to poor 'model' simulation in the ground regime, it is difficult to assess the controllability in the flare."

Task 5 – One engine inoperative landing (CHR=3 / BWR=2)

"Easily controllable in yaw. A lot more thrust is required to remain on glideslope, (to be expected on loss of engine) remains easily controllable."

Task 6 – Approach for longitudinal offset (CHR=3 / BWR=2)

"Relatively easy to fly one dot high on glide slope. Easy to correct to visual approach, PAPI. Still the problem of speed control exists. It is much more noticeable as would expect on approach."

Task 7 – Approach for lateral offset (CHR=4 / BWR=4)

"At 600ft, plenty of room to manoeuvre to control flight path to achieve desired point of touchdown."

General comments:

"In general this is a flyable model for a large transport aircraft (a/c) and the simulation replicates quite well, the flying and handling qualities of a similar sized a/c that I am familiar with: B737."

"The ground model does not appear to work well, apart from the immediate touch down. The a/c does not 'rotate' properly on takeoff, with a long and noticeable 'dead-band' (similar to a hydraulic control system failure).

Nothing happens for a while before the a/c lifts off, and it appears not to respond initially to elevator control on the runway when pulled back."

"Pitch and roll control of flight path is good and replicates a B737-400 series (heavy). Would suggest that the approach speed is too high for all normally useable runways and if could be reduced to 170-160 would be easier to control, in terms of stopping on the runway."

E.3.3 PILOT C (Simulation trials at 10 / Dec / 2002)

Task 1 – Normal takeoff
1.1 Select and maintain 10 deg pitch attitude: CHR=3 / BWR=3
1.2 Maintain 5000ft while accelerating: CHR=3 / BWR=4
1.3 Maintain 250kt at 5000ft: CHR=3 / BWR=3

Note: subtask 1.2 gave a bit more work because the acceleration was a bit high so the altitude was overshoot and gave some work to the pilot.

Task 2 – Critical engine failure takeoff
2.1 Maintain runway centreline after engine failure: CHR=3 / BWR=5

"Easy to maintain centreline, as a result of that, difficult to identify failed engine."

2.2 Maintain a wings level climb after takeoff: CHR – 5 / BWR – 6

"Difficult to hold heading and bank angle due to dutch rolling."

Task 3 – Normal approach and landing
3.1 Approach till 200ft: CHR=4 / BWR=4
3.2 Landing, flare and touchdown: CHR=4 / BWR=4

"Flew ILS glideslope until PAPIs visible. Then flew 2white/2red PAPI till touchdown. Very small flare required."

Task 4 – Crosswind landing
Note: Not evaluated, task deleted from the trial.

Task 5 – One engine inoperative landing
5.1 Maintain runway centreline after engine failure: CHR=5 / BWR=6
"The FCS seems to compensate fully for the asymmetric thrust so control of heading and bank is normal. However there is sufficient excess thrust for reliable flight path control. If the pilot allows the aircrafts to get slightly low and/or slow he will be unable to recover the situation."

Task 6 – Approach for longitudinal offset

6.1 Regain 2white/2red PAPI after 600ft at 180kts: CHR=5 / BWR=4

6.2 Landing (as before): CHR=4 / BWR=4

"There was a tendency for a small flight path PIO after the correction which was difficult to damp out. This made accurate touchdown more difficult."

Task 7 – Approach for lateral offset

7.1 Regain centreline by 200ft height: CHR=4 / BWR=4

7.2 Landing as before: CHR=4 / BWR=5

"Lateral correction was easy but attention is necessary to maintain speed and flight path during correction. Possible to regain centreline by 180ft height and land on centreline."

E.3.4 PILOT D (Simulation trials at 11 / Dec / 2002)

Task 1 – Normal Takeoff

1.1 Select and maintain 10 deg pitch attitude: CHR=3 / BWR=3

1.2 Maintain 5000ft while accelerating: CHR=3 / BWR=3

1.3 Maintain 250kt at 5000ft: CHR=4 / BWR=4

"Minimal pitch activity to maintain ±2 deg, not fully 'hands free'. Continuous adjustment of EPR ±0.04. Perhaps the tolerances could be tightened to unearth the underlying pitch/power couple."

Task 2 – Critical engine failure takeoff

2.1 Maintain runway centreline after engine failure: CHR=3 / BWR=3

2.2 Maintain a wings level climb after takeoff (heading): CHR=3 / BWR=3

2.3 Maintain wings level climb after takeoff (bank): CHR=4 / BWR=4

"Lateral activity slightly increased over 3 engines case, and so, those comments still apply to 2 engines case (the longitudinal evaluation). I found the pitch capture slightly more difficult (maybe inexperience?), i.e., capture of ±2 deg, so, as the previous evaluation (CHR=4 / BWR=4)."

Task 3 – Normal approach and landing:

3.1 Approach till 200ft: CHR=4 / BWR=5

3.2 Landing, flare and touchdown: CHR=4 / BWR=6 ("*lack of familiarity*")

"**>200ft**: *Distracting in lateral sense (1/Ps cause me to overshoot desired track resulting in ±2 deg oscillation in Hdg).* **<200ft**: *I found it difficult to track the runway (rwy) centreline (c/l) once visual which resulted in me landing on R ½ of runway (rwy). Glideslope (G/S) and PAPIs not coincident*

(may have been the cause of initial distraction). Still difficult to fly Hdg ±2 deg."

Task 4 – Crosswind landing
Note: Not evaluated, task deleted from the trial

Task 5 – One engine inoperative landing
5.1 Maintain runway centreline after engine failure: CHR=3 / BWR=3
5.2 Landing (as before below 200ft): CHR=4 / BWR=5

"Engine fail not obvious, i.e., no warning and/or aerodynamics insignificant yaw (is it good?). 1st notice speed decay: easily recovered to V_{app}. Lateral activity still continuous but minimal directional 1/p required. However, if rudder were used for primary control of Hdg, i.e. to reduce lateral activity, oscillations were of greater amplitude ±3deg."

Task 6 – Approach for longitudinal offset
6.1 Regain 2w/2r PAPI after 600ft at 180kts: CHR=3 / BWR=3
6.2 Landing (as before): CHR=4 / BWR=3

"In 6.1, power adjustment easy, trend vector helps a great deal. In 6.2, lateral problem still exits but I am 'learning' the task."

Task 7 – Approach for lateral offset
7.1 Regain centreline by 200ft height: CHR=6 / BWR=7
(w/sidestick: CHR=4 / BWR=5)
7.2 Landing as before: CHR=6 / BWR=7
(w/sidestick: CHR=4 / BWR=3)

"From 600ft RA the initial turn towards the centreline was easy. I found (after 3 gos!) more anticipation than I expected to use was needed for the reversal (which I did from approximately 400ftRA). The Lat/Dir controllability felt much reduced during this transient phase. Using the side stick for this manoeuvre resulted in a more successful acquiring of the centreline."